Cognitive Radio in HF Communications: Selective Transmission and Broadband Acquisition

Radio Cognitiva en Comunicaciones HF: Transmisión Selectiva y Adquisición de Banda Ancha

Laura Beatriz Melián Gutiérrez

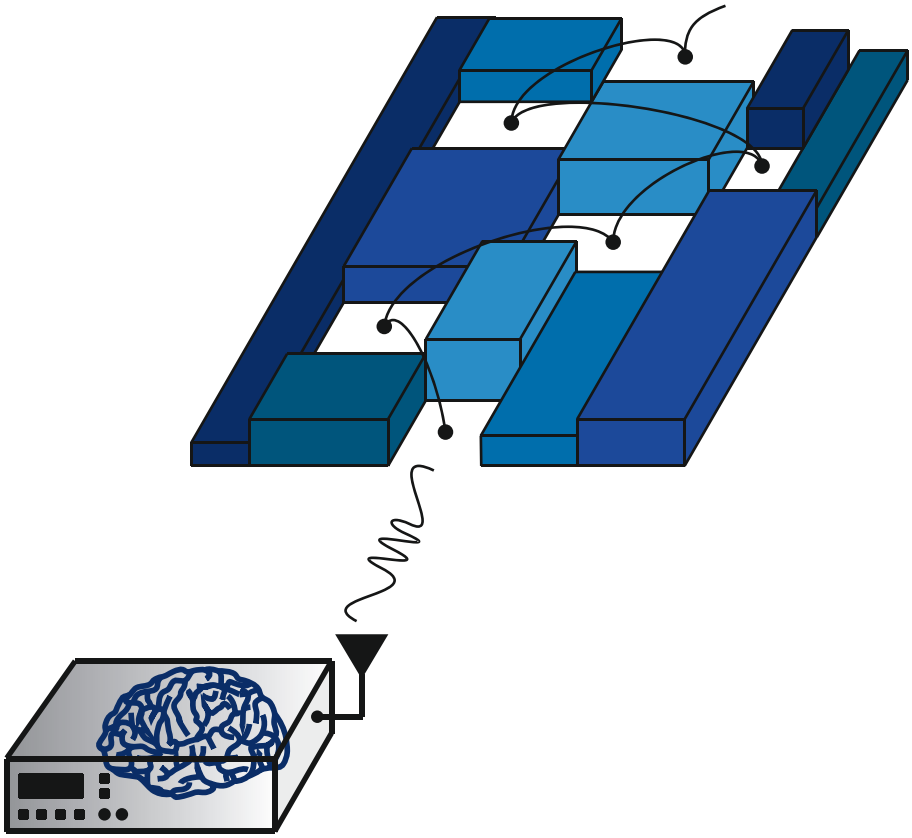

TESIS DOCTORAL

UNIVERSIDAD DE LAS PALMAS DE GRAN CANARIA
Instituto Universitario de Ciencias y Tecnologías Cibernéticas

Las Palmas de Gran Canaria, Enero 2016

UNIVERSIDAD DE LAS PALMAS DE GRAN CANARIA
Instituto Universitario de Ciencias
y Tecnologías Cibernéticas

D. AGUSTÍN J. SÁNCHEZ MEDINA, SECRETARIO DEL INSTITUTO UNIVERSITARIO DE CIENCIAS Y TECNOLOGÍAS CIBERNÉTICAS DE LA UNIVERSIDAD DE LAS PALMAS DE GRAN CANARIA

CERTIFICA,

Que la Comisión Ejecutiva del Instituto, en su sesión de fecha quince de febrero de dos mil dieciséis, tomó el acuerdo de dar el consentimiento para su tramitación a la tesis doctoral titulada "Cognitive Radio in HF Communications: Selective Transmission and Broadband Acquisition (Radio Cognitiva en Comunicaciones HF: Trasmisión Selectiva y Adquisición de Banda Ancha)", presentada por la doctoranda Dª Laura Beatriz Melián Gutiérrez y dirigida por los doctores D. Iván Alejandro Pérez Álvarez y D. Santiago Zazo Bello.

Y para que así conste, y a efectos de lo previsto en el artículo 6 del Reglamento para la elaboración, tribunal, defensa y evaluación de tesis doctorales de esta Universidad, firmo la presente en Las Palmas de Gran Canaria a quince de febrero de dos mil dieciséis.----------
---

UNIVERSIDAD DE LAS PALMAS DE GRAN CANARIA

INSTITUTO UNIVERSITARIO DE CIENCIAS Y TECNOLOGÍAS CIBERNÉTICAS

Doctorado en Cibernética y Telecomunicación

TESIS DOCTORAL

COGNITIVE RADIO IN HF COMMUNICATIONS: SELECTIVE TRANSMISSION AND BROADBAND ACQUISITION

RADIO COGNITIVA EN COMUNICACIONES HF: TRANSMISIÓN SELECTIVA Y ADQUISICIÓN DE BANDA ANCHA

Autora:	Director:	Codirector:
LAURA BEATRIZ MELIÁN GUTIÉRREZ	Dr. IVÁN ALEJANDRO PÉREZ ÁLVAREZ	Dr. SANTIAGO ZAZO BELLO

Las Palmas de Gran Canaria, Enero 2016

UNIVERSIDAD DE LAS PALMAS DE GRAN CANARIA

INSTITUTO UNIVERSITARIO DE CIENCIAS Y TECNOLOGÍAS CIBERNÉTICAS

Doctorado en Cibernética y Telecomunicación

TESIS DOCTORAL

COGNITIVE RADIO IN HF COMMUNICATIONS: SELECTIVE TRANSMISSION AND BROADBAND ACQUISITION

RADIO COGNITIVA EN COMUNICACIONES HF: TRANSMISIÓN SELECTIVA Y ADQUISICIÓN DE BANDA ANCHA

Autora: **LAURA BEATRIZ MELIÁN GUTIÉRREZ**

Directores: **Dr. IVÁN ALEJANDRO PÉREZ ÁLVAREZ**
Dr. SANTIAGO ZAZO BELLO

Las Palmas de Gran Canaria, Enero 2016

Abstract

The HF band (3-30 MHz) promotes the establishment of trans-horizon radio links by using the ionosphere as a passive reflector. Although HF radio links have this trans-horizon behaviour, most HF stations are allocated by national regulators. This allocation results in multiple collisions between HF users even if they are legacy users in their respective countries. Furthermore, HF communications make use of the Automatic Link Establishment (ALE) protocol, which has been referred to as an example of a primitive form of cognitive radio. It is based on a listen-before-transmit strategy to avoid interfering with on-going communications. However, the ALE protocol has several limitations: it does not manage the spectrum in a wide-band sense and it does not monitor the evolution of the users' activity in the channels. Due to these limitations, more dynamic techniques than the ALE protocol must be implemented in HF stations to reduce the amount of collisions between users. New capabilities such as adaptability and cognition have to be introduced in HF stations to reduce the inefficient use of this band in terms of successful access to the spectrum resources.

In this Thesis, the application of cognitive radio principles is proposed to reduce the amount of collisions between HF users and to reduce the inefficient use of this band. The cycle of tasks that a cognitive radio should face can be divided into three main tasks: *Observe*, *Learn*, and *Decide & Act*. They represent the cycle from the spectrum acquisition to the selection of the best channel to transmit, according to the observed and learned activity of other users.

A database of real measurements of the activity in the HF band is created in order to evaluate and validate the proposed cognitive techniques in this Thesis. This database contains wideband measurements of the power spectrum of the HF band. By using an energy detector to perform the spectrum sensing task, the acquired power spectrum is converted into users' activity information. The energy detector is the most appropriate technique in such a heterogeneous environment as the HF band.

One of the challenges that the acquisition of wideband measurements faces is the effect of narrowband interference (NBI) in wideband receivers. NBI causes a reduction in the effective number of bits used for the digitalisation of the signals of interest, and the quantization noise can exceed the thermal noise and the desired signal itself. Since NBI has to be mitigated in the analog domain, a compressive sensing based NBI detector is proposed to identify NBI before the digital front-end in wideband HF receivers.

Two learning strategies are defined and validated in this Thesis. An activity model based on Hidden Markov Models (HMM) is designed and validated for long-term predic-

tions of the activity in a particular HF channel. Another learning strategy is validated for short-term predictions in HF channels, the Upper Confidence Bound (UCB) algorithm. Besides its use for short-term predictions it also allows for decision-making to select the best channel to transmit in terms of availability.

Finally, a hybrid system combining previous learning strategies is defined in this Thesis. This hybrid UCB-HMM system can be seen as a metacognitive engine, which is able to adapt its data transmissions, i.e. it is able to select the most appropriate cognitive engine to transmit, according to the observed changes in the environment. Besides its adaptability to the changes in the environment, it is also shown that the amount of signalling information exchanged between transmitter and receiver is significantly decreased.

A mi familia

"*In the new era, thought itself*
will be transmitted by radio."

"*En la nueva era, el pensamiento mismo*
se transmitirá por radio"

Guglielmo Marconi (1874-1937)

Acknowledgements

When I look back on the long process of this work, I think of the people who have contributed in some way to its development. First of all, I would like to thank my supervisor Prof. Iván Pérez for giving me the opportunity to join his research team quite a few years ago, and for sharing his knowledge and experience during all these years. I would also like to thank my supervisor Prof. Santiago Zazo for advising me throughout this time. I am extremely grateful for their good advice.

I would like to thank Prof. Carlos Bader, Prof. Christophe Moy, and Navik from CentraleSupélec - Rennes, for their willingness to face new challenges. I would also like to thank the rest of members of the SCEE group, for their hospitality and kindness during my stay.

I would like to thank Prof. Hamed Ahmadi for accepting an invitation to review this work. I really appreciate his good advice, which has significantly improved it.

I can only recall having great moments with my colleagues at IDeTIC. Since I started working there, I have only met kind people with whom I have worked and shared meals, chats, and laughs. Thanks a lot!

I cannot forget Nelson, José Luis, Virginia, and Henar from Madrid, those who shared a huge amount of biscuits and good advice with me when I was starting this journey. I would especially thank José Luis for gladly advising me in the first tasks of this work.

I am deeply indebted to my family, especially to my parents, for their patience and support, they have always trusted in me. I am also very grateful to Javi, who has been always there, listening to all my concerns related to this work and helping me to deal with them.

Thanks to all of you who have been there for so long.

Table of Contents

List of Figures

List of Tables

Glossary

A

ABC Artificial Bee Colony

ACO Ant Colony Optimization

ADC Analog to Digital Converter

AGC Automatic Gain Control

ALE Automatic Link Establishment

ANN Artificial Neural Network

ARRL American Radio Relay League

AWGN Additive White Gaussian Noise

B

BER Bit Error Rate

BLOS Beyond-line-of-sight

C

CEPT European Conference of Postal and Telecommunications Administrations

CoSaMP Compressive Sampling Matching Pursuit

CPC Cognitive Pilot Channel

CS Compressive Sensing

CUS Collective Use of Spectrum

CW Continuous Wave

D

DSA Dynamic Spectrum Access

DVB-T Digital Video Broadcasting - Terrestrial

F

FCC Federal Communications Commission

FFT Fast Fourier Transform

FSK Frequency Shift Keying

G

GEV Generalised Extreme Value

H

HF High Frequency

HFDVL HF Data+Voice Link

HMM Hidden Markov Model

I

IARU International Amateur Radio Union

IDeTIC Instituto para el Desarrollo Tecnológico y la Innovación en Comunicaciones

IEEE Institute of Electrical and Electronics Engineers

IF Intermediate Frequency

ITU International Telecommunication Union

L

LBT Listen Before Transmit

LQA Link Quality Analysis

LSA Licensed Shared Access

M

MAB Multi-armed Bandit

MDP Markov Decision Process

ML Machine Learning

N

NBI Narrowband Interference

O

OFDM Orthogonal Frequency Division Multiplexing

OFDM-CDM Orthogonal Frequency Division Multiplexing - Code Division Multiplexing

OMP Orthogonal Matching Pursuit

OSA Opportunistic Spectrum Access

P

PCAST President's Council of Advisors on Science and Technology

POMDP Partially-observable Markov Decision Process

PSD Power Spectral Density

PSK31 Phase Shift Keying, 31 Baud

PSO Particle Swarm Optimization

Q

QoS Quality of Service

R

RD Random Demodulator

RF Radio Frequency

RIP Restricted Isometry Property

RL Reinforcement Learning

ROC Receiver Operating Characteristics

S

SDR Software-Defined Radio

SNR Signal to Noise Ratio

SSB Single-Sideband Modulation

STANAG NATO Standardisation Agreement

U

UCB Upper Confidence Bound

UCB_1 Upper Confidence Bound 1

UCB_1-M Upper Confidence Bound 1 - Multiple Plays

V

VSA Vector Signal Analyzer

Chapter

1

INTRODUCTION

MORE than 3000 km away across the Atlantic Ocean had the first over-the-horizon link established in December 1901. It was Guglielmo Marconi who received a telegraphic signal containing the Morse code for the letter *S* from Poldhu, United Kingdom, at Newfoundland, now in Canada (Simons, 1996). The first over-the-horizon radio transmission convinced Marconi that a transatlantic radio service was possible. He believed that radio waves could follow the curvature of the Earth, thus, if stations of sufficient size and power were used, over-the-horizon links could be established.

By that moment, there was no scientific evidence of how radio waves could cross the Atlantic ocean and reach the American coast, since the common belief at that time (Ratcliffe, 1974), after Maxwell and Hertz studies (Maxwell, 1873) (Hertz, 1893), was that radio waves should travel in straight lines like light, only deflecting if they found any barrier with different electrical properties. Therefore, limiting radio communications to line-of-sight distances. Physicist and mathematicians focussed their attention towards solving the problem of diffraction of waves by a spherical surface. Nevertheless, calculations demonstrated that the diffraction effect could not adequately explain the reflection of radio waves to reach remote places (Ratcliffe, 1974) (Maslin, 1987).

A year after Marconi's first over-the-horizon link, in 1902, two scientists: Arthur Kennelly and Oliver Heaviside postulated the existence of a conducting layer in the Earth's atmosphere (Kennelly, 1902), referred to as Kennelly-Heaviside layer (Ratcliffe, 1974). They suggested that radio waves could be reflected by this layer and thus, it could allow the propagation of radio waves thousands of kilometres far away, making possible the establishment of beyond-line-of-sight (BLOS) links. But, until 1925, no direct evidence for the Kennelly-Heaviside layer was achieved, meanwhile several long-distance

transmissions were successfully carried out by both professional and amateur users. That year, Appleton and Barnett obtained the first direct evidence of the so called Kennelly-Heaviside layer (Appleton, 1932). While establishing a long-distance transmission, they compared the effect of fading on the received signals at two different antennas simultaneously. Each received signal had different propagation paths, and this proved the existence of several layers at different altitudes in the atmosphere where radio waves were reflected to the Earth, i.e. several layers that made sky wave propagation feasible. Since it was thought that these layers were composed by ions (as it was later demonstrated), this region became known as ionosphere.

The ionosphere is a region of electrically charged particles and gases in the Earth's atmosphere, which extends from approximately 50 km to 600 km above the Earth's surface (NTIA/ITS, 1998). Solar radiation induces the ionisation process in which electrons are stripped from atoms and electrically charged particles, i.e. ions, are produced. These ions are placed in stratified layers with different ionisation. As shown in Figure 1.1, the placement of these layers varies with the time of day. They also vary over the Earth's surface since the strength of sun's radiation varies with geographic latitude, time of day, season and sunspot cycles (NTIA/ITS, 1998).

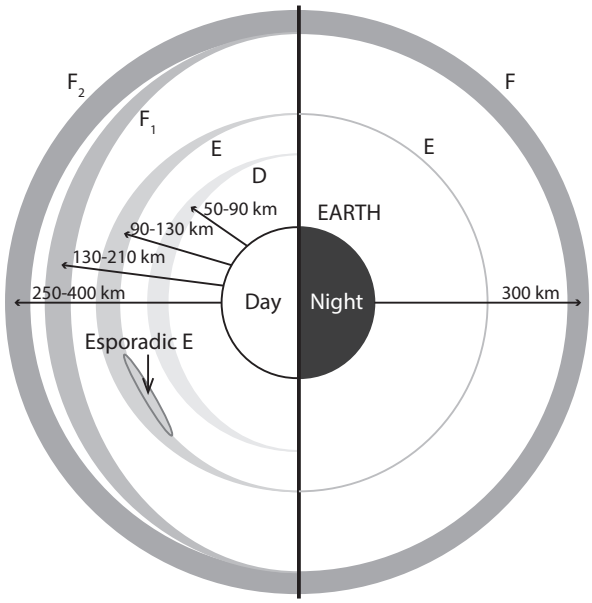

FIGURE 1.1. Layers of the ionosphere and their placement.

When radio waves hit these ionised layers, some are completely absorbed whereas others are reflected to the Earth, depending on their frequency. It is the High Frequency (HF) band from 3 to 30 MHz that enables the sky wave propagation (Maslin, 1987). Within this band, most of the radio waves hit the ionosphere and are reflected to the Earth in one or multiple hops. Depending on frequency, time of day, and ionospheric ionisation conditions, a signal can bounce several times before reaching a receiver which may be thousands of kilometres away.

Within the ionosphere, there are three layers: D, E, and F layers that have an influence

on HF communications (Maslin, 1987). The D-layer is the lowest region that affects HF transmissions. It is in this region where the main absorption takes place. However, due to the fact that absorption is inversely proportional to frequency, the D-layer has a smaller effect on frequencies above about 10 MHz, whereas, during daylight, the lower frequencies of the HF band are almost completely absorbed.

The E-layer is the lowest region of the ionosphere useful for sky wave propagation. It is comprised by the 'normal' and 'sporadic' E layers. The former is a regular layer that is important for daytime HF propagation at distances less than 2000 km but it has a residual ionisation at night. The 'sporadic' E-layer is formed by irregular layers of a higher ionisation with a cloud-shape that are latitude dependent. This layer can support long-distance transmissions at the upper end of the HF band and beyond, at frequencies that normally pass through this layer to reflect from higher layers.

Finally, the F-layer, which is the highest and most ionised layer of the ionosphere, is the most important for long-distance HF communications. During daylight, it is formed by two distinct layers: F_1 and F_2 layers, placed at different altitudes. The F_1-layer only exists during daylight and it is occasionally the reflection region for HF transmissions, but in general, it introduces further absorption since radio waves that penetrate the E-layer also penetrate the F_1-layer and are reflected by the F_2-layer. The F_2-layer is the highest ionospheric layer and it is the principal reflection region for long-distance HF communications. Although, it reaches maximum ionisation at noon, it remains charged at night, merging with the F_1-layer to form the F-layer at night.

Due to this structure of the ionosphere, during the day, HF sky waves of frequencies between 10 and 30 MHz pass through D and E layers to be reflected by the F_2-layer, whereas, during the night, only HF sky waves of frequencies from 3 to 8 MHz are reflected by the F-layer and they do not pass into outer space.

It can be observed from the previous description of the ionosphere that HF communications highly depend on natural factors such as solar radiation, geographical location, time of day, season, or sunspots cycles. Therefore, different propagation characteristics will be encountered by each HF communication link. Furthermore, after satellite communications emerged in the early 1970s, the interest in HF communications declined and HF equipment was usually preserved as a back-up (Maslin, 1987). However, it became clear some time later that satellites had several limitations and this is the reason why the HF band is still widely used for many civil and military applications to establish BLOS links. In fact, it is usually considered as a vital alternative to satellite links in tactical and mobile environments because, in case of natural or human disasters, it offers a worldwide coverage and it is always available for emergency services to establish BLOS communications.

As previously stated, the HF band covers the radio frequency spectrum from 3 to 30 MHz. Since it is a worldwide communications band, it is subject to international and national regulations. The International Telecommunication Union (ITU) has defined a

primary allocation within this band according to the service type: fixed, mobile, aeronautical mobile, maritime mobile, land mobile, broadcasting, amateur or standard frequency (Maslin, 1987). However, as contradictory as it may seem, most HF stations are allocated by national regulators, in other words, their frequency bands are assigned per country. This results in multiple collisions between HF users even if they transmit in their licensed bands, because HF transmissions in licensed channels in a particular country can interfere with other HF licensed users in another countries due to the trans-horizon behaviour of the band.

1.1 Motivation

Standard HF communications make use of the Automatic Link Establishment (ALE) protocol. It is the worldwide de facto standard for the establishment of HF radio communications over HF single sideband (SSB) links (NTIA/ITS, 1998). Based on a Listen Before Transmit (LBT) strategy to avoid interfering with on-going communications, the ALE protocol is usually referred to as an example of a primitive form of cognitive radio (Fette, 2009).

ALE represents the evolution from several calling technologies and protocols from different American manufacturers that were merged in the second generation ALE (2G ALE), defined in MIL-STD-188-141A and FED-STD-1045. Although a third generation (3G ALE) of the protocol was defined in MIL-STD-188-141B (Appendix C) and adopted in STANAG 4538, 2G ALE is still heavily used today (Furman & Koski, 2009).

ALE was designed to automatically select the best channel according to an internal ranking based on the propagation statistics of each possible link between two stations. An HF station that makes use of 2G or 3G ALE scans a list of pre-selected channels while it is not transmitting voice or data to evaluate the link quality with a particular HF station in that channel. By decoding the received ALE waveforms from other stations, the Bit Error Rate (BER), the Signal-plus-Noise-plus-Distortion to Noise-plus-Distortion Ratio (SINAD) and Multi-Path (MP) statistics are computed to conform the Link Quality Analysis (LQA) table. This LQA table contains the ranked list of each channel-station pair according to the computed propagation statistics.

Both 2G and 3G ALE stations use a LBT strategy to transmit and LQA statistics to select the best channel to transmit. However, 2G and 3G ALE have several drawbacks: they neither manage the spectrum as a whole, in a wide-band sense, nor support a real time channel evaluation operation where channels are probed prior to use (Furman & Koski, 2009). Furthermore, channel selection in 2G and 3G ALE can last for several seconds and these protocols do not monitor users' activity in those channels in the recent past. Thus, in order to reduce collisions between users even if they are licensed or they use the ALE protocol, more dynamic techniques than ALE must be implemented in HF stations for a further improvement of HF communications.

As previously stated, the HF band has a narrow bandwidth of 27 MHz where worldwide voice and data communications are established by multiple users mostly allocated by national regulators. Smart and dynamic mechanisms are needed to efficiently manage the HF spectrum, i.e., to avoid interfering with on-going communications and to take advantage of new transmission opportunities that may arise. New capabilities such as adaptability and cognition have to be introduced in HF stations to reduce the inefficient use of this band in terms of successful access to the spectrum resources.

Cognitive radio has emerged as a solution to the spectral scarcity problem by introducing opportunistic usage of the frequency bands that are not heavily occupied by licensed users (Haykin, 2005) (Federal Communications Commission, 2005). The main objective behind the use of cognitive radio principles is to provide the required intelligence to communications systems in order to learn from the environment and to adapt to its statistical variations in order to transmit in the frequency bands that are not being used by licensed users. If cognitive radio principles are applied, a more efficient use of the spectrum resources will be achieved.

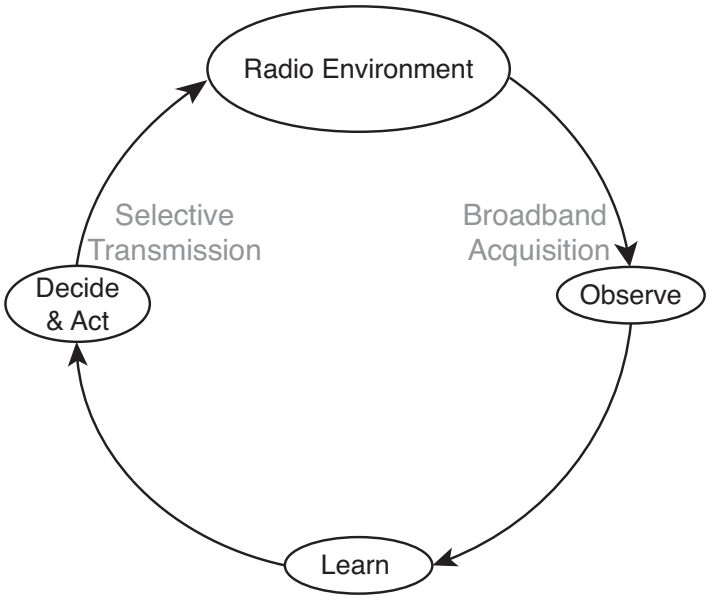

FIGURE 1.2. Simplified cognition cycle of tasks: *Observe*, *Learn* and *Decide & Act*.

The cognitive process encompasses three main tasks that are executed following the so called cognitive cycle (Mitola & Maguire, 1999; Mitola, 2000; Haykin, 2005), whose simplified version is depicted in Figure 1.2. These tasks are *Observe*, *Learn* and *Decide & Act*. They represent the cycle from the spectrum acquisition to the selection of the best channel to transmit in terms of availability, according to the observed and learned activity of other users.

- OBSERVE: The first step is the spectrum sensing task (Yucek & Arslan, 2009), which consists in the acquisition of the power spectrum to monitor users' activity within the acquisition bandwidth.
- LEARN: Cognitive radios take a further step, they learn from the acquired knowledge

with the spectrum sensing task by analysing the observed activity and by predicting future patterns of activity.

- DECIDE & ACT: Once the learning phase is complete, a decision must be made to select the best strategy to access the spectrum and transmit. This is referred to as the spectrum decision or decision-making phase (Hossain & Bhargava, 2007)(Hossain, Niyato, & Han, 2009) and it is normally related to spectrum access strategies.

Different works discussed the challenges and opportunities of applying cognitive radio to HF communications (Koski & Furman, 2009; Furman & Koski, 2009; Vanninen, Linden, Raustia, & Saarnisaari, 2014), in which the authors emphasised that multiple changes must be done to avoid collisions between HF users. They proposed new specifications based on cognitive radio principles for the next generation of the ALE protocol. Particularly, frequency management, channel selection, link establishment and link maintenance must be endowed with adaptability and cognition to be able to follow the changes in the environment and avoid collisions with other HF users.

1.2 Goals of this Thesis

It is likely that as long as cognitive radio principles are introduced in stations and mobile platforms of the HF band (hereafter, both referred to as HF stations), the radio frequency spectrum of this band from 3 to 30 MHz could be exploited in a more efficient way as HF stations will become aware of their surrounding environment and learn from it. In order to achieve such improvements in the band, these cognitive stations should have the capability to change their operating parameters in order to adapt their transmissions to the available spectrum holes which are to be predicted by using the acquired knowledge.

Hence, the primary goal of this Thesis is to evaluate and to show the feasibility of the application of cognitive radio principles to HF communication systems. Since they must be endowed with cognition and adaptability to execute the cognitive cycle of tasks depicted in Figure 1.2, different secondary goals in this Thesis are derived from this cognitive cycle of tasks.

- OBSERVE: Different goals must be fulfilled to properly execute the spectrum sensing task in the HF environment:
  - In order to test the developed work in this Thesis in a real environment, create a database of wideband measurements of the power spectrum of the HF band with the wideband HF transceiver developed in (Pérez-Díaz et al., 2009). By using a wideband transceiver multiple channels can be simultaneously scanned and cognitive strategies can be applied and evaluated.

  - Define and evaluate a strategy for the spectrum sensing task in the HF environment to convert the acquired power spectrum into users' activity information.
  - Design a narrowband interference (NBI) detector for wideband receivers that could be implemented in the analog domain. The presence of surface waves besides BLOS (Maslin, 1987) causes a reduction in the effective number of bits used for the digitalization of the signals of interest and thus, the quantization noise exceeds the thermal noise and the desired signal itself (Pérez-Díaz et al., 2012).

- LEARN: A secondary goal is identified in the learning phase:
  - Define and validate a strategy to learn the activity of HF users. It has also to be able to predict if a particular HF channel will be occupied, or not, both in the short-term and in the long-term.

- DECIDE & ACT: In order to perform a selective transmission, the following secondary goal has to be fulfilled:
  - Define and validate a strategy for decision-making, i.e. for the selection of the best strategy to transmit according to what the cognitive system has previously observed and learned.

1.3 Document structure

The contents of this Thesis are organised as follows:

- Chapter 2 includes an overview of the state of the art of cognitive radio. Several works have introduced the concept of cognitive radio and have proposed different techniques for each task of the cognitive cycle. Related work to the application of cognitive radio principles to HF communications is also analysed in this Chapter.

- Chapter 3 describes the database of real wideband measurements of the HF band acquired in this Thesis. Moreover, this Chapter includes the description of the proposed spectrum sensing technique for the HF environment.

- Due to the problematic acquisition with wideband receivers when there exists strong NBI, a solution for NBI detection based on compressive sensing is proposed in Chapter 4.

- Chapter 5 describes the first solution proposed in this work for the learning task. A spectrum activity model based on Hidden Markov Models (HMM) is designed and its structure provides a long-term prediction of the activity in a particular HF channel.

- Another learning strategy for the HF environment is proposed in Chapter 6. Based on reinforcement learning (Sutton & Barto, 1998), the Upper Confidence Bound (UCB) algorithm is demonstrated to be a feasible solution for activity prediction in the short-term as well as for decision-making.
- In order to improve the adaptability and reliability of the proposed solutions for learning and decision-making in Chapters 5 and 6, a hybrid UCB-HMM solution is proposed in Chapter 7.
- Finally, Chapter 8 draws the main conclusions of this work likewise future related work to this Thesis.

1.4 Related Contributions

As a result of the work described in this Thesis, several contributions have been published in peer-reviewed conferences and journal papers. The updated list of publications of the author of this Thesis is provided hereafter. The relation between these publications and the chapters of this Thesis is detailed in Table 1.1.

MELIÁN-GUTIÉRREZ, L., MODI, N., MOY, C., BADER, F., PÉREZ-ÁLVAREZ, I., & ZAZO, S. (2016). Hybrid UCB-HMM: A Machine Learning Strategy for Cognitive Radio in HF Band. *IEEE Transactions on Cognitive Communications and Networking*. doi: 10.1109/TCCN.2016.2527021

MELIÁN-GUTIÉRREZ, L., GARCIA-RODRIGUEZ, A., PÉREZ-ÁLVAREZ, I., & ZAZO, S. (2015). Compressive Narrowband Interference Detection for Wideband Cognitive HF Front-Ends. *Springer Wireless Personal Communications (Submitted)*.

MELIÁN-GUTIÉRREZ, L., MODI, N., MOY, C., PÉREZ-ÁLVAREZ, I., BADER, F., & ZAZO, S. (2015a, May). DSA with Reinforcement Learning in HF Band. In *1st URSI Atlantic Radio Science Conference (AT-RASC)*. Gran Canaria, Spain.

MELIÁN-GUTIÉRREZ, L., MODI, N., MOY, C., PÉREZ-ÁLVAREZ, I., BADER, F., & ZAZO, S. (2015b, June). Upper Confidence Bound Learning Approach for Real HF Measurements. In *IEEE International Conference on Communications Workshops (ICC Workshops)* (p. 281-286). London, UK.

MELIÁN-GUTIÉRREZ, L., ZAZO, S., BLANCO-MURILLO, J., PÉREZ-ÁLVAREZ, I., GARCÍA-RODRÍGUEZ, A., & PÉREZ-DÍAZ, B. (2013). HF spectrum activity prediction model based on HMM for cognitive radio applications. *Elsevier Physical Communication*, *9*, 199 - 211.

MELIÁN-GUTIÉRREZ, L., ZAZO, S., BLANCO-MURILLO, J., PÉREZ-ÁLVAREZ, I., GARCÍA-RODRÍGUEZ, A., & PÉREZ-DÍAZ, B. (2012, May). Efficiency improvement of HF communications using cognitive radio principles. In *12th International Conference on Ionospheric Radio Systems and Techniques (IRST12)* (p. 1-5). York, UK.

PÉREZ-DÍAZ, B., ZAZO, S., PÉREZ-ÁLVAREZ, I., LÓPEZ-PÉREZ, J., MELIÁN-GUTIÉRREZ, L., & JIMÉNEZ-YGUACEL, E. (2012, May). Theory and practice for modelling the broadband acquisition in HF transmissions. In *12th International Conference on Ionospheric Radio Systems and Techniques (IRST12)*. York, UK.

TABLE 1.1. Relation between Chapters and peer-reviewed publications.

CHAPTER	PUBLICATIONS
3. HF Spectrum Activity Database	(Melián-Gutiérrez et al., 2013)
4. Narrowband Interference Detection: A Solution Based on Compressive Sensing	(Melián-Gutiérrez, Garcia-Rodriguez, et al., 2015)
5. HF Primary User Dynamics Model	(Melián-Gutiérrez et al., 2012), (Melián-Gutiérrez et al., 2013)
6. Decision Making with Upper Confidence Bound Algorithms	(Melián-Gutiérrez, Modi, et al., 2015a), (Melián-Gutiérrez, Modi, et al., 2015b), (Melián-Gutiérrez et al., 2016)
7. Hybrid UCB-HMM Learning Scheme - A Metacognitive Engine	(Melián-Gutiérrez et al., 2016)

1.5 Collaborative work

The research work described in this Thesis has been carried out at *División de Ingeniería de Comunicaciones* at *Instituto Universitario para el Desarrollo Tecnológico y la Innovación en Comunicaciones* (IDeTIC). It has been partially funded by *Universidad de Las Palmas de Gran Canaria* with a fellowship for doctorate studies (*Programa propio de becas de postgrado y contratos - Convocatoria 2010*). During the development of this Thesis, the author has participated in the national research projects:

CR4HFDVL: Improving HF Data+Voice Link (HFDVL) using Cognitive Radio principles (TEC2010-21217-C02-01). Funded by *Ministerio de Ciencia e Innovación*. Partners: IDeTIC-ULPGC and SSR-UPM. Duration: January 2011 - December 2013.

UNDERWORLD: Underwater Radiocommunications for Optimized Monitoring using Multirelay Devices (TEC2013-46011-C3-2-R). Funded by *Ministerio de Economía y Competitividad*. Partners: IDeTIC-ULPGC, SSR-UPM and PLOCAN. Duration: January 2014 - December 2016.

The author has also collaborated in the following publications related to these projects:

LÓPEZ-PÉREZ, J., MELIÁN-GUTIÉRREZ, L., PÉREZ-ÁLVAREZ, I., ZAZO, S., RAOS, I., & PÉREZ-DÍAZ, B. (2012, May). Selection of CSI-based precoding techniques in the HF channel. In *12th International Conference on Ionospheric Radio Systems and Techniques (IRST12)*. York, UK.

RAOS, I., ZAZO-BELLO, S., PÉREZ-ÁLVAREZ, I., LÓPEZ-PÉREZ, J., MELIÁN-GUTIÉRREZ, L., & PÉREZ-DÍAZ, B. (2012, May). Optimization of ARQ parameters of STANAG 5066 for the HFDVL Modem. In *12th International Conference on Ionospheric Radio Systems and Techniques (IRST12)*. York, UK.

ZAZO, S., PÉREZ-ÁLVAREZ, I., LÓPEZ-PÉREZ, J., PÉREZ-DÍAZ, B., JIMÉNEZ-YGUACEL, E., MELIÁN-GUTIÉRREZ, L., & SANZ-GONZÁLEZ, J. (2012, May). Spatial domain mitigation of out of band strong interferers in HF wide band acquisition using analog beamforming principles. In *12th International Conference on Ionospheric Radio Systems and Techniques (IRST12)*. York, UK.

ZAZO, S., SANZ-GONZÁLEZ, J., PÉREZ-DÍAZ, B., PÉREZ-ÁLVAREZ, I., LÓPEZ-PÉREZ, J., & MELIÁN-GUTIÉRREZ, L. (2012, May). Analog mitigation of out of band strong interferers in wide band acquisition for multiband HF transmissions. In *12th International Conference on Ionospheric Radio Systems and Techniques (IRST12)*. York, UK.

Chapter

2

Cognitive Radio

In 2002, the Federal Communications Commission (FCC) carried out a campaign of measurements of the spectrum use below 1 GHz in several major cities of the United States. They revealed that, while some bands are heavily used, many other bands are not it use or are used only part of the time (Federal Communications Commision, 2002). This phenomenon was also observed in later campaigns in other countries such as Germany (Wellens, Wu, & Mähönen, 2007; Wellens & Mähönen, 2010), New Zealand (Chiang, Rowe, & Sowerby, 2007), Singapore (Islam et al., 2008), and Spain (López-Benítez, Casadevall, et al., 2009; López-Benítez, Umbert, & Casadevall, 2009). Furthermore, in many bands, spectrum access is a more significant problem than physical scarcity of spectrum, in large part due to command-and-control regulation, since spectrum bands are licensed for exclusive use of the entities assigned and unlicensed users are not allowed to use them (Federal Communications Commision, 2002) (Buddhikot, 2007) (Hossain et al., 2009). The FCC's spectrum use study reinforced the idea that spectrum opportunities may arise to new radio users to exploit more efficiently the spectrum resources.

These spectrum opportunities are usually referred to as spectrum holes in the literature (Hossain et al., 2009), defined as frequency bands assigned to licensed users, but at a particular time and specific geographic location, not being utilised by these licensed users (Haykin, 2005). An example of these spectrum holes is represented in Figure 2.1, where the dynamics of the spectrum use for a particular region are shown and several spectrum holes are identified.

If these spectrum holes were used by new radio users for transmission albeit not being licensed in these bands, an efficient use of the spectrum resources would be achieved. In order to do that, these new radio systems must be endowed with new capabilities to cor-

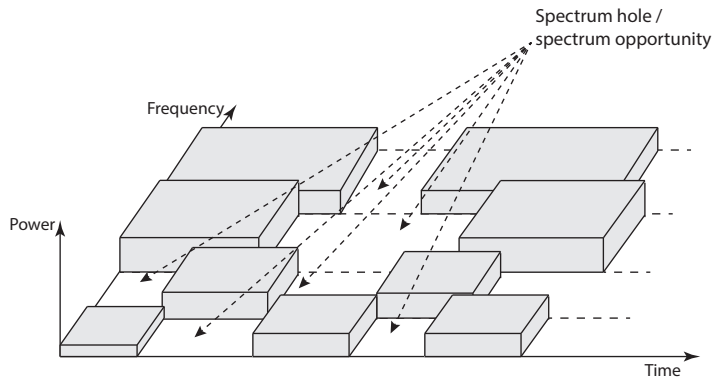

FIGURE 2.1. Spectrum holes / spectrum opportunities.

rectly identify and use spectrum holes for their transmissions while avoiding interference to licensed users.

By introducing opportunistic usage of the frequency bands that are not heavily occupied by licensed users, cogntive radio came out as a possible solution to the inefficient use of the spectrum (Haykin, 2005) (Federal Communications Commission, 2005). Since Mitola III proposed this concept in 1999 (Mitola & Maguire, 1999; Mitola, 1999), different scientists and communications-related entities (Haykin, 2005; Jondral, 2005; Federal Communications Commission, 2005; The SDR Forum, 2008; ITU-R, 2009) have defined the concept of Cognitive Radio, emphasising the fact that a cognitive radio must be an autonomous system with the following capabilities: intelligence, adaptivity, learning, reliability, efficiency and awareness. In addition to the previous cognitive capabilities, a cognitive radio is also endowed with reconfigurability. It can be achieved by using software-defined radio (SDR) platforms in order to automatically adapt cognitive radio's internal parameters according to the changes of the surrounding environment (Haykin, 2005; Jondral, 2005; Akyildiz, Lee, Vuran, & Mohanty, 2006).

All these capabilities are resumed in the cognition cycle depicted in Figure 2.2. A cognitive radio interacts with the surrounding environment following this cognition cycle: it continually observes the environment, orients itself, creates plans, decides, and then acts (Mitola & Maguire, 1999; Mitola, 2000). For a better comprehension, this cognitive cycle was simplified in Figure 1.2.

In the cognitive radio context, two types of users are identified: primary and secondary users. The former are the users that hold a license to transmit in a particular band of the spectrum whereas secondary users, which are also known as cognitive users, are unlicensed users that will access the spectrum assigned to primary users without causing interference. Secondary users will execute the cognition cycle of tasks in order to take advantage of available spectrum holes for transmission while primary users use current technology without cognitive capabilities (Buddhikot, 2007; Doyle, 2009; Hossain et al., 2009).

The following sections will introduce a set of techniques and strategies that could be

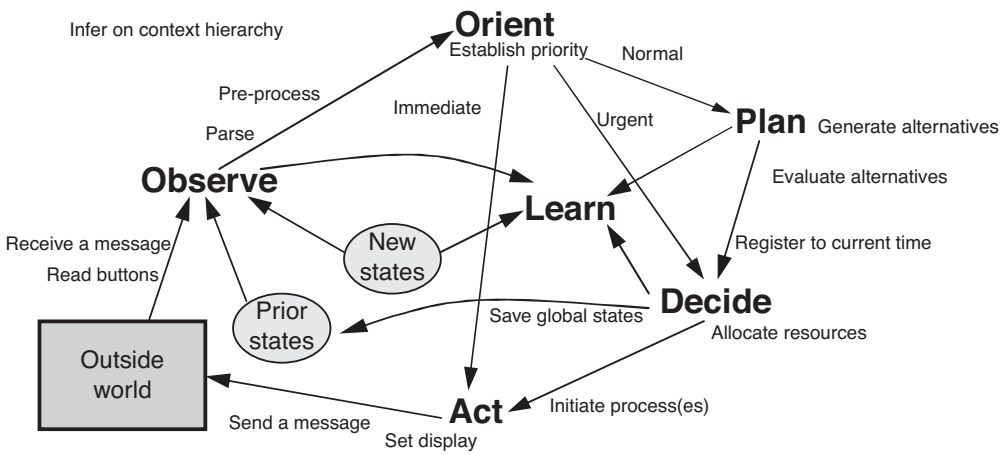

FIGURE 2.2. Cognition Cycle of tasks (Mitola & Maguire, 1999; Mitola, 2000).

used to implement each task of the cognition cycle of tasks. Firstly, Section 2.1 details different models of spectrum access that depict the coexistence of primary and secondary users in a particular frequency band. In the simplified cognition cycle of tasks in Figure 1.2 three main tasks were identified, namely: OBSERVE, LEARN, and DECIDE & ACT. Section 2.2 covers the existing techniques in the literature to observe the activity of primary users. The following task is dedicated to learn from the observed activity and the techniques dedicated to learn primary users activity are detailed in Section 2.3. Finally, a decision must be made according to the observed and learned information about primary users activity. Thus, Section 2.4 describes the strategies for decision making.

2.1 Spectrum access in Cognitive Radio

A static spectrum allocation has been traditionally offered to radio users due to the command and control model applied by international and national regulators. In this traditional licensing scheme, the spectrum licensee, the type of service and granularity of the spectrum are unchangeable, being an inflexible access scheme which results in spectrum underutilisation. Furthermore, it neither allows a flexible spectrum usage according to the time-varying demands of the user (Buddhikot, 2007).

Alternative spectrum access models have emerged under the name of Dynamic Spectrum Access (DSA), defined by the IEEE as the near real-time adjustment of spectrum utilisation in response to changing circumstances and objectives (IEEE Communications Society, 2008). DSA models are categorized in three major access models as described in Figure 2.3, namely, exclusive-use, shared-use of primary licensed spectrum, and commons model. Finally, new sharing models have been defined for spectrum sharing by regulatory bodies of the European Union and the United States.

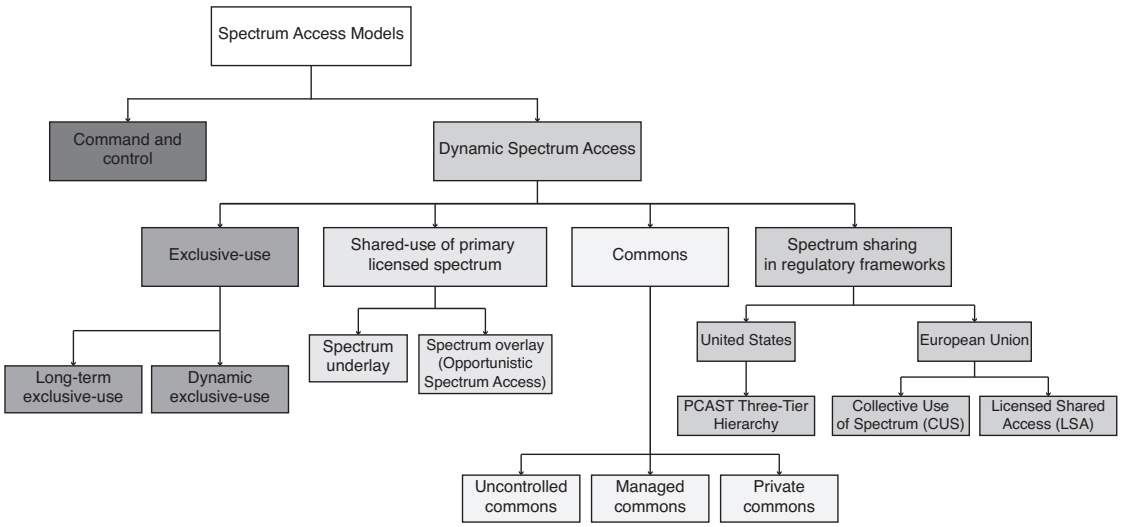

FIGURE 2.3. Spectrum access models

2.1.1 Exclusive-use model

The exclusive-use model allocates the spectrum to an entity that will have exclusive rights to use the spectrum under certain constraints. If the entity, a licensed user, does not use the allocated spectrum, it can lease the spectrum access rights to cognitive users, i.e. unlicensed users, that explicitly request permission from the licensed user. There are two variants: long-term exclusive-use model and dynamic exclusive-use model (Buddhikot, 2007; Hossain et al., 2009). The main difference between them is that the spectrum is allocated to licensed users for prolonged periods of time in long-term exclusive-use models, whereas spectrum allocation can be performed at a finer scale in dynamic exclusive-use models.

Under the restriction that only one user can exclusively use the spectrum at any time, a licensed user can trade its allocated spectrum to a cognitive user in the dynamic exclusive-use model. Therefore, the licensed user can earn revenue while the spectrum is being accessed by cognitive users for a certain period of time. This is the basis of secondary markets (Federal Communications Commission, 2000a, 2000b; Peha & Panichpapiboon, 2004), previously presented in Section 2.2 as a passive awareness technique since primary users inform secondary users of available spectrum holes. The spectrum allocation of cognitive users can be established in different ways (Hossain et al., 2009): before the spectrum is accessed (non-real-time secondary markets), in an on-demand basis for a fixed wireless service type (real-time secondary markets for homogeneous multi-operator sharing), or in an on-demand basis for a different wireless service type (real-time secondary markets for heterogeneous multi-operator sharing). By establishing a charge of use, licensed users have an incentive to share the spectrum while unlicensed users benefit from spectrum opportunities that they have to take advantage of (Peha & Panichpapiboon, 2004).

2.1.2 Shared-use model

Primary/licensed users and secondary/unlicensed users can simultaneously use the spectrum in the shared-use model as long as secondary users do not interrupt primary users. Unlike the exclusive-use model, the shared-use model allows secondary access with no request for permission to primary users, i.e. secondary access remains transparent to primary users (Hossain et al., 2009).

In the shared-use model, the transmissions of secondary users are expected to have minimal impact on primary users' operating conditions (Buddhikot, 2007). They are allowed to access the spectrum without damaging primary users in two ways (see Figure 2.4): spectrum overlay, also known as Opportunistic Spectrum Access (OSA), and spectrum underlay.

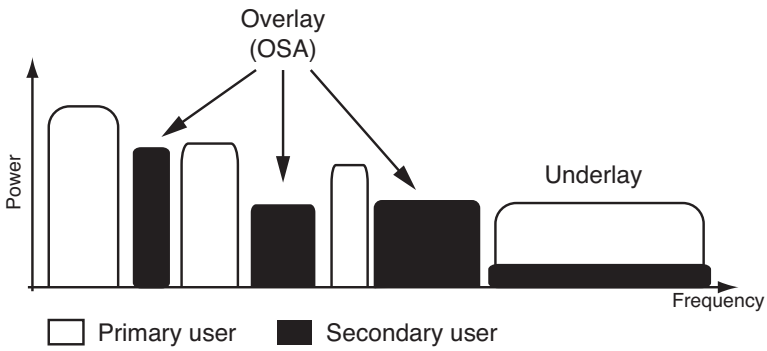

FIGURE 2.4. Shared-use of primary licensed spectrum: spectrum overlay (OSA) vs. spectrum underlay

On the one hand, spectrum overlay, mostly referred to as opportunistic spectrum access (Q. Zhao & Sadler, 2007), is widely considered in cognitive radio based schemes. In this model, primary users have license to transmit in a particular band and region. Nevertheless, if the allocated spectrum is not being used by a primary user at a particular time, it can be opportunistically accessed by a secondary user without power restrictions until the primary user starts to transmit.

On the other hand, in the spectrum underlay model, the secondary user concurrently shares with a primary user its allocated spectrum by transmitting with such a low power that it operates without interfering primary users. The interference temperature based sensing can be imposed on secondary users' transmission power so that the interference at a primary user's receiver is within the interference temperature limit (B. Wang & Liu, 2011). Spread spectrum or ultra wideband (UWB) radio systems can access the spectrum in the underlay mode (Doyle, 2009).

2.1.3 Commons model

Commons refers to an access model where all users have the same right to access the radio spectrum (Hossain et al., 2009). There are three variants (Buddhikot, 2007;

Hossain et al., 2009), namely, uncontrolled commons, managed commons and private commons. The difference between these variants resides in the existence or absence of some entity that controls the use of the spectrum resources.

The simplest variant is the uncontrolled commons in which the spectrum is not owned by any entity and there is no restriction in the number of users accessing the spectrum. This is the case of the ISM (2.4 GHz) and U-NII (5 GHz) unlicensed bands where no user has spectrum access rights. However, in uncontrolled commons they suffer from interference from other users of the unlicensed band, or from external transmissions of other wireless services such as IEEE 802.11b/g networks in the 2.4 GHz band (Buddhikot, 2007). On the contrary, in the managed commons model there is a group of users that jointly control the use of the spectrum resources. All users accessing the spectrum under this commons variant must follow the imposed restrictions to access the band but no user owns exclusive use license. Finally, the private commons model enables secondary users to access licensed bands at the discretion of the spectrum owner of that band. Unlike the shared-use model, primary users must approve the protocol and technology used by secondary users to access its allocated spectrum (Hossain et al., 2009).

2.1.4 Spectrum sharing in regulatory frameworks

Given the impact of new proposals on dynamic spectrum access to reduce the inefficient use of the spectrum, regulatory bodies of the European Union and the United States are working in new regulatory frameworks for spectrum sharing. Particularly, the Radio Spectrum Policy Group that assist the European Commission and the CEPT Electronic Communications Committee have proposed two spectrum sharing models to be applied in Europe: Collective Use of Spectrum (CUS) and Licensed Shared Access (LSA). While in the United States, the President's Council of Advisors on Science and Technology (PCAST) has proposed the Three-Tier Hierarchy model of spectrum sharing. The following sections are dedicated to these new spectrum sharing models as introduced by their respective regulatory bodies.

2.1.4.1 Licensed Shared Access

The Radio Spectrum Policy Group of the European Commission introduced in (Radio Spectrum Policy Group, 2013) a new spectrum sharing framework named as Licensed Shared Access (LSA), which has been studied by the CEPT Electronic Communications Committee in (Electronic Communications Committee, 2014). LSA was defined in (Radio Spectrum Policy Group, 2013) as: '*A regulatory approach aiming to facilitate the introduction of radiocommunication systems operated by a limited number of licensees under an individual licensing regime in a frequency band already assigned or expected to be assigned to one or more incumbent users. Under the Licensed Shared Access (LSA) approach, the additional users are authorised to use the spectrum (or part of the spectrum) in accordance with*

sharing rules included in their rights of use of spectrum, thereby allowing all the authorized users, including incumbents, to provide a certain Quality of Service (QoS).'

LSA fits under an 'individual licensing regime' (Electronic Communications Committee, 2014) where the incumbent user holds a license of spectrum rights and is able to share the spectrum assigned to it with one or several new users, named as LSA licensees, in accordance with a set of conditions negotiated between them and implemented by the National Regulation Authority (Radio Spectrum Policy Group, 2011; Matinmikko et al., 2014). In contrast to OSA where secondary users have no protection from primary users, LSA aims to ensure a certain level of guarantee in terms of spectrum access and protection from harmful interference for both incumbent and LSA licensees. With this protection, a predictive QoS is provided to incumbent and LSA licensees (Electronic Communications Committee, 2014).

2.1.4.2 Collective Use of Spectrum

Another model defined by the Radio Spectrum Policy Group of the European Commission is Collective Use of Spectrum (CUS), which is defined in (Radio Spectrum Policy Group, 2011) as follows: '*Collective Use of Spectrum allows an unlimited number of independent users and/or devices to access spectrum in the same range of designated CUS frequencies at the same time and in a particular geographic area under a well-defined set of conditions.*'

CUS is based on general authorisation, where an unlimited number of users are allowed to use the bands that they find available through their own mechanisms (Radio Spectrum Policy Group, 2011). Therefore, they have to rely on intelligent mechanisms such as cognitive radio to identify spectrum opportunities and, as opposed to LSA, they do not have interference protection. Since the offered QoS depends on the number of CUS users and the existing congestion level, there is no guarantee on the QoS for the users of this framework (Matinmikko et al., 2014).

2.1.4.3 PCAST Three-Tier Hierarchy

The President's Council of Advisors on Science and Technology (PCAST) proposed a Three-Tier Hierarchy model of spectrum sharing in (President's Council of Advisors on Science and Technology, 2012). The use of underutilised spectrum assigned to Federal users is promoted, while ensuring that primary Federal operations are both protected from interference. This spectrum sharing framework is based on the use of a geo-location database to enable reservation based dynamic sharing (Matinmikko et al., 2014).

The main difference of the Three-Tier Hierarchy model with respect to LSA is that it identifies three types of spectrum access (President's Council of Advisors on Science

and Technology, 2012), namely: Federal primary access, secondary access, and general authorised access. Federal users are legacy users with the highest priority. They have to register their deployments in a database to be protected from harmful interference in their deployed areas. When a particular frequency band in a specified geographic area is not in use by Federal primary users, secondary users are given priority access to register in the database in order to use the spectrum and they will be protected from interference caused by general authorised users. Nevertheless, if a Federal primary user registers a conflicting deployment in the database, the secondary user has to vacate it. Finally, general authorised users are allowed to opportunistically access the unoccupied spectrum when neither Federal primary users nor secondary users are registered in the database. As opposed to CUS users, generalised authorised users have to report its spectrum usage to the geo-location database (Matinmikko et al., 2014).

2.2 Techniques to observe the environment in Cognitive Radio

Following the previous description, secondary/cognitive users have to be aware of the surrounding environment in order to efficiently exploit the spectrum resources. Therefore, they have to observe their environment as a first step.

Spectrum awareness can be actively or passively achieved (Fujii & Suzuki, 2005; Fitzek & Katz, 2007). In passive awareness, secondary users receive the information of the available spectrum resources from an external agent whereas in active awareness, they sense their surrounding environment by themselves to obtain measurements of the spectrum usage. In fact, active awareness is usually referred to as spectrum sensing. A summary of the different techniques of passive and active awareness is depicted in Figure 2.5.

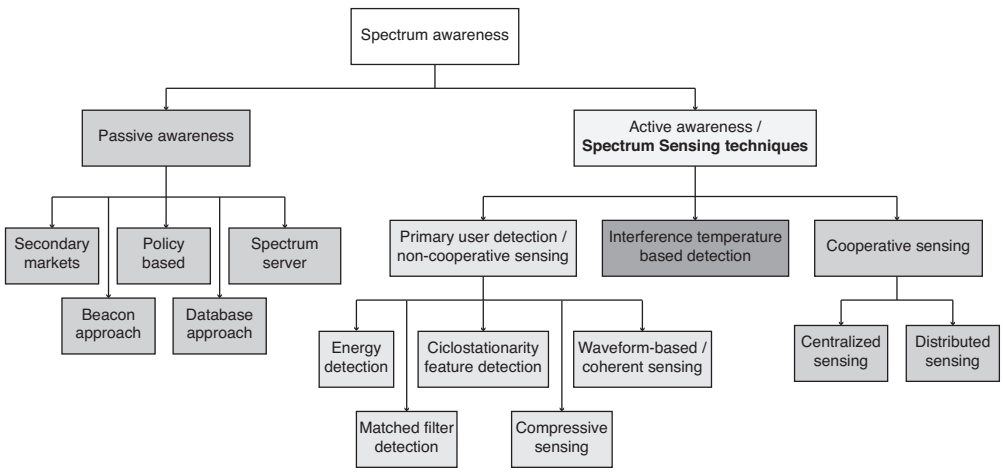

FIGURE 2.5. Types of spectrum awareness and spectrum sensing techniques.

In scenarios with passive awareness, primary users or regulatory authorities inform secondary users whether they can transmit, in which frequency band and for how long. Primary users can send beacons that advertise the availability of licensed spectrum to

secondary usage (Brown, 2005; Hulbert, 2005; Mangold, Jarosch, & Monney, 2006), or they can establish a secondary market where they lease their rights to secondary users to temporarily access the spectrum (Peha & Panichpapiboon, 2004). In the same way as primary users, if regulatory authorities identify previously licensed band with a low use by its licensed users, these can be assigned for secondary use according to a set of policies that provides rules and constrains concerning how to use this band (Mangold, Zhong, Challapali, & Chou, 2004). Furthermore, primary users, regulatory authorities, or external agents can maintain a database of the available spectrum resources in a particular area, being accessible to both primary and secondary users to update it (Brown, 2005; Gurney, Buchwald, Ecklund, Kuffner, & Grosspietsch, 2008; Murty, Chandra, Moscibroda, & Bahl, 2012). Finally, the last approach in passive awareness is based on a spectrum server with the information of the available resources, which offers suggestions to secondary users for an efficient use of the spectrum (Raman, Yates, & Mandayam, 2005; Yates, Raman, & Mandayam, 2006).

Spectrum awareness schemes combining passive awareness via geo-location databases and spectrum sensing have been proposed in (Mueck, Di Renzo, Debbah, & Renk, 2010; Ribeiro et al., 2012), showing that both types of awareness can be jointly used to acquire a better knowledge of the surrounding environment. In the following subsections, the attention is focussed on active awareness, i.e. spectrum sensing techniques that secondary users can carry out by themselves without interacting with primary users. As depicted in Figure 2.5, these techniques are divided into three main categories: primary user detection / non-cooperative sensing, interference temperature based techniques and cooperative sensing.

2.2.1 Primary user detection

The spectrum sensing task involves deciding whether the transmission of the primary user is present or not from the observed measurements by the secondary user. It can be generally formulated as a binary signal detection problem (Kay, 1998) with the following two hypotheses (Ghasemi & Sousa, 2005; Fitzek & Katz, 2007; Ma, Li, & Juang, 2009):

$$H_0: \quad y[n] = w[n] \qquad n = 1, \cdots, N-1 \tag{2.1a}$$

$$H_1: \quad y[n] = s[n] + w[n] \qquad n = 1, \cdots, N-1 \tag{2.1b}$$

where $y[n]$ is the signal received by the secondary user, $s[n]$ is the transmitted signal by the primary user at the channel's output, and $w[n]$ is the additive white Gaussian noise (AWGN). The null hypothesis H_0 states that no primary user is present in the observed measurements whereas the alternative hypothesis H_1 states that a transmission of a primary user may exist.

Different techniques based on the detection of a primary user's transmission by a single secondary user have been presented and evaluated in the literature. The most representative are included in Figure 2.5 and detailed hereafter. The selection of a par-

ticular technique must satisfy a trade-off between required accuracy, sensing duration, complexity, and whether secondary users have some knowledge about the primary user's transmission or not.

2.2.1.1 Energy detection

The energy detector, also known as radiometer, measures the energy of the received signal over a specific time interval as depicted in Figure 2.6, and performs the detection by comparing it with a threshold that depends on the noise floor (Urkowitz, 1967).

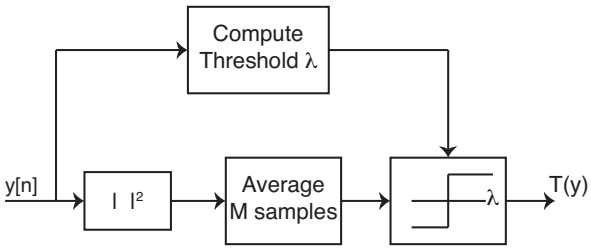

FIGURE 2.6. Block diagram of an energy detector.

The behaviour of the energy detector can be summarized in the test statistic:

$$T(y) = \frac{1}{M}\sum_{n=1}^{M}|y[n]|^2 \underset{H_0}{\overset{H_1}{\gtrless}} \lambda, \tag{2.2}$$

where $T(y)$ is the test statistic, M is the number of averaged samples of the received signal $y[n]$, and λ is the detection threshold. If $T(y) > \lambda$, the hypothesis H_1 holds and a primary transmission may exist, otherwise, if $T(y) < \lambda$, the null hypothesis H_0 holds and no primary transmission has been detected.

Energy detection is a suitable solution for spectrum sensing when the secondary user has any a priori knowledge of the primary transmission. In fact, it is the most simple solution but it also has some drawbacks as it is highly susceptible to unknown or changing noise levels and it does not work efficiently for detecting spread spectrum signals (Cabric, Mishra, & Brodersen, 2004). Nevertheless, it has been widely proposed for different cognitive radio applications in the literature such as (Ghasemi & Sousa, 2005; Cabric, Tkachenko, & Brodersen, 2006); or (López-Benítez & Casadevall, 2012; Nastase, Martian, Vladeanu, & Marghescu, 2014), where the energy detector has been enhanced for performance improvement.

2.2.1.2 Matched filter detection

Matched filter detection is known as the optimum detector of primary transmissions when these are known and corrupted by AWGN, since it maximises the received signal-to-noise ratio (SNR) (Proakis, 2000). Therefore, it is the optimum detector when the

secondary user has perfect knowledge of primary users' transmissions such as bandwidth, operating frequency, modulation type and order, and pulse shaping.

Matched filter detection is generally used to detect a signal by comparing a known signal or template with the input signal. When the secondary user does not have the template to compare or it is incorrect, its performance degrades significantly (Hossain et al., 2009). Since the detection is performed with a known signal, the matched filter needs less time to achieve high processing gain (Cabric et al., 2004; Sahai, Hoven, & Tandra, 2004). However, any receiver with matched filter detection will require a dedicated spectrum sensing receiver for each type of primary user signal type (Cabric et al., 2004; Yucek & Arslan, 2009).

2.2.1.3 Waveform-based detection / coherent sensing

Waveform-based detection, also known as coherent sensing (Yucek & Arslan, 2009), can only be performed when there exists a known pattern of the primary user's signal. In this technique, sensing is performed by correlating the received signal at the secondary user with this pattern of the primary user's signal (Tang, 2005; Arslan, 2007).

The detection is performed by comparing the waveform-based metric S with a pre-established threshold λ, similarly to the test statistic of the energy detector defined in Equation (2.2):

$$S = \Re\left[\sum_{n=1}^{N} y[n]s^*[n]\right] \underset{H_0}{\overset{H_1}{\gtrless}} \lambda, \tag{2.3}$$

where S is the waveform-based metric defined in the discrete time domain (Tang, 2005), $y[n]$ is the received signal by the secondary user and N is the number of samples of the known pattern $s^*[n]$. This pattern is the complex conjugate of the signal transmitted by the primary user $s[n]$. When the null hypothesis of Equation 2.1 holds, the waveform-based metric is

$$S = \Re\left[\sum_{n=1}^{N} w[n]s^*[n]\right], \tag{2.4}$$

whereas if the alternative hypothesis H_1 in Equation (2.1) holds, the waveform-based metric becomes

$$S = \sum_{n=1}^{N} |s[n]|^2 + \Re\left[\sum_{n=1}^{N} w[n]s^*[n]\right]. \tag{2.5}$$

The main advantage of waveform-based detection is that it outperforms energy detection at low SNR (Tang, 2005). Nevertheless, this technique is only applicable to systems with known signal patterns such as preambles, pilot patterns or spreading sequences used for synchronization or for other purposes (Yucek & Arslan, 2009).

2.2.1.4 Cyclostationary feature detection

Modulated signals are in general coupled with sine wave carriers, pulse trains, repeating spreading, hoping sequences, or cyclic prefixes, which result in built-in periodicity. Cyclostationary feature detection is a method for detection of primary user's transmissions by exploiting the cyclostationarity features of the received signals (Cabric et al., 2004). In the case wide-sense cyclostationary processes, second-order statistics such as the autocorrelation, vary periodically with time (Gardner, 1987).

Cyclostationary feature detection is realised by analysing the cyclic autocorrelation function of the received signal at the secondary user, $y[n]$, or, equivalently, its spectral correlation density function or cyclic spectral density function (Ma et al., 2009). The cyclic autocorrelation function of $y[n]$ is defined as

$$R_y^{\alpha}[\tau] \triangleq \langle y[n+\frac{\tau}{2}]y^*[n-\frac{\tau}{2}]e^{-2\pi j\alpha n}\rangle, \tag{2.6}$$

where α is called cyclic frequency, and $R_y^{\alpha}(\tau)$ is different from zero for some values of α (Gardner, 1987). The Fourier transform of the cyclic autocorrelation is the spectral correlation density function (Gardner, 1987), defined as

$$S_y^{\alpha}(f) = \sum_{\tau=-\infty}^{\infty} R_y^{\alpha}[\tau]e^{-2\pi jf\tau}. \tag{2.7}$$

The main advantage of cyclostationary feature detection is that it is able to differentiate the primary user signal from interference and noise, which do not exhibit spectral correlation (Gardner, 1987; Cabric et al., 2004). However, the detection process is complex and requires long observation periods to perform the spectrum sensing task (Hossain et al., 2009).

Cyclostationary feature detection has been proposed in (Goh, Lei, & Chin, 2007; Jallon, 2008) to perform the detection of DVB-T signals in TV bands authorised to secondary access as the FCC proposed in (Federal Communications Commission, 2004). The DVB-T standard defines digital TV signals as OFDM signals with a cyclic prefix which shows cyclostationary properties (Jallon, 2008). Accordingly to these properties, secondary users opportunistically accessing TV bands can detect via cyclostationary feature detection existing primary users in TV bands, i.e. existing TV broadcasters.

2.2.1.5 Other primary user detectors

Alternative methods have been proposed in the literature to perform primary user detection. While the computation of the wavelet transform of the received signal is proposed in (Tian & Giannakis, 2006; Ma et al., 2009) to identify spectrum holes, the randomised Hough transform is used in (Challapali, Mangold, & Zhong, 2004) for radar

pulse detection. Furthermore, test statistics derived from the covariance matrix of the received signal are used in (Ma et al., 2009; Zeng & Liang, 2009) since the statistical covariance matrices of the received signal and noise are generally different. The use of filter banks for spectrum sensing is proposed in (Farhang-Boroujeny, 2008), and the multitaper spectrum estimation, which can also be thought as a filter bank based estimator (B. Wang & Liu, 2011), is proposed in (Haykin, 2005). Finally, compressive sensing is used in (Tian & Giannakis, 2007) for primary user detection.

2.2.2 Interference temperature based sensing

Interference temperature is a new model introduced in (Federal Communications Commision, 2003) for measuring interference in cognitive radio scenarios. This concept is useful for secondary users since it is a reference to compute the maximum transmission power without damaging the transmission of the primary user. Interference temperature was defined by the FCC (Federal Communications Commision, 2003) as a measure of the RF power generated by undesired emitters plus noise sources that are present in a receiver per unit of bandwidth. The concept of interference temperature is identical to that of noise temperature (T. C. Clancy, 2007) since it is the temperature equivalent of this power measured in units of Kelvin (K):

$$T_I\left(f_c, B\right) = \frac{P_I\left(f_c, B\right)}{kB} \tag{2.8}$$

where $P_I\left(f_c, B\right)$ is the average interference power in Watts centred at f_c, covering a bandwidth B measured in Hertz, and k is the Boltzmann's constant whose is $1.38 \cdot 10^{-23}$ Joules per Kelvin degree. The emissions from undesired transmitters include both out-of band transmissions from users operating in adjacent frequency bands and in-band transmissions.

The goal of this approach is that by taking a single measurement, secondary users can jointly characterise both interference and noise. For a given geographic area, a maximum amount of tolerable interference for a given frequency band is established: the interference temperature limit, T_L. Therefore, secondary users must guarantee that their transmissions added to the existing interference must not exceed the interference temperature limit at a primary user (Federal Communications Commision, 2003; T. C. Clancy, 2007), as shown in Figure 2.7.

However, as detailed in (T. Clancy, 2009), the achievable capacity by secondary users from the interference temperature is low, compared to the amount of interference it can cause to primary users. Furthermore, the interference temperature based detection has also been considered by the FCC as an unworkable concept that would result in increased interference in the frequency bands where it would be used (B. Wang & Liu, 2011).

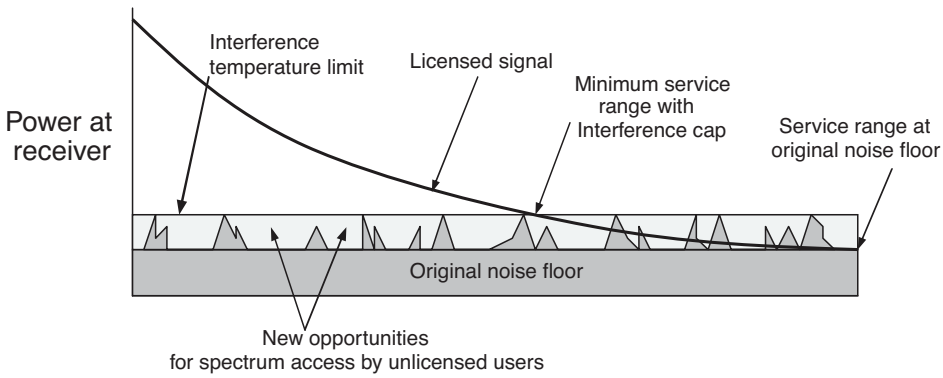

FIGURE 2.7. Interference temperature model (Federal Communications Commision, 2003).

2.2.3 Cooperative spectrum sensing

Spectrum sensing techniques based on primary user detection are also referred to as non-cooperative sensing due to the fact that they are performed in a single secondary user. When multiple primary and secondary users take part in a cognitive radio network, the hidden primary user problem may arise, since a secondary user may not always be able to detect all existing transmissions from primary users due to noise uncertainty, shadowing or channel fading (Yucek & Arslan, 2009; Hossain et al., 2009).

Cooperative sensing has been proposed in the literature to handle with the hidden primary user problem and to improve detection performance in each secondary user (Cabric et al., 2004; Ghasemi & Sousa, 2005; Ganesan & Li, 2005). By exploiting the spatial diversity in the sensed information by spatially located secondary users, the deficiency of individual sensing at each secondary user can be overcame and global sensing performance can be enhanced (Akyildiz, Lo, & Balakrishnan, 2011). However, it incurs in a communication overhead compared to non-cooperative sensing (Hossain et al., 2009).

Cooperation can be achieved in two different ways (Ganesan & Li, 2005): centralised or distributed. In centralised sensing, secondary users send sensing information via a common control channel to a central unit, which identifies available spectrum holes and broadcasts this information to other secondary users (Ma, Zhao, & Li, 2008; Lundén, Koivunen, Huttunen, & Poor, 2009). On the contrary, in distributed sensing schemes, each secondary user performs spectrum sensing and decision making based on the sensing results of the whole set or a fraction secondary users of the network (Cabric et al., 2004; J. Zhao, Zheng, & Yang, 2005). Independently of the cooperation scheme, each secondary user performs local spectrum sensing with the previously described primary user detectors. As an example, energy detection is used in (Unnikrishnan & Veeravalli, 2008; Ma et al., 2008), while cyclostationary feature detection is proposed in (Lundén et al., 2009; Derakhshani, Le-Ngoc, & Nasiri-Kenari, 2011).

2.3 Learning primary user dynamics

Besides primary user detection via spectrum sensing, there remains a need for monitoring primary users activity to improve secondary users' prediction of spectrum holes. One of the strategies that secondary users could accomplish is to learn from the observed activity of primary users in such a way that they could later predict their behaviour. Machine learning strategies have been widely used in the literature to learn primary user dynamics and to build models of their behaviour in the band. It may be possible that different types of users are present in a particular band but activity models will be definitely helpful for secondary users. In this section, the most utilised techniques for learning primary user dynamics are presented.

2.3.1 Artificial Neural Networks

Artificial Neural networks (ANN) have been designed to model the way in which the brain performs a particular task. An ANN is defined as a parallel distributed processor made up of simple processing units referred to as neurons, which is able to keep experiential knowledge and making it available for use (Haykin, 1998). In order to achieve good performance, ANNs have a massive interconnection of neurons and this interconnection is modified by learning to achieve a design objective.

In the context of cognitive radio, ANNs have been applied to model the activity of primary users. These models were used by secondary users to predict future primary users activity. This is the case of (Tumuluru, Wang, & Niyato, 2010), which proposed an ANN based spectrum prediction scheme. This ANN has a multilayer perceptron (MLP) architecture, i.e. it is formed by an input layer of sensor units, one or several hidden layers of neurons, and an output layer of neurons (Haykin, 1998). It was shown in (Tumuluru et al., 2010) that, after training the ANN with primary user traffic data following a Poisson process, there was an improvement in spectrum utilisation if the proposed model is used by secondary users for prediction. Furthermore, it was also proved that the required sensing energy could be significantly decreased since the prediction model allowed for the reduction in the number of channels to sense. In addition, a cognitive engine based on artificial neural networks was evaluated in (Baldo, Tamma, Manoj, Rao, & Zorzi, 2009). It learnt how environmental measurements affected the performance experienced on different channels of an IEEE 802.11 wireless network.

2.3.2 Hidden Markov Models

A Hidden Markov Model (HMM) is defined as a doubly embedded process with an underlying stochastic process that is not observable. This hidden process (state) can only be evaluated through another set of processes that produce sequences that actually can

be observed (Rabiner & Juang, 1993). An HMM can be used as an observation process of the cognitive engine to recognize or classify received stimuli and achieve awareness because it can model complicated statistical processes. In addition, since it can reproduce the training sequences, it can be used for prediction based on previous experiences (He et al., 2010).

Attending to the modelling and detection problems, Hidden Markov Models are widely used for speech recognition (Rabiner & Juang, 1993) but more recently they have also been used on cognitive applications for primary user detection and prediction, where they have achieved remarkable results. A spectrum detection system based on several HMMs, each trained for a particular signal spectrum, was presented in (Z. Chen, Hu, & Qiu, 2009). Besides, channel state prediction models based on HMMs were proposed in (Park, Kim, Lim, & Song, 2007) and (Z. Chen & Qiu, 2010). The one addressed in (Park et al., 2007) could only predict the channel state for deterministic observation sequences of a 1 symbol period or 2 symbols period; and could not carry out the prediction of non periodic sequences as real measurements from a frequency band actually are. Furthermore, the model proposed in (Z. Chen & Qiu, 2010) was based on Higher-Order HMM and took into account the latency between spectrum sensing and Wi-Fi data transmissions.

Another schemes for channel status prediction based on HMMs were proposed in (Akbar & Tranter, 2007) and (Ahmadi, Chew, Tang, & Nijsure, 2011), where it was assumed that primary users' traffic followed a Poisson distribution with channel occupancy ratio of more than 50% (i.e. every primary user utilises the spectrum for more than 50% of the time). Both schemes can be used by secondary users to predict the channel activity, (Ahmadi et al., 2011) demonstrated its prediction accuracy but no results in these terms were provided in (Akbar & Tranter, 2007).

As opposed to previous works, an underlay spectrum access was considered in (Sharma, Sahoo, & Nayak, 2008) for secondary users based on interference temperature metrics. A Hidden Markov Model was proposed to model the interference temperature dynamics of a primary channel. The trained HMM could be also used as a sequence generator to predict the interference temperature of a particular channel in the future.

Finally, few of the HMM based activity prediction schemes have been tested and validated in real scenarios. This is the case of the model proposed in (Z. Chen & Qiu, 2010), which was further developed and tested in (Z. Chen, Guo, Hu, & Qiu, 2011) jointly with a cooperative strategy among secondary users, and the 2-state HMM prediction scheme proposed in (Chatziantoniou, Allen, & Velisavljevic, 2013). Acquired Wi-Fi signals in an indoor placement were used to train the proposed model in (Z. Chen et al., 2011), whereas both Wi-Fi and Bluetooth signals in the 2.4 GHz band were considered in (Chatziantoniou et al., 2013). Moreover, the prediction accuracy of the model proposed in (Ahmadi et al., 2011) was further evaluated in (Ahmadi, Macaluso, & DaSilva, 2013) and (Macaluso, Ahmadi, & DaSilva, 2015) with synthetic data and real measurements of the 2.4 GHz ISM and GSM 1800 bands acquired by the RWTH Aachen University (Wellens

& Mähönen, 2010). The results showed that the prediction accuracy of the model proposed in (Ahmadi et al., 2011) depends on the duty cycle of the observed channel and on the complexity of the channel occupancy by the primary user.

2.4 Strategies for decision making in Cognitive Radio

As previously stated, opportunistic spectrum access (OSA) is the spectrum access model widely considered in cognitive radio literature for secondary users. Several solutions have been proposed as decision making strategies for secondary users to opportunistically access the spectrum. As depicted in Figure 2.8, some of them are applied to single agent scenarios where only a secondary user opportunistically access the spectrum, whereas other solutions are set in scenarios with multiple secondary users simultaneously accessing the spectrum.

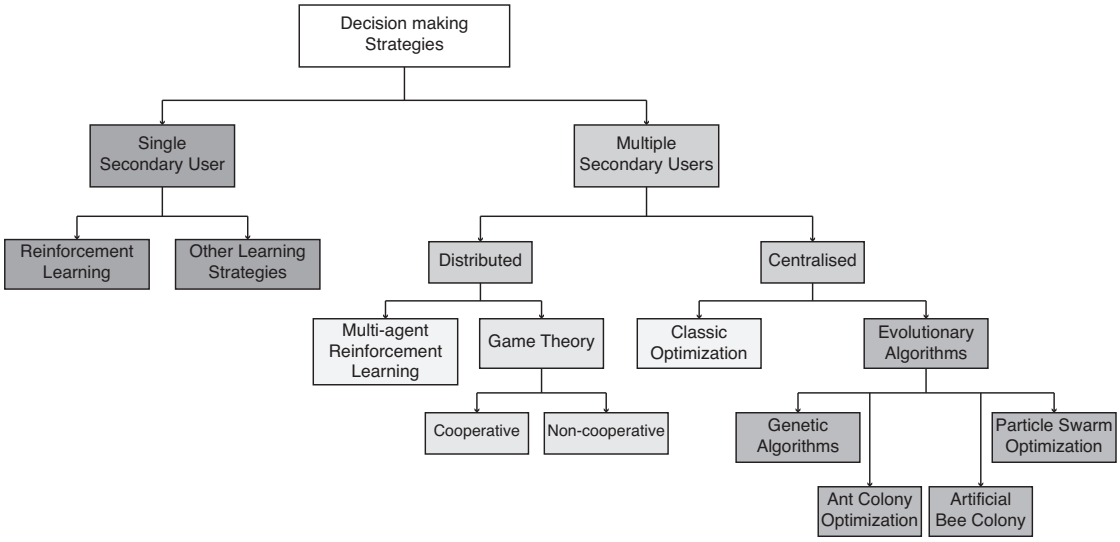

FIGURE 2.8. Decision making strategies.

2.4.1 Reinforcement Learning in single-agent scenarios

Reinforcement learning characterises learning problems that involve learning while interacting with an environment without requiring models of the dynamics of the environment (Sutton & Barto, 1998). In other words, reinforcement learning consists of an agent that interacts with the environment following a policy that describes its behaviour as a consequence of the changes in the environment. Differently to most forms of machine learning where the agent is told which actions to take, in reinforcement learning the learner must discover which actions generate the most reward by trying them (Sutton & Barto, 1998).

The agent-environment interaction in reinforcement learning is defined by the block diagram depicted in Figure 2.9. It is shown that after an interaction with the environment

by making an action a_t, the agent receives a reward r_{t+1} that informs the agent if the previous action was correct or not. Furthermore, after executing action a_t, the state of the environment changes from s_t to s_{t+1}.

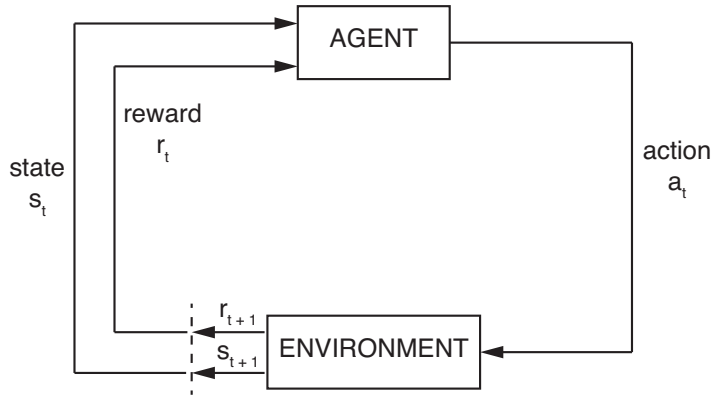

FIGURE 2.9. The agent-environment interaction in reinforcement learning (Sutton & Barto, 1998).

In the context of decision making for cognitive radio, an OSA scenario can be described as a reinforcement learning problem where the agent is a secondary user and the environment is the primary user spectrum to be accessed. The set of actions corresponds to the set of channels where the secondary could opportunistically transmit and the reward will inform the secondary user if it has selected an available channel or not, or some measure about the quality of the transmission performed in the selected channel.

Multi-armed bandit (MAB) problems (Robbins, 1952) and Markov Decision Processes (MDP) (Sutton & Barto, 1998) are two mathematical frameworks to describe the reinforcement learning problem, being MAB a simplified setting of reinforcement learning where only one state is considered instead of multiple states as in MDP. In the context of decision-making for OSA, MAB is a straightforward approach where the agent can only be at one state and the set of actions corresponds to a set of transmission channels. However, when an MDP is considered to model the OSA scenario, the set of actions also corresponds to a set of transmission channels but there are multiple states where the agent can be, and the transitions between them represent the complexity to change from one channel to another (Berthold, Fu, van der Schaar, & Jondral, 2008). An opportunistic spectrum access for cognitive radio based systems has been defined in the literature as an MAB in (Berthold et al., 2008; Jouini, Ernst, Moy, & Palicot, 2009; Jiang, Grace, & Liu, 2011; Robert, Moy, & Wang, 2014), an MDP in (Berthold et al., 2008; Hamdaoui, Venkatraman, & Guizani, 2009), or a partially-observable MDP (POMDP) in (Hoang, Liang, Wong, Zeng, & Zhang, 2009; Unnikrishnan & Veeravalli, 2010), where a POMDP is an MDP in which the states are not observable, but another signal stochastically related to the states is observable (Sutton & Barto, 1998).

Different algorithms have been proposed to solve both frameworks of reinforcement learning in the literature. All of them share a common characteristic: they look for a trade-off between exploitation and exploration, i.e. the continuous selection of an action previously rewarded or the search for new actions that could provide, or not, more

reward than those previously exploited. Particularly, softmax action-selection (Sutton & Barto, 1998), Upper Confidence Bound (UCB) (Agrawal, 1995; Auer, Cesa-Bianchi, & Fischer, 2002), and weight-driven (Jiang, Grace, & Liu, 2011) have been proposed for MAB problems, whereas time-difference learning methods such as Q-learning (Watkins & Dayan, 1992), Sarsa (Sutton & Barto, 1998) and actor-critic methods (Sutton & Barto, 1998) have been proposed for MDP.

These algorithms have also been proposed in previous cited works related to the application of reinforcement learning to opportunistically access the spectrum. In order to solve the associated MAB problem to OSA, softmax action-selection was selected in (Berthold et al., 2008), UCB was proposed in (Jouini et al., 2009; Jouini, Ernst, Moy, & Palicot, 2010), and weight-driven in (Jiang, Grace, & Liu, 2011; Jiang, Grace, & Mitchell, 2011). Furthermore, a comparative between UCB and weight-driven in these MAB setting for OSA was detailed in (Robert et al., 2014). In the particular case of MDP framework, Q-learning was proposed in (Hamdaoui et al., 2009; Yau, Komisarczuk, & Teal, 2010; Macaluso, Finn, Ozgul, & DaSilva, 2013) whereas the actor-critic method was selected in (Berthold et al., 2008).

2.4.2 Distributed strategies for multiple secondary users

When dealing with multiple secondary users in decision making problems, there are two types of scenarios: distributed or centralised, as shown in Figure 2.8. Similarly to cooperative sensing strategies, in a distributed decision making scenario, each secondary user performs its own decision according to its observations and the observations of other secondary users. On the contrary, decision making is carried out by a central authority or agent in a centralised scenario. When a distributed scenario with multiple secondary users is considered, multi-agent reinforcement learning and game theory are two suitable solutions for the decision making problem.

2.4.2.1 Multi-agent Reinforcement Learning

Besides its application to single-agent scenarios, some proposals on reinforcement learning have dealt with multi-agent scenarios where several secondary users try to simultaneously access the spectrum. A modified version of Q-learning, named to as decentralized Q-learning, was proposed in (Galindo-Serrano & Giupponi, 2010) for a set of secondary users whose cognitive system was based on the IEEE 802.22 standard (Cordeiro, Challapali, Birru, & Sai Shankar, 2005), which is the first standard that proposes an opportunistic spectrum access to TV broadcasting frequency bands to provide access to rural areas. However, the simultaneous learning process of different nodes could generate oscillating behaviours in a decentralized setting (Giupponi, Galindo-Serrano, Blasco, & Dohler, 2010). As a solution, the term *docition* was introduced for multi-agent scenarios

in (Giupponi et al., 2010), which referred to radios that teach to other radios by exchanging information about the performance of their learning processes, thus, resulting in an improvement of the learning process.

2.4.2.2 Game Theory

Game theory is a mathematical tool that attempts to model the behaviour of rational entities in an environment of conflict (Bkassiny, Li, & Jayaweera, 2013). One of the main challenges in opportunistic spectrum access is the interaction among multiple secondary users (Xu et al., 2013). When multiple secondary users in a cognitive radio network have to simultaneously decide which channel is better for their transmissions, i.e. multiple secondary users have to be allocated in the spectrum at the same time, they interact to avoid collisions between them. This interaction can be analysed by game theory where each secondary user is a player and two types of games can be played: cooperative and non-cooperative, based on whether the secondary users exchange information regarding their decisions or not, respectively. Game theory has been widely used for cognitive spectrum allocation algorithms in both cooperative or non-cooperative scenarios (Tragos, Zeadally, Fragkiadakis, & Siris, 2013; B. Wang, Wu, & Liu, 2010): as an example, adaptive channel allocation schemes for cooperative and non-cooperative scenarios were presented in (Nie & Comaniciu, 2006), whereas dynamic spectrum sharing based on game theory in cooperative and non-cooperative settings was analysed in (Ji & Liu, 2007).

A repeated game was proposed in (Wu, Wang, Liu, & Clancy, 2009) to share the spectrum between secondary users in a cooperative mode. The proposed game follows a cheat-proof strategy in order to evaluate how fair were secondary users while sharing their observations. Another cooperative game was proposed in (Suris, DaSilva, Han, & MacKenzie, 2007) where several nodes in a multi-hop wireless network needed to agree on a fair allocation of spectrum. On the contrary, a non-cooperative scenario is considered in (Malanchini, Cesana, & Gatti, 2009) where a repeated game is proposed to model the selection of the best spectrum opportunities by secondary users with a cost associated with spectrum mobility.

2.4.3 Centralised strategies for multiple secondary users

The following sections deal with decision making in centralised scenarios with multiple users. In a centralised setting, a central authority or agent is in charge of looking for an allocation of spectrum resources according to different terms such as maximum total throughput, minimum interference between users, or minimum power consumption in the network. Classic Optimization techniques and evolutionary algorithms are two suitable strategies to deal with centralised decision making in cognitive radio.

2.4.3.1 Classic Optimization

Mathematical optimization techniques such as linear programming or gradient-based methods have been utilised to solve decision making problems in cognitive radio. Particularly, most of these works were focussed on spectrum allocation of multiple secondary users and their power/rate scheduling. An example of these works was proposed in (Masmoudi, Belmega, Fijalkow, & Sellami, 2015), where a sub-gradient algorithm was used to solve a joint scheduling and power allocation problem. The objective of the problem proposed is to minimise the power consumption of all secondary users under QoS, maximum peak and average interference to primary users constraints. Another proposal was included in (Ngo & Le-Ngoc, 2011), where a joint subcarrier and power allocation problem was set out in cognitive radio networks with orthogonal frequency-division multiple-access (OFDMA), and solved with a sub-gradient algorithm.

2.4.3.2 Evolutionary Algorithms

Evolutionary algorithms are stochastic search methods that mimic natural evolution and the social behaviour of species (Tragos et al., 2013). Genetic algorithms, Particle Swarm Optimization, Ant Colony Optimization and Artificial Bee Colony are some of the algorithms categorized as evolutionary that have been proposed for decision making in cognitive radio.

Genetic algorithms mimic the process of natural selection. A solution to a given problem is represented in the form of a string called 'chromosome', consisting of 'genes' which hold a set of values for the optimization variables (Goldberg, 1989). The proposal enclosed in (Thilakawardana & Moessner, 2007) is a genetic algorithm based cell-by-cell dynamic spectrum allocation scheme that achieved better spectral efficiency than fixed spectrum allocation. In addition, (Kim et al., 2008) proposed a genetic algorithm based cognitive engine for dynamic spectrum access. It was designed to optimise transmission parameters, such as carrier frequency, bandwidth, transmit power and modulation type, in order to maximise the spectrum efficiency and minimise interference to primary users. A centralised setting with a spectrum broker in a real-time secondary spectrum market was proposed in (Bourdena, Kormentzas, Pallis, & Mastorakis, 2012) where the decision making strategy was based on genetic algorithms. The efficiency of the broker operation was evaluated in terms of maximum utilisation of spectrum opportunities and minimum fragmentation. Finally, (Z. Zhao, Peng, Zheng, & Shang, 2009) proposed a genetic algorithm based spectrum allocation scheme to maximise network utilization by secondary users.

Ant Colony Optimization (ACO) is inspired by the behaviour of ants in finding shortest paths from their colony to food sources (Dorigo & Blum, 2005; He et al., 2010), while Artificial Bee Colony (ABC) is inspired by honey bee foraging (Karaboga & Basturk, 2007).

An ABC algorithm is proposed in (Cheng & Jiang, 2011) to optimise the spectrum allocation in a cognitive radio network with two goals: efficiency and fairness. The results obtained in (Cheng & Jiang, 2011) showed that ABC algorithm outperforms a genetic algorithm in terms of convergence speed and computational complexity.

Particle Swarm Optimization (PSO) is inspired by the social behaviour of a flock of birds trying to find their destination during migration (Kennedy & Eberhart, 1995; Z. Zhao et al., 2009). Besides genetic algorithms, (Z. Zhao et al., 2009) also proposed a PSO based spectrum allocation scheme to maximise network utilization. When compared with the genetic algorithm based allocation scheme, PSO was generally found to perform better than genetic algorithm. Decision making is modelled as a joint power control and channel assignment problem in (Yu, Liu, & Hu, 2010), and solved with binary PSO to maximise the network capacity and minimise the power consumption.

2.5 Metacognitive Radio Engine

The algorithms that provide a cognitive radio with learning and decision-making capabilities are referred to as the cognitive engine of the cognitive radio (Gadhiok, Amanna, Price, & Reed, 2011). One of the challenges that a cognitive radio faces is how to adapt to the changes of the surrounding environment. The algorithms that are part of the cognitive engine may not be feasible nor reliable for all situations. Due to this fact, the adoption of the *metacognition* concept of psychology to cognitive radio is proposed in (Gadhiok et al., 2011) and (Asadi, Volos, Marefat, & Bose, 2015).

A metacognitive radio engine is a cognitive radio formed by several cognitive engines and it has the ability to dynamically match the appropriate learning algorithm with the dynamically changing environment (Asadi et al., 2015). In other words, a metacognitive engine can be seen as a higher-level agent inside the cognitive radio architecture that selects the most appropriate learning and decision-making strategies according to the observed changes in the environment. By doing this, the cognitive radio behaviour will not be limited by the use of an unique cognitive engine.

2.6 Cognitive Radio and HF communications

Little work in the literature of cognitive radio has focussed its attention to the application of cognitive radio to HF communications due to the fact that most of the research in this matter is related to communication bands above the HF band. Albeit Automatic Link Establishment (ALE) protocol for HF radios has been presented as a primitive form of cognitive radio (Fette, 2009), a more dynamic mechanism that ALE is required to efficiently apply cognitive radio principles to HF communications.

Having the ALE protocol as a starting point to implement cognitive capabilities, there

are some proposals on new specifications for the ALE protocol in (Furman & Koski, 2009) and (Koski & Furman, 2009). Particularly, frequency management, channel selection, link establishment and link maintenance must be endowed with adaptability and cognition to be able to follow the changes in the environment. Moreover, (Vanninen et al., 2014) also analysed the current limitations of HF communications and ALE protocol to include the dynamic capabilities required by cognitive radios, thus also enumerating some modifications of the ALE protocol to provide cognitive radio to HF systems. None of these works presented a real or simulated strategy based on the proposed modifications to ALE protocol. Nevertheless, (Shahid, Ahmad, Akram, & Khan, 2010) analysed how primary user detectors such as: energy detection, matched filter detection and cyclostationary feature detection could outperform the Listen Before Transmit (LBT) technique in ALE protocol for occupancy detection.

(Shukla, Jackson-Booth, & Arthur, 2012) also introduced how cognitive radio can improve HF communications by analysing the IEEE 802.22 standard for wireless regional area networks (Cordeiro et al., 2005). The QinetiQ HF policy box was introduced in (Shukla et al., 2012) as a system that could derive user policies of optimum frequency and best waveform for the current and future statistical ionospheric conditions. The authors indicated which were the required capabilities or functions that should be considered in a future version of their policy box in order to add cognition to the HF user. No evidence on how these modifications must be applied was provided in (Shukla et al., 2012).

The relevance of machine learning to fulfil cognitive radio requirements has been highlighted throughout this Chapter. However, there is little work on the application of machine learning for cognitive radio in HF communications. A model of activity prediction in terms of congestion suffered by HF broadcast users was proposed in (Haralambous & Papadopoulos, 2009). The model was developed with artificial neural networks and trained with real measurements of the HF band. Besides this work, ionospheric propagation characteristics have been widely modelled with machine learning techniques as in (Altinay, Tulunay, & Tulunay, 1997) and (Chu & Conn, 1999).

Chapter

3

HF Spectrum Activity Database

Wideband power measurements of the HF band have been acquired during the development of this Thesis to test and evaluate the proposed cognitive techniques for the HF environment. The acquisition setup was located at IDeTIC facilities in Las Palmas de Gran Canaria and it is shown in Figure 3.1. A wideband transceiver previously built in the research group where this Thesis has been developed (Pérez-Díaz et al., 2009) has been used followed by a Vector Signal Analyzer (VSA) (Agilent Technologies, 2010b) and SystemVue Software (Agilent Technologies, 2010a), both from Agilent Technologies (currently Keysight Technologies), to collect the time data from the Yagi antenna and convert it into frequency data (spectrum) by means of the Fast Fourier Transform (FFT) with the required characteristics. Several parameters, such as span, resolution bandwidth and number of bins for the FFT, must be adjusted while a suitable balance between them has to be observed to obtain the desired spectrum information.

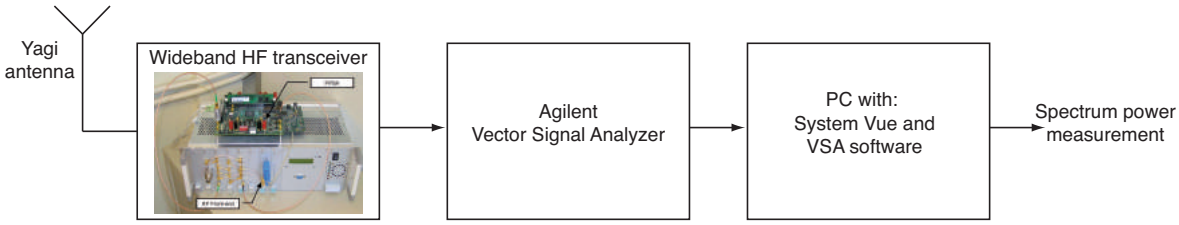

FIGURE 3.1. Measurement acquisition setup located at IDeTIC facilities in Las Palmas de Gran Canaria, Spain.

3.1 Wideband HF transceiver

Since the sensitivity of the VSA was not high enough and could not be used to reliably identify most of the HF signals in the band, the wideband HF transceiver designed in (Pérez-Díaz et al., 2009) was required in the measurement system to collect data from the antenna which was then sent onto the Vector Signal Analyzer, as shown in Figure 3.1. This digital transceiver has 1 MHz bandwidth and it was designed for the HF band (3-30 MHz). Despite its bandwidth, it was not meant for the transmission of a single wideband signal but to establish flexible multichannel communications by using narrowband modulations (Pérez-Díaz et al., 2009).

A photograph of this transceiver is shown in Figure 3.2, which consists of a radio frequency (RF) front-end and a field-programmable gate array (FPGA) that executes the digital part (Pérez-Díaz et al., 2009). The wideband RF front-end has a double-conversion superheterodyne (Puvaneswari & Sidek, 2004) architecture. As detailed in the receiver block diagram in Figure 3.3, the signal at the antenna is filtered in the HF band (3-30 MHz) to be then amplified. There are two conversion stages, the first mixer moves the filtered RF band to the first intermediate frequency (IF). At this IF, the signal is amplified and moved to the second IF frequency, where it is filtered and amplified again before its digitalisation with an analog-to-digital converter (ADC). At this point, the signal is amplified according to the Automatic Gain Control (AGC) because it has to be adapted to the dynamic range of the ADC.

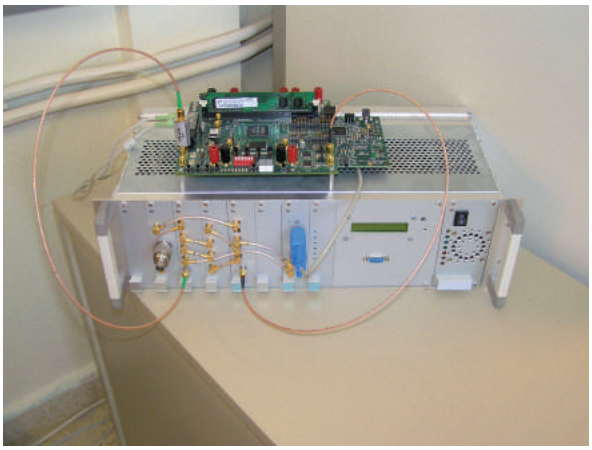

FIGURE 3.2. Wideband HF transceiver (Pérez-Díaz et al., 2009)

The same architecture of double-conversion syperheterodyne is used in the transmitter, as detailed in the transmitter block diagram in Figure 3.4. After its digital-to-analog conversion, the baseband signal is filtered, amplified if necessary, and moved from the first IF to the second IF. Then, it is again filtered and moved to the RF frequency range (3-30 MHz) by using the output mixer. Finally, the RF signal is amplified according to the automatic level control that keeps a constant power level at the output to prevent the power amplifier from working outside its dynamic range.

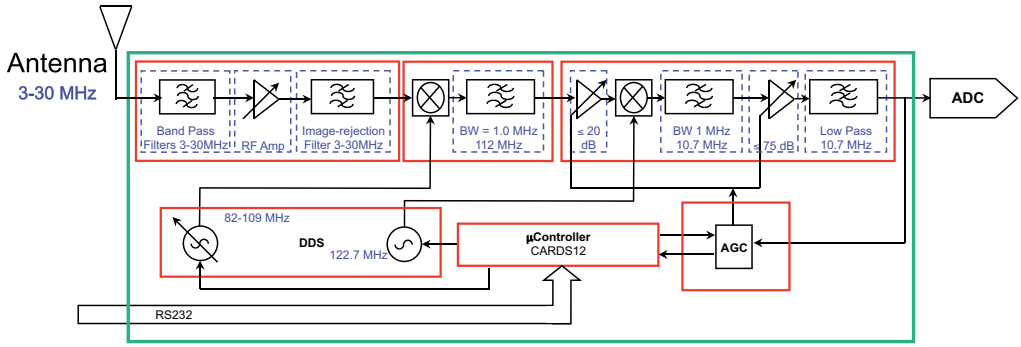

FIGURE 3.3. Receiver block diagram of the wideband HF transceiver (Pérez-Díaz et al., 2009).

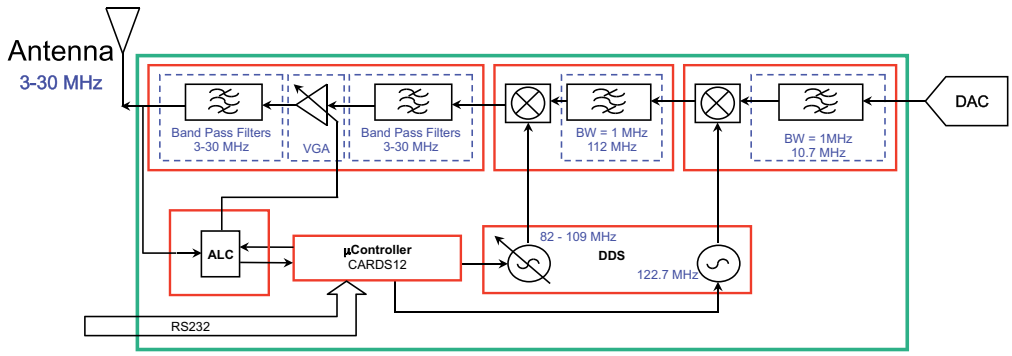

FIGURE 3.4. Transmitter block diagram of the wideband HF transceiver (Pérez-Díaz et al., 2009).

The digital part of this transceiver compromises a multichannel Digital Down Converter (DDC) and, inversely, a multichannel Digital Up Converter (DUC), which are implemented in an FPGA (Pérez-Díaz et al., 2009). The DDC translates the selected frequency band to baseband and downsamples the digitalised signal, whereas the DUC executes the inverse process.

In the acquisition setup for wideband HF measurements depicted in Figure 3.1, the input signal at the VSA is the filtered signal at the second IF of the wideband HF receiver, i.e. the analog signal before its digitalisation. This signal has been already modified by the AGC to fit into the dynamic range of the ADC, therefore, it can show the effect of narrowband interference (NBI) as it will be thoroughly detailed in Chapter 4.

3.2 Measurement campaign

Sequential measurements of the 14 MHz, 21 MHz and 28 MHz amateur bands were carried out during several days, which are specified in Table 3.1 and Table 3.2. These spectrum power measurements were collected in sample batches with a duration of nine or ten minutes, separated by intervals of ten or fifteen minutes. Additionally, the time resolution was defined in samples of approximately two seconds long.

The analysis has been restricted to these bands and mainly focused on the 14 MHz amateur band due to the limited bandwidth and receiving characteristics of the antennas.

Nevertheless, the high activity and the presence of all kinds of transmissions, both data and voice, observed within these bands seemed to be a remarkable scenario to test and validate the proposed cognitive techniques in this Thesis.

TABLE 3.1. Measurement campaign of the 14 MHz band.

Date	Bandwidth	Amateur Radio Contest
3 June 2011	640 kHz	– (Acquired on weekday)
10 June 2011	640 kHz	– (Acquired on weekday)
24 September 2011	640 kHz	First Greek Telegraphy Club CW Cup
23-24 June 2012	640 kHz	ARRL Field Day 2012
14-15 July 2012	1.28 MHz	IARU HF World Championship 2012
25-26 May 2013	640 kHz	CQ World Wide WPX CW Contest 2013
22-23 June 2013	640 kHz	ARRL Field Day 2013
13-14 July 2013	640 kHz	IARU HF World Championship 2013
23-24 November 2013	640 kHz	CQ World Wide DX CW Contest 2013
15 February 2014	640 kHz	ARRL Int. DX CW Contest 2014
1-2 March 2014	640 kHz	ARRL Int. DX Phone Contest 2014
28-29 June 2014	640 kHz	ARRL Field Day 2014
12-13 July 2014	640 kHz	IARU HF World Championship 2014
25-26 October 2014	640 kHz	CQ World Wide DX SSB Contest 2014
21-22 February 2015	640 kHz	ARRL Int. DX CW Contest 2015
27-28 June 2015	640 kHz	ARRL Int. DX Phone Contest 2015
11-12 July 2015	640 kHz	IARU HF World Championship 2015

As shown in Table 3.1 and Table 3.2, several amateur radio contests have been recorded during the measurement campaigns. This is due to the fact that, depending on the day, amateur bands have different degrees of activity: there is normal activity on weekdays, while a huge amount of activity can be found at weekends, especially in those when amateur radio contests are scheduled. Thus, by recording amateur radio contests, the database can include different transmission patterns in a tough scenario.

From the whole set of acquired measurements, two different subsets of measurements of the 14 MHz amateur band in Table 3.1 have been used in the following chap-

TABLE 3.2. Measurement campaigns of other amateur HF bands: 21 MHz and 28 MHz.

Date	Bandwidth	Band	Amateur Radio Contest
16-17 February 2013	640 kHz	21 MHz	ARRL Int. DX CW Contest 2013
14-15 December 2013	1.28 MHz	28 MHz	ARRL 10 m Contest 2013
13-14 December 2014	1.28 MHz	28 MHz	ARRL 10 m Contest 2014

ters of this Thesis. These databases have been named as HFSA_IDeTIC_F1_V01 and HFSA_IDeTIC_F1_V02, where HFSA stands for *HF Spectrum Activity*, IDeTIC stands for *Instituto Universitario para el Desarrollo Tecnológico y la Innovación en Comunicaciones*, the research institute where this Thesis was developed, F1 refers to the acquisition system in the frequency domain used (VSA), and V01 and V02 stand for the version of the database.

The 14 MHz amateur band is in frequencies from 14000 kHz to 14350 kHz and it is divided into three sub-bands:

- 14000 kHz - 14065 kHz: CW signals.
- 14065 kHz - 14100 kHz: Digital modulations such as PSK31 or 2-FSK.
- 14100 kHz - 14350 kHz: SSB analog modulations.

In order to acquire spectral information from the whole band, the selected central frequency was 14175 kHz with a span of 500 kHz or 1 MHz, though the collected bandwidth by VSA was actually wider than the specified span, 640 kHz and 1.28 MHz, respectively. With these parameters, measurements of the amateur band and also channels outside of it that correspond to other radio stations were obtained. Given that all kinds of transmissions and activities take place in the acquired bandwidth, the 14 MHz band measurements are fairly representative of the main activities and transmissions that can be found in the whole HF band.

The collected measurements of the 21 MHz amateur band had 21225 kHz as central frequency and 640 kHz bandwidth. These measurements included the activity of this amateur band, which is in frequencies from 21000 kHz to 21450 kHz:

- 21000 kHz - 21070 kHz: CW signals.
- 21070 kHz - 21150 kHz: Digital modulations.
- 21150 kHz - 21450 kHz: SSB analog modulations.

Finally, the measurements of the 28 MHz amateur band had 28500 kHz as central frequency and 1.28 MHz bandwidth. This amateur band is in frequencies from 28000 kHz to 29700 kHz and it is mainly divided into:

- 28000 kHz - 28070 kHz: CW signals.
- 28070 kHz - 28190 kHz: Digital modulations.
- 28225 kHz - 29700 kHz: SSB analog modulations.

3.3 HFSA_IDeTIC_F1_V01 database

A selection of the acquired measurements of the 14 MHz amateur band is included in the HFSA_IDeTIC_F1_V01 database and specified in Table 3.3. These are wideband measurements of 640 kHz bandwidth each, which represents more than 200 HF channels of 3 kHz bandwidth during nine or ten minutes. In this database, 49 measurements were acquired on weekdays as the example shown in Figure 3.5 whereas 14 of them were acquired during an amateur radio contest as the example shown in Figure 3.6.

TABLE 3.3. Selection of wideband HF measurements of the 14 MHz band included in the HFSA_IDeTIC_F1_V01 database.

Date	Bandwidth	Number of Measurements	Amateur Radio Contest
3 June 2011	640 kHz	20	– (Acquired on weekday)
10 June 2011	640 kHz	29	– (Acquired on weekday)
24 September 2011	640 kHz	14	First Greek Telegraphy Club CW Cup

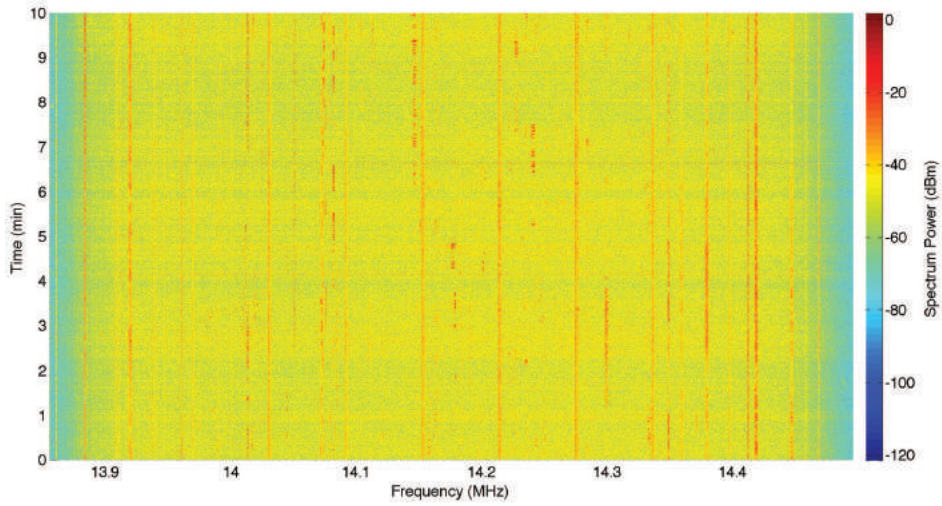

FIGURE 3.5. Example of the acquired HF spectrum of the 14 MHz band with central frequency 14175 kHz, span of 640 kHz and a duration of 10 minutes. Weekday - Normal activity scenario.

This database will be used in to train and validate the learning and decision making techniques proposed in Chapters 5, 6 and 7 of this Thesis. In order to do that, these

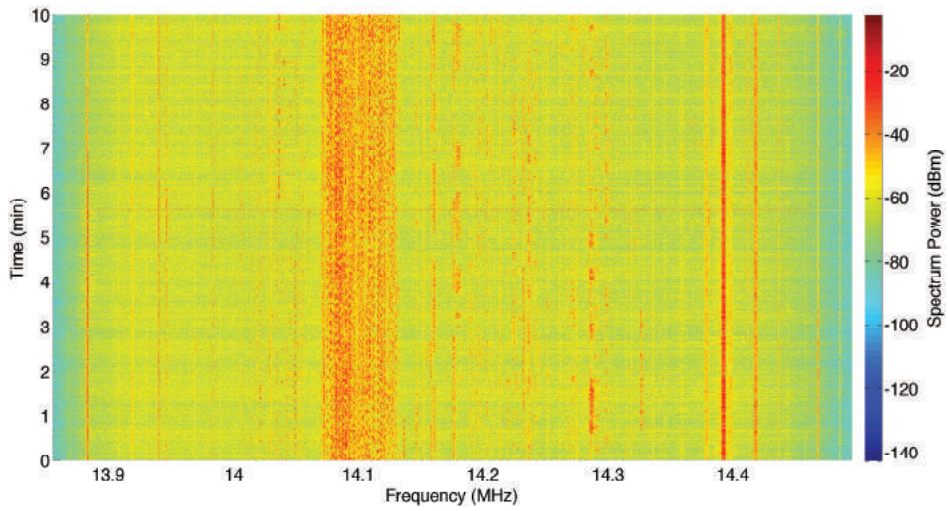

FIGURE 3.6. Example of the acquired HF spectrum of the 14 MHz band with central frequency 14175 kHz, span of 640 kHz and a duration of 10 minutes. Weekend - High activity scenario.

measurements will be segmented into shorter sequences, which will be classified according to the observed activity in the HF band into: *available*, *unavailable*, and *partially available*. The segmentation and classification of the measurements contained in the HFSA_IDeTIC_F1_V01 database is later detailed in Chapter 5.

3.4 HFSA_IDeTIC_F1_V02 database

The HFSA_IDeTIC_F1_V02 database is an extended version of the HFSA_IDeTIC_F1_V01 database. It includes the selection of acquired measurements specified in Table 3.4 with both 640 kHz and 1.28 MHz bandwidth. Since the effect of narrowband interference (NBI) was observed during the measurement campaign in June 2011 and June-July 2012, these measurements are included in this version and will be used in Chapter 4 to test the proposed solution for NBI detection. As it will be later explained in Chapter 4, the proposed NBI detector has a power wideband measurement as input, thus, neither the energy detection depicted in Section 3.5 nor the classification and segmentation tasks implemented for the HFSA_IDeTIC_F1_V01 database in Chapter 5 are required. An example of these measurements with the solely presence of NBI is shown in Figure 3.7.

3.5 Spectrum sensing via Energy detection

A solution based on active awareness is considered in this Thesis to observe the HF environment. Particularly, the proposed cognitive front-end will execute the spectrum sensing task by primary user detection. It has been observed from the acquired measurement databases that the HF band is a heterogeneous environment where different

TABLE 3.4. Selection of wideband HF measurements of the 14 MHz band included in the HFSA_IDeTIC_F1_V02 database.

Date	Bandwidth	Number of Measurements	Amateur Radio Contest
3 June 2011	640 kHz	20	– (Acquired on weekday)
10 June 2011	640 kHz	29	– (Acquired on weekday)
24 September 2011	640 kHz	14	First Greek Telegraphy Club CW Cup
23-24 June 2012	640 kHz	72	ARRL Field Day 2012
14-15 July 2012	1.28 MHz	72	IARU HF World Championship 2012

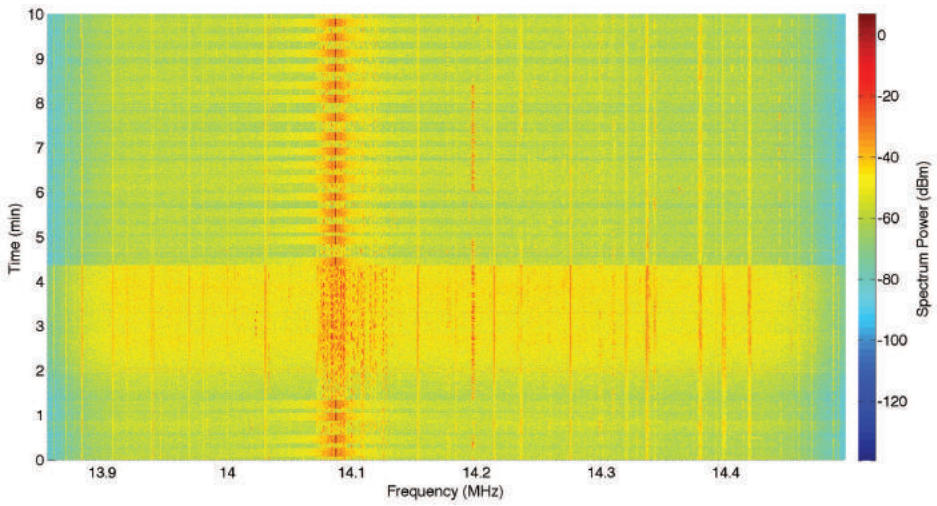

FIGURE 3.7. Example of the acquired HF spectrum of the 14 MHz band with central frequency 14175 kHz, span of 640 kHz and a duration of 10 minutes. High activity scenario with the presence of NBI.

transmission types and patterns can be observed. Since a secondary user in this environment does not have prior knowledge about licensed users' transmissions, the energy detector is the most appropriate sensing technique as previously detailed in Chapter 2 (see Section 2.2.1.1). In fact, energy detection is also suitable for wideband spectrum sensing, since simultaneous sensing of several bands can be realized by scanning the power spectral density (PSD) of the received wideband signal (Ma et al., 2009).

As depicted in Figure 3.8, the energy detector computes the mean power of the acquired signal in the frequency domain over a specific time interval. Afterwards, the signal detection is performed by comparing the signal's mean power with a threshold that depends on the noise floor (Urkowitz, 1967).

Once the VSA has captured the spectrum information by means of FFT, a pre-

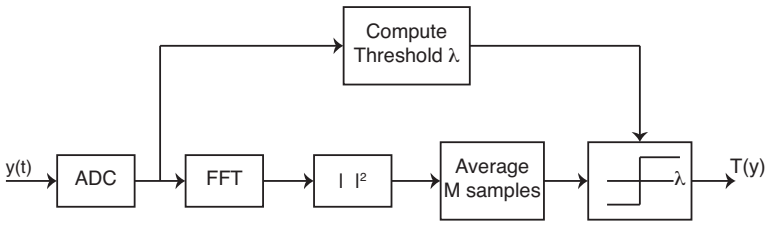

FIGURE 3.8. Implementation of an energy detector.

processing step is applied in the frequency domain to obtain samples representing a 3 kHz HF channel, i.e. the collected spectrum is uniformly divided into channels of 3 kHz bandwidth, and the mean power is computed for each channel. At this point, each sample of the processed measurements represents the mean power in a 3 kHz channel within a time slot of 2 seconds. Afterwards, the remaining steps of the energy detector are applied to each channel, the mean power of each channel is averaged over a time window of the previous 8 seconds in order to best characterise the time evolution of the transmissions and avoid samples which represent the nulls of the HF channel and the typical impulsive noise present in this band.

Finally, the signal detection problem is set out to transform the power samples into normalised values that will represent primary users' activity. For this purpose, two hypotheses were defined for the primary user detection in Equation (2.1), which are repeated here for a better readability:

$$H_0: \quad y[n] = w[n] \qquad n = 1, \cdots, N-1 \tag{3.1a}$$

$$H_1: \quad y[n] = s[n] + w[n] \qquad n = 1, \cdots, N-1 \tag{3.1b}$$

H_0 holds when there is only noise, $w[n]$, in the channel at sample n, while H_1 is true when there is a signal, $s[n]$, in the channel with additive noise at sample n.

The detector that maximises the detection probability for a given false alarm probability is defined through the likelihood ratio test formulated in (3.2) as specified by the Neyman-Pearson lemma (Kay, 1998):

$$L(\mathbf{y}) = \frac{p\left(\mathbf{y}; H_1\right)}{p\left(\mathbf{y}; H_0\right)} > \lambda \tag{3.2}$$

where $p\left(\mathbf{y}; H_1\right)$ is the probability distribution function for occupied-channel samples, $p\left(\mathbf{y}; H_0\right)$ the probability distribution for only-noise samples and the threshold λ of the detector is derived from the false alarm constraint

$$P_{FA} = \int_{\lambda}^{\infty} p\left(\mathbf{y}; H_0\right) d\mathbf{y} = \alpha. \tag{3.3}$$

The way to assess such a detector is to plot the Receiver Operating Characteristics (ROC) curve, which represents the detection probability (P_D) versus the false alarm probability (P_{FA}) for different thresholds λ. Given the constrained false alarm probability α,

the corresponding value of the threshold that maximises the detection probability can be found just by using the estimated ROC curve.

For the acquired measurements the probability distributions for both hypotheses, $p(\mathbf{y};H_0)$ and $p(\mathbf{y};H_1)$, are estimated by computing the normalised histogram of the power of only-noise samples and occupied-channel samples, respectively. These estimations are plotted in Figure 3.9 and as a result, threshold λ can be defined. Furthermore, in order to evaluate the ROC curve, the only-noise probability distribution has been fitted to a normal distribution $N(\mu_0,\sigma_0)$ with mean $\mu_0 = -58.82$, standard deviation $\sigma_0 = 3.23$ and probability density function

$$p(\mathbf{y};H_0) = \frac{1}{\sigma_0\sqrt{2\pi}} e^{-\frac{(y-\mu_0)^2}{2\sigma_0^2}}, \tag{3.4}$$

whereas the occupied-channel probability distribution has been fitted to a Generalised Extreme Value (GEV) distribution with location parameter $\mu = -47.125$, scale parameter $\sigma = 3.882$, shape parameter $\xi = -0.015$ and probability density function

$$p(\mathbf{y};H_1) = \frac{1}{\sigma}\left(1+\xi\frac{y-\mu}{\sigma}\right)^{-\frac{\xi+1}{\xi}} e^{-\left(1+\xi\frac{y-\mu}{\sigma}\right)^{-\frac{1}{\xi}}}. \tag{3.5}$$

As it can be observed in Figure 3.9, the estimated probability distribution for hypothesis H_1 can not be completely fitted to the proposed GEV distribution, but it is the best accurate fitting as it allows us to define the asymmetry of the estimated probability distribution from the acquired measurements. As opposed to the normal distribution, the GEV distribution can be used to fit data with non-zero skewness.

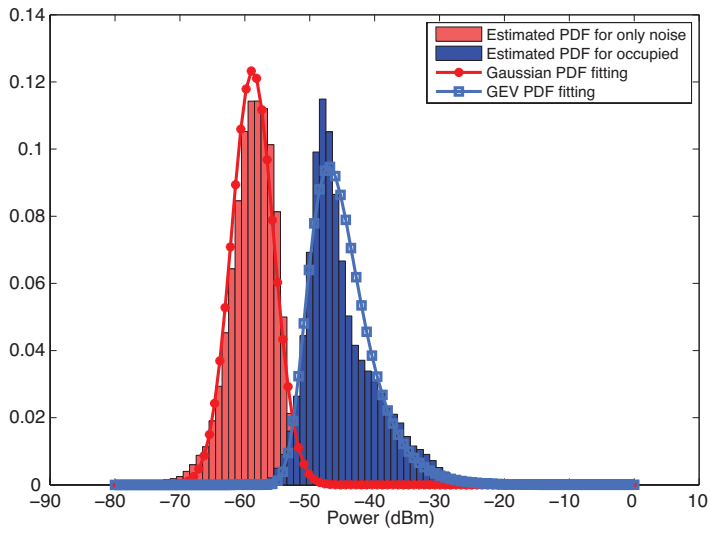

FIGURE 3.9. Estimation of the probability distribution of only noise-samples and occupied-channel samples and statistical fitting.

Once both distributions are fitted, the false alarm probability (P_{FA}) and the detection probability (P_D) are computed to represent the analytic ROC plotted in Figure 3.10 where

$$P_{FA} = \int_{\lambda}^{\infty} p(\mathbf{y};H_0)\,dy = \int_{\lambda}^{\infty} \frac{1}{\sigma_0\sqrt{2\pi}} e^{-\frac{(y-\mu_0)^2}{2\sigma_0^2}}\,dy = Q\left(\frac{\lambda-\mu_0}{\sigma_0}\right) \tag{3.6}$$

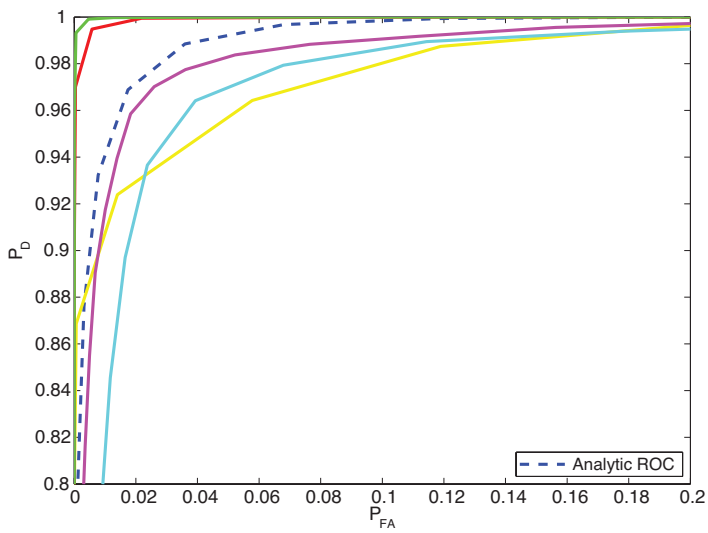

FIGURE 3.10. Receiver Operating Characteristics (ROC)

$$
\begin{aligned}
P_D &= \int_{\lambda}^{\infty} p\left(\mathbf{y}; H_1\right) dy = \\
&= \int_{\lambda}^{\infty} \frac{1}{\sigma}\left(1+\xi\frac{y-\mu}{\sigma}\right)^{-\frac{\xi+1}{\xi}} e^{-\left(1+\xi\frac{y-\mu}{\sigma}\right)^{-\frac{1}{\xi}}} dy = 1-e^{-\left(1+\xi\frac{\lambda-\mu}{\sigma}\right)^{-\frac{1}{\xi}}}
\end{aligned}
\tag{3.7}
$$

and λ is the detection threshold.

As it can be observed in Figure 3.10, the analytic ROC could represent the mean behaviour of the acquired measurements as some experimental ROC curves are above the analytic ROC whereas others are below it.

3.6 Summary

This Chapter introduces the characteristics of the acquired wideband measurements of the HF band during the development of this Thesis. A selection of measurements of the 14 MHz band has been included in the HFSA_IDeTIC_F1_V01 database. These measurements have 640 kHz bandwidth, a duration of nine or ten minutes, and samples that represent the mean power in a 3 kHz HF channel for 2 seconds. An extended version of this database, named to as HFSA_IDeTIC_F1_V02, includes new measurements where the effect of NBI was observed during their acquisition. This extended version also includes measurements with 1.28 MHz bandwidth, taking advantage of the previously developed wideband HF transceiver in the research group (Pérez-Díaz et al., 2009). Both databases are available for the research community.

Due to the heterogeneity observed in the HF band, an energy detector has been proposed and designed to perform the spectrum sensing task. By computing the likelihood ratio test specified by the Neyman-Pearson lemma (Kay, 1998), it has been designed as the detector that maximises the detection probability for a given false alarm probability.

After the execution of the designed energy detector, power measurements of each 3 kHz HF channel are translated into binary observation sequences that represent primary users' activity in each channel.

Chapter

4

Narrowband Interference Detection: A Solution based on Compressive Sensing

HF communications are widely established with single-channel receivers of 3 kHz bandwidth (Maslin, 1987). However, wideband transceivers have been recently specified in MIL-STD-188-110C to increase the achievable data rates. Besides this improvement, multi-channel communication strategies can be applied with these wideband receivers to make a more efficient use of the HF band. Among them, the application of cognitive radio principles (Haykin, 2005) is proposed in this Thesis, due to the fact that HF stations can be endowed with adaptability and cognition to better exploit the spectrum resources.

The use of wideband receivers, which can be extremely helpful for cognitive radios, entails new challenges such as the effect of narrowband interference (NBI). This is because the HF environment promotes the propagation of high-powered surface waves, transmitted within a radius of tens of kilometres from the receiver (Maslin, 1987), which significantly affect the performance of wideband HF receivers, since the wideband signal's amplitude must be adapted to the dynamic range of the Analog to Digital Converter (ADC) (Pérez-Díaz et al., 2012). In other words, the presence of NBI in the received wideband signal causes a reduction in the effective number of bits used for the digitalization of the signals of interest and thus, the quantization noise exceeds the thermal noise and the desired signal itself (Pérez-Díaz et al., 2012). Providing a method to detect these harmful interfering transmissions in the analog domain is critical since, once their frequency location is known, they can be mitigated in the analog domain, before the digital front-end. By doing this, an increase in the effective number of bits used to digitize the desired signals at the ADC of the wideband receiver could be achieved, thus, resulting in a higher signal to noise ratio (SNR). Moreover, the acquired knowledge of their frequency location could also be used to improve dynamic spectrum access protocols that are implemented in cognitive radio systems (Fette, 2009).

In fact, the development of interference mitigation techniques in all the frequency bands is one of the innovations in the *Top 10 Most Wanted Innovations* defined by the Wireless Innovation Forum (Wireless Innovation Forum, 2012), formerly the SDR (Software-Defined Radio) Forum. This corporation of commercial, defence and civil government organizations has stated that 'better mechanisms are needed to reduce destructive interference on the communications signal, and thus improve the signal's quality of service and/or communications range'.

Based on the above, two steps are required to reduce the destructive effect of NBI on wideband receivers: detection and mitigation. Several solutions have been proposed for NBI detection and mitigation in HF systems, mostly HF radars (G. Chen, Zhao, Zhu, Huang, & Li, 2010; Kanterakis & Bruno, 1994). These solutions are based on NBI cancellation with wideband signals such as Direct Sequence - Spread Spectrum (DS-SS) in (Kanterakis & Bruno, 1994) as desired signals. Further work has focussed on the mitigation of NBI via Compressive Sensing (CS) schemes in (Davenport, Boufounos, & Baraniuk, 2009), (Davenport et al., 2010) and (Hwang, Jang, Kim, & Seo, 2010). In these works, NBI is cancelled by applying a projection matrix after applying CS to the received signal. In order to do that, the frequency location of NBI is assumed to be known and a low-rate ADC is used. Finally, another proposal to avoid strong NBI in a ultra-wideband (UWB) system with low-rate ADCs is presented in (F. Wang & Tian, 2008).

In this Thesis, a low-complexity solution is proposed for the detection of NBI based on CS. The considered NBI detector will be used in parallel with a wideband receiver executing the spectrum sensing task for a cognitive radio application in the HF band. Therefore, the main goal of the proposed scheme is to efficiently detect NBI while the cognitive radio is simultaneously monitoring multiple HF channels to observe primary users' activity. Nevertheless, the proposed design can also be implemented in wideband receivers of any frequency band where NBI mitigation is required.

Furthermore, its performance is validated with the HFSA_IDeTIC_F1_V02 database of real wideband measurements. As previously detailed in Chapter 3, these measurements are composed by multiple narrowband transmissions, where both desired and interfering signals are narrowband signals. Due to this fact, previous solutions for HF radars (G. Chen et al., 2010; Kanterakis & Bruno, 1994) and the solution based on low-rate ADCs proposed in (F. Wang & Tian, 2008) cannot be applied to this real scenario since they were designed for schemes where desired signals were wideband signals such as direct sequence - spread spectrum or ultra wideband signals. Furthermore, the proposal of (G. Chen et al., 2010) has not been designed to cope with the effect of strong NBI at the input of the ADC, as it includes the detection phase in the digital domain. Thus, the performance of the scheme developed in (G. Chen et al., 2010) is only guaranteed when the interference power is low enough to ensure an accurate digitization of the desired signals. Finally, the CS-schemes presented in (Davenport et al., 2009), (Davenport et al., 2010), and (Hwang et al., 2010), assume that the frequency location of NBI is known. In contrast, in this Thesis a realistic assumption is considered, i.e. both the number and

the frequency location of the interferers are unknown. This automatically entails that the cancellation via projection matrices employed in (Davenport et al., 2009), (Davenport et al., 2010) and (Hwang et al., 2010) cannot be applied, since the prior knowledge of the above-mentioned data is required for a successful detection in these schemes.

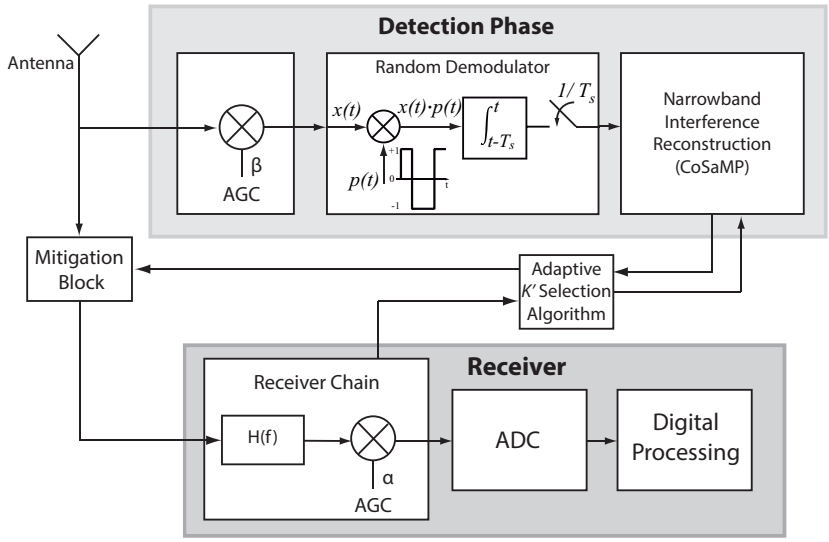

FIGURE 4.1. Architecture of a wideband receiver with the proposed compressive NBI detector.

The proposed detection scheme is referred to as detection phase in Figure 4.1 and the components that comprise it and their behaviour will be described in Section 4.3. The detection phase is a parallel analog system to the receiver before its digitalization phase as shown in Figure 4.1. This ensures that the strong interfering signals that affect the performance of the wideband HF receiver are accurately detected and mitigated in the analog domain, which ensures that a sufficient number of bits are dedicated to digitize desired transmissions. For this, the NBI detector self-adapts its configuration to detect a number of narrowband interfering signals guided by the status of the Automatic Gain Control (AGC). This strategy allows a premature detection of NBI with a low complexity so that a wideband signal without harmful narrowband transmissions is provided to the digital receiver after the mitigation phase.

The low complexity offered by the proposed scheme is a consequence of the application of CS principles to NBI detection. Nowadays, ADCs are pushed to their limits when working with wideband signals in order to fulfil the Nyquist theorem (Tropp, Laska, Duarte, Romberg, & Baraniuk, 2010). However, CS techniques are applied to signals that contain a little amount of information when being represented in a certain domain (Candès, 2006; Donoho, 2006), known as sparse, and the CS theory takes advantage of their properties to digitize them at a lower rate than the specified by the Nyquist theorem, hence promoting the use of low-rate ADCs. This is the particular case of the HF band because the Fourier spectrum of the acquired wideband signal is comprised by several narrowband signals with significant spectrum holes between them.

In the proposed NBI detector, the low-rate ADC is based on a CS system that is able to digitize wideband analog signals with low-rate ADCs: the random demodulator (RD)

(Tropp et al., 2010). As previously stated, the detector's practical feasibility has been validated with real wideband measurements of the HF band. Furthermore, the RD's performance in real scenarios has been evaluated, and the characterization of its behaviour in real scenarios compared against the theoretical study with a controlled environment presented in (Tropp et al., 2010).

The contents of this Chapter are divided as follows: the effect of NBI on wideband receivers is depicted in Section 4.1. Section 4.2 includes a description of CS background. Afterwards, the design of the proposed compressive NBI detector is described in Section 4.3. Finally, the performance of the proposed NBI detector in the HF environment and the characterization of the RD in a real scenario are described in Section 4.4.

4.1 NBI Effect on Wideband Receivers

The behaviour of the proposed NBI detector in this Thesis is based on the AGC response of the wideband HF receiver developed in (Pérez-Díaz et al., 2009). For completeness, the response of the AGC of this wideband HF receiver is depicted versus the input power in terms of inverse gain in Figure 4.2. The main goal of the AGC is to adapt its input power to a desired output power related to the dynamic range of the ADC of the wideband receiver. When the power of the input signal is very small, named as *Low-powered input signal* in Figure 4.2, the AGC gain has its maximum value until the input power reaches the P_L threshold, which is the beginning of the *AGC working range*. From P_L, as the input power increases, the AGC gain decreases until it reaches its minimum value and the input power reaches the P_H threshold. From this input power threshold, named as *Saturated AGC* in Figure 4.2, the output signal of the AGC cannot be adapted to the dynamic range of the ADC and a clipping effect occurs in the signal conversion from analog to digital, hence degrading the final performance of the wideband receiver. This undesired operating condition is usually provoked by the appearance of strong NBI and detecting its appearance is the main focus of the proposed NBI detector in this Chapter.

Figure 4.3 illustrates how the presence of NBI affects to the whole wideband received signal both in the frequency (Figure 4.3 (a) and Figure 4.3 (b)) and time (Figure 4.3 (c) and Figure 4.3 (d)) domains. The amplitude of these wideband signals in the time domain has been normalised to represent the AGC accommodation to the dynamic range of the ADC. In Figure 4.3 (b), there is a low-frequency NBI with a received power of 25 dB over the rest of narrowband signals. Figure 4.3 (d) shows that, when compared to Figure 4.3 (c), narrowband signals, including desired signals, are completely masked by NBI. This entails that only a few bits would be used to digitize the intended signals, hence preventing a correct detection with the required SNR. Based on the above, it is clear that the mitigation of NBI must be held in the analog domain to ensure that desired signals are digitized with enough bits to perform a correct detection. This is due to the fact that, once the wideband signal with NBI is digitized, the SNR of the desired signals

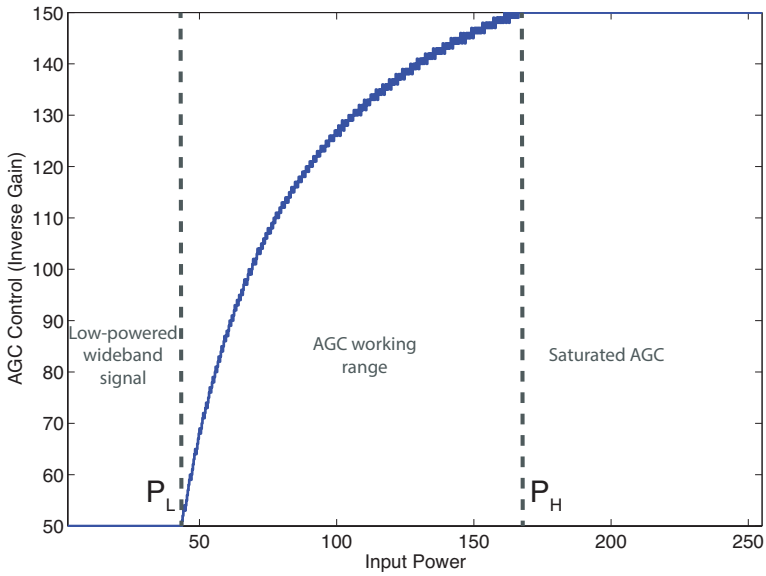

FIGURE 4.2. Inverse AGC gain of the wideband HF transceiver.

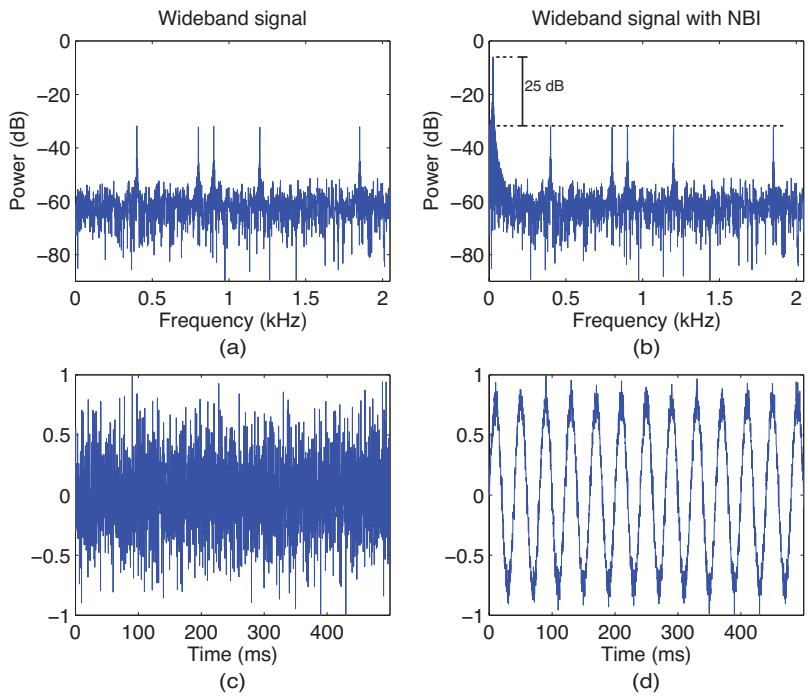

FIGURE 4.3. An example of a wideband signal with and without NBI.

is reduced to the dynamic range of the ADC due to the AGC adaptation. At this point of the reception chain, the effective SNR of the desired signals cannot be increased when its power is comparable to the quantification noise since only a few bits have been used for their digitization.

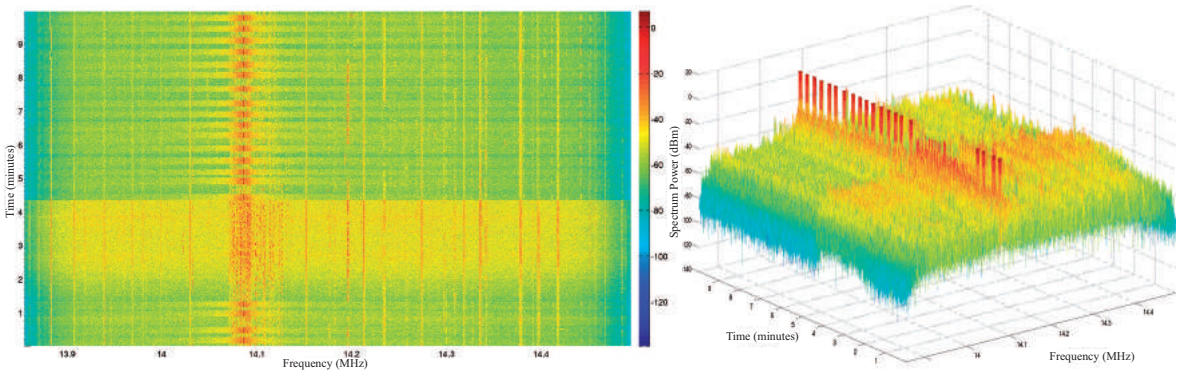

FIGURE 4.4. Example of an acquisition of a 600 kHz bandwidth spectrum (200 standard 3 kHz channels) around 14 MHz during 10 minutes with an intermittent strong NBI in 14.09 MHz.

A real example of the NBI effect on a wideband HF receiver is shown in Figure 4.4. This figure represents a real spectrum acquired during a period of ten minutes with the wideband HF receiver developed in (Pérez-Díaz et al., 2009) and contained in the HFSA_IDeTIC_F1_V02 database. It can be observed that there is an intermittent interfering signal around 14.1 MHz whose power level is 40 dB over the rest of narrowband transmissions. Its existence induces the adaptation of the entire signal to the dynamic range of the ADC by attenuating all the components at its input. As a consequence, desired signals and others transmissions are attenuated below the noise floor and cannot be detected.

4.2 Compressive Sensing Background

Compressive Sensing (CS) has established a new approach to the acquisition of wideband signals by allowing the use of ADCs with a sampling rate much lower than the Nyquist rate (Candès, 2006; Donoho, 2006). Formally, the measurements $\mathbf{y} \in \mathbb{R}^M$ in the CS acquisition procedure can be expressed as

$$\mathbf{y} = \mathbf{\Phi}\mathbf{x} + \mathbf{e} = \mathbf{\Phi}\mathbf{\Psi}\mathbf{s} + \mathbf{e}, \tag{4.1}$$

where $\mathbf{x} \in \mathbb{R}^N$ represents the Nyquist-rate samples of the time signal over a specific time window, $\mathbf{\Phi}$ is a $M \times N$ matrix often referred to as measurement matrix, $\mathbf{e} \in \mathbb{R}^M$ is a measurement error term, $\mathbf{\Psi}$ is an orthonormal basis matrix, and $\mathbf{s}$ contains the coefficients of the signal in the compressive domain. In particular, CS focuses on scenarios where the number of acquired measurements is much smaller than the number of samples specified by the Nyquist theorem, i.e., $M \ll N$. The CS theory focuses on signals $\mathbf{s}$ where only a few coefficients in the basis $\mathbf{\Psi}$ contain the signal's energy while the rest of them are

zero. In this context, $\mathbf{s}$ is defined as a K-sparse signal if it has K coefficients different from zero (Candès, 2006; Donoho, 2006). In practice, a few coefficients of the signal in the basis $\mathbf{\Psi}$ contain most of the signal's energy whereas the rest contain a residual part. For instance, the Fourier spectrum of wideband scenarios is usually composed by narrowband transmissions with spectrum holes between them, therefore making possible its approximation by a sparse signal with $\mathbf{\Psi}$ being the Fourier basis $\mathbf{F}$. This is the case of HF communications, where some narrowband users are usually active whereas the rest of bands are generally unused as shown in Figures 3.5 and 3.6.

Furthermore, the acquisition of measurements in a CS system must ensure that the information of the original signal is not damaged by the inherent dimensionality reduction (Candès, 2006). For this, the *Restricted Isometry Property* (RIP) (Candès & Tao, 2005) determines whether these recovery guarantees are fulfilled or not for any measurement system characterized by a system matrix $\mathbf{A} = \mathbf{\Phi\Psi}$. The RIP of order K is defined for a system matrix $\mathbf{A}$ and for any K-sparse signal $\mathbf{s}$ as (Candès & Tao, 2005)

$$(1-\delta_K)\|\mathbf{s}\|_{l_2}^2 \leq \|\mathbf{As}\|_{l_2}^2 \leq (1+\delta_K)\|\mathbf{s}\|_{l_2}^2, \tag{4.2}$$

where $\|\cdot\|_{l_2}$ denotes the Euclidean norm and the constant $\delta_K \in (0,1)$ determines how much energy of the original signal is preserved in the measurement process (Candès & Tao, 2005). In the ideal case, all the energy of the original signal should be conserved, i.e. $\delta_K = 0$, and no loss of information should occur, hence enabling an accurate signal reconstruction in spite of the solely availability of low-dimensionality measurements. However, it is common to assert that a measurement system satisfies the RIP if the constant δ_K is not too far from zero (Candès & Tao, 2005).

Once the undersampled measurements, $\mathbf{y}$, have been acquired satisfying (4.2), the remaining step is to recover the original signal $\mathbf{s} \in \mathbb{R}^N$. As stated in (Candès, Romberg, & Tao, 2006), an accurate reconstruction can be obtained by solving

$$\begin{aligned} \underset{\mathbf{s}\in\Re^N}{\text{minimize}} \quad & \|\mathbf{s}\|_{l_1} \\ \text{subject to} \quad & \|\mathbf{As}-\mathbf{y}\|_{l_2} \leq \epsilon \end{aligned} \tag{4.3}$$

provided that $\delta_{2K} < \sqrt{2}-1$. Here, $\|\mathbf{s}\|_{l_1}$ refers to the standard l_1 norm and the constant ϵ limits the measurement noise $\|e\|_{l_2} \leq \epsilon$.

From the discrete theory introduced above, the problem of acquiring continuous time signals with CS techniques can be divided into two main parts: the one that deals with the problem of ensuring that most of the information is preserved even though a low-rate ADC is used, and another one which is concerned about how to reconstruct the digitized version of the original signal, $\mathbf{x}$, or its sparse representation, $\mathbf{s}$, from just $M \ll N$ samples (Candès, 2006).

4.3 NBI Detector based on Compressive Sensing

As previously stated in Section 4.1, the presence of NBI in the acquisition bandwidth of wideband receivers degrades their performance, which makes the receiver blind to receive desired transmissions (Pérez-Díaz et al., 2012). To solve this problem, the addition of a compressive NBI detector to wideband receivers is proposed in this Thesis. This structure is referred to as detection phase in Figure 4.1 and it aims at identifying the frequency locations of the most harmful signals within the acquisition bandwidth so that they can be mitigated before the input of the ADC.

In the proposed design depicted in Figure 4.1 in Page 49, the signal from the antenna is split into two paths to the detection phase and to the mitigation block placed before the wideband receiver side. The received wideband signal from the antenna, which contains the harmful interfering signals, is the input of the detection phase, whose structure is divided into two steps: the signal acquisition with a lower rate than Nyquist rate but satisfying the RIP (4.2), and its reconstruction (4.3). In this case, the signal is acquired with a random demodulator (Tropp et al., 2010) that digitizes it by using a low-rate ADC and then reconstructed with the Compressive Sampling Matching Pursuit (CoSaMP) algorithm (Needell & Tropp, 2009). The CoSaMP algorithm extracts the location in the frequency domain of the strongest narrowband transmissions in the band. What is more, an approximation of the amplitude and phase of these harmful signals can also be obtained if desired. NBI frequency locations obtained by the CoSaMP algorithm are then provided to the mitigation block to apply cancellation techniques to guarantee that the performance of the wideband receiver is not affected by the presence of NBI. During this process, it is assumed that the transceiver knows where its communication links are being held so that desired signals are not mitigated.

It is important to remark here that the proposed system is adapted according to the status of the AGC of the wideband receiver, i.e. whether the input of the receiver is saturated or not. If the received signal cannot be processed because the input power at the AGC is higher than P_H, the mitigation block is driven by the output of CoSaMP to attenuate detected NBI. This allows the wideband receiver to receive the signal without NBI and operate normally. Otherwise, if the power of the received signal is within AGC working range, no action is taken by the mitigation block.

First, the attention is focussed on the signal acquisition employed. The choice of the random demodulator (RD) is supported by the intention of reducing the hardware burden to a minimum (Tropp et al., 2010). Specifically, the RD is a single-channel measurement system that satisfies the RIP provided that a minimum number of samples are acquired (Tropp et al., 2010). Hence, the main advantage of using this scheme with regard to a traditional wideband acquisition system is that the total hardware cost is reduced: no expensive high-rate ADCs are required, since the sampling rate is lowered.

The RD's block diagram is depicted in Figure 4.5. It is composed by a random ±1

source ($p(t)$), a mixer, and a traditional integrate-and-dump ADC (Tropp et al., 2010). The effect of the RD on the frequency-sparse input $x(t)$ starts by mixing this signal with the chipping sequence $p(t)$. This square signal is independent of the input and it alternates between ± 1 amplitude levels at the Nyquist rate $f_{\text{NYQ}} = 1/T_{\text{NYQ}}$. Then, the output of the mixer confronts an integrator (low-pass filter) which is reset each time a new sample is acquired. Finally, the resulting signal faces a subsampling stage with a low-rate ADC that produces a new sample each $T_s > T_{\text{NYQ}}$ seconds.

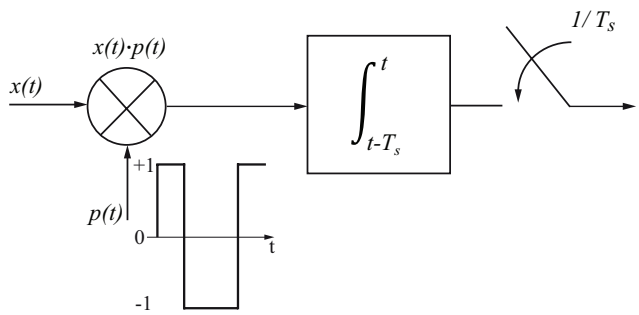

FIGURE 4.5. Block diagram of the random demodulator (RD).

The effect of this sampling system on a discrete-time setting over the equivalent Nyquist-rate samples of the input signal can be modelled by the measurement matrix $\mathbf{\Phi}$ (Tropp et al., 2010). Basically, this matrix describes the acquisition procedure of the analog hardware, therefore allowing the use of an equivalent discrete model to reproduce the result at its output. The entries of the measurement matrix depend on two factors: the chipping sequence and the chosen sampling rate $1/T_s$. In general, the measurement matrix of the RD has the following structure

$$\mathbf{\Phi} = \begin{bmatrix} p[1] & \cdots & p[P] & 0 & 0 & 0 & 0 & 0 & 0 \\ 0 & 0 & 0 & p[P+1] & \cdots & p[2P] & 0 & 0 & 0 \\ 0 & 0 & 0 & 0 & 0 & 0 & p[2P+1] & \cdots & p[3P] \end{bmatrix}, \tag{4.4}$$

where $p[n]$ represents the Nyquist-rate samples of the chipping sequence and P is the number of samples in each row of the equivalent measurement matrix. In general, P depends on the relationship between the Nyquist rate and the selected sampling rate (Tropp et al., 2010). For instance, if the Nyquist rate f_{NYQ} is an integer multiple of the sampling rate $f_s = 1/T_s$, then the number of samples of $p[n]$ in each row is $P = f_{\text{NYQ}}/f_s$. Non-integer relationships can also be described by adding non-unit normed coefficients in each row (Tropp et al., 2010).

After the received wideband signal has been undersampled, the last process of the proposed scheme consists in accurately detecting the strong interfering signals that might be harming the receiver's performance as shown in Figure 4.1. In order to reconstruct the input signal of the detector, the optimization problem (4.3) has to be solved. Since solving this convex problem is computationally intensive, faster alternatives such as greedy algorithms are often used instead (Needell, Tropp, & Vershynin, 2008). These algorithms go through an iterative process which adds new frequency components to reduce the approximation error in each iteration, i.e., the largest Fourier coefficients are iteratively recov-

ered. Several greedy alternatives that are able to achieve identical reconstruction guarantees as convex algorithms have been proposed: Orthogonal Matching Pursuit (OMP) (Tropp & Gilbert, 2007), tree-based OMP (La & Do, 2006), Regularized OMP (Needell & Vershynin, 2009) or Compressive Sampling Matching Pursuit (CoSaMP) (Needell & Tropp, 2009). In this Thesis, the CoSaMP algorithm is selected due to its optimal recovery guarantees and rigorous computational costs (Needell & Tropp, 2009).

The CoSaMP algorithm requires as an input parameter the sparsity order of the signal to be reconstructed K' to achieve the same reconstruction problem. This poses a new consideration when applied to realistic scenarios such as the ones of this Thesis. This is due to the fact that K' can control the desired number of interfering signals to be detected since it coincides with the number of frequency components to be produced by CoSaMP. Thus, in order to detect all the most harmful interfering signals at the input of the wideband receiver in this proposal, the reconstruction sparsity order K' will be controlled according to the input power of the AGC of the wideband receiver as detailed in Section 4.3.1.

4.3.1 Algorithm for the selection of K'

The selection of a proper value of the number of frequency components to detect in order to optimize the performance of NBI detector should be handled by a cognitive system (Haykin, 2005). For this purpose, an algorithm for the selection of K' has been designed according to the AGC status of the wideband receiver. This algorithm will be executed by the cognitive system, providing the NBI detector with adaptability to the environment's changes. During its execution, the cognitive system always knows the frequency location of the desired signals in order to prevent their mitigation, the current sparsity order K' and a mitigation list containing the frequencies of NBI previously detected.

Considering this, the value of the reconstruction sparsity order K' is modified in accordance to the AGC's specific operating region as described in Figure 4.2. Three cases can be identified in the algorithm's flowchart depicted in Figure 4.6:

- *Saturated AGC*: When the input power at the AGC is higher than P_H, the input wideband signal contains at least one strong NBI and AGC reduces the input signal for adapting it to the maximum ADC input range (Pérez-Díaz et al., 2012). If this occurs, the cognitive system will execute the left-hand side of the flowchart represented in Figure 4.6 also named here as 'Saturated AGC'. The value of K' will be increased in one unit in order to detect a new frequency component and the detection phase is re-executed with the additional information. If the result of CoSaMP contains the frequency of one of the desired signals, K' will be restored to the previous value and this frequency will not be included in the mitigation list. However, if the reconstructed frequency component is not a desired signal, i.e. it is a new interfering signal, its frequency will be included in the mitigation list and the mitigation

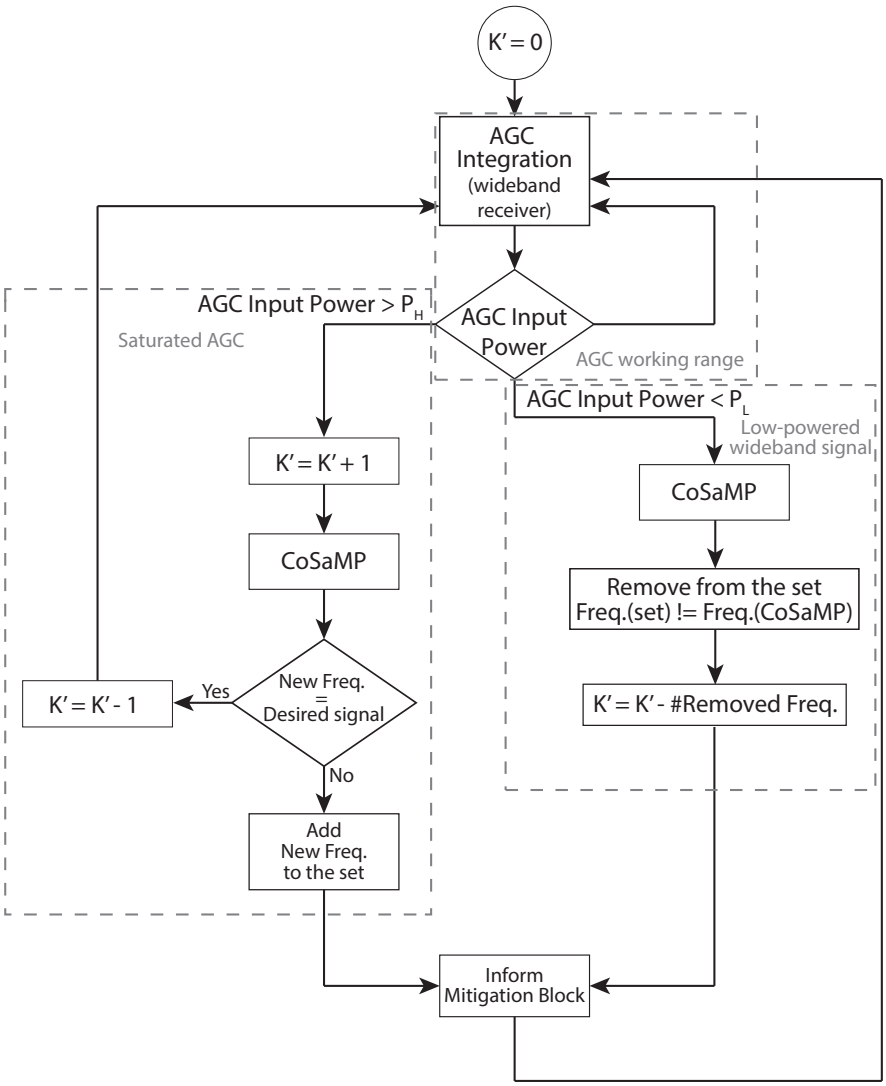

FIGURE 4.6. Flowchart of the algorithm for the selection of the reconstruction sparsity order K'.

block will be informed to apply cancelling techniques in those frequencies.

- *Low-powered wideband signal*: If the input power at the AGC is lower than P_L, i.e. it is in the 'Low-powered wideband signal' area, the cognitive system will execute the right-hand side of the flowchart represented in Figure 4.6 also named as 'Low-powered wideband signal'. The detection phase will be active and the output of the CoSaMP algorithm with a reconstruction sparsity order equal to the current value of K' will be compared with the set of frequencies stored in the mitigation list. If the CoSaMP algorithm does not detect the frequency of one or more interfering signals that were previously detected, they are removed from the mitigation list. The reconstruction sparsity order K' will be decreased in accordance to the number of frequency components that have been removed from the mitigation list.

- *AGC working range*: When the previous cases are not held, the AGC of the wideband receiver will continue its integration and the proposed detection phase will be inactive.

4.4 Experiments

To illustrate the benefits of the proposed NBI detector, a wideband compressive detector with a sampling rate eight times lower than the Nyquist rate has been designed for the detection phase. This decision allows the reduction of the complex sampling rate of 1 MHz to 125 kHz in the detection phase of the proposed scheme. Specifically, blocks of $N = 4096$ Nyquist-rate samples corresponding to a fixed time window are placed at the input of the random demodulator. From these samples, the random demodulator produces $M = 512$ compressive measurements that are required by the CoSaMP algorithm to obtain the location of NBI. In general, the above experimental setup enables the simulation of the continuous-time process of acquiring HF signals with a compressive system by using its digital equivalent.

The CoSaMP algorithm is configured by modifying the reconstruction sparsity order K' with the algorithm introduced in Section 4.3.1 for the selection of K'. In order to show the importance of the algorithm for the selection of K', the sparsity order of the algorithm is varied naively and the resulting detection performance analysed. For this, different tests were carried out by modifying the sparsity order of the signal to reconstruct and the channel activity conditions. The set of frequency components recovered by CoSaMP is compared with the set of frequency components with the highest power levels in each measurement to compute the detection rate and the false alarm rate of the proposed NBI detector. Although the proposed NBI detector is evaluated in these terms, it cannot be evaluated as an energy detector based on the Neyman-Pearson lemma (Kay, 1998) due to the fact that its architecture is based on a low-complexity wideband receiver and no power threshold can be established for signal detection.

Due to the variability of the activity in the HF band, the acquired measurements of the HFSA_IDeTIC_F1_V02 database have been classified in three different categories according to the activity level: 41.67% of them in a normal activity scenario during two different weekdays, 41.67% have been acquired during two weekends when amateur radio contests were scheduled and they have been classified as high activity, and 16.66% of measurements include strong NBI as the one presented in Figure 4.4. Measurements of both normal and high activity scenarios do not contain strong NBI since they were acquired when the AGC of the wideband HF receiver was in its working range.

The results obtained for the detection rate and the false alarm rate are shown in Figure 4.7 and Figure 4.8, respectively, for the three scenarios previously defined, namely: normal activity, high activity and scenarios only with NBI. As it was expected, Figure 4.7 and Figure 4.8 show that the performance of the proposed NBI detector depends on both the sparsity order K' and the activity level in the considered scenario.

A particularly interesting case to test the performance of the proposed compressive NBI detector is when only the position of the strongest narrowband transmission is desired to be detected ($K' = 1$). With these conditions, the system's performance is max-

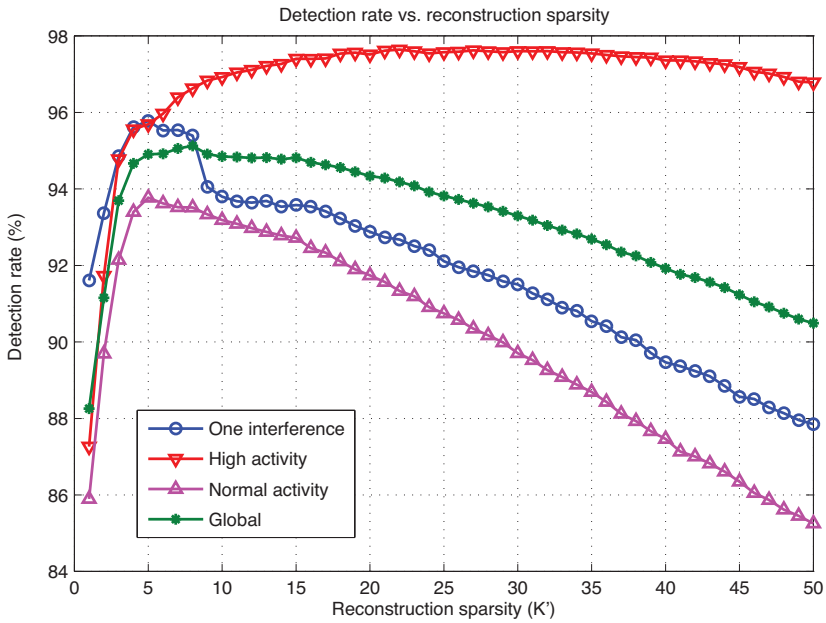

FIGURE 4.7. Variation of the detection rate with the sparsity order of the reconstruction.

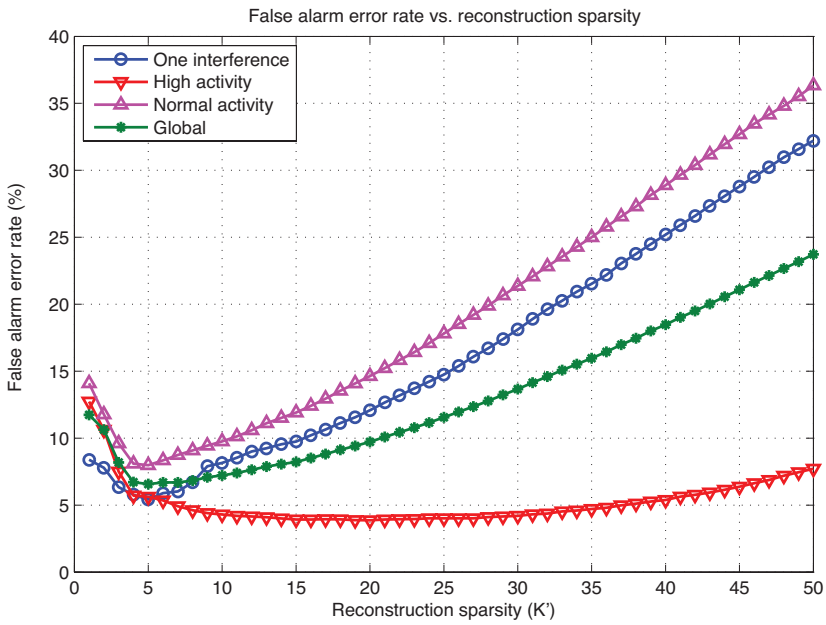

FIGURE 4.8. Variation of the false alarm error rate with the sparsity order of the reconstruction.

imized in scenarios in which there is only one strong interfering signal, achieving a detection rate of 92% and a false alarm rate of 8%. It is important to remark here that the detection rate is a 4% higher when $K' = 5$ than when $K' = 1$ due to the measurements' characteristics. As depicted in Figure 4.9, each frequency component that CoSaMP recovers has a narrower bandwidth of 600 Hz versus the 3 kHz of conventional HF transmissions. In other words, there are multiple components that belong to the same HF transmission. The proposed NBI detector is also able to achieve a detection rate of 86% and 87% in normal and high activity scenarios, respectively. Since most of the narrowband signals in each wideband measurement have similar power levels in normal and high activity scenarios, the CoSaMP algorithm detects another transmission with a power level similar to the strongest one.

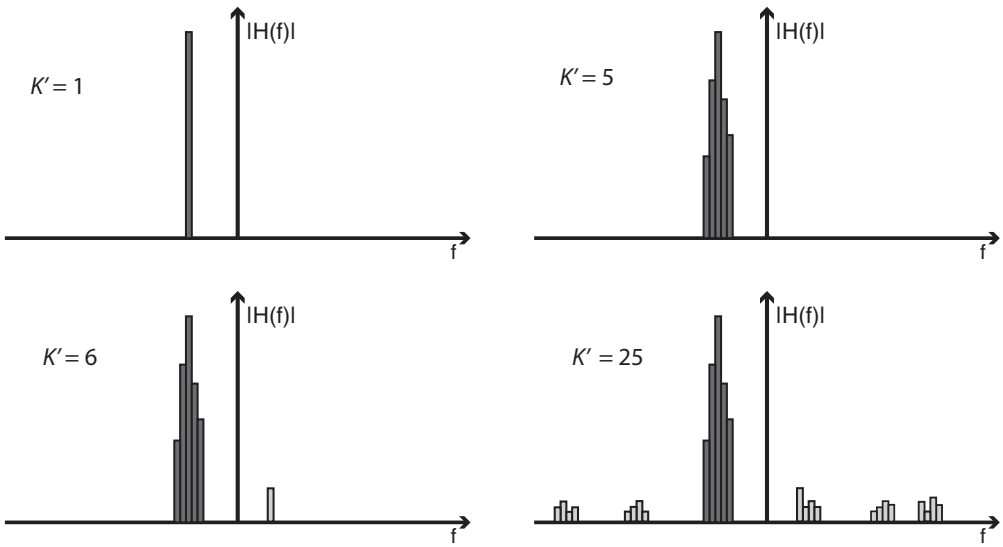

FIGURE 4.9. CoSaMP reconstruction of acquired HF measurements with NBI vs. reconstruction sparsity order K'.

The importance of the selection of an adequate value of interfering signals to detect as detailed in Section 4.3 can also be seen in Figure 4.7 and Figure 4.8. When there are multiple interfering signals and the AGC of the wideband receiver is saturated, the cognitive system increases the reconstruction sparsity order K' to detect more than one interfering signal. It can be seen in Figure 4.7 and Figure 4.8 that detection and false alarm error rates improve in the high activity scenario from sparsity order $K' = 15$ to $K' = 30$ reaching 97.8% detection rate and 4% false alarm rate. However, in those situations with not many representative interfering signals such as the ones with normal activity or a strong NBI, as K' increases so does the error rate. This effect is due to the significant power difference between the strongest transmissions and the rest of signals, i.e., once all the frequency components with the highest power levels are reconstructed, the remaining recovered coefficients appear in locations where no strong interfering signals are present. When this ocurrs, the AGC will not reach the *Saturated AGC* region and thus, the algorithm depicted in Figure 4.6 will not increase K' beyond the value of K' where the maximum detection rate was achieved.

4.4.1 Characterization of the RD's behaviour in real scenarios

The results obtained in the experimental study of Section 4.4 allow the characterization the RD's behaviour in a real scenario. They also allow the comparative with the theoretical study of (Tropp et al., 2010) in a controlled scenario. In that work, an empirical rule is used to determine the relationship between the sampling rate R that is necessary to identify a K-sparse signal with a bandwidth of W Hz using the RD and the controlled signal model proposed in (Tropp et al., 2010).

For the purpose of characterizing the RD's behaviour in a real scenario, the same procedure is followed in this Thesis, but using real wideband HF measurements of the HFSA_IDeTIC_F1_V02 database detailed in Section 3.4. In this process, the signal bandwidth is equal to the wideband HF transceiver, 1 MHz, and for each K-R pair, the number of measurements used is equivalent to an hour recording during five days.

Since, in contrast with (Tropp et al., 2010), the real measurements have noise, interference, and different types of transmissions with unknown characteristics; in this Thesis the minimum sampling rate R for a false alarm rate lower than 10% is computed. Experiments' results are depicted in Figure 4.10 for a sparsity order K from 2 to 100 and the sampling rate R being the quotient W/P with discrete values $P = 3, 4, ..., 10$ (blue horizontal lines represent these values in Figure 4.10). This entails that the results depicted in Figure 4.10 have an upper limit, $W/3$, and a lower limit, $W/10$, corresponding to the values of $P = 3$ and $P = 10$ respectively.

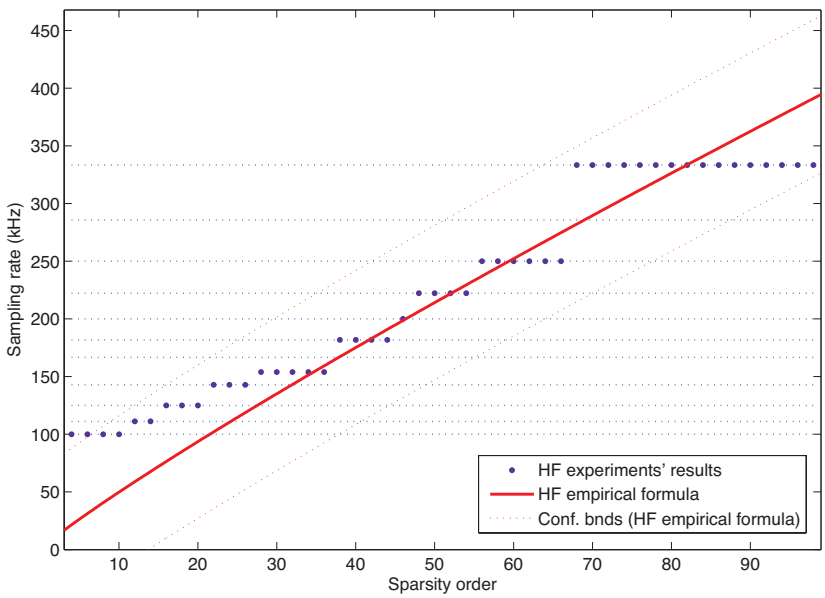

FIGURE 4.10. Results' fitting to the empirical formula (4.5) with confidence bounds.

In order to characterize the behaviour of the RD in the HF scenario, an analysis of how the results obtained in Section 4.4 fit with the empirical formula obtained in (Tropp

et al., 2010) is presented. This empirical formula is:

$$R \approx CK \log\left(\frac{W}{K} + 1\right), \tag{4.5}$$

where log is the natural logarithm and C is the fitted parameter to the experiments' results. A goodness-of-fit test has been made to illustrate how close is the behaviour of the RD in real scenarios compared to the theoretical behaviour. For the HF environment, the fitted parameter has a value of 432.4 with 95% confidence bounds $(415.1, 449.6)$. This parameter must be fitted according to the scenario under test. Since an acquisition bandwidth W of 1 MHz is being considered in this work, which is higher than the bandwidth considered in (Tropp et al., 2010) (512 Hz), the value of C is two orders of magnitude higher than the obtained for a controlled scenario in (Tropp et al., 2010). It is important to highlight that, despite this difference in the value of C, Figure 4.10 shows that the experiments are located between the obtained confidence bounds and the fitting in real scenarios follows the same trend as the theoretical behaviour. Furthermore, the R-Square statistic has been also computed since it measures how successful the fit is in explaining the variation of the data and it can take on any value between 0 and 1, with a value closer to 1 indicating that a greater proportion of variance is accounted for by the model (James, Witten, Hastie, & Tibshirani, 2013). For this fitting, the R-Square has a value of 0.8594, i.e. the fit of our experiments to the empirical formula of the RD's proposal explains the 85.94 % of the total variation in the data about the average. This shows that the attainable detection performance when real scenarios are considered is close to the theoretical performance shown in (Tropp et al., 2010).

4.5 Summary

The detection of strong NBI is crucial to guarantee the operation of wideband receivers without performance degradation. For this reason, the design of a NBI based on compressive sensing techniques for a wideband HF transceiver is presented in this Chapter. The proposed NBI detector reduces the hardware complexity of standard approaches by using a sampling system with a low-rate ADC, i.e. the random demodulator, and it has been provided with adaptability to the environment's conditions according to the status of the AGC of the wideband receiver.

Based on different tests under real conditions, it has been shown that the proposed NBI detector is able to locate the strongest signals in HF scenarios with different degrees of activity. Moreover, the performance of the NBI detector has been characterized depending on the number of interfering signals to detect or the activity scenario, hence showing the possibility of including this compressive NBI detector in wideband HF schemes to further improve their performance. Finally, the random demodulator's behaviour has been characterized in a real scenario, and compared against the theoretical study of the random demodulator showing that the empirical performance with signals from real environments has the same trend as the theoretical behaviour.

Chapter

5

HF Primary User Dynamics Model

A model of primary user dynamics in the band is extremely useful to make the best from the acquired knowledge in predicting the activity of primary users in the channel. A model for long-term predictions is derived in this Thesis for the HF band based on a set of Hidden Markov Models (HMM). It has been trained and validated on real data from the HF band with the HFSA_IDeTIC_F1_V01 database as a first step towards a fully operative cognitive radio scheme.

The proposed HF primary user dynamics model is based on HMMs because they are a powerful and robust tool for modelling stochastic random processes, as they are able to model a large variety of processes achieving high accuracy with relatively low model complexity. They have been extensively used in a myriad of signal processing applications during the last 20 years, mainly for fitting experimental data onto a parametric model which can be used for real-time pattern recognition, and to make predictions based on the available prior knowledge (Rabiner & Juang, 1993). HMMs are also widely used in prediction problems due to its strong theoretical foundations and tractability (Akbar & Tranter, 2007), property that is not always guaranteed in artificial neural networks (Blum & Rivest, 1992).

This Chapter is divided as follows: Hidden Markov Models are introduced in Section 5.1. To reduce the variability of the HMM training, the measurements of the HFSA_IDeTIC_F1_V01 database are segmented and classified in terms of users activity in Section 5.2. The proposed HF primary user dynamics model is described in Section 5.3, where the training and validation processes are presented; whereas the prediction scheme developed and tested on top of this model is described in Section 5.4.

5.1 Hidden Markov Models

A Hidden Markov Model is defined as a doubly embedded process with an underlying stochastic process that is not observable. This hidden process (state) can only be evaluated through another set of processes that produce sequences that actually can be observed (Rabiner & Juang, 1993). An HMM for discrete symbol observations is defined by the the following elements:

- **A**: State transition probability distribution matrix $A = \{a_{ij}\}$ of size N^2 where N is the number of states in the model and

$$a_{ij} = P\left[q_{t+1} = S_j | q_t = S_i\right], \qquad 1 \leq i, j \leq N. \tag{5.1}$$

  The set of individual states is $S = \{S_1, S_2, \cdots, S_N\}$ and the state at time t is denoted as q_t.

- **B**: The observation symbol probability distribution for state i, $B = \{b_i(k)\}$, where

$$b_i(k) = P\left[O_t = V_k | q_t = S_i\right], \qquad 1 \leq i \leq N; \quad 1 \leq k \leq M, \tag{5.2}$$

  O_t is the observation at time t and M is the number of distinct observation symbols per state. The observation symbols correspond to the physical output of the system being modelled and are denoted as $V = \{V_1, V_2, \cdots, V_M\}$.

- π: The initial state probability distribution $\pi = \{\pi_i\}$ where

$$\pi_i = P\left[q_1 = S_i\right], \qquad 1 \leq i \leq N. \tag{5.3}$$

- **O**: Observation sequence

$$O = O_1 O_2 \cdots O_T \tag{5.4}$$

  where each observation O_t is one of the symbols from V and T is the number of observations in an observed sequence.

Thus, a complete definition of an HMM involves: two model parameters (N and M), the specification of the observations symbols and the specification of **A**, **B** and π. In practise the compact notation used for an HMM is

$$\lambda = (\mathbf{A}, \mathbf{B}, \pi) \tag{5.5}$$

Regarding the structure of the transition matrix **A**, HMMs can be classified into different groups. In an ergodic or fully-connected HMM every state of the model can be reached from any other state in the model after a finite number of steps. However, transitions between HMM's states are most frequently limited. An example of these models is the left-right or Bakis HMM which has the property that as time increases the state index either increases or stays the same. Such model was introduced to fit signals which

changed over time in a successive manner, and is characterised by its transition matrix which forbids non-causal transitions within the models, i.e. its state transition coefficients have the property

$$a_{ij} = 0, \qquad j < i \tag{5.6}$$

as no transitions are allowed to states whose indexes are lower than that of the current state. Another relevant characteristic of a left-right HMM is that the state sequence must begin in state 1 and end in state N, so the initial probability distribution has the following property

$$\pi_i = \begin{cases} 0 & \text{if } i \neq 1 \\ 1 & \text{if } i = 1 \end{cases} \tag{5.7}$$

Additionally, from an implementation perspective, such simplification introduces both a hard restriction and a relevant simplification for the model to be derived, as the number of parameters in the transition matrix decreases dramatically by almost a factor of two.

Three major tasks must be fulfilled for a Hidden Markov Model defined as (5.5) to be useful in practical applications (Rabiner & Juang, 1993):

1. *Evaluation*: Given an observed data sequence and a set of models to be compared, the probability that the provided sequence was produced by each of them, $P(O|\lambda_k)$, is to be computed as the cumulative product of the likelihood obtained by each evaluated sample. This is calculated through the sum of the so called, terminal forward variables, $\alpha_T(i)$, defined in the "forward-backward" algorithm (Rabiner & Juang, 1993). From the perspective of the Neyman-Pearson lemma, this can be considered as a scoring problem, in which the resulting scores will be used to decide which of the models fits the observed sequence better (i.e. obtained the largest accumulated likelihood value).

2. *Decoding*: Given an observation sequence, the state sequence that is optimal in some meaningful sense is chosen. By doing this, the hidden part of the model can be uncovered according to some criteria. The most widely used criteria is to find the best state sequence that maximises the probability $P(Q, O|\lambda)$ using the well-known Viterbi algorithm (Forney, 1973).

3. *Learning*: The parameters of a particular model are adapted in order to maximise its likelihood when a set of sequences which correspond to the class it models is observed. The learning task is also referred as the training of the model in which it is attempted to find the model parameters which best describe the observed sequence (the training sequence). An iterative procedure such as the Baum-Welch method (Rabiner & Juang, 1993) is used to locally maximise the likelihood of the model defined as $P(O|\lambda)$.

Sections 5.3 and 5.4 are devoted to describe how the three tasks were developed in order to train and test the model, and also, to use them for prediction using a previously

trained model.

5.2 HFSA_IDeTIC_F1_V01: data classification and segmentation

Once the spectrum sensing task was completed, acquired wideband measurements in the HFSA_IDeTIC_F1_V01 database have been translated into binary observation sequences where each one represents a 3 kHz HF channel for ten or nine minutes. Each sequence has '0' and '1' values which represent only-noise samples or occupied-channel samples, respectively. Subsequently, these observation sequences are segmented into smaller sequences with a duration of one minute and classified in order to reduce the complexity of the model to be defined in Section 5.3.

As observed in Figures 3.5 and 3.6, different degrees of activity can be identified in the acquired measurements of the HF band. There are several channels which are almost unoccupied for long-time slots, while other channels remain occupied for the same amount of time and could not be used to transmit. Finally, there are other channels which could be used by a secondary user to transmit and make an efficient use of the band. Thus, a classification of the observation sequences is proposed prior to the modelling of the primary user's dynamics in Section 5.3. This classification is based on the degrees of activity observed in the acquired measurements and the secondary user's behaviour in a cognitive radio system, that is:

- *Available channels* where the secondary user can transmit.
- *Unavailable channels* where a primary user is in the band and the secondary user cannot transmit.
- *Partially available channels* in which there are time intervals during which the secondary user can transmit until a primary user appears.

Observation sequences of ten and nine minutes long were segmented into one minute-long sequences as it can be seen in Figure 5.1. These short sequences could be classified as 'Available', 'Unavailable' and 'Partially available' channels and encoded as $\{1, 2, 3\}$, respectively, to reduce the complexity of the model to be trained in Section 5.3.

The criteria followed to classify the observation sequences of each channel is based on the maximum time that a secondary user will need to transmit a data frame. Two thresholds were defined: one for minimum percentage of occupation by a primary user in unavailable channels, in such a way that the secondary user can transmit its maximum length data frame, and another for the maximum percentage of occupation in available channels. In order to derive both thresholds, it is necessary to get the worst case of channel occupation as secondary users in HF data communications. This worst case scenario comes from assuming a maximum length for data frames to be transmitted by the

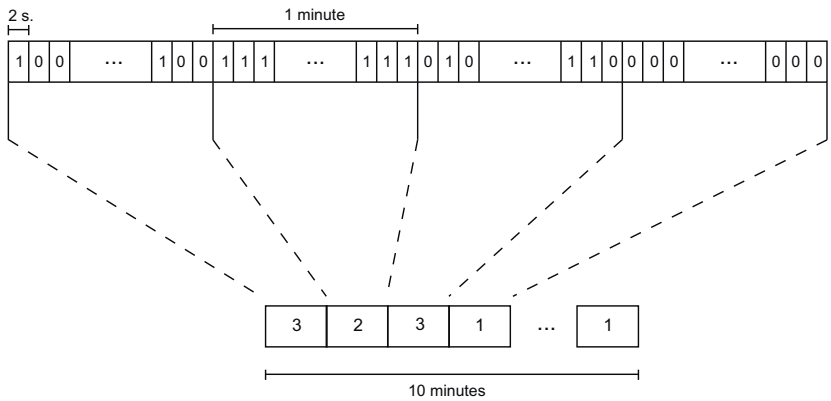

FIGURE 5.1. Data classification and segmentation.

secondary user. In this work, the frame of maximum length defined by the NATO Standardisation Agreement STANAG 5066 (STANAG 5066, 2008) has been considered for the HF stations as secondary users. This standard establishes the profile for professional HF data communications and defines frames, called D-PDU, that have 46 bytes of overhead and up to 1023 bytes of user data. Most HF data communications use a data rate of 600 bps or 1200 bps, and, with these parameters, the longest D-PDU frame resulting would last for 14.25 seconds (1069 bytes at 600 bps), which represents the worst case of channel occupation by the secondary user to be considered in this work.

Therefore, observation sequences with at least 45 seconds occupied within a minute were considered to belong to the unavailable channels group as secondary users will not be able to transmit the largest frame during the remaining 15 seconds. Similarly, available channels were defined as those observation sequences with a maximum of 15 seconds occupation in one minute. Finally, the rest of the observation sequences were classified as partially available channels where secondary users could transmit for less than 45 seconds to avoid collisions with primary users.

5.3 HF primary user dynamics model

In this Thesis Hidden Markov Models were used to model the primary users activity dynamics in the 14 MHz band. As it was previously described, such a model could be used by HF stations, acting as secondary users, to predict the presence of a primary user, preventing interferences in their own transmissions. Therefore, this prediction would be the main source of information to avoid collisions with licensed users of the band, and consequently, to make the best possible use of the available channels.

Once data from the HF band has been processed and classified, the activity model can be defined and trained. Due to the proposed classification of the observation sequences, the model has a hierarchical structure and is defined as an ergodic HMM with three states interconnecting three underlying submodels, one for each class (i.e. available,

unavailable and partially available channel) as it can be seen in Figure 5.2. These type of structures are commonly used in HMM based generative models as the one presented in (García-Frías & Crespo, 1997) for burst error characterisation.

Each submodel was trained with a set of one minute-long observation sequences from the corresponding class as previously defined (see Section 5.2) to derive a suitable model for the group at hand. Consequently, the first submodel was meant to characterise available channel sequences, the second submodel for unavailable channel sequences and the third one for partially available channel sequences. These submodels were implemented as left-right HMMs as the particular structure of the transition matrix they exhibit is quite suited to model the time evolution of the samples in the observation sequences, definitely better than ergodic models can, and with a reduced number of parameters to be trained.

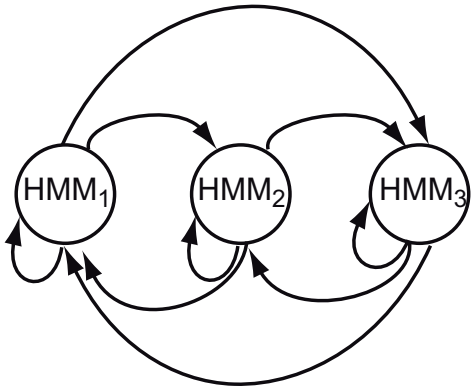

FIGURE 5.2. High-level HMM of the primary user dynamics model.

In the end, the proposed model for primary user's dynamics was built through the combination of a high-level, ergodic HMM with three states, each of them corresponding to available, unavailable or partially available channels respectively, and a set of three left-right submodels. Each state in the upper model emits an observation sequence of a minute long which is generated by the submodel corresponding to that state. To simplify the training and evaluation of the high-level model, this was trained as an independent HMM where each state only emits one single value representing the state, independently from the scores provided by the low-level submodels. That is, state S_1 only emits symbol '1' and it represents the observation sequence generated by submodel 1. This also happens for states S_2 and S_3 emitting symbols '2' and '3', respectively. So, the observation matrix for the high-level ergodic model, $\mathbf{B}$, would actually be the identity matrix. Under this specification, observation symbols generated by the high-level model would be also the transitions between its states, that is, the transitions between the underlying submodels. When the whole model is evaluated, the symbols for each state $\{1, 2, 3\}$ correspond to the observation sequences generated by the respective submodels for each of these states { 1 (Available channels), 2 (Unavailable channels), 3 (Partially available channels) } respectively and not these symbols.

Moreover, while submodels were trained to characterise one minute-long observation sequences from available, unavailable or partially available channels, the high-level

model was trained to characterise the evolution of a particular channel for ten and nine minute-long sequences, in which states are classified according to one minute-long sequences.

Once defined, the proposed model was trained and validated with the acquired data in the HFSA_IDeTIC_F1_V01 database. The observation sequences contained in this database have been segmented and classified as detailed in Section 5.2 in order to reduce the variability of the proposed HF primary user dynamics model. Furthermore, they have been divided into two sets as depicted in Figure 5.3: 70% of each class of observation sequences is used to train the model whereas the remaining 30% of each class of observation sequences is used to validate it.

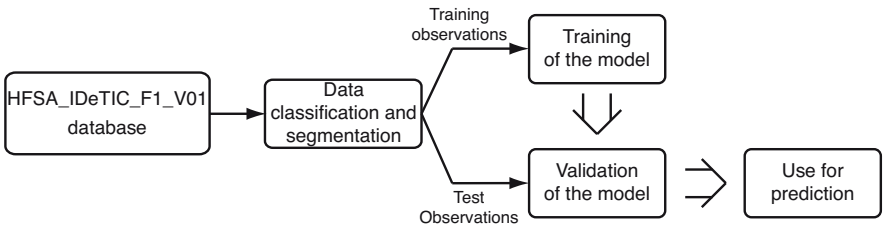

FIGURE 5.3. Block diagram for the training, testing and usage of the proposed HF primary user dynamics model in classification and prediction tasks.

5.3.1 Training of the model

The learning problem was established in terms of the optimisation of the HMMs' parameters (5.5) through the maximisation of $P(O|\lambda)$, that is, to identify the model which maximises the probability that the observation sequences used for training were actually generated by the model. The Baum-Welch algorithm (Rabiner & Juang, 1993), based on the Expectation-Maximisation method, was used to train both submodels and the high-level model. Randomly initialised matrices were used for the first iteration of the Baum-Welch method, as no prior knowledge on the structure of the sequences was provided, and the amount of collected data seemed to be quite enough.

Due to the differences in the selected structures for the high-level model and the three sumbodels, two different training protocols were carried out. Whereas the number of states of the high-level model was pre-fixed –3– due to the prior classification of the observations, the number of states for each submodel still had to be chosen. On the one hand, in training the proposed ergodic high-level model, the major concern was related to the initialisation of the values due to the ergodic structure itself. This structure had to be trained to be independent on the initial point, assuming that its execution could begin at any time, i.e. any of the three defined states could be the first. Thus, the transition matrix **A**, containing the estimated probability of going from one state to another regardless of the previous history, was initialised with different random seeds to reinforce the model stability, and trained on previously classified observation sequences including one minute-long available, unavailable and partially available segments.

On the other hand, the non-ergodic, left-right structure of the submodels largely reduced the complexity and cost for their training; unlike the high-level model for which no specific structure could be established. The number of states for the submodels, designed as left-right HMMs including three-states-long transitions (i.e. on each intermediate state, the incoming and outgoing transitions is equal and fixed to 4), was chosen according to the procedure previously described, based on the likelihood scores computed on every one minute-long observation sequences. For these submodels, matrices **A** and **B** were randomly initialised with a common seed, while π was initialised as in (5.7) due to the left-right structure which forces the models to begin at the first state. Different configurations for these models including 20 to 45 states were trained with their own one minute-long observed sequences including binary samples containing information on channels' occupancy: the available channel submodel was trained with all sequences classified as available channels, and the same was done for unavailable and partially available channel submodels.

Once trained, submodels' accumulated likelihood scores were obtained according to the evaluation task described in Section 5.1, and the model with the maximum likelihood (highest $P(O|\lambda)$ among all trained models) was identified. However, a normalisation model built from the combination of all samples included was artificially introduced to normalise the likelihood scores and prevent spurious effects during their estimation. This slight modification causes the former likelihood values to be bounded and behave as averaged likelihood ratios resulting from comparing different models to a common one, and therefore allows positive and negative values. However, to compare the scores from two different models, the subtraction of these scores would still provide a relative cumulative log-likelihood ratio measure, independent from the intermediate artificial model introduced. Their assessment was carried out attending to the results depicted in Figure 5.4. Focusing on the curves included in this Figure and corresponding to unavailable and partially available channel submodels, it should be noticed that the log-likelihood scores reach a local maximum for the configuration in which forty states were included, while log-likelihood scores corresponding to the available channel submodel were very small (see curve scale on 10^{-10}) for any number of states. Consequently, according to this result a suitable left-right HMM to model sequences included in the latter group could be built on any number of states from 20 to 45 without major differences. However, from a practical point of view, if all submodels included the same number of states their comparison would be easier once the whole model was trained and used for prediction. Therefore, all submodels discussed hereafter are left-right Hidden Markov Models including forty states, as a trade-off between submodels' log-likelihood scores, and up to three-states-long transitions as the one in Figure 5.5.

Being the number of states for the submodels adequately chosen, each of the models was trained over a sample including 70% of the observed sequences corresponding to it, and the model parameters maximising $P(O|\lambda)$ were then identified. The Baum-Welch algorithm was applied to randomly initialised HMM matrices **A** and **B** with the same seed used in the previous step. Matrices were obtained after ten iterations of the algorithm to

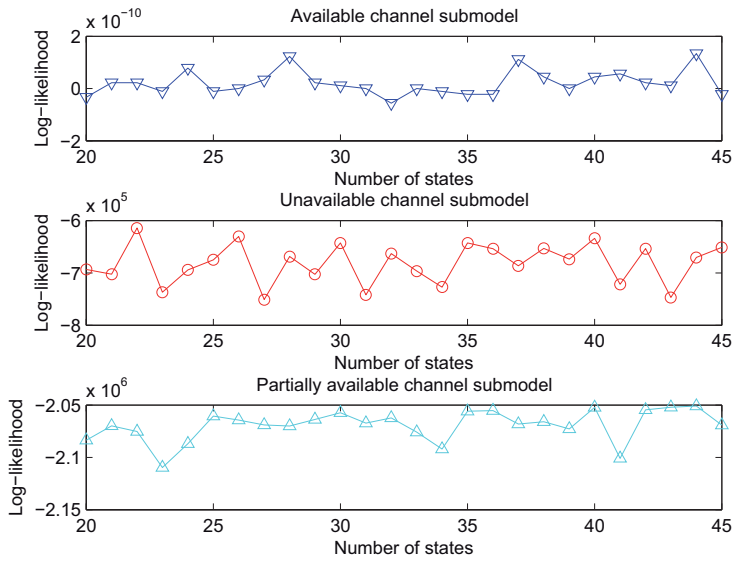

FIGURE 5.4. Evolution of submodel log-likelihoods versus the number of states.

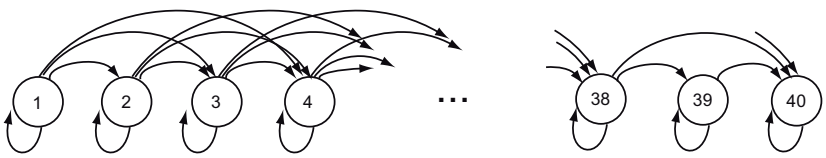

FIGURE 5.5. Left-right HMM with forty states and up to three states transitions.

prevent over-fitting. The rest of the acquired sequences were evaluated on the proposed models to re-estimate likelihood scores and then compared to the values obtained on the training sequences to check that the models did not over-fit the training data. It has been specifically checked that these matrices represent stable models, that is, there is a transition with a high probability in each row of the transition matrices and if the transition probabilities along the matrix are analysed, the final state is always reached for any observation sequence.

5.3.2 Validating the proposed model

From the initial set of collected data, once the 70% have been put aside for the training of the HF primary user dynamics model, the remaining 30% were left to evaluate the trained model and validate it. As the HF primary user dynamics model was based on three submodels and a high-level model, the evaluation protocol required two steps: first, submodel likelihoods were evaluated with binary one minute-long sequences indicating the channel occupancy, and afterwards, the high-level model probabilities were calculated for each observation sequence of ten or nine minutes.

To compare all submodels, the evaluation problem must be solved taking the submodel with the highest likelihood as the local solution. A matrix containing values

$\{1, 2, 3\}$ was built from these decisions with its rows corresponding to the observation sequences of ten and nine minutes. Due to the definition of the high-level model in Section 5.3, these observation sequences were also equivalent to the transitions of the high-level model. By computing the difference between this generated matrix and the real one, an estimation of the percentage of wrong decisions could be estimated, which reached the 5% of one minute-long test observation sequences.

As previously stated, the resulting matrix with $\{1, 2, 3\}$ values contained the observation sequences for the high-level model and could be used to evaluate it. At this point it was not possible to compare models in order to solve the evaluation problem, but as these observation sequences were the same as the transition sequences due to the initial restriction on matrix **B** of the model, the decoding problem could be evaluated using the Viterbi algorithm (Forney, 1973). The Viterbi algorithm was developed to identify the state sequence which maximises the probability $P(Q, O|\lambda)$, so that this state sequence can be directly compared to the observation matrix. The percentage of errors obtained was actually the same as the one obtained in the previous step, so, the high-level model can emit sequences such as the ones used in this test. Furthermore, if it is thought in terms of a pseudo-random sequence generator, it would be able to emit random sequences statistically close to the real measurements used for its training, i.e similar to the actual occupancy sequences present in the HF band.

5.4 Prediction scheme based on the HF primary user dynamics model

Bearing in mind the principles under cognitive radio and that the main goal of this model is to make an efficient use of the HF band, its use to predict in the long-term the activity of primary users in a particular HF channel is proposed in this Thesis. The following procedure was designed to predict whether a channel will be used by a primary user within the next minute or not, and it is based on the combination of the high-level model and the underlying submodels parametrised as HMMs, as described in the previous sections. A one minute prediction span is chosen to allow long-term data transmissions according to these predictions. As it will be later detailed in Chapter 6, another learning strategies are more suitable for short-term prediction schemes. Besides, it will be demonstrated in Chapter 7 that the joint use of two prediction spans, short-term and long-term spans according to two different learning strategies, achieves better performance than each learning strategy working independently.

The developed architecture shall operate according to the flow shown in Figure 5.6. While a secondary user is sensing different channels in order to select the one that can be used to transmit without interfering with a primary user, it shall process the spectrum measurement corresponding to the last minute of a particular channel and use it as an observation sequence O_T to evaluate the three submodels for available, unavailable and partially available channels. By evaluating the “forward-backward” algorithm, their like-

lihoods are computed and, instead of choosing the submodel with highest likelihood like in the evaluation process, the resulting probabilities can be used in the high-level model as updated entries for its observation matrix **B**.

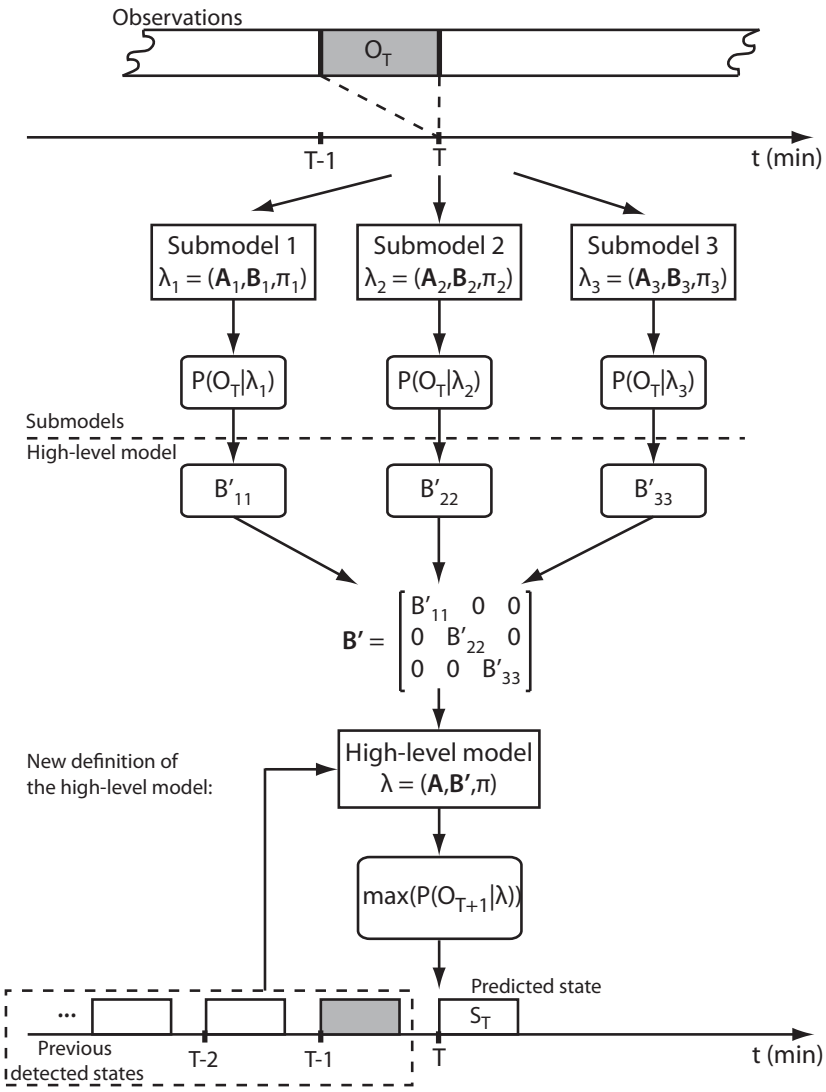

FIGURE 5.6. Block diagram of the prediction procedure.

Subsequently, the "forward-backward" algorithm is evaluated in the high-level model on the sequence of states corresponding to the prior T minutes and the three possible states for the next minute are evaluated: {1 (Available channels), 2 (Unavailable channels), 3 (Partially available channels)}. The state with the highest likelihood will be considered to be the predicted state for the channel in the next minute.

The average error rate of the prediction model with a prediction span of one minute is plotted in Figure 5.7. Due to the time restriction on the data acquisition process which lasted for ten minutes, most of the test sequences actually have a duration of nine minutes and thus, the maximum time span of the acquired knowledge is eight minutes.

In addition to the global performance of the prediction model, performances for normal and high activity scenarios in the HF band are also presented in Figure 5.7. As it was

previously stated, the 14 MHz amateur band has a different behaviour depending on the day: there is a huge amount of activity at weekends, especially when amateur contests are scheduled, whereas there is a normal amount of activity on weekdays. Both situations have been considered in the training stage of the HF primary user dynamics model, so, the trained model will be able to predict whether a primary user will be present in the channel or not within the next minute in both situations.

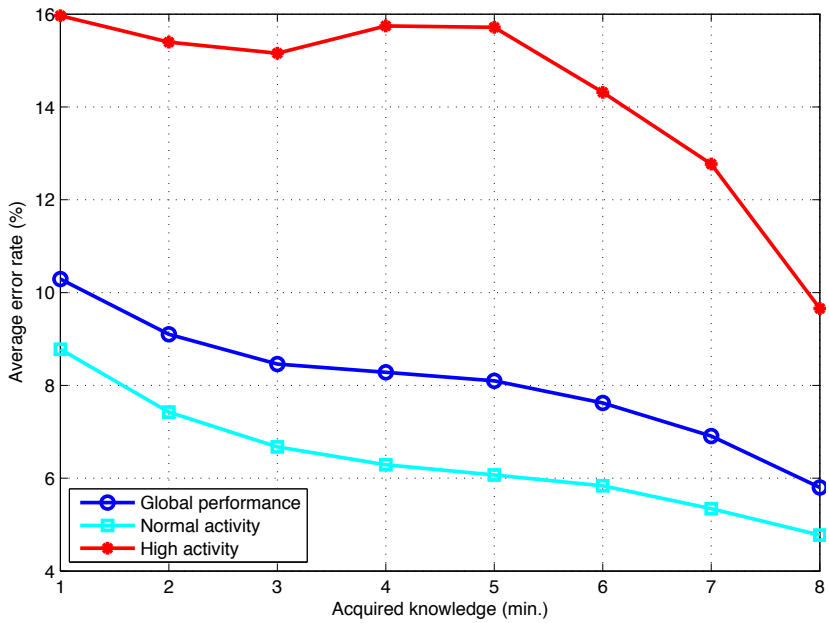

FIGURE 5.7. Average error rate of the prediction model.

As shown in Figure 5.7 for the global performance, when the secondary user has listened the previous minute and no past information is available, the model has an average error rate of 10.3% but, as the acquired knowledge of the channel increases, this error rate decreases monotonically. In fact, if the secondary user could access the channel state memory of the previous eight minutes, the error rate is reduced to a 5.8%.

For high activity environments, the average error rate of the prediction model increases to 16% when the secondary user has only listened the previous minute. Once it has listened for at least five minutes, the average error rate heavily decreases, and it is reduced to 9.6% if the secondary user has a channel state memory of the previous eight minutes. However, the average error rate decreases (respect to the global performance) to 8.7% in normal activity environments with a channel state memory of the last minute and decreases to 4.7% when the secondary user has listened the previous eight minutes.

5.5 Summary

A primary user dynamics model for the HF band based on Hidden Markov Models has been presented in this Chapter. Due to the regulatory bandwidth restrictions and propagation characteristics of this frequency band, the use of this model to make pre-

dictions within the next minute of the activity in a particular channel is considered to be extremely helpful for cognitive stations. It has been designed to perform long-term predictions of the activity in a particular HF channel to increase the length of secondary users' data transmissions.

As a first step, the acquired observation sequences in the HFSA_IDeTIC_F1_V01 database have been segmented into short observation sequences of one minute long, and classified according to the observed activity in available, unavailable and partially available sequences. The main goal achieved by this classification is a reduction in the variability of the learning strategies proposed in this Chapter.

The proposed model has been trained and validated with real measurements collected from the 14 MHz band of the HFSA_IDeTIC_F1_V01 database. It is built from three interconnected submodels which describe three types of channels: available channels, unavailable channels and partially available channels. Finally, this model was used to predict the activity in a channel within the next minute: it achieved an average 10.3% error rate when the acquired knowledge of the channel has a duration of one minute, and it reached an average 5.8% error rate with a downward trend when this knowledge is extended to the previous eight minutes. Since it has a prediction span of a minute, it allows long-term data transmissions without executing the proposed prediction model for further predictions within this minute.

Finally, it has been designed as a single-channel prediction model due to its simplicity, since one HMM based model that learns multiple channels simultaneously is more complex than multiple single-channel HMM based models working in parallel (Melián-Gutiérrez et al., 2013).

Chapter

6

Decision-Making with Upper Confidence Bound Algorithms

In the previous Chapter, a long-term prediction scheme with the HMM based primary user dynamics model was described. A one minute prediction span was chosen to increase the length of HF users' data transmissions, and it was designed as a single-channel prediction model due to its simplicity. However, its straight application in a multi-channel scenario for opportunistic spectrum access (OSA) requires as much HMM based prediction models as the number of channels to sense and transmit. Therefore, a decision-making strategy and a short-term prediction scheme are required to complement the HMM based prediction model in a cognitive radio based HF station.

In this Thesis, an opportunistic spectrum access is proposed for secondary users in the HF band based on the application of the Upper Confidence Bound (UCB) algorithm as introduced in (Jouini et al., 2009). Such a mechanism will help HF users to decide which are the best channels in terms of availability at each particular time. Furthermore, it allows for short-term predictions during its execution. It could be used with wideband transceivers or with single-channel transceivers with an automatic frequency tuning.

As previously described in Chapter 2, the Multi-armed Bandit (MAB) framework used in reinforcement learning is a straightforward approach of decision-making for OSA. In this MAB framework, the agent is a secondary user that selects within a set of actions that corresponds to a set of transmission channels. From the set of algorithms detailed in Chapter 2 to solve MAB problems, the UCB algorithm has been presented as an efficient solution for this type of problems (Auer et al., 2002). Furthermore, the extensive work performed in (Jouini et al., 2009, 2010; Moy, 2014; Robert et al., 2014) has shown the feasibility of UCB algorithms for cognitive radio scenarios via simulations and experiments. Thus, it seems that it is also an appropriate a feasible solution for the application

of cognitive radio in HF communications.

In this Chapter, the feasibility of UCB algorithms in the HF band is demonstrated. From the HFSA_IDeTIC_F1_V01 database, a selection of the measurements with the worst conditions in terms of availability is employed to validate the performance of UCB algorithms. This selection includes amateur channels of 3 kHz each located from 14.07 MHz to 14.14 MHz (see Figure 3.6), and recorded when the 14 MHz amateur band was heavily occupied. For a better readability, the sample time slot of 2 seconds of this database is referred hereafter as T_{UCB} whereas the duration of the whole acquired measurement of 10 minutes is referred hereafter as T_{TEST}.

The outline of this Chapter is as follows. The UCB algorithm is described in Section 6.1, where UCB for single channel selection and UCB-M for multiple channel selection strategies are presented. The performance of the UCB algorithm in the HF environment is compared to different channel selection approaches: *best channel selection*, *worst channel selection*, *uniform random selection*, and *best opportunistic selection*, which are defined in Section 6.2. An overview of how the UCB algorithm behaves in the HF environment compared to previously detailed selection approaches is given in Section 6.3. The validation of UCB algorithms in the HF band is detailed in Section 6.4 and Section 6.5, including the analysis and validation of the exploration vs. exploitation dilemma for both single and multiple channel selection UCB, respectively. Finally, a short discussion on the complexity introduced by UCB and UCB-M algorithms for learning and decision making in the HF band is included in Section 6.6.

6.1 Upper Confidence Bound algorithm

The Upper Confidence Bound (UCB) algorithm is one of the algorithms based on reinforcement learning (RL) that was introduced in (Agrawal, 1995) and (Auer et al., 2002) as an approach for solving the Multi-Armed Bandit (MAB) framework (Robbins, 1952). The MAB framework is analogous to the traditional slot machine but with more than one lever. In (Jouini et al., 2009), the UCB algorithm was proposed for cognitive radio in order to provide secondary users with opportunistic spectrum access through a set of channels following the MAB framework. In this framework, the spectrum is divided into a set of N channels, each one with the same bandwidth and modulation scheme, and each represents one lever of the MAB. At each time slot, the algorithm plays one or multiple levers and obtains a reward from each one.

The UCB algorithm allows decision making in an OSA cognitive radio context to maximise the transmission opportunities of secondary users. In this Chapter, the following model has been used for OSA: at each time slot, only one channel (single-channel UCB) or M channels (multi-channel UCB) within a group of N channels (with $M < N$) are sensed but all N channels are ranked; if the selected channels by the algorithm are free, they will be used to transmit and they will be rewarded. However, if they are occupied

by another user, neither a reward will be granted nor a transmission will be established to avoid a collision with primary users' transmissions.

Since UCB is based on RL, it learns from previously observed rewards starting from scratch, e.g. without any a priori knowledge of the activity within the set of channels. The UCB algorithm continuously learns (in the exploration phase) and predicts the next available channel to transmit on within the set of channels (in the exploitation phase) during the entire process. One of the advantages of the UCB algorithm is that the exploitation phase starts at the beginning of the process even when the knowledge is not mature enough (Moy, 2014). Reciprocally, the exploration is maintained along the overall process, even during exploitation. Thus, both exploration and exploitation are continuously superposed for improved management of the exploration versus exploitation dilemma.

At each time slot t, the algorithm updates UCB indices named as $B_{t,k,T_k(t)}$, where $T_k(t)$ is the number of times channel k has been selected by the algorithm in previous slots, and returns the channel index k of the maximum UCB index (see Algorithm 6.1 on Page 80). From the different UCB indices existing in the literature, UCB_1 index (Auer et al., 2002) is computed in this Thesis and evaluated with single-channel (UCB_1) or multiple-channel (UCB_1-M, known as UCB_1 - multiple plays) selection of the most available channels within the set. Other algorithms based on the computation of UCB indices could also have been considered but the use of UCB_1 produces no loss of generality. The UCB_1 index is defined as follows:

$$B_{t,k,T_k(t)} = \overline{X}_{k,T_k(t)} + A_{t,k,T_k(t)}, \tag{6.1}$$

where $\overline{X}_{k,T_k(t)}$ and $A_{t,k,T_k(t)}$ are two terms that represent the exploitation and the exploration contributions, respectively. $\overline{X}_{k,T_k(t)}$ is the empirical mean and it is defined as

$$\overline{X}_{k,T_k(t)} = \frac{\sum_{m=0}^{t-1} r_m \mathbf{1}_{\{a_m=k\}}}{T_k(t)}, \tag{6.2}$$

where r_m and a_m are the achieved reward and selected channel, respectively, at the m-th time slot, and the indicator function is as follows

$$\mathbf{1}_{\{a_m=k\}} = \begin{cases} 1 & \text{if } a_m = k \\ 0 & \text{if } a_m \neq k \end{cases} \tag{6.3}$$

The empirical mean is also proportional to the accumulated throughput by the UCB_1 algorithm when channel k has been selected. $A_{t,k,T_k(t)}$ is the UCB_1 bias (Auer et al., 2002) defined as follows

$$A_{t,k,T_k(t)} = \sqrt{\frac{\alpha \ln(t)}{T_k(t)}}, \tag{6.4}$$

where α is the exploitation-exploration factor of the algorithm. If α increases, UCB_1 bias $A_{t,k,T_k(t)}$ dominates and UCB_1 algorithm explores new channels. Otherwise, if α decreases, UCB_1 bias also does and $\overline{X}_{k,T_k(t)}$ dominates the UCB_1 index $B_{t,k,T_k(t)}$ forcing the algorithm to mostly exploit previous channels (Jouini et al., 2009).

Algorithm 6.1 UCB_1 algorithm

Require: $N, \alpha, \{a_0, r_0, a_1, r_1, \ldots, a_{t-1,} r_{t-1}\}$

Ensure: a_t

```
loop
    if t ≤ N then
        a_t = t + 1
    else
        T_k(t) ← Σ_{m=0}^{t-1} 1_{{a_m=k}}, ∀k
        X̄_{k,T_k(t)} ← (Σ_{m=0}^{t-1} r_m 1_{{a_m=k}}) / T_k(t), ∀k
        A_{t,k,T_k(t)} ← √(α ln(t) / T_k(t)), ∀k
        B_{t,k,T_k(t)} ← X̄_{k,T_k(t)} + A_{t,k,T_k(t)}, ∀k
        a_t = arg max_k (B_{t,k,T_k(t)})
    end if
    return a_t
end loop
```

6.2 Analysed approaches for performance evaluation

UCB_1 and UCB_1-M performances are evaluated in this Thesis from a radio communication point of view in a cognitive radio context instead of the metrics typically used in the machine learning (ML) community. It is worth highlighting that in a ML context, the final goal is to find and to subsequently exploit the best channel in terms of availability, whereas in a cognitive radio context the goal is to find and to exploit any possible available channel to efficiently use the spectrum opportunities. Thus, the selection of the best available channel is not as important as the selection of any available channel at each time slot to establish the communication link. Considering the cognitive radio context, new performance metrics for RL algorithms were presented in (Robert et al., 2014) in terms of transmission opportunities effectively obtained and utilised for data transmission. These new metrics are based on the percentage of time that the RL algorithm selects an available channel, named as 'percentage of successful trials', which can be also seen as the successful transmission rate obtained by RL algorithm.

In this Thesis, the performance evaluations of UCB_1 and UCB_1-M are based on the percentage of successful trials achieved within a set of channels. The metric 'successful transmission rate' is defined as the percentage of transmission opportunities effectively

detected and used to transmit by a secondary user during the whole testing time period. In order to show UCB_1 and UCB_1-M performances in these terms, the following approaches have been defined to facilitate comparisons:

- *Uniform random selection*: the first question that should be answered is: 'Is it worth applying RL for decision making in the HF environment?' If so, 'how much can the performances be improved compared to a non intelligent approach?' Thus, the successful transmission rate achieved by a uniform random channel selection in each set of channels is computed to establish a reference level where no learning is used.
- *Best channel*: from the set of evaluated channels, it is the channel with the longest availability time within the overall testing time (10 minutes), which is considered as the maximum performance achievable under the ML perspective.
- *Worst channel*: it is the channel with the shortest availability time within the overall testing time from the set of evaluated channels.
- *Best opportunistic selection*: Since the algorithm is evaluated for a cognitive radio application, the performances of UCB_1 and UCB_1-M algorithms will be compared with a kind of genie-aided policy, i.e. a policy with a perfect knowledge of the environment's behaviour, where all spectrum holes within the set of evaluated channels are used for transmission achieving a more efficient use of the band. In this approach, the system will use any detected free channel, independently of being or not the channel with the longest availability time.

6.3 An overview of single-channel UCB_1 performance in the HF band

In order to introduce the differences between UCB algorithms and the channel selection approaches defined in Section 6.2, a comparative of the successful transmission rate achieved by each of them is detailed in the following paragraphs. Two parameters must be set in advance to evaluate the UCB_1 algorithm with single-channel selection, the number of channels per group N, and the parameter α that sets the compromise between exploration and exploitation. Here, the selected values correspond to the best configuration of single-channel UCB_1 in the HF band achieved and demonstrated in the evaluation of the exploration vs. exploitation dilemma in Section 6.4: $N = 8$ and $\alpha = 0.4$. With this configuration, the UCB_1 algorithm mainly exploits previously rewarded channels although it explores in a small group where it can take advantage of other existing transmission opportunities.

The comparative of the successful transmission rates achieved by different groups of $N = 8$ channels after the whole execution time (T_{TEST}) of the UCB_1 algorithm and the different approaches presented in Section 6.2 is depicted in Figure 6.1. In spite of the

fact that the comparative of only a short selection of groups of $N = 8$ channels is included in Figure 6.1, they are a representative example of the different cases that can be found in this environment.

The successful transmission rate achieved by the UCB_1 algorithm is compared to (as stated in Section 6.2): the successful transmission rate achieved with a uniform random selection of channels, the best channel's successful transmission rate, the worst channel's successful transmission rate and the maximum successful transmission rate that a cognitive agent could achieve by applying a genie-aided policy with prior knowledge of existing transmission opportunities.

It is shown in Figure 6.1 that the UCB_1 algorithm always outperforms the *uniform random selection* approach. Hence, these results demonstrate that it is worth applying reinforcement learning to dynamically access the HF band.

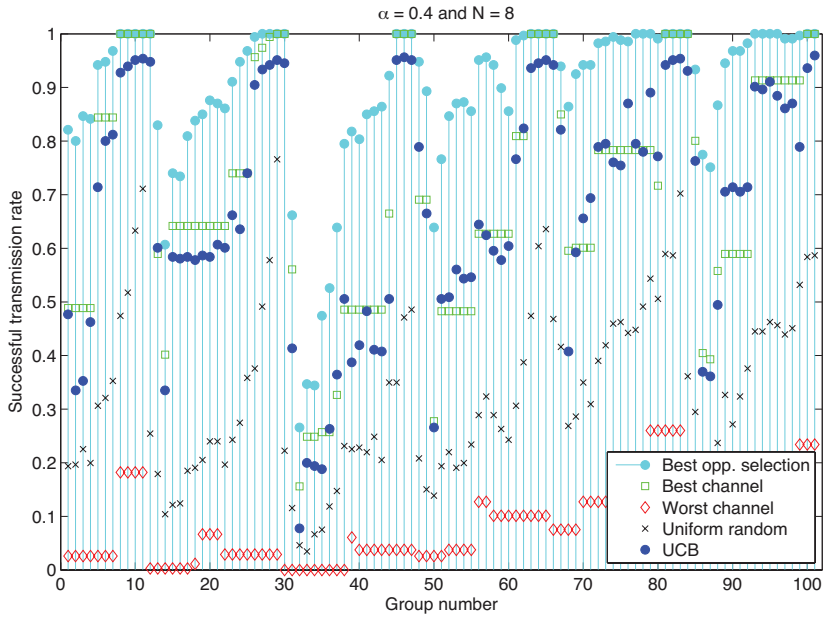

FIGURE 6.1. Comparative of the successful transmission rate per group with $\alpha = 0.4$ and $N = 8$.

Figure 6.2a shows the performance of the UCB_1 algorithm when there are more transmission opportunities than the best available channel, so that the secondary HF user could take advantage of. This occurs when the successful transmission rate of *best channel selection* is lower than the successful transmission rate achieved by the *best opportunistic selection* approach because there are other available channels in the group when the best channel is unavailable. Since the main goal of a cognitive radio is the use of any channel for transmission as long as it is available, the successful transmission rate achieved by the *best opportunistic selection* approach will indicate if the UCB_1 algorithm is suitable for a cognitive radio application. In the framed groups of Figure 6.2a, the UCB_1 algorithm sometimes outperforms the best available channel, but in other groups it cannot outperform it because the successful transmission rate achieved also depends on the occupancy level of the whole set of channels within the group, which directly affects the performance of the algorithm.

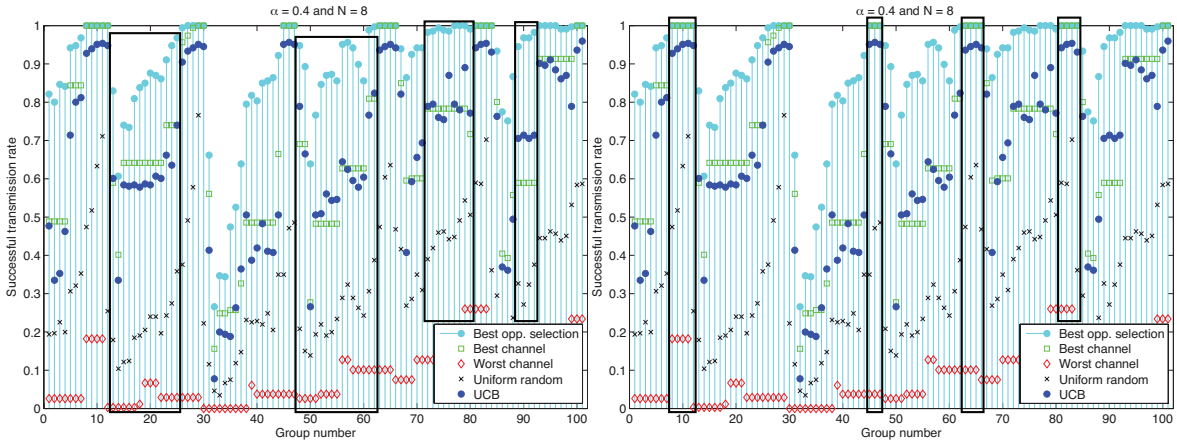

A: UCB_1 outperforms *best channel selection* or it is close to its performance.

B: UCB_1 cannot reach *best opportunistic selection* and *best channel selection* performances.

FIGURE 6.2. Detail of the comparative of the successful transmission rate per group with $\alpha = 0.4$ and $N = 8$.

Figure 6.2b shows the performance of the UCB_1 algorithm when there is a channel available for the whole execution time. In these groups, the successful transmission rate of *best opportunistic selection* is equal to the successful transmission rate of *best channel selection* and equal to one in the comparative in Figure 6.2b. As expected, UCB_1 loses the opportunity to transmit due to the exploration phase of the algorithm but it is close to *best opportunistic selection* in some groups. In addition, its successful transmission rate remains always higher than the successful transmission rate achieved by a *uniform random selection*.

An overview of the performance of single-channel UCB_1 in the HF band has been introduced so far. However, as previously stated, the UCB_1 algorithm can select one (UCB_1) or multiple channels (UCB_1-M) at each time slot. Therefore, the sections that follow will analyse the performance of this algorithm using both single and multiple channel selection strategies by evaluating the influence of the UCB parameters α, N, and M (only for UCB_1-M) on its performance in the HF band.

6.4 The exploration vs. exploitation dilemma in single-channel UCB_1

As previously stated, two parameters must be set before executing the UCB_1 algorithm: the total number N of channels considered within a set, e.g. the number of arms in a MAB approach, and the exploitation-exploration factor α. The value of α is chosen depending on the environment's conditions in terms of activity or presence of primary users, whereas N is determined by the final system restrictions such as the number of channels to explore or the limited number of assigned channels. This section shows how the performance of UCB_1 algorithm with single-channel selection varies according to N

and α parameters, i.e. the exploration vs. exploitation dilemma.

The *best opportunistic selection* approach, i.e. the genie-aided policy, is used for numerical comparisons of the UCB_1 algorithm performance with the other approaches given in Section 6.2. This approach is selected as a reference of the best possible performance because it has prior knowledge of the activity in the band. Therefore, the percentage of successful transmission rate achieved by each approach after 10 minutes of testing time (T_{TEST}) is computed with respect to the successful transmission rate of the *best opportunistic selection* after T_{TEST}, i.e. the maximum achievable successful transmission rate. As previously stated, the maximum testing time is about 10 minutes according to the duration of the acquired measurements in the HFSA_IDeTIC_F1_V01. This time period corresponds to 300 samples of 2 seconds (T_{UCB}) that could not be considered as a large enough amount of samples from a ML perspective which allow for convergence. However, it has been stated and experimentally verified in (Moy, 2014) that in an OSA context UCB_1 learning is sufficient after a small number of time slots.

Figure 6.3 depicts the obtained results when comparing the UCB_1 algorithm and the *best opportunistic selection* for $\alpha \in [0, 5]$, and sets of $N = \{4, 8, 16\}$ channels. It can be observed that for different values of N the best performance is reached at $\alpha = 0.4$. When $N = 4$, UCB_1 can achieve a 81% of the successful transmission rate achieved by *best opportunistic selection* for $\alpha \in [0.4, 1.8]$, and it remains close to this maximum for $\alpha > 1.8$. Nevertheless, when the number of channels within a set increases to $N = 8$ or $N = 16$, the number of channels that UCB_1 has to explore also increases. Thus, if the exploitation-exploration factor α is high, the UCB_1 algorithm will tend to explore more than to exploit the channels that have been previously labelled as available. This fact explains why, when $N = 8$, the best performance (77%) is achieved for $\alpha \in [0.3, 0.4]$, whereas it reaches 79% for $N = 16$ and $\alpha \in [0.2, 0.4]$.

Best channel selection, *uniform random selection*, and *worst channel selection* approaches are also compared in terms of mean percentage of achieved successful transmission rate with respect to the *best opportunistic selection* approach in Table 6.1. Both UCB_1 and *best channel selection* approach surmount in these terms the performance of *uniform random selection* and *worst channel selection* approaches.

TABLE 6.1. Single-channel selection: Mean percentage of successful transmission rate achieved by each approach with respect to best opportunistic selection approach.

	$N = 4$	$N = 8$	$N = 16$
UCB_1 ($\alpha = 0.4$)	81%	77%	79%
Best channel selection	83%	81%	88%
Uniform random selection	53%	39%	35%
Worst channel selection	27%	9%	3%

Another metric that reveals how the UCB_1 algorithm performs in a cognitive radio

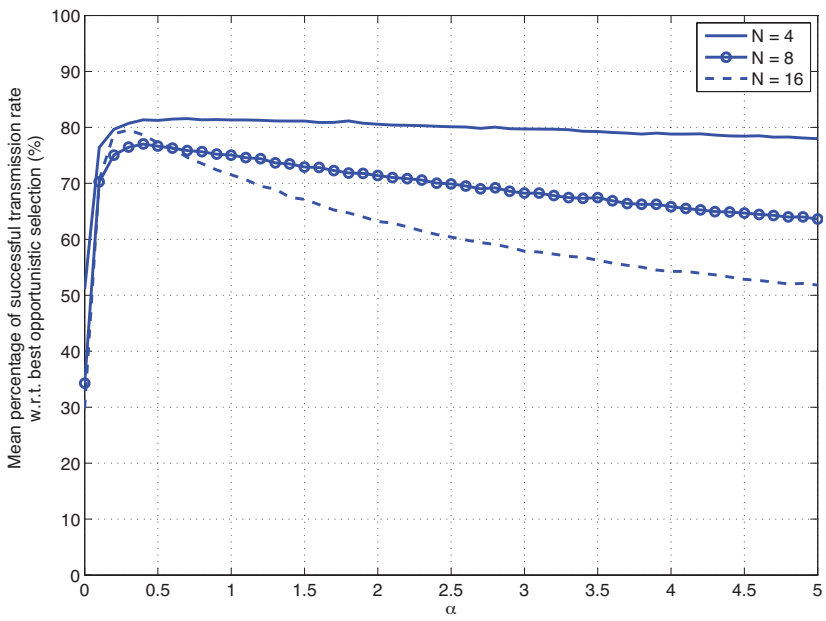

FIGURE 6.3. UCB_1: Mean percentage of successful transmission rate with respect to best opportunistic selection approach vs. α with $N = \{4, 8, 16\}$.

context is the mean percentage of improvement in the successful transmission rate with respect to a uniform random selection of channels, since it also reflects the improvement of applying learning in OSA for the HF environment. This is analysed in Figure 6.4 with $\alpha \in [0, 5]$, and with sets of $N = \{4, 8, 16\}$ channels. The mean percentage of improvement when the size of the set of channels is small ($N = 4$) remains close to 178% for any value of α within the interval $[0.4, 5]$, which is nearly twice as much as that with respect to *uniform random selection* approach. However, the maximum percentage of improvement is reached at $\alpha = 0.4$, with 228% for $N = 8$ and 245% for $N = 16$. This behaviour exhibits the same trend as obtained performances in terms of mean percentage of successful transmission rate with respect to *best opportunistic selection* approach in Figure 6.3. If there is a small set of channels, there are fewer to explore and the variability in the exploitation-exploration factor α does not strongly influence UCB_1 performance. Otherwise, when the size of the set of channels increases, the UCB_1 algorithm will tend to explore more as α increases, thus, it results in a decrease in the percentage of improvement with respect to a uniform random selection.

Note that in Figure 6.3 and Figure 6.4 the exploration vs. exploitation dilemma is highly dependent on the size of the set of channels N. As N increases, the sensitivity of α is higher, the UCB_1 algorithm is forced to explore more channels and the transmissions opportunities are reduced. Due to this fact, in Figure 6.3 and Figure 6.4, as N increases, the interval of values of α where the best performance is reached is also reduced at α close to 0.4.

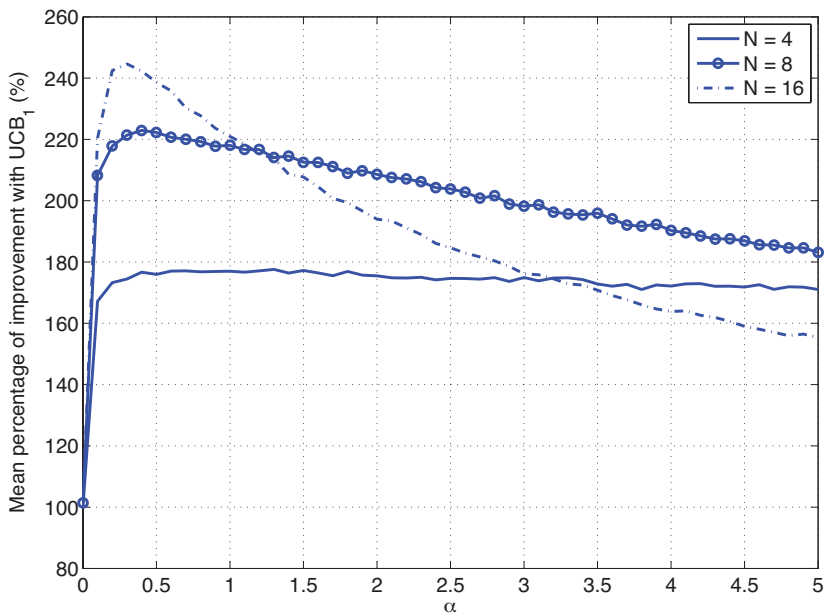

FIGURE 6.4. Percentage of improvement using UCB_1 with respect to uniform random selection approach vs. α with $N = \{4, 8, 16\}$.

6.5 The exploration vs. exploitation dilemma in multi-channel UCB_1 (UCB_1-M)

This Section analyses how the UCB_1 algorithm with multiple-channel selection (UCB_1-M), known as UCB_1-multiple plays, behaves. In order to do that, the same performance metrics and strategies followed in Section 6.4 for the validation of the UCB_1 algorithm with single-channel selection are used. Therefore, an evaluation of the mean percentage of successful transmission rate achieved by each approach defined in Section 6.2 compared to the best possible performance, i.e. *best opportunistic selection* approach, is performed. Unlike the UCB_1 algorithm in the previous analysis where two parameters were defined: N and α, a third parameter is introduced here which is the number of channels M (being $M < N$) that will be selected by the algorithm to transmit.

The obtained results for the UCB_1-M algorithm in the HF environment in terms of mean percentage of successful transmission rate with respect to *best opportunistic selection* are depicted in Figure 6.5. These results are represented for different values of $\alpha \in [0, 5]$, and ratios of $M/N = \{1/8, 1/4, 1/2\}$ with $12 \leq N \leq 30$. When the ratio M/N is high ($M/N = 1/2$), i.e. a higher percentage of channels of N can be jointly selected by the algorithm, the maximum percentage of successful transmission rate achieved by UCB_1-M is equal to 88% of the achieved successful transmission rate achieved by *best opportunistic selection* for values of α within the studied interval. Therefore, it can be concluded that UCB_1-M performance does not strongly depend on α for $M/N = 1/2$. However, when M/N decreases because there are fewer channels for data transmission that can be chosen by the UCB_1-M algorithm ($M/N = 1/4$ and $M/N = 1/8$), its

maximum performance is achieved at $\alpha \in [0.2, 0.4]$ when $M/N = 1/8$, and $\alpha = 0.4$ if $M/N = 1/4$. It is worth noting that this behaviour is identical to single-channel selection UCB_1 in Figure 6.3 when the size of the set of channels N increases. In this case, the UCB_1-M algorithm has a larger set of channels to explore and if α increases, it is forced to explore instead of exploiting the channels previously labelled as available, and consequently it will lose transmission opportunities. This phenomenon is shown in Figure 6.5 for $\alpha = 5$, where the mean percentage of successful transmission rate achieved by UCB_1-M with $M/N = 1/4$ decreases in 6% compared to its maximum at $\alpha = 0.4$, and it decreases in 17% compared to its maximum at $\alpha \in [0.2, 0.4]$ when $M/N = 1/8$.

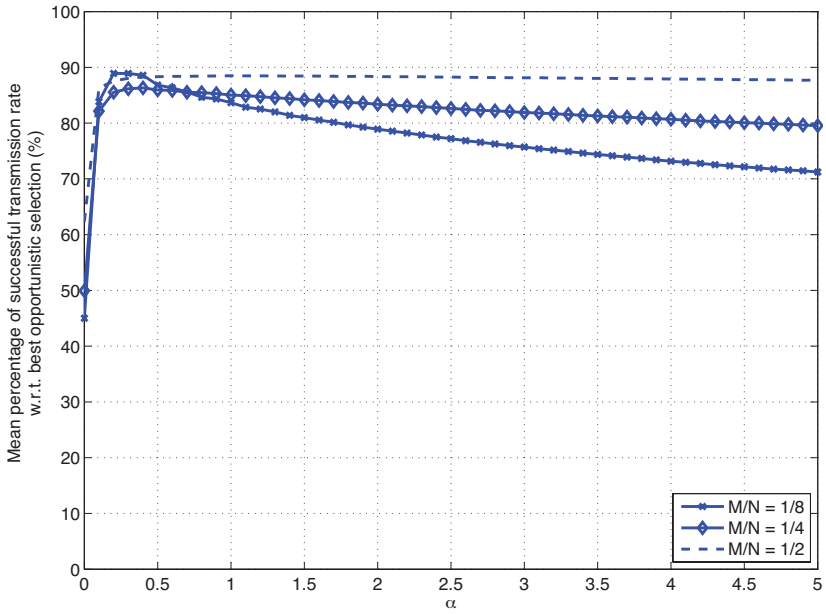

FIGURE 6.5. UCB_1-M: Mean percentage of successful transmission rate with respect to best opportunistic selection approach vs. α with $M/N = \{1/8, 1/4, 1/2\}$.

In Table 6.2, the performance of the UCB_1-M algorithm is also compared to *best channel selection*, *uniform random selection*, and *worst channel selection* approaches. It can be observed that *best channel selection* performs similarly to *best opportunistic selection* because when $M > 1$, these sets of M channels contain channels that are available during the whole testing time, therefore, both achieve the maximum performance. Furthermore, similar to UCB_1 results in Table 6.1, both UCB_1-M and *best channel selection* surmount the performance of *uniform random selection* and *worst channel selection* approaches.

Finally, the mean percentage of improvement using UCB_1-M with respect to a uniform random selection of channels is shown in Figure 6.6, and has been computed as the percentage of improvement in terms of achieved successful transmission rates for values of $\alpha \in [0, 5]$ and $M/N = \{1/8, 1/4, 1/2\}$. When the number of channels that can be selected by the UCB_1-M algorithm is high, i.e. $M/N = 1/2$, UCB_1-M outperforms the uniform random selection by 140% when $\alpha \in [0.4, 5]$. As M/N ratio decreases, the percentage of improvement increases. When $M/N = 1/4$ the percentage of improvement is equal to a 180% for $\alpha \in [0.3, 0.7]$, whereas for $M/N = 1/8$, the maximum percentage

TABLE 6.2. Multi-channel selection: Mean percentage of successful transmission rate achieved by each approach compared w.r.t. best opportunistic selection.

	$M/N = 1/8$	$M/N = 1/4$	$M/N = 1/2$
UCB_1-M ($\alpha = 0.4$)	88%	86%	88%
Best channel selection	100%	92%	92%
Uniform random selection	48%	52%	64%
Worst channel selection	4%	14%	37%

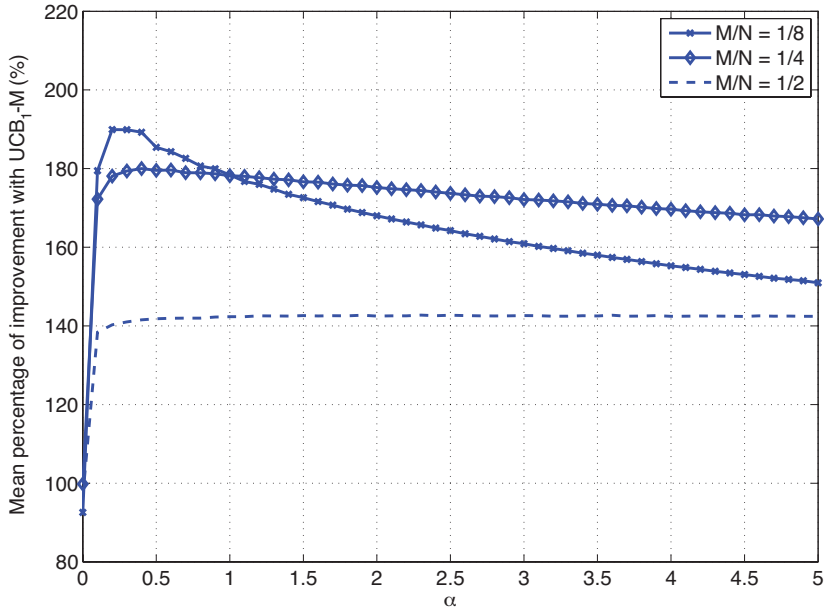

FIGURE 6.6. Percentage of improvement using UCB_1-M with respect to uniform random selection approach vs. α with $M/N = \{1/8, 1/4, 1/2\}$.

of improvement is reached for $\alpha \in [0.3, 0.4]$ and is equal to 190%, being the successful transmission rate of the UCB_1-M algorithm nearly three times higher than the successful transmission rate of the uniform random selection.

As seen in Figure 6.5 and Figure 6.6, the UCB_1-M algorithm performs best in terms of successful transmission rate when the exploitation-exploration factor α is close to 0.4 and $M/N = 1/8$.

6.6 Learning complexity discussion

Currently, the fact that learning is a time demanding task and thus, it can reduce the global system improvement, is a common belief. The successful transmission rate has been evaluated so far as the rate of transmission opportunities successfully used without considering that the UCB_1 algorithm may require some time in the 2 seconds slot (T_{UCB}) for its learning stage. Nevertheless, in this section we will show that the

execution time required by UCB_1 is marginal compared to the set time slot of 2 seconds of the HFSA_IDeTIC_F1_V01 database.

Generally speaking, a simple study of how this common belief could affect the global performance to compare it with a uniform random selection, a non-learning approach, is here introduced. This study depicted in Figure 6.7 shows the mean required time by both approaches to transmit a certain quantity of data, 100 KB and 150 KB, with respect to the learning time. It is assumed that, for each T_{UCB} slot, the execution of the learning technique requires some percentage of time within the T_{UCB} slot and, in case of a successful transmission, the transmission data rate is 3600 bps, which is one of the transmission rates of the HFDVL system (Pérez-Álvarez et al., 2009). Since the measurements of the HFSA_IDeTIC_F1_V01 database have a duration of $T_{TEST} = 10$ minutes and the transmission data rate is 3600 bps, the maximum amount of data that could be transmitted would be 270 KB in this case study.

In Figure 6.7 it is shown that to transmit 100 KB, a learning technique such as UCB_1 would require less time to transmit than a uniform random selection when the learning phase lasts for less than a second, which is a 50% of the considered time slot. If the data size increases to 150 KB, the learning technique would also outperform a uniform random selection when the learning phase lasts for less than 0.8 seconds, a 40% of the considered time slot.

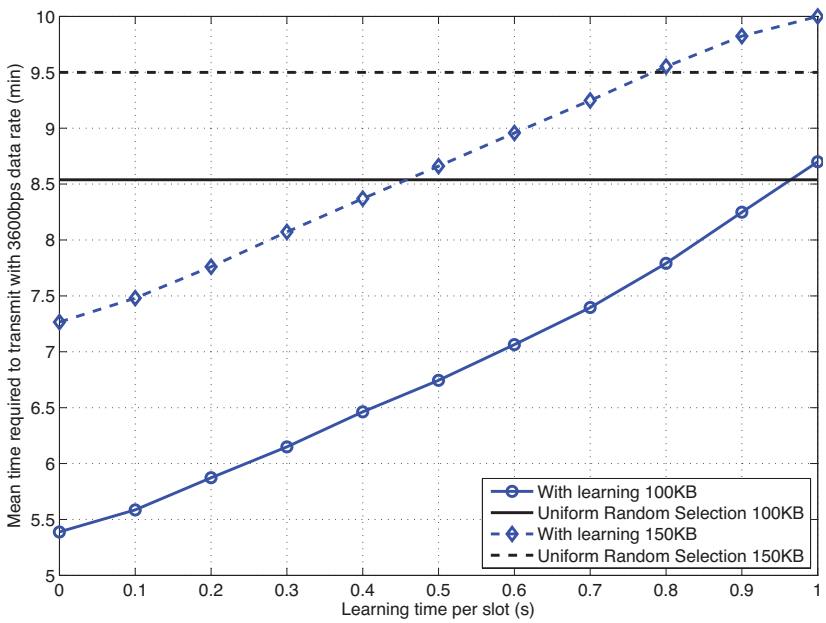

FIGURE 6.7. Required time to transmit 100 KB and 150 KB with 3600 bps data rate vs. learning time.

Nonetheless, the learning phase of UCB_1 algorithm only computes a few operations at each T_{UCB}. For the set of N channels, the UCB_1 index and the exploration contribution $A_{k,T_k(t)}$ are updated following Equations (6.1) and (6.4), respectively. However, the empirical mean can be updated according to the selection made in the previous iteration $t-1$ with Equation (6.5). In other words, it will be updated depending on whether

channel k was the action selected in the previous iteration as a_{t-1} or not.

$$\overline{X}_{k,T_k(t)} = \begin{cases} \frac{r_{t-1}-\overline{X}_{k,T_k(t-1)}}{T_k(t)} + \overline{X}_{k,T_k(t-1)} & \text{if } a_{t-1} = k \\ \overline{X}_{k,T_k(t-1)} & \text{if } a_{t-1} \neq k \end{cases} \tag{6.5}$$

where the number of times that channel k has been selected by the algorithm in previous iterations, $T_k(t)$, is updated as

$$T_k(t) = \begin{cases} T_k(t-1)+1 & \text{if } a_{t-1} = k \\ T_k(t-1) & \text{if } a_{t-1} \neq k \end{cases} \tag{6.6}$$

If a general-purpose microprocessor is considered to be used to run the UCB_1 algorithm, its execution time will depend on its own structure and its task scheduling. Although it could be guessed that most of the computations required to run UCB_1 are mathematical operations that may be executed in a few clock cycles, the global execution time cannot be estimated without considering a particular architecture.

Despite this, an example is included here to give a better idea of the mathematical complexity of UCB_1 and UCB_1-M algorithms. In this example, the UCB_1 learning workload is compared to the sensing workload with an energy detector in terms of mathematical operations to compute. If it is assumed that the energy detector takes 100 ms to sense a channel with 3 kHz bandwidth and 10 kHz sampling rate, it will take 1000 samples in 100 ms. Therefore, it will have to compute the squared modulus of each sample and sum up all the samples of each slot, that is, 2 squares and 2 additions per sample. Since 1000 samples are obtained each slot, the energy detector computes 4000 mathematical operations. On the contrary, as detailed before, the UCB_1 algorithm computes N times Equations (6.1) and (6.4), and only once for the selected channel Equations (6.5) and (6.6). These equations result in $N+2$ additions, $N+1$ divisions, N square roots, N multiplications, N natural logarithms and 1 subtraction, in all $5\times N+4$ mathematical operations each slot. For the best configuration of UCB_1 in the HF band ($N = 8$ and $\alpha = 0.4$) this results in 44 mathematical operations each slot. This UCB_1 learning workload is a 1.1% of the sensing workload, thus showing that the workload of the UCB_1 algorithm is marginal compared to the sensing workload. It can be also concluded that the required execution time by the UCB_1 algorithm is marginal compared to the T_{UCB} slot of acquired HF measurements in the HFSA_IDeTIC_F1_V01 database.

Therefore, the obtained results in Figure 6.7 for a learning time equal to zero seconds can be considered as the real performance of the UCB_1 algorithm showing that UCB_1 outperforms a random uniform selection. In average, UCB_1 takes 5.5 minutes instead of 8.5 minutes to transmit 100 KB of data and 7.3 minutes instead of 9.5 minutes to transmit 150 KB.

Furthermore, if the multi-channel selection UCB_1 (UCB_1-M) algorithm is considered, it computes N times Equations (6.1) and (6.4), and M times Equations (6.5) and (6.6) for the set of selected channels to transmit. These equations result in $N+2\times M$ additions, $N+$

M divisions, N square roots, N multiplications, N natural logarithms and M subtractions, in all $5\times N+4\times M$ mathematical operations each slot. For the best configuration of UCB_1-M in the HF band, which corresponds to $M/N = 1/8$ with $N = 24$ and $\alpha = 0.4$, this results in 132 mathematical operations. Its learning workload is a 3.3% of the sensing workload, therefore showing that the workload of the UCB_1-M algorithm is also marginal compared to the sensing workload, and thus, its execution time is also marginal compared to the T_{UCB} slot of the used database.

From previous examples, it may seem that an unfair comparison has been made between energy detection and UCB_1 and UCB_1-M algorithms since all the mathematical operations have been considered equivalent in terms of computational complexity. Spectrum sensing via energy detection only computes additions and multiplications, but UCB_1 and UCB_1-M algorithms also compute divisions, square roots, and natural logarithms. However, the computation of divisions and square roots of n digits has the same computational complexity as the selected algorithm for the computation of multiplications ($O(M(n))$) (Brent & Zimmermann, 2010). Therefore, the only mathematical operation that UCB_1 and UCB_1-M require with a higher computational complexity than those required by energy detection is the natural logarithm, whose complexity is $O(M(n)\cdot\ln(n))$ if the arithmetic-geometric mean algorithm is used (Brent & Zimmermann, 2010). Although the natural logarithm has a higher complexity, there is still a significant difference between learning and sensing in terms of mathematical operations to compute as previously detailed.

6.7 Summary

In this Chapter, the use of Upper Confidence Bound algorithms has been proposed for HF users to dynamically access the spectrum. Both single-channel and multiple-channel strategies of UCB_1 (UCB_1 and UCB_1-M) have been tested under an opportunistic spectrum access model with the HFSA_IDeTIC_F1_V01 database of real measurements of the HF band.

Since the metrics of the machine learning community do not reflect if the UCB_1 algorithm is suitable for a cognitive radio context, a new metric based on the successful transmission rate achievable in different approaches has been proposed. The obtained results demonstrate that both UCB_1 and UCB_1-M outperforms a random uniform selection even in the worst conditions in terms of availability. Hence, they confirm that it is worth applying reinforcement learning to opportunistically access the HF band.

The feasibility in the HF band of the Upper Confidence Bound (UCB) algorithm has been also demonstrated by analysing the exploration vs. exploitation dilemma. Both single-channel and multiple-channel versions of UCB_1 (UCB_1 and UCB_1-M) achieve the best trade-off between exploration and exploitation in the HF environment when the exploitation-exploration factor α is equal to 0.4, meaning that UCB_1 and UCB_1-M try

to exploit more the channels previously labelled as *available* instead of exploring new channels.

Finally, the complexity introduced by UCB_1 and UCB_1-M algorithms has been analysed. A comparative between UCB_1 and UCB_1-M algorithms and an energy detector for spectrum sensing has been presented in terms of mathematical operations to compute. Although all these mathematical operations do not have the same computational complexity, it has been shown that UCB_1 and UCB_1-M algorithms require mathematical operations such as divisions and square roots that have the same complexity as multiplications, and the only mathematical operation with a higher complexity is the natural logarithm. The results of the comparative evidenced that UCB_1 and UCB_1-M learning workloads are marginal compared to the sensing workload with an energy detector. Therefore, their execution time is also marginal compared to the T_{UCB} slot of the used database, showing that UCB_1 and UCB_1-M learning can be executed within a short time interval of the considered T_{UCB} slot of the database.

Chapter

7

Hybrid UCB-HMM Learning Scheme - A Metacognitive Engine

The cognitive engine of a cognitive radio is formed by the algorithms that provide a cognitive radio with learning and decision-making capabilities (Gadhiok et al., 2011). A metacognitive engine has been recently presented in the literature (Asadi et al., 2015) as a higher-layer agent that selects a specific cognitive engine according to the observed changes in the environment. Since each cognitive engine cannot be reliable for all situations in the surrounding environment, the most suitable is dynamically selected.

In this Thesis, two learning methods have been presented and can be considered as cognitive engines: the HF primary user dynamics prediction model based on HMMs developed in Chapter 5 and the UCB_1-M algorithm evaluated in Chapter 6. The HMM based prediction model proposed in Chapter 5 was designed to make long-term predictions (1 minute duration) with low complexity in a specific HF channel. However, its straight application in a multi-band scenario for opportunistic spectrum access requires as much HMM based prediction models as the number of channels to sense and transmit. It is worth mentioning that the HMM based prediction model was designed as a single-channel prediction model due to its simplicity, while one HMM based prediction model that learns multiple channels simultaneously is more complex than multiple HMM based prediction models working in parallel (Melián-Gutiérrez et al., 2013).

Furthermore, the UCB_1-M algorithm evaluated in Chapter 6 was presented as a solution to select the best channels for data transmission. While the HMM based prediction model predicts the activity in a specific HF channel in the long-term, the UCB_1-M algorithm performs short-term predictions (2 seconds duration) and allows for a decision-making strategy.

A significant aspect that has not been considered so far in this Thesis is that signalling

is required to coordinate any transmission and reception processes. Both sides of the communication link can be interconnected for link management with an in-band or an out-band channel. In fact, cognitive radio systems do require link management, for instance a Cognitive Pilot Channel (CPC) has been proposed in (Cordier *et al.*, 2006). This link management could be an in-band or out-band channel that informs secondary users about the channels' status. In this Chapter, channel signalling is considered to coordinate transmitter and receiver sides in HF communications. Due to HF communication rate limitation and its link instability, whatever the adopted signalling solution is, it is highly recommended to efficiently manage the amount of signalling information to be exchanged between transmitter and receiver. Therefore, in this Thesis, channel signalling is defined as the amount of transmissions needed to inform the receiver about the selected channels for data transmission.

A hybrid solution combining learning with HMM and reinforcement learning with UCB_1-M is proposed in this Chapter as a metacognitive engine approach. If the conditions of the environment allow the establishment of long-term data transmissions according to the predictions of the HMM based prediction model, channel signalling can be significantly decreased with respect to short-term prediction methods such as UCB_1-M since it is only updated once in a period of one minute. On the contrary, if the environment's conditions worsen, short-term data transmissions can be established though required channel signalling increases. Therefore, the main goals of the hybrid UCB-HMM system are: (1) to decrease the amount of signalling information exchanged between transmitter and receiver, (2) to reduce the complexity of N HMM based models working in parallel, and (3) to adapt slots of data transmission to the behaviour of the environment. Finally, it is worth noting that the application of this metacognitive solution in the HF environment arises new requirements on current HF systems, which will be discussed in Chapter 8.

7.1 Hybrid UCB-HMM system description

The UCB_1-M and HMM learning methods run in parallel in the proposed scheme over two transmission slots; a short-term slot of 2 seconds with UCB_1-M (T_{UCB}), and a long-term slot using HMM predictions of 1 minute duration (T_{HMM}). The same data segmentation of the HFSA_IDeTIC_F1_V01 database (see Figure 5.1) is hereafter considered.

Achievable data rates in the HF environment are very small, which make longer transmissions preferable when sending higher amounts of data. The proposed scheme is able to automatically adapt its configuration to the changes in channels' activity, which means that if there are plenty of available channels for transmission during a minute, the hybrid UCB-HMM system will switch to long-term transmission slots following the predictions of M HMMs working in parallel (M-HMMs), being $M < N$. Nevertheless, if the environment changes and most of the channels are unavailable or partially-available, it will transmit in a short-term slot following the decisions of the UCB_1-M algorithm. This is

indeed a cognitive radio procedure that selects different cognitive engines according to the conditions of the environment, e.g. a metacognitive radio engine (Asadi et al., 2015).

If only short-term predictions and transmissions are accomplished, the channel signalling used for link management between transmitter and receiver will increase. This increase occurs if UCB_1-M is only used in the system, as it has to predict channels' activity every 2 seconds (T_{UCB}) and, therefore, it will require a higher number of signalling transmissions. However, in the proposed hybrid scheme, channel signalling will decrease when it switches to M-HMMs to transmit according to their predictions over a minute (T_{HMM}). For each channel predicted as available in the next minute by a HMM, the transmitter will send selected channel frequency to the receiver only once during this one minute slot, thereby reducing thirty times (T_{HMM}/T_{UCB}) the channel signalling and, therefore, increasing feedback information capacity. This reduction factor remains at a constant value throughout the entire execution of the proposed hybrid scheme since M-HMMs are trained before their use for prediction and there is no added workload.

Furthermore, the hybrid UCB-HMM allows for a reduction in the complexity of N HMM working in parallel by combining two learning methods. This combination only requires M HMM with $M < N$ and the UCB_1-M algorithm to select the M best channels in terms of availability from a larger set of N channels, which is not nearly as complex (Melián-Gutiérrez, Modi, et al., 2015b). The sections that follow will show that the best of both learning methods is exploited in the hybrid UCB-HMM scheme.

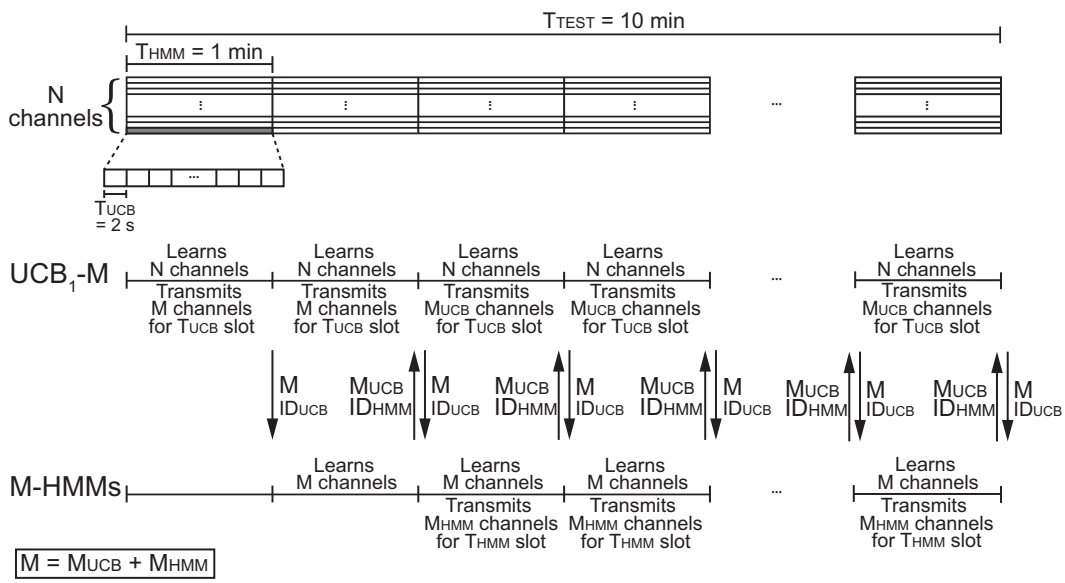

FIGURE 7.1. Time execution of the hybrid UCB-HMM system with M HMM based prediction models and UCB_1-M algorithm.

The hybrid UCB-HMM system is described in Algorithm 7.1 (Page 96) and Figure 7.1, where a simplified diagram is depicted. During its execution, the UCB_1-M algorithm selects the M best channels with short-term predictions in T_{UCB} slots, and subsequently, these channels are learnt by M-HMMs to predict their activity in a long-term slot, T_{HMM}. Hence, M-HMMs' effort is optimised as M-HMMs are executed in the M best available

Algorithm 7.1 Hybrid UCB-HMM algorithm

Require: N, M, α

Init.: $\mathrm{M_{UCB}} = M$, $\mathrm{M_{HMM}} = 0$, slot $= 0$, $\mathrm{T_{UCB}} = 2$ s, $\mathrm{T_{HMM}} = 1$ min, $\mathrm{ID_{UCB}} = \varnothing$, $\mathrm{ID_{HMM}} = \varnothing$

```
loop
  if t = slot + T_HMM then
    slot ← t
    if ID_UCB ≠ ∅ then
      Predict with M-HMMs
      ID_HMM ← indices (channels predicted as free)
      M_HMM ← size (ID_HMM)
      M_UCB ← M − M_HMM
      M-HMMs SEND UCB_1-M: M_UCB, ID_HMM
    end if
    ID_UCB ← indices (M highest B_{t,k,T_k(t)})
    UCB_1-M SENDS M-HMMs: M, ID_UCB
  end if
  t ← t + T_UCB
  Compute UCB_1-M
  TX in M_UCB channels ∈ N \ ID_HMM
  if ID_UCB ≠ ∅ then
    M-HMMs save sensing information of ID_UCB channels
    if ID_HMM ≠ ∅ then
      TX in M_HMM channels ∈ ID_HMM
    end if
  end if
end loop
```

channels of the whole set of N channels, e.g. in those channels with the longest availability time during next T_{HMM} to establish longer data transmissions.

Two sets are modified during the execution of the hybrid UCB-HMM system to avoid any conflict between both learning methods: ID_{UCB}, which contains the M best channels selected by UCB_1-M, and ID_{HMM}, which includes channels predicted by M-HMMs as available for the next T_{HMM} slot. Both learning methods update and transmit their sets to each other at every T_{HMM} according to their predictions as described in lines 9 and 12 of Algorithm 7.1.

There is an initialization phase where only UCB_1-M is learning during T_{HMM} over N channels until it extracts which are the M best available channels (see line 11 of Algorithm 7.1 and Figure 7.1). After the first T_{HMM} slot, it transmits the M best channels in the set ID_{UCB} to M-HMMs. During the second T_{HMM} slot (see Figure 7.1), each HMM will learn one of the M best channels to predict which of them will be available, partially available or unavailable for the next T_{HMM} slot. While M-HMMs are learning, UCB_1-M continues its execution and transmits in at most M channels in T_{UCB} slots. Once M-HMMs have learnt for a T_{HMM} slot, ID_{HMM} set is modified to contain those channels predicted as available for the next T_{HMM} slot, and sent to UCB_1-M algorithm jointly with the maximum number of channels M_{UCB} where UCB_1-M can transmit in the next T_{HMM} slot (see lines 4-10 of Algorithm 7.1). At this instant (at the beginning of the third T_{HMM} slot) both learning methods start transmitting in their corresponding channels, M-HMMs in M_{HMM} channels from the set ID_{HMM} and UCB_1-M in M_{UCB} channels from the relative complement of ID_{HMM} in N ($N \setminus ID_{HMM}$), being $M = M_{UCB} + M_{HMM}$. Thus, the hybrid UCB-HMM system always tries to transmit in the M maximum number of assigned channels. Note that M-HMMs execution is restricted to T_{TEST} - $2 \cdot T_{HMM}$ due to the initialization phase of the proposed hybrid UCB-HMM system shown in Figure 7.1.

7.2 Performance evaluation

The performance of the proposed hybrid UCB-HMM system is hereafter evaluated by depicting the benefits of the combination of the UCB_1-M and HMM learning methods. The same selection of measurements of the HFSA_IDeTIC_F1_V01 database used in Chapter 6 to evaluate UCB_1 and UCB_1 algorithms is used to evaluate the proposed hybrid UCB-HMM system in this Chapter. This selection contains the measurements with the worst conditions in terms of availability: amateur channels of 3 kHz each located from 14.07 MHz to 14.14 MHz (see Figure 3.6), and recorded when the 14 MHz amateur band was heavily occupied.

In the subsequent Sections, the proposed hybrid UCB-HMM system is evaluated with the exploitation-exploration factor $\alpha = 0.4$, according to the configuration of the UCB_1-M algorithm that attained the best performance in Chapter 6. The ratio between the number of channels that the algorithm can use to transmit (M) and the total number of

channels within a set (N) is set to $M/N = \{1/8, 1/4, 1/2\}$ where M changes its value but N remains at a constant value equal to 24.

7.2.1 Successful transmission rate

The validation of the UCB_1-M algorithm in Section 6.5 was carried out based on successful transmission rates, attaining its best performance for $\alpha = 0.4$ and $M/N = 1/8$. Figure 7.2 depicts the comparison of the achieved successful transmission rate after each T_{HMM} slot by the hybrid UCB-HMM system and the UCB_1-M algorithm with $\alpha = 0.4$ and $M/N = \{1/8, 1/4, 1/2\}$. As described in Figure 7.1, T_{TEST} is restricted to 10 minutes and long-term data transmissions according to M-HMMs predictions start after $2{\cdot}\text{T}_{\text{HMM}}$ slots (2 minutes). It can be observed in Figure 7.2 that the UCB_1-M algorithm and the hybrid UCB-HMM scheme learning gradually increases and so does the successful transmission rate from minute 1 to minute 1.7. At this point, both UCB_1-M and the proposed hybrid scheme are close to their maximum performances for $M/N = \{1/8, 1/4, 1/2\}$. The best successful transmission rate is achieved by the proposed hybrid UCB-HMM with $M/N = 1/8$, since it exploits 99% of the transmission opportunities from the third minute when M-HMMs start transmitting and the learning process is almost done (see Figure 7.2 at minute 3). This successful transmission rate is 4% higher than that achieved when $M/N = 1/4$, and 20% higher than that achieved when $M/N = 1/2$. Note that the global performance of the proposed hybrid UCB-HMM is highly dependent on the initial selection of the M best channels made by the UCB_1-M algorithm and, as shown in Section 6.5 for UCB_1-M, the best performance is achieved for $\alpha = 0.4$ and $M/N = 1/8$.

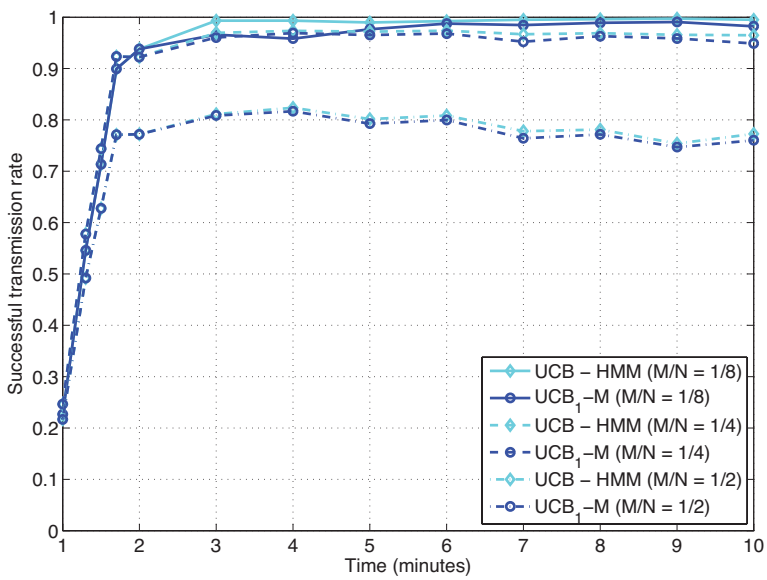

FIGURE 7.2. Successful transmission rate of the hybrid UCB-HMM system and UCB_1-M with $\alpha = 0.4$ and $M/N = \{1/8, 1/4, 1/2\}$.

7.2.2 Metacognitive strategy

As previously stated, the proposed hybrid UCB-HMM solution exhibits the same behaviour as a metacognitive radio engine (Asadi et al., 2015) since it changes its learning method, also known as cognitive engine, based on changes in the environment. The proposed solution switches from short-term transmissions to long-term transmissions when there is an improvement in the environment's conditions as regards availability. Nevertheless, if the environment's conditions worsen, it will switch from long-term transmissions to short-term transmissions. It is important to remark that this adaptability enhances the proposed hybrid UCB-HMM performance to achieve its goals, namely to transmit data in long-term slots when the environment is favourable and to reduce the amount of channel signalling between transmitter and receiver.

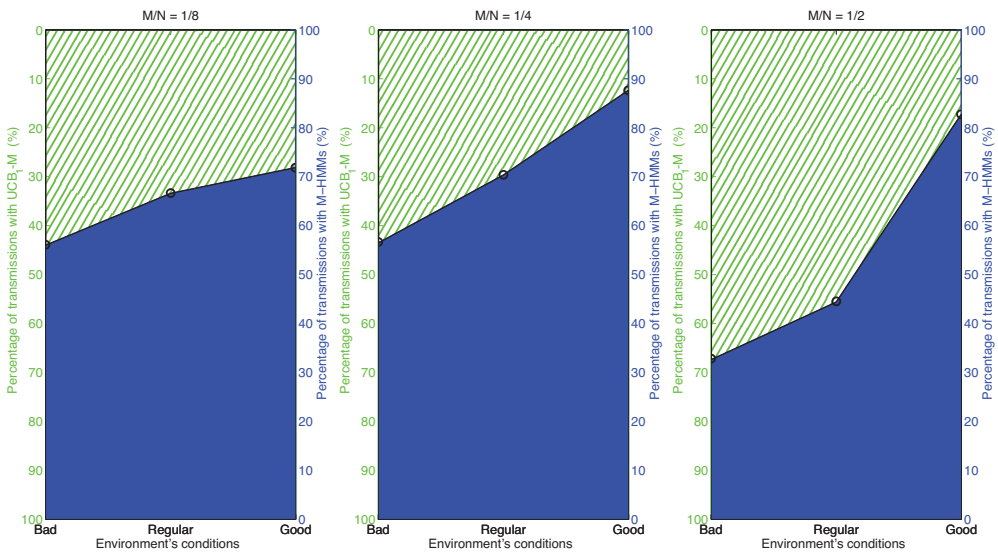

FIGURE 7.3. Mean percentage of long-term (M-HMMs) and short-term (UCB_1-M) transmissions in the proposed hybrid UCB-HMM system with $M/N = \{1/8, 1/4, 1/2\}$ vs. environment's conditions.

Figure 7.3 illustrates the transmission adaptability of the proposed hybrid UCB-HMM scheme for $M/N = \{1/8, 1/4, 1/2\}$. The mean percentage of channels used for transmission by each cognitive engine (UCB_1-M or M-HMMs) is represented versus the status of the environment in terms of availability. Three different scenarios are defined following the same classification of the HFSA_IDeTIC_F1_V01 database: a 'good scenario' where most of the N channels are completely available, a 'regular scenario' where most of the N channels are partially available, and a 'bad scenario' where most of the N channels are unavailable.

Figure 7.3 shows that an increase in the number of channels classified as *available* lead to a decrease in the percentage of channels used for short-term transmissions according to UCB_1-M predictions, whereas the percentage of channels transmitting in a long-term basis according to M-HMMs predictions increases. This increase in the percentage of channels used for long-term transmissions (or inversely the decrease in the percentage of channels used for short-term transmissions) when the environment's conditions improve

is about 16% for $M/N = 1/8$, 31% for $M/N = 1/4$, and 50% for $M/N = 1/2$. It is shown that the highest increase in the percentage of channels used for long-term transmissions is reached when $M/N = 1/2$. It occurs because as M increases, the proposed hybrid UCB-HMM has to transmit in a higher number of channels, and, in 'bad scenarios', it is more difficult to take advantage of all possible transmission opportunities within the total set of N channels. Thus, in 'bad scenarios' it switches to UCB_1-M for 68% of data transmissions in the short-term whereas in 'good scenarios' it reaches 83% of data transmissions in the long-term.

7.2.3 Analysis of the duration of data transmission's slots

An analysis of the duration of data transmission's slots of each cognitive engine of the proposed hybrid UCB-HMM is also noteworthy. Figure 7.4 and Figure 7.5 show the histogram of data transmission's slots made by both learning methods when they are executed in this hybrid UCB-HMM scheme with respect to their slots' duration. These results include the performance of the proposed hybrid UCB-HMM with $M/N = \{1/8, 1/4, 1/2\}$.

Figure 7.4 shows that, for $M/N = 1/8$, 94% of data transmission's slots according to UCB_1-M predictions have a duration of less than 0.2 minutes (12 seconds). As M/N increases to $M/N = 1/4$ and $M/N = 1/2$, i.e., the number of channels for transmission increases, UCB_1-M transmission's slots also increase their duration to at most 2 minutes. Therefore, the percentage of transmissions' slots with a duration less than 12 seconds is reduced to 70%. This reduction is due to the fact that the set of channels that can be chosen to transmit is larger and thus, the probability of having more available channels for longer periods also increases.

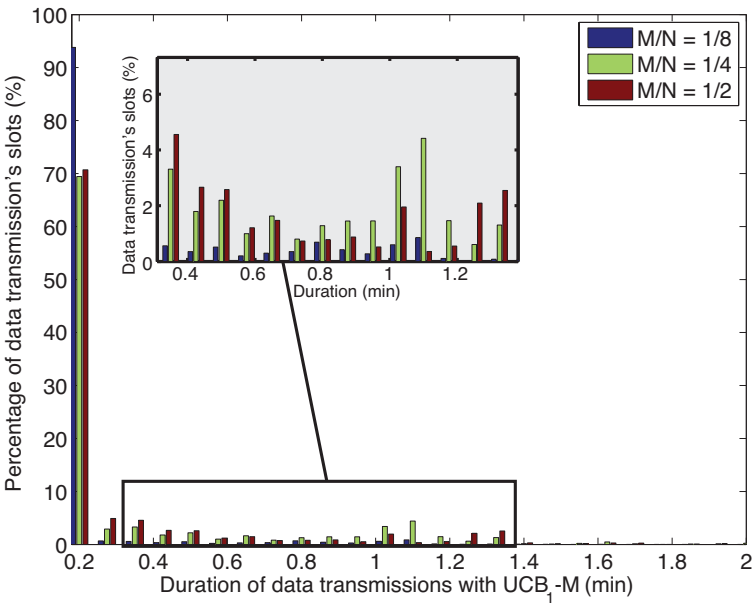

FIGURE 7.4. Histogram of data transmission's slots according to UCB_1-M predictions in the proposed hybrid UCB-HMM system vs. slots' duration.

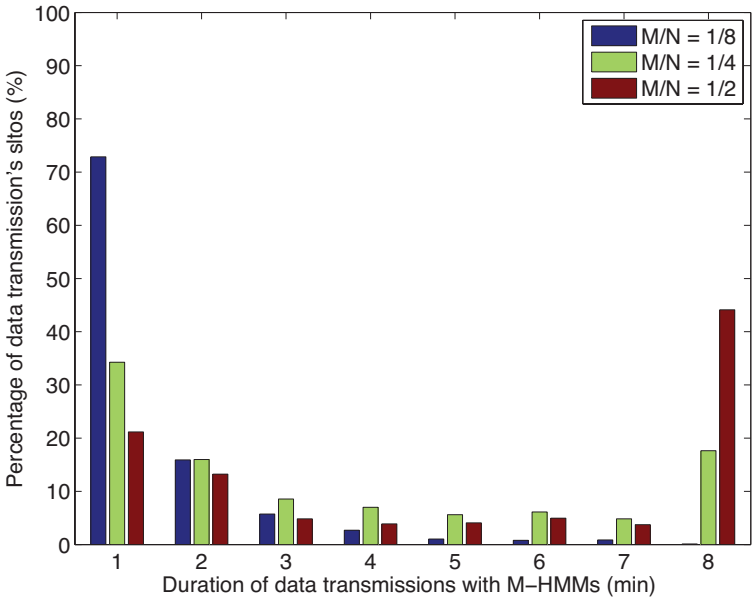

FIGURE 7.5. Histogram of data transmission's slots according to M-HMMs predictions in the proposed hybrid UCB-HMM system vs. slots' duration.

This effect can also be observed in Figure 7.5, where the histogram of data transmission's slots according to M-HMMs predictions is depicted. When the value of the ratio M/N is small ($M/N = 1/8$), 73% of data transmission's slots have only one minute length according to M-HMMs predictions. However, as M/N increases to $1/4$ and $1/2$, this percentage decreases to 34% when $M/N = 1/4$ and to 21% when $M/N = 1/2$, whereas the percentage of data transmission's slots of 8 minutes according to M-HMMs predictions without shifting to other channels increases to 18% when $M/N = 1/4$ and to 44% when $M/N = 1/2$. Therefore, in order to exploit longer data transmissions, M/N must be set to $1/2$ or $1/4$.

7.2.4 Channel signalling improvement

A reduction in the complexity of N parallel HMM based prediction models is not the only aim of the hybrid UCB-HMM system. A second objective is to simplify the link management between transmitter and receiver. This simplification can be seen as a reduction in the channel signalling due to the possibility of establishing long-term transmissions by using slots of $T_{HMM} = 1$ min with M-HMMs predictions instead of short-term transmissions during slots of $T_{UCB} = 2$ s with UCB_1-M predictions. This Section demonstrates that the channel signalling load of the hybrid UCB-HMM scheme is affordable to be used in the HF environment.

A comparison of the proposed UCB-HMM system to the M parallel HMMs and UCB_1-M algorithms working separately and independently is shown in Figure 7.6 with the aim of analysing the amount of required channel signalling. As mentioned previously, channel signalling is the amount of transmissions needed to inform the receiver about

the selected channels for data transmission. Therefore, when M-HMMs are used for prediction and transmission, the selection of M channels for data transmission is updated and transmitted to the receiver once every T_{HMM} slot. Nevertheless, UCB_1-M requires more channel signalling because it updates and transmits the selection of M channels every T_{UCB} slots.

Figure 7.6 shows that the required channel signalling by the proposed hybrid UCB-HMM scheme with $M/N = \{1/8, 1/4, 1/2\}$ after T_{TEST} is higher than that of M-HMMs but lower than UCB_1-M. It is important to remark that the required channel signalling by M-HMMs, hybrid UCB-HMM system, and UCB_1-M algorithm increases when M/N also does due to the fact that the number of channels that can be used to transmit (M) is increasing too. However, even if the maximum number of channels to explore in the hybrid UCB-HMM system is considered ($N = 30$), the amount of signalling transmissions and channel signalling load required to coordinate transmitter and receiver are totally affordable, even if coding and redundancy are considered to protect the channel signalling load. The most demanding configuration of the hybrid scheme is when $N = 30$ and $M/N = 1/2$, which allows simultaneous data transmissions in at most $M = 15$ channels. In this configuration, 5 bits are needed to identify each channel for the set of $N = 30$. The highest channel signalling load to send will be $5 \times M = 5 \times 15 = 75$ bits every 2 seconds, i.e. when only UCB_1-M is used to transmit in the short-term due to poor environment's conditions. If these conditions improve, less than M channels will be used in the short-term and the channel signalling load will decrease.

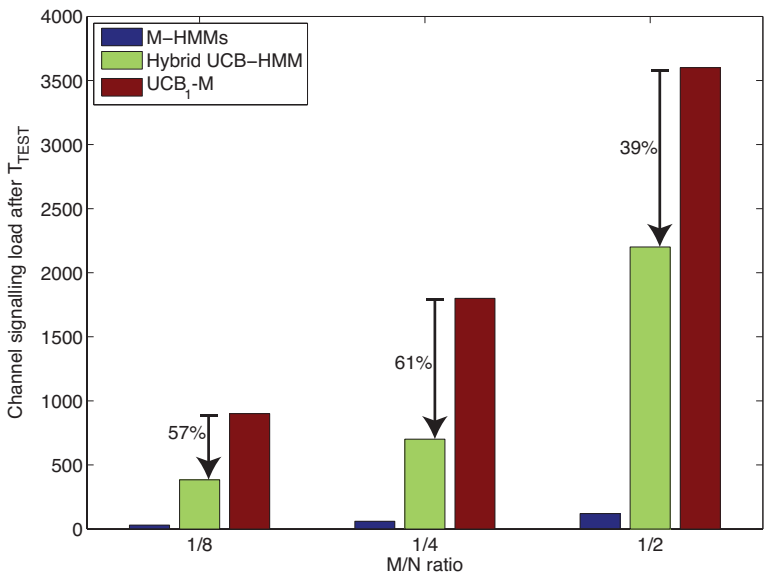

FIGURE 7.6. Required channel signalling by M-HMMs, UCB_1-M and proposed hybrid UCB-HMM system vs. M/N ratio.

The attained reduction in channel signalling by the proposed hybrid UCB-HMM with respect to that required by the UCB_1-M algorithm was also computed. It is worth mentioning that as UCB_1-M updates the selection of channels for data transmission every T_{UCB} slots, it is the learning method that requires the highest amount of channel signalling as

defined in this Thesis. Figure 7.6 shows that required channel signalling by the hybrid UCB-HMM system is equivalent to a reduction of 57% when $M/N = 1/8$, 61% when $M/N = 1/4$ and 39% when $M/N = 1/2$. It was shown in Figure 7.2 that the proposed UCB-HMM system has similar successful transmission rates to UCB_1-M. However, as the proposed hybrid UCB-HMM system switches to long-term transmissions, required channel signalling is significantly reduced for all M/N ratios. This clearly demonstrates the benefits of the proposed hybrid UCB-HMM system compared to each learning method used separately.

In order to exploit hybrid UCB-HMM system's capability to transmit data for longer slots according to the environment's conditions, a trade-off between achieved successful transmission rate, the duration of data transmissions, and the reduction of channel signalling must be found. The depicted results reveal that this trade-off can be accomplished by selecting $M/N = 1/4$. With this configuration, the proposed hybrid UCB-HMM achieves 95% successful transmission rate, and reduces by 61% required channel signalling compared to that required by the UCB_1-M algorithm.

7.3 Summary

A new hybrid scheme based on a metacognitive engine approach has been proposed in this Chapter. This hybrid scheme combines two separate cognitive engines: the UCB_1-M algorithm (evaluated in Chapter 6) and M parallel HMM based prediction models for the HF band (described in Chapter 5 and named in this Chapter as M-HMMs).

The hybrid UCB-HMM system adapts its transmission strategy according to the changes in the environment. If the conditions of the environment are favourable, long-term data transmissions can be established according to M-HMMs predictions, thereby reducing required channel signalling as defined in this Thesis. When these conditions worsen, the hybrid UCB-HMM system establishes short-term data transmissions according to UCB_1-M predictions.

The proposed hybrid UCB-HMM system with $\alpha = 0.4$ and ratio $M/N = 1/4$ achieves its best performance: 95% of successful transmission rate is achieved as long as it automatically adapts its configuration to the changes in the environment. An 88% of data transmissions are established in the long-term (1 minute) according to M-HMMs predictions when the activity in the band decreases whereas 44% of the data transmissions are established in the short-term (2 seconds) according to UCB_1-M predictions when the activity in the band increases.

Furthermore, the link management of cognitive radio can be significantly reduced by using the proposed hybrid UCB-HMM since long-term transmissions are established, and required channel signalling is reduced by 61% with respect to that required by the UCB_1-M algorithm. These results were obtained by evaluating the proposed hybrid system with

real measurements of the HFSA_IDeTIC_F1_V01 database.

Chapter

8

Conclusions and Future Work

Cognitive Radio has been proposed in this Thesis as a solution for the inefficient use of the HF band. This band allows the establishment of beyond-line-of-sight links but multiple collisions between HF users arise even if they are legacy users. These collisions occur because frequency bands are mainly assigned by national regulators. Thus, any HF user is a legacy user within its frontiers but it establishes a link that can surpass them.

The Automatic Link Establishment (ALE) protocol for HF radios has been presented as a primitive form of cognitive radio in the literature (Fette, 2009). Although it is based on a listen before transmit strategy to avoid interfering with on-going communications, channels are only ranked according to their propagation characteristics since ALE does not monitor the users' activity in the recent past. Furthermore, this mechanism can take several seconds to correctly establish a link in a single channel. Due to these limitations, it could not be applied in its current form since cognitive radio requires a more dynamic mechanism than ALE to perform dynamic spectrum access.

The cognitive cycle presented by Mitola in (Mitola & Maguire, 1999; Mitola, 2000) resumes the tasks that a cognitive radio should face. In this Thesis, it has been simplified to three main phases: Observe, Learn, and Decide & Act, and a solution for the application of each phase in the HF environment has been proposed.

Observe

A cognitive radio must listen its surrounding environment to be aware of the changes that occur and to be aware of the activity of primary and other cognitive users. Once it has observed, it has to perform the spectrum sensing task, i.e. translate the acquired knowledge into other means of information that reveal the existence of spectrum holes

for future transmissions.

In this Thesis, a database of real measurements of the HF band has been created to show the feasibility of the application of cognitive radio in this band. As detailed in Chapter 3, this database contains wideband power measurements of 200-300 HF channels of 3 kHz bandwidth recorded simultaneously during 10 minutes. This amount of channels correspond to measurements with a span of 640 kHz - 1.28 MHz. The 14 MHz band was selected due to the presence of amateur and non-amateur HF users, who generate several activity patterns. A selection of the acquired measurements of 640 kHz was included in the HFSA_IDeTIC_F1_V01 database, which has been used to test and validate the proposals of Chapters 5, 6 and 7. An extended version of this database with measurements of 1.28 MHz (HFSA_IDeTIC_F1_V02) has been utilised to evaluate the proposal of Chapter 4.

An energy detector has been proposed in Chapter 3 to perform the spectrum sensing task. The energy detector transforms power samples into normalised values that represent primary users' activity. This primary user detection technique was selected due to the heterogeneity observed during the acquisition campaign of the database. The designed energy detector maximises the detection probability for a given false alarm following the Neyman-Pearson lemma (Kay, 1998) to establish the power threshold that differentiates occupied-channels samples from only-noise samples.

One of the disadvantages of sensing the spectrum with wideband receivers is that they can suffer from narrowband interference (NBI). This effect was observed during the acquisition campaign of the database with the wideband HF transceiver developed in (Pérez-Díaz et al., 2009). The presence of NBI in the received wideband signal causes a reduction in the effective number of bits used for the digitalization of the signals of interest and thus, the quantization noise exceeds the thermal noise and the desired signal itself (Pérez-Díaz et al., 2012).

A solution for NBI detection in wideband HF receivers has been proposed in Chapter 4. The NBI detector is based on compressive sensing techniques that allow for a reduction in the hardware complexity since a sampling system with a low-rate ADC is used. Two steps must be performed in compressive based systems (Candès, 2006): the acquisition with a low-rate ADC and the signal reconstruction from the compressed samples. In this Thesis, the random demodulator (Tropp et al., 2010) is the sampling system due to its hardware simplicity and the CoSaMP algorithm (Needell & Tropp, 2009) is the selected algorithm to identify the frequency location of the most representative components in the wideband signal.

The proposed NBI detector works in parallel with a wideband receiver. It has been provided with adaptability to the changes in the environment by modifying its configuration according to the status of the AGC of the wideband receiver. Therefore, its performance has been characterised depending on the number of interfering signals to detect. When there is only one strong interfering signal, it achieves a detection rate of 92% and

a false alarm rate of 8% if only one component is desired to be detected. Nevertheless, in those scenarios where there are more representative signals, the proposed NBI detector is able to reach a 97.8% detection rate and 4% false alarm rate if more than 15 frequency components are desired to be detected.

Finally, the behaviour of the random demodulator has been characterised in a real scenario and compared against its theoretical study in (Tropp et al., 2010). The obtained results reveal that the empirical performance with signals from real environments has the same trend as the theoretical behaviour.

LEARN

One of the capabilities that characterise a cognitive radio is learning. By learning from the environment, a cognitive radio can predict the activity of primary users and, therefore, improve its performance as well as make a more efficient use of the spectrum resources.

Two learning strategies have been proposed in Chapters 5 and 6 with different prediction spans. A long-term prediction scheme based on learning with Hidden Markov Models (Rabiner & Juang, 1993) have been presented in Chapter 5, while a short-term prediction scheme based on reinforcement learning, particularly the Upper Confidence Bound algorithm (Agrawal, 1995; Auer et al., 2002), has been proposed in Chapter 6.

The prediction model defined in Chapter 5, which is based on Hidden Markov Models (Rabiner & Juang, 1993), models the dynamics of primary users in the HF band. It is based on HMMs because they are a powerful and robust tool for modelling stochastic random processes. The proposed model is built from three interconnected submodels that describe three type of channels: available channels, unavailable channels and partially available channels.

Since the proposed model was trained and validated with real measurements of the HF band, it could be used as a sequence generator of the activity patterns of different HF users, but its use as a predictive model has been proposed in this Thesis. This model predicts the activity in a specific channel within the next minute. Therefore, it allows for long-term transmissions without executing the prediction model within a minute for further predictions. It has been designed as a single-channel prediction model due to its simplicity, since one HMM based prediction model that learns multiple channels simultaneously is more complex than multiple HMM based prediction models working in parallel.

The obtained results with real measurements of the HF band show that the proposed model can predict the activity within next minute with an average 10.3% error rate when it has learned the activity for the last minute. If the acquired knowledge from the channel activity extends to the previous 8 minutes, the error rate is reduced to 5.8%.

A second learning strategy has been defined in Chapter 6. The Upper Confidence

Bound algorithm has been presented as a solution for learning the activity of HF primary users in the short-term as well as a solution for decision-making in an opportunistic spectrum access scenario.

DECIDE & ACT

Learning is followed by decision making in a cognitive radio. Once the cognitive radio has learned, it has to decide which are the best channels to transmit and which configuration is the more suitable for the observed environment. In many proposals likewise the work of this Thesis, learning and decision making can be executed at the same time. This occurs when the proposed UCB_1 and UCB_1-M algorithms in Chapter 6 are executed, since they learn from the observed channels and they also decide which are the best available channels in the next time slot.

UCB_1 and UCB_1-M algorithms have been proposed in Chapter 6 to opportunistically access the HF band. UCB_1 selects the best channel to transmit in terms of availability within a set of N explored channels, whereas UCB_1-M is able to select the M best available channels within a set of N, being $M < N$. Differently to the HMM based prediction model, these algorithms are executed in a short-term time slot of 2 seconds to perform predictions and decisions in the short-term. They have been evaluated with the acquired measurements from the HF band, and by analysing the exploration vs. exploitation dilemma, it has been demonstrated that these algorithms are feasible in this band.

The metric "successful transmission rate" was defined as the percentage of transmission opportunities effectively detected and used to transmit by a secondary user during the whole testing time period. It has been used to compare UCB_1 and UCB_1 algorithm with the selection of the best available channel, the selection of the worst available channel, a uniform random selection of channels, and the best opportunistic selection of channels which is a genie-aided policy with perfect knowledge of the environment's behaviour.

The obtained results show that UCB_1 and UCB_1-M achieve the best trade-off between exploration and exploitation in the HF environment when the exploitation-exploration factor α is equal to 0.4. With this value of α, UCB_1 and UCB_1-M try to exploit more the channels previously labelled as available instead of trying to explore new channels. Furthermore, these results reveal the benefits of applying reinforcement learning to opportunistically access the HF spectrum with respect to a uniform random selection of channels. The mean percentage of improvement can be as high as 245% for UCB_1 and 190% for UCB_1-M with respect to a uniform random selection of channels.

Finally, a hybrid UCB-HMM system is proposed in Chapter 7 as a metacognitive engine approach which combines learning with HMMs and the UCB_1-M algorithm. Each cognitive engine is selected according to the conditions of the environment as regards availability. Both learning methods run in parallel in the proposed scheme over two transmission slots; a short-term slot with UCB_1-M and a long-term slot with the HMM based prediction model. This hybrid scheme also allows for decision making over these

two time slots according to the predictions of both learning strategies.

The hybrid UCB-HMM system comes up as a solution with a lower complexity than N HMM based prediction models working in parallel in a multi-channel system. Furthermore, it also reduces the required channel signalling between transmitter and receiver sides compared to that required by the UCB_1-M algorithm since long-term transmissions can be established according to the long-term predictions of the HMM based prediction models. Therefore, the hybrid UCB-HMM system has been designed to meet three main goals: to decrease the amount of signalling information exchanged between transmitter and receiver, to reduce the complexity of N HMM based prediction models working in parallel, and to adapt slots of data transmission to the behaviour of the environment.

The proposed hybrid system has also been evaluated with real measurements of the HF band. The obtained results reveal that it is able to automatically adapt its configuration to the changes in channels' activity. The proposed solution switches from short-term transmissions to long-term transmissions when there is an improvement in the environment's conditions as regards availability. Nevertheless, if the environment's conditions worsen, it switches from long-term transmissions to short-term transmissions.

The proposed hybrid UCB-HMM system performs best when $\alpha = 0.4$ and the ratio between the number of channels for transmission and the number of channels for exploration M/N is equal to $1/4$. With this configuration, 95% of successful transmission rate is achieved as long as it automatically adapts its configuration to the changes in the environment. An 88% of data transmissions are established in the long-term (1 minute) according to M-HMMs predictions when the activity in the band decreases whereas 44% of the data transmissions are established in the short-term (2 seconds) according to UCB_1-M predictions when the activity in the band increases. Furthermore, the required channel signalling for link management is significantly reduced by 61% with respect to that required by the UCB_1-M algorithm.

8.1 Future Work

In this Thesis, the feasibility of the proposed learning strategies has been demonstrated via simulations with real measurements of the HF band in a high-level platform such as Matlab. A future work is their implementation in hardware, e.g. by means of application-specific integrated circuits (ASIC) or field-programmable gate arrays (FPGA).

However, there are some considerations that must be examined before. Classical HF systems, such as STANAG 4285 or STANAG 4539, are frame-based systems based on single-carrier modulation which, in order to be robust, require long interleavers of several seconds (in some cases more than tens of seconds), equalizers, and high densities of pilot symbols. This overhead surpass the short-term time slot of 2 seconds considered in this Thesis for UCB_1 and UCB_1-M algorithms and the hybrid UCB-HMM scheme. Fur-

thermore, current HF standards for link management, such as STANAG 5066, incur in more overhead and do not support a dynamic spectrum access as required by cognitive radio. Thus, new HF communication strategies should be considered to implement the cognitive based proposals of this Thesis.

Following the trend of new standards in radio communications such as Long-Term Evolution (LTE) (3GPP TS 36.201, 2015) or Digital Video Broadcasting - Terrestrial (DVB-T) (ETSI EN 301 701, 2008), the use of multi-carrier modulations such as Orthogonal Frequency Division Multiplexing (OFDM) has also been proposed for HF communications. One of these multi-carrier modems for HF communications, named as HF Data+Voice Link (HFDVL), has been designed and evaluated in the HF band by the research group where this Thesis has been developed in (Pérez-Álvarez et al., 2003), (Santana-Sosa, Pérez-Álvarez, et al., 2006), and (Pérez-Álvarez et al., 2009). This system is based on Orthogonal Frequency Division Multiplexing - Code Division Multiplexing (OFDM-CDM), which does not require interleavers, and has a point-to-point transmission delay of 125 ms with a net data rate of 2460 bps. Therefore, it is an appropriate physical layer platform to implement the cognitive based proposals of this Thesis.

As a future work of this Thesis, a protocol with lower overhead than STANAG 5066 has to be designed to support the channel signalling exchange in the hybrid UCB-HMM system proposed in Chapter 7. As demonstrated in Section 7.2.4, the channel signalling load required by this hybrid system to coordinate transmitter and receiver is totally affordable for use in the HF environment, even if coding and redundancy are used to protect the channel signalling load. Thus, the remaining tasks are the design and implementation of a simpler mechanism with a light overhead for link management than the specified by the STANAG 5066.

Finally, another issue that is proposed for future work of this Thesis is the design and implementation of a narrowband interference mitigation scheme. In Chapter 4, a NBI detector has been defined and validated for wideband HF receivers. Once NBI is detected before the digitalisation phase, there remains a need to mitigate NBI in the analog domain as detailed in the scheme proposed in Section 4.3. Although this restriction entails a higher complexity in the design and implementation of this mitigation system, there is no alternative to implement it in the digital domain because the signal degradation occurs in the analog domain.

Appendix

A

Radio Cognitiva en Comunicaciones HF: Transmisión Selectiva y Adquisición de Banda Ancha

Más de 3000 kilómetros recorrió la primera señal telegráfica enviada desde Poldhu, Reino Unido, y recibida por Guglielmo Marconi en Newfoundland, ahora en Canadá (Simons, 1996), en diciembre de 1901. Se trataba del establecimiento del primer enlace radio transoceánico y, de hecho, fue lo que convenció a Marconi de que se podía implantar un servicio de radiocomunicaciones transoceánico.

Hasta el momento no había evidencia científica que demostrara cómo era la propagación de las ondas de radio en estos enlaces transoceánicos. Los científicos de la época, tras los estudios de Maxwell y Hertz (Maxwell, 1873) (Hertz, 1893), compartían la idea de que las ondas de radio se propagaban en línea recta al igual que la luz, limitando las comunicaciones radio a enlaces con visión directa entre transmisor y receptor. Sin embargo, los estudios realizados basados en la difracción de las ondas en una superficie esférica no explicaban la reflexión de las ondas de radio que permitía enlaces a mayores distancias que los enlaces con visión directa (Ratcliffe, 1974) (Maslin, 1987).

Fue en 1902, un año después del primer enlace transoceánico realizado por Marconi, cuando los científicos Arthur Kennelly and Oliver Heaviside afirmaron que existía una capa conductora en la atmósfera terrestre responsable de la reflexión de las ondas de radio (Kennelly, 1902). Esta capa, conocida también como la capa Kennelly-Heaviside (Ratcliffe, 1974), permitía el establecimiento de enlaces radio más allá del horizonte. Pero no fue hasta 1925 cuando se obtuvo una evidencia clara de la existencia de esta capa (Appleton, 1932). Appleton y Barnett compararon el efecto del desvanecimiento en cada

Este apéndice contiene un resumen en Español del trabajo realizado en esta Tesis. No incluye todos los detalles descritos en los capítulos previos.

una de las señales recibidas. Al haberse propagado por diferentes caminos, consiguieron demostrar que cada una había sido reflejada por varias capas en la atmósfera situadas a diferente alturas y juntas componían una zona ionizada de la atmósfera: la ionosfera.

Cuando las ondas de radio llegan a las capas ionizadas de la atmósfera, algunas son completamente absorbidas mientras que otras son reflejadas hacia la Tierra, dependiendo de su frecuencia. Es precisamente la banda de frecuencias de HF la que permite la transmisión de ondas de radio de frecuencias entre 3 y 30 MHz, ya que son reflejadas por la ionosfera. Dependiendo de la frecuencia, la hora del día o la ionización de la ionosfera, una señal puede rebotar una o múltiples veces hasta llegar al receptor que puede estar situado a miles de kilómetros del receptor.

De las capas que forman la ionosfera, tres de ellas son las que influyen en el establecimiento de las comunicaciones HF: las capas D, E y F. La capa más baja, la capa D, es donde tiene lugar la mayor absorción. La capa E permite la propagación durante el día en enlaces de menos de 2000 km pero, al caer la noche, su ionización es residual. Finalmente, la capa F es la más importante en el establecimiento de comunicaciones HF ya que tiene una mayor ionización. Se divide en las capas F_1 y F_2 durante el día, y durante la noche, ambas se fusionan para formar la capa F. La mayoría de las ondas con frecuencias en el rango de la banda de HF atraviesan la capa F_1 y son reflejadas por la capa F_2, siendo la capa F_2 la principal capa de reflexión de las comunicaciones en la banda de HF. Debido a esta estructura de la ionosfera, las ondas con frecuencias entre 10 y 30 MHz atraviesan las capas D y E y son reflejadas por la capa F_2 durante el día. Sin embargo, durante la noche, sólo las ondas con frecuencias entre 3 y 8 MHz son reflejadas por la capa F.

Al depender significativamente de factores naturales como la radiación solar, la localización geográfica, la hora del día o los ciclos de actividad solar, cada enlace establecido en la banda de HF puede sufrir diferentes condiciones de propagación. Esta limitación hizo que el interés en las comunicaciones HF decayera en la década de 1970 al comenzar las comunicaciones vía satélite (Maslin, 1987). Sin embargo, las propias limitaciones de las comunicaciones vía satélite demostraron con el paso de los años que las comunicaciones HF son necesarias y, en casos de emergencia como desastres naturales o humanos, son la alternativa vital a las comunicaciones vía satélite para establecer enlaces sin visión directa entre transmisor y receptor.

Dado que la banda de HF es una banda de comunicaciones global, está sujeta a regulaciones internacionales por parte de la Unión Internacional de Telecomunicaciones (ITU, International Telecommunication Union) y de reguladores nacionales. Aunque pueda parecer contradictorio, la mayoría de las frecuencias de esta banda son asignadas por reguladores nacionales. Ello conlleva a la aparición de múltiples colisiones entre usuarios con licencia de diferentes países, ya que, gracias al carácter transoceánico de las comunicaciones HF, éstas pueden cruzar las fronteras de sus respectivos países.

A.1 Motivación

Las comunicaciones HF hacen generalmente uso del protocolo de establecimiento automático del enlace ALE (Automatic Link Establishment). Se trata del estándar de facto aceptado a nivel global para el establecimiento de enlaces HF (NTIA/ITS, 1998). El protocolo ALE está basado en la estrategia de escuchar antes de transmitir (LBT, Listen Before Transmit) para evitar interferir a otros usuarios y, es por ello, que se ha presentado en la literatura como una forma primitiva de radio cognitiva (Fette, 2009).

Existen dos versiones del protocolo ALE, 2G ALE definido en los estándares MIL-STD-188-141A y FED-STD-1045, y 3G ALE definido en el estándar MIL-STD-188-141B (Apéndice C) y adoptado por STANAG 4538, aunque no tan utilizado actualmente como el 2G ALE (Furman & Koski, 2009). Ambas generaciones del protocolo ALE fueron diseñadas para seleccionar automáticamente el mejor canal según una clasificación interna de canales en función de las características de propagación de cada enlace posible entre dos estaciones. Las estaciones HF que hacen uso del protocolo ALE escanean la lista de canales preseleccionados cuando no están transmitiendo para evaluar la calidad del enlace con otra estación HF y con cada uno de los canales. Tras la decodificación de las formas de onda definidas en el protocolo ALE, se calculan la tasa de error de bit (BER, bit error rate), la relación señal más ruido más distorsión respecto a ruido más distorsión (SINAD) y las estadísticas sobre multi-trayecto para clasificar los enlaces entre estaciones y con un determinado canal en la tabla sobre la calidad del enlace (LQA, Link Quality Analysis).

A pesar de que ambas versiones del protocolo ALE siguen la estrategia de escuchar antes de transmitir y seleccionan los canales acorde a las estadísticas de propagación recogidas en la tabla LQA, ambos tienen varios inconvenientes: no monitorizan el espectro con un sistema de banda ancha, no evalúan a tiempo real cada uno de los canales antes de utilizarlos (Furman & Koski, 2009) ni monitorizan la actividad de otros usuarios en ellos. Además, ambos protocolos pueden tardar varios segundos en establecer el enlace. Por lo tanto, es necesario implementar nuevos mecanismos que permitan establecer enlaces HF de una manera más dinámica y sin colisionar con otros usuarios con licencia. Nuevas capacidades como adaptabilidad y cognición deben ser incluidas en las estaciones HF para reducir el uso ineficiente de la banda en términos de acceso satisfactorio al espectro.

Los principios de radio cognitiva surgieron como una posible solución a la escasez de recursos disponibles en el espectro. Proponen un uso oportunista de las bandas que no estén siendo utilizados por los usuarios con licencia para transmitir en ellas (Haykin, 2005) (Federal Communications Commission, 2005). El objetivo principal de radio cognitiva es dotar de inteligencia a los sistemas de comunicaciones de manera que sean capaces de aprender del entorno radio y adaptar su configuración para transmitir en las bandas que no estén siendo utilizadas por los usuarios con licencia en ellas. Así, al aplicarse los principios de radio cognitiva, se utilizarán los recursos disponibles en el espectro

eficientemente.

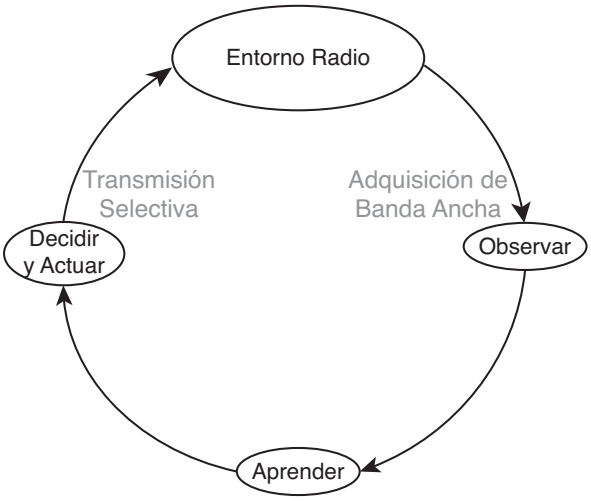

FIGURA A.1. Ciclo simplificado de tareas cognitivas: *Observar*, *Aprender* y *Decidir y Actuar*.

El proceso cognitivo conlleva tres principales tareas que se ejecutan en el orden establecido por el denominado ciclo cognitivo (Mitola & Maguire, 1999; Mitola, 2000; Haykin, 2005), cuya versión simplificada está representada en la Figura A.1. Se trata de las tareas de *Observar*, *Aprender* y *Decidir y Actuar* que representan el ciclo desde la adquisición de información sobre el estado del espectro hasta la selección del mejor canal de transmisión de acuerdo con lo observado y aprendido de la actividad del resto de usuarios.

- OBSERVAR: El primer paso a realizar es la detección de actividad de otros usuarios, *spectrum sensing* (Yucek & Arslan, 2009). Consiste en la adquisición del espectro en términos de potencia para monitorizar la actividad de los usuarios en la banda analizada.
- APRENDER: La radio cognitiva aprende la información obtenida durante la tarea de *spectrum sensing* y analiza la actividad de los usuarios en la banda para predecir futuros patrones de actividad.
- DECIDIR Y ACTUAR: Una vez que ha aprendido sobre la actividad en la banda, toma la decisión sobre cuál es la mejor estrategia para acceder al espectro disponible y transmitir. Esta tarea es conocida en la literatura como *decision-making* (Hossain & Bhargava, 2007)(Hossain et al., 2009), y está relacionada con las diferentes estrategias de acceso al espectro.

Varios estudios han analizado los retos y las oportunidades de la aplicación de radio cognitiva en las comunicaciones de HF (Koski & Furman, 2009; Furman & Koski, 2009; Vanninen et al., 2014). En ellos, los autores han destacado que múltiples cambios han de aplicarse en los sistemas HF para evitar las colisiones entre usuarios. Además, han propuesto nuevas especificaciones para futuras versiones del protocolo ALE basadas en los principios de radio cognitiva.

A.2 Objetivos y Metodología

Si los principios de radio cognitiva son incluidos en las estaciones HF, se estima que el espectro podría ser explotado de una manera más eficiente ya que las estaciones HF serían conscientes de los cambios en el entorno y podrían aprender de él. Para lograr esta mejora, las estaciones deberán ser capaces de cambiar su configuración para adaptar sus transmisiones a las zonas del espectro que ellas mismas han predicho como disponibles.

Por lo tanto, el objetivo principal de esta Tesis es evaluar y demostrar la viabilidad de la aplicación de radio cognitiva a las comunicaciones HF. Dado que las estaciones HF han de ejecutar el ciclo cognitivo de tareas dibujado en la Figura A.1, se definen los objetivos secundarios de esta Tesis a partir de este ciclo cognitivo.

- OBSERVAR: Varios objetivos han de cumplirse para poder implementar adecuadamente la tarea de *spectrum sensing*:
  - Para poder evaluar el trabajo realizado en esta Tesis en un entorno real debe crearse una base de datos de medidas del espectro de HF. Éstas han de ser medidas de banda ancha que contengan la potencia observada en la banda de HF con el transceptor de HF desarrollado en (Pérez-Díaz et al., 2009). Al utilizar un transceptor de banda ancha, se pueden detectar múltiples canales simultáneamente así como evaluar las estrategias cognitivas propuestas.
  - Definir y evaluar una estrategia para realizar la tarea de *spectrum sensing* que convierta la información del entorno HF en datos sobre la actividad de sus usuarios.
  - Diseñar un detector de interferencias de banda estrecha (NBI, narrowband interference) para receptores de banda ancha que pueda ser implementado en el dominio analógico. La existencia de ondas de superficie en la banda de HF (Maslin, 1987) disminuye el número efectivo de bits utilizados para la digitalización de las señales de interés, provocando que el ruido de cuantificación sea superior al ruido térmico y a las señales de interés (Pérez-Díaz et al., 2012).
- APRENDER: Se define un único objetivo secundario en la fase de aprendizaje:
  - Definir y validar una estrategia de aprendizaje de la actividad de los usuarios de HF. Debe ser capaz de predecir si un determinado canal HF estará ocupado o no, tanto a corto plazo como a largo plazo.
- DECIDIR Y ACTUAR:
  - Definir y validar una estrategia de *decision-making* para seleccionar la mejor estrategia de transmisión acorde a lo observado y aprendido por el sistema cognitivo previamente.

A.3 Publicaciones relacionadas con la Tesis

Como resultado del trabajo realizado en esta Tesis, varios trabajos han sido presentados a congresos y revistas internacionales. A continuación se detalla la lista de publicaciones actualizada de la autora de esta Tesis.

MELIÁN-GUTIÉRREZ, L., MODI, N., MOY, C., BADER, F., PÉREZ-ÁLVAREZ, I., & ZAZO, S. (2016). Hybrid UCB-HMM: A Machine Learning Strategy for Cognitive Radio in HF Band. *IEEE Transactions on Cognitive Communications and Networking*. doi: 10.1109/TCCN.2016.2527021

MELIÁN-GUTIÉRREZ, L., GARCIA-RODRIGUEZ, A., PÉREZ-ÁLVAREZ, I., & ZAZO, S. (2015). Compressive Narrowband Interference Detection for Wideband Cognitive HF Front-Ends. *Wireless Personal Communications (Submitted)*.

MELIÁN-GUTIÉRREZ, L., MODI, N., MOY, C., PÉREZ-ÁLVAREZ, I., BADER, F., & ZAZO, S. (2015a, May). DSA with Reinforcement Learning in HF Band. In *1st URSI Atlantic Radio Science Conference (AT-RASC)*. Gran Canaria, Spain.

MELIÁN-GUTIÉRREZ, L., MODI, N., MOY, C., PÉREZ-ÁLVAREZ, I., BADER, F., & ZAZO, S. (2015b, June). Upper Confidence Bound Learning Approach for Real HF Measurements. In *IEEE International Conference on Communications Workshops (ICC Workshops)* (p. 281-286). London, UK.

MELIÁN-GUTIÉRREZ, L., ZAZO, S., BLANCO-MURILLO, J., PÉREZ-ÁLVAREZ, I., GARCÍA-RODRÍGUEZ, A., & PÉREZ-DÍAZ, B. (2013). HF spectrum activity prediction model based on HMM for cognitive radio applications. *Physical Communication*, *9*, 199 - 211.

MELIÁN-GUTIÉRREZ, L., ZAZO, S., BLANCO-MURILLO, J., PÉREZ-ÁLVAREZ, I., GARCÍA-RODRÍGUEZ, A., & PÉREZ-DÍAZ, B. (2012, May). Efficiency improvement of HF communications using cognitive radio principles. In *12th International Conference on Ionospheric Radio Systems and Techniques (IRST12)* (p. 1-5). York, UK.

PÉREZ-DÍAZ, B., ZAZO, S., PÉREZ-ÁLVAREZ, I., LÓPEZ-PÉREZ, J., MELIÁN-GUTIÉRREZ, L., & JIMÉNEZ-YGUACEL, E. (2012, May). Theory and practice for modelling the broadband acquisition in HF transmissions. In *The 12th International Conference on Ionospheric Radio Systems and Techniques (IRST12)*. York, UK.

A.4 Trabajos en colaboración

El trabajo realizado en esta Tesis se ha llevado a cabo en la *División de Ingeniería de Comunicaciones* del *Instituto Universitario para el Desarrollo Tecnológico y la Innovación en Comunicaciones* (IDeTIC). Ha sido parcialmente financiado por la *Universidad de Las*

Palmas de Gran Canaria con una beca para estudios de doctorado del *Programa propio de becas de postgrado y contratos - Convocatoria 2010*. Durante el desarrollo de esta Tesis, la autora ha participado en los proyectos de investigación nacionales:

CR4HFDVL: Improving HF Data+Voice Link (HFDVL) using Cognitive Radio principles (TEC2010-21217-C02-01). Financiado por *Ministerio de Ciencia e Innovación*. Entidades: IDeTIC-ULPGC y SSR-UPM. Duración: Enero 2011 - Diciembre 2013.

UNDERWORLD: Underwater Radiocommunications for Optimized Monitoring using Multirelay Devices (TEC2013-46011-C3-2-R). Financiado por *Ministerio de Economía y Competitividad*. Entidades: IDeTIC-ULPGC, SSR-UPM y PLOCAN. Duración: Enero 2014 - Diciembre 2016.

También ha colaborado en las siguientes publicaciones derivadas de los proyectos mencionados:

López-Pérez, J., Melián-Gutiérrez, L., Pérez-Álvarez, I., Zazo, S., Raos, I., & Pérez-Díaz, B. (2012, May). Selection of CSI-based precoding techniques in the HF channel. In *12th International Conference on Ionospheric Radio Systems and Techniques (IRST12)*. York, UK.

Raos, I., Zazo-Bello, S., Pérez-Álvarez, I., López-Pérez, J., Melián-Gutiérrez, L., & Pérez-Díaz, B. (2012, May). Optimization of ARQ parameters of STANAG 5066 for the HFDVL Modem. In *12th International Conference on Ionospheric Radio Systems and Techniques (IRST12)*. York, UK.

Zazo, S., Pérez-Álvarez, I., López-Pérez, J., Pérez-Díaz, B., Jiménez-Yguacel, E., Melián-Gutiérrez, L., & Sanz-González, J. (2012, May). Spatial domain mitigation of out of band strong interferers in HF wide band acquisition using analog beamforming principles. In *12th International Conference on Ionospheric Radio Systems and Techniques (IRST12)*. York, UK.

Zazo, S., Sanz-González, J., Pérez-Díaz, B., Pérez-Álvarez, I., López-Pérez, J., & Melián-Gutiérrez, L. (2012, May). Analog mitigation of out of band strong interferers in wide band acquisition for multiband HF transmissions. In *12th International Conference on Ionospheric Radio Systems and Techniques (IRST12)*. York, UK.

A.5 Radio cognitiva

La campaña de medidas llevada a cabo por la Comisión Federal de Comunicaciones (FCC, Federal Communications Commission) en las ciudades más grandes de Estados Unidos reveló que el uso del espectro situado por debajo de 1 GHz está mal distribuido. Mientras algunas bandas están prácticamente saturadas, el resto de bandas no están en uso o sólo durante una parte del tiempo (Federal Communications Commision, 2002). Este fenómeno también fue observado en otros estudios en Alemania (Wellens et al., 2007),

Nueva Zelanda (Chiang et al., 2007), Singapur (Islam et al., 2008) y España (López-Benítez, Casadevall, et al., 2009; López-Benítez, Umbert, & Casadevall, 2009). Más que un problema de escasez de recursos, la FCC destaca que se trata de un problema de acceso al espectro debido a la asignación actual de frecuencias para uso exclusivo de los usuarios con licencia (Federal Communications Commision, 2002)(Buddhikot, 2007)(Hossain et al., 2009). Estas campañas de medidas reforzaban la idea de que nuevas oportunidades de uso del espectro podían surgir para usuarios sin licencia y así poder explotar de forma más eficiente los recursos del espectro.

Estas oportunidades han sido denominadas como *spectrum holes* en la literatura (Hossain et al., 2009) y hacen referencia a aquellas bandas asignadas a usuarios con licencia que, durante un determinado intervalo de tiempo y en un lugar concreto, no están siendo utilizadas por dichos usuarios (Haykin, 2005). Un ejemplo de este tipo de oportunidades o *spectrum holes* está representado en la Figura A.2.

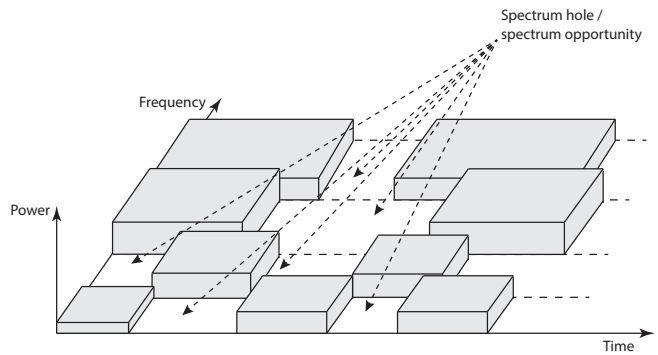

FIGURA A.2. Oportunidades de uso del espectro / *spectrum holes*.

Si estas oportunidades fueran utilizadas por nuevos usuarios aunque no tuvieran licencia para transmitir se lograría un uso más eficiente de los recursos espectrales. Por lo tanto, los nuevos usuarios deben ser dotados con nuevas capacidades para identificar y utilizar correctamente los *spectrum holes* disponibles sin interferir a los usuarios con licencia.

Radio cognitiva surgió como una posible solución al uso ineficiente del espectro permitiendo un uso oportunista de las bandas no ocupadas por usuarios con licencia (Haykin, 2005),(Federal Communications Commission, 2005). Además de Mitola, que propuso este concepto en 1999 (Mitola & Maguire, 1999; Mitola, 1999), otros científicos y entidades relacionadas con las comunicaciones (Haykin, 2005; Jondral, 2005; Federal Communications Commission, 2005; The SDR Forum, 2008; ITU-R, 2009) han definido también el concepto de radio cognitiva, enfatizando que una radio cognitiva ha de ser un sistema autónomo con las siguientes capacidades: inteligencia, adaptabilidad, aprendizaje, fiable, eficiente y consciente del entorno. Además, deben ser reconfigurables para adaptar automáticamente su configuración a los cambios en el entorno (Haykin, 2005; Jondral, 2005; Akyildiz et al., 2006). Todas estas capacidades están resumidas en el ciclo de tareas cognitivas de la Figura A.3.

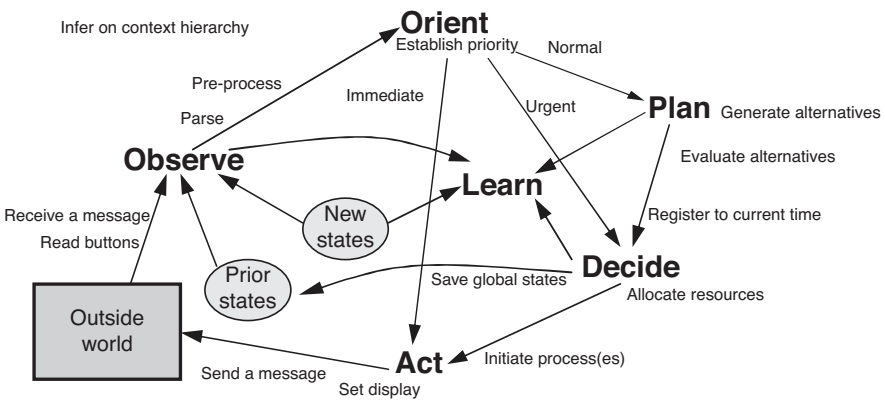

FIGURA A.3. Ciclo cognitivo de tareas. (Mitola & Maguire, 1999; Mitola, 2000).

Se identifican dos tipos de usuarios en radio cognitiva: usuarios primarios y usuarios secundarios. Los usuarios primarios son los usuarios con licencia de transmisión en una determinada banda mientras que los usuarios secundarios, también conocidos como usuarios cognitivos, son usuarios sin licencia que pueden acceder al espectro asignado a los primarios cuando éstos no estén haciendo uso de él para no interferir con ellos. Son los usuarios secundarios los que ejecutan el ciclo cognitivo de tareas para aprovechar las oportunidades de transmisión que surjan, mientras que los usuarios primarios utilizan la tecnología actual sin capacidades cognitivas (Buddhikot, 2007; Doyle, 2009; Hossain et al., 2009).

A.5.1 Técnicas de acceso al espectro en Radio Cognitiva

El sistema actual de asignación de frecuencias está basado en el modelo *command and control*, aplicado por organismos reguladores internacionales y nacionales. En este sistema, tanto el usuario que tiene licencia como el tipo de servicio y la canalización del espectro son fijos, siendo un esquema de acceso al espectro inflexible (Buddhikot, 2007). Otros esquemas de acceso al espectro alternativos han surgido bajo el nombre de acceso dinámico al espectro (DSA, Dynamic Spectrum Access). Los modelos de acceso basados en DSA se dividen en tres categorías principales como se muestra en la Figura A.4: uso exclusivo, uso compartido del espectro asignado a los usuarios primarios y el modelo de uso común del espectro. Además, nuevos modelos de uso compartido del espectro han sido definidos por las entidades reguladoras de la Unión Europea y Estados Unidos.

A.5.1.1 Acceso exclusivo al espectro

El modelo de acceso exclusivo asigna una banda de frecuencias a una entidad que tendrá acceso exclusivo bajo una serie de restricciones. Si un usuario con licencia no utiliza el espectro asignado, puede ceder sus derechos de acceso a usuarios cognitivos, sin licencia, que hayan solicitado el uso del espectro no utilizado. Existen dos variantes: un

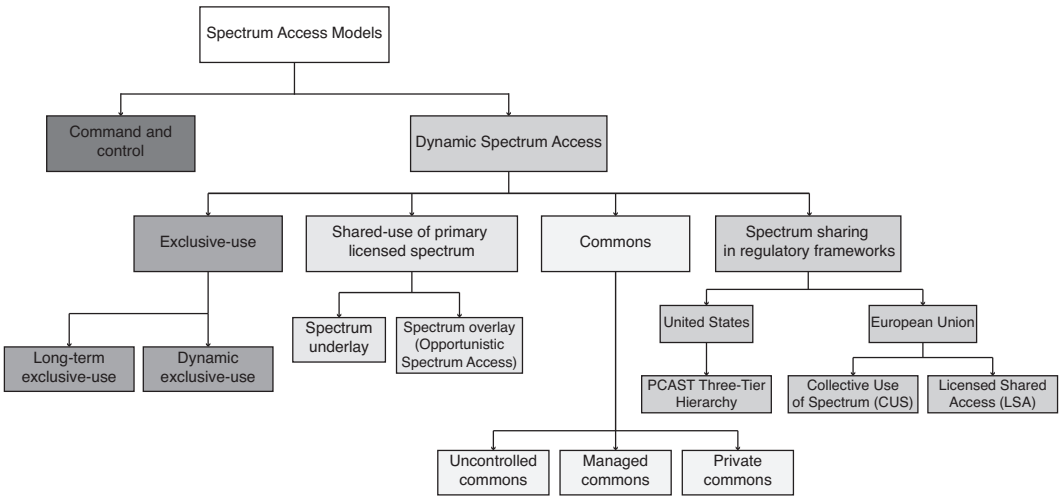

FIGURA A.4. Modelos de acceso al espectro.

uso exclusivo a largo plazo y un modelo de uso exclusivo dinámico (Buddhikot, 2007). La principal diferencia entre ambos es que la asignación del espectro a los usuarios primarios se realiza con una mayor duración en el primero que en el modelo dinámico.

Bajo la restricción de que sólo un único usuario puede utilizar el espectro, los usuarios con licencia pueden negociar con los usuarios secundarios el acceso al espectro asignado. De esta manera, los usuarios con licencia pueden obtener beneficios mientras los usuarios cognitivos acceden a sus bandas de frecuencias. Ésta es la base de los mercados secundarios (Federal Communications Commission, 2000b, 2000a; Peha & Panichpapiboon, 2004), descritos en la Sección A.5.2 como una técnica de observación del espectro pasiva.

A.5.1.2 Uso compartido del espectro asignado al usuario primario

Los usuarios primarios y los usuarios secundarios pueden utilizar simultáneamente el espectro en este modelo de uso compartido siempre y cuando los usuarios secundarios no interfieran a los usuarios primarios (Buddhikot, 2007). Además, los usuarios secundarios no tienen que pedir permiso a los usuarios primarios, es un acceso transparente a ellos (Hossain et al., 2009). Existen dos estrategias de acceso al espectro para los usuarios secundarios (ver Figura A.5): *overlay*, también conocida como acceso oportunista al espectro (OSA, Opportunistic Spectrum Access) (Q. Zhao & Sadler, 2007), y *underlay*.

La estrategia *overlay* es la más utilizada en los sistemas basados en radio cognitiva. En ella, los usuarios primarios tienen licencia de transmisión en una determinada banda y región. Sin embargo, si no utilizan la banda asignada, los usuarios secundarios pueden acceder a la misma de una manera oportunista sin restricciones de potencia hasta que el usuario primario vuelve. Por otro lado, en la estrategia *underlay*, los usuarios secundarios acceden al espectro junto con los usuarios primarios pero con niveles de potencia muy bajos para no interferir a los primarios.

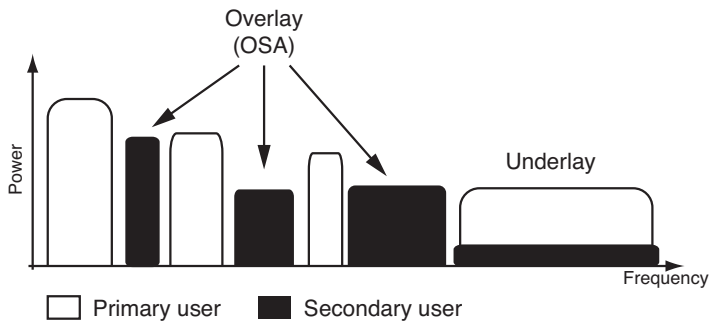

FIGURA A.5. Uso compartido del espectro asignado al usuario primario: *overlay* (OSA) vs. *underlay*.

A.5.1.3 Modelo de uso común del espectro

El modelo de uso común del espectro no considera diferentes a los usuarios secundarios de los primarios, ya que ninguno tiene uso exclusivo de los recursos del espectro (Buddhikot, 2007). Existen tres variantes (Buddhikot, 2007; Hossain et al., 2009) en función de si no hay control o sólo por parte de algunos usuarios sobre las bandas de frecuencia: el modelo no controlado aplicado a las bandas ISM (2.4 GHz) y U-NII (5 GHz), el modelo gestionado por un grupo de usuarios y el modelo privado que permite el acceso a usuarios secundarios que cumplan con el protocolo y tecnología asignados a la banda.

A.5.1.4 Modelos de uso compartido en la regulación

Dado el impacto de las nuevas propuestas basadas en el acceso dinámico al espectro, las entidades reguladores de la Unión Europea y de los Estados Unidos están trabajando actualmente en la regulación del uso compartido del espectro. En el caso de la Unión Europea se han propuesto dos modelos: *Collective Use of Spectrum* (CUS) (Radio Spectrum Policy Group, 2011) y *Licensed Shared Access* (LSA) (Radio Spectrum Policy Group, 2013; Electronic Communications Committee, 2014), mientras que un modelo jerárquico con tres tipos de usuarios (*Three-Tier Hierarchy model of spectrum sharing*) ha sido propuesto por el consejo de asesores del presidente en ciencia y tecnología (PCAST) en Estados Unidos (President's Council of Advisors on Science and Technology, 2012).

A.5.2 Técnicas de observación del entorno en Radio Cognitiva

De acuerdo con el ciclo cognitivo de la Figura A.1, el primer paso que realiza una radio cognitiva es observar el entorno. Lo puede hacer siguiendo una estrategia activa o pasiva (Fujii & Suzuki, 2005; Fitzek & Katz, 2007). Si se trata de una estrategia pasiva, los usuarios secundarios reciben información sobre los recursos espectrales disponibles de un agente externo, mientras que si se trata de una estrategia activa, los usuarios secundarios escuchan el entorno para obtener medidas del uso del espectro. Este tipo de estrategias son conocidas en la literatura como *spectrum sensing*. La Figura A.6 recoge un

diagrama que resumen las diferentes técnicas tanto activas como pasivas de observación del entorno.

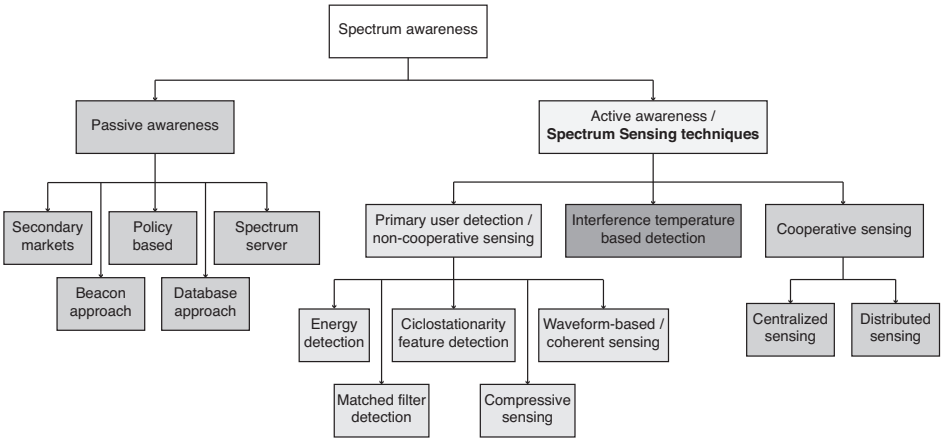

FIGURA A.6. Estrategias de observación del entorno y técnicas de *spectrum sensing*.

En los escenarios con estrategias pasivas, los usuarios primarios o las entidades reguladoras informan a los usuarios secundarios si pueden transmitir, en qué frecuencia y por cuánto tiempo (Brown, 2005; Hulbert, 2005; Mangold et al., 2006) y (Mangold et al., 2004), o los usuarios primarios pueden establecer un mercado secundario donde ceden temporalmente sus licencias a usuarios secundarios (Peha & Panichpapiboon, 2004). Tanto los usuarios primarios como las entidades reguladoras pueden crear también bases de datos con información actualizada sobre los recursos espectrales disponibles en una determinada área (Brown, 2005; Gurney et al., 2008; Murty et al., 2012).

Existen también combinaciones de estrategias activas y pasivas de observación del espectro. En (Mueck et al., 2010; Ribeiro et al., 2012) se propuso la combinación de *spectrum sensing* con bases de datos geolocalizadas. Sin embargo, en la literatura se presta una mayor atención a las estrategias activas de observación del espectro, i.e., *spectrum sensing*. Tal y como se demuestra en la Figura A.6, estas técnicas se dividen en tres categorías: detección de usuarios primarios / *sensing* no cooperativo, técnicas basadas en el cálculo de la temperatura de interferencia y *sensing* cooperativo.

A.5.2.1 Detección de usuarios primarios

Las tareas de *spectrum sensing* deciden a partir las medidas adquiridas del entorno si un usuario primario está transmitiendo o no. Generalmente se puede plantear como un problema de detección de señal binaria (Kay, 1998) con las siguientes dos hipótesis (Ghasemi & Sousa, 2005; Fitzek & Katz, 2007; Ma et al., 2009):

$$H_0: \quad y[n] = w[n] \qquad n = 1, \cdots, N-1 \tag{A.1a}$$

$$H_1: \quad y[n] = s[n] + w[n] \qquad n = 1, \cdots, N-1 \tag{A.1b}$$

donde $y[n]$ es la señal recibida por el usuario secundario, $s[n]$ es la señal transmitida por el usuario primario, y $w[n]$ es el ruido blanco Gaussiano aditivo (AWGN, additive white Gaussian noise). La hipótesis nula H_0 indica que no hay un usuario primario en las medidas adquiridas mientras que la hipótesis alternativa H_1 indica que puede existir una transmisión de un usuario primario.

Múltiples técnicas de detección de usuarios primarios han sido propuestas y evaluadas en la literatura. Las más representativas han sido incluidas en la Figura A.6. La selección de una técnica u otra dependerá del compromiso entre factores como la precisión en la detección, el tiempo para llevarla a cabo, la complejidad, o de si los usuarios secundarios tienen alguna información sobre el tipo de transmisión de los usuarios primarios.

Cuando los usuarios secundarios no disponen de las características de transmisión de los usuarios primarios, el detector de energía es la solución más adecuada. Este detector mide la energía de la señal recibida en un intervalo de tiempo y detecta si hay una transmisión de un usuario primario comparando la energía medida con un umbral que depende del piso de ruido (Urkowitz, 1967). Se trata de la técnica de detección de usuarios primarios más sencilla aunque su comportamiento varía según el nivel de ruido y no puede detectar señales de espectro ensanchado (Cabric et al., 2004). A pesar de ello, ha sido utilizada en múltiples trabajos de radio cognitiva como (Ghasemi & Sousa, 2005; Cabric et al., 2006), o (López-Benítez & Casadevall, 2012; Nastase et al., 2014) donde se modifica el detector de energía para mejorar su rendimiento.

En los escenarios donde los usuarios secundarios tienen alguna información sobre la transmisión de los usuarios primarios se puede utilizar un *matched filter*, un detector cicloestacionario o un detector de la forma de onda de la señal recibida. Si el usuario secundario conoce perfectamente las características de transmisión del usuario primario como el ancho de banda, la frecuencia de trabajo o la modulación, y la transmisión sólo está contaminada por ruido AWGN, el detector óptimo es el *matched filter* (Proakis, 2000). Sin embargo, cuando esta información es incompleta, su rendimiento cae significativamente. Además, en el caso de recibir diferentes señales de usuarios primarios, se requiere un *matched filter* para cada una de las señales (Cabric et al., 2004; Yucek & Arslan, 2009).

Los detectores basados en las características cicloestacionarias de la señal recibida analizan la autocorrelación cíclica de la señal recibida o la función de densidad espectral cíclica (Ma et al., 2008). Su principal ventaja es que son capaces de diferenciar la señal del usuario primario de interferencias y ruido que no tienen correlación espectral (Gardner, 1987; Cabric et al., 2004). Sin embargo, requieren de periodos de observación bastante largos para detectar correctamente la señal del usuario primario (Hossain et al., 2009). Este tipo de detectores ha sido propuesto en (Goh et al., 2007; Jallon, 2008) para la detección de señales de televisión digital (DVB-T) en bandas de televisión autorizadas para uso secundario.

Existe otro detector basado en la detección de la forma de onda de la señal transmi-

tida por el usuario primario, conocido también como *coherent sensing* (Yucek & Arslan, 2009). Su principal ventaja es que tiene mejores prestaciones que el detector de energía (Tang, 2005). No obstante, sólo puede ser aplicado si el usuario secundario conoce algún patrón en la transmisión del usuario primario como los pilotos o las secuencias de ensanchamiento (Yucek & Arslan, 2009).

Finalmente, otras técnicas han sido aplicadas para la detección de usuarios primarios. La transformada Wavelet se propuso en (Tian & Giannakis, 2006; Ma et al., 2009) mientras que la transformada Hough aleatoria se propuso en (Challapali et al., 2004) para la detección de pulsos radar. Las estadísticas extraídas de la matriz de covarianzas de la señal recibida se utilizan en (Ma et al., 2009; Zeng & Liang, 2009).

A.5.2.2 Detección a partir de la temperatura de interferencia

La temperatura de interferencia es un concepto definido por la FCC (Federal Communications Commision, 2003) para medir las interferencias existentes en un escenario de radio cognitiva. Se trata de la medida de la potencia RF generada por emisores no deseados junto con las fuentes de ruido que están presentes en el receptor por unidad de ancho de banda. La temperatura de interferencia es idéntica a la temperatura de ruido (T. C. Clancy, 2007) ya que es equivalente a la potencia medida en unidades Kelvin (K). Por cada zona geográfica y por cada banda de frecuencia existirá una cantidad de temperatura de interferencia máxima tolerable por los usuarios primarios, la denominada temperatura de interferencia límite, T_L. De esta manera, los usuarios secundarios deberán garantizar que sus transmisiones junto con el resto de transmisiones existentes en la banda no sobrepasan la temperatura de interferencia límite en un usuario primario (Federal Communications Commision, 2003; T. C. Clancy, 2007).

A.5.2.3 *Sensing* cooperativo

Las técnicas de detección de usuarios primarios descritas en la Sección A.5.2.3 son también denominadas como *sensing* no cooperativo, ya que son ejecutadas en un único usuario secundario. Cuando existen múltiples usuarios primarios y secundarios en una red de radio cognitiva, puede suceder que un usuario secundario no pueda detectar siempre todas las transmisiones de los usuarios primarios a causa del ruido, las zonas de sombra o el desvanecimiento del canal (Yucek & Arslan, 2009; Hossain et al., 2009).

El *sensing* cooperativo ha sido propuesto en la literatura para resolver este problema y para mejorar las prestaciones de detección de los usuarios secundarios (Cabric et al., 2004; Ghasemi & Sousa, 2005; Ganesan & Li, 2005). Los usuarios secundarios pueden cooperar de dos maneras (Ganesan & Li, 2005): centralizada o distribuida. Si se trata de una cooperación centralizada, los usuarios secundarios envían la información observada a través de un canal de control común a una unidad central, que es responsable de iden-

tificar las oportunidades de transmisión y de reenviar esta información (Ma et al., 2008; Lundén et al., 2009). Por lo contrario, en los escenarios con cooperación distribuida, cada usuario secundario ejecuta su tarea de *spectrum sensing* y decide en función de lo que ha observado todo el conjunto de usuarios secundarios de la red (Cabric et al., 2004; J. Zhao et al., 2005).

A.5.3 Aprendizaje de la actividad de los usuarios primarios

Además de observar la actividad de los usuarios primarios ejecutando la tarea de *spectrum sensing*, existe la necesidad de monitorizar dicha actividad para mejorar las predicciones de los usuarios secundarios sobre las futuras oportunidades de transmisión. Puede suceder que existan diferentes tipos de usuarios en una determinada banda pero los modelos de actividad pueden ser muy útiles para los usuarios secundarios. En esta Sección se describen las técnicas más utilizadas para el modelado de la actividad de los usuarios primarios.

A.5.3.1 Redes Neuronales

Las redes neuronales (ANN, Artificial Neural Networks) han sido diseñadas para modelar la manera en que el cerebro realiza una determinada tarea. Se definen como un procesador paralelo distribuido formado por unidades sencillas de procesamiento denominadas neuronas. Estas neuronas son capaces de mantener el conocimiento adquirido a través de la experiencia previa teniéndolo disponible para su uso (Haykin, 1998). En el contexto de radio cognitiva, las redes neuronales han sido aplicadas como modelos de actividad de usuarios primarios que son utilizados por los usuarios secundarios para predecir la actividad de los usuarios primarios. Uno de estos modelos fue presentado en (Tumuluru et al., 2010).

A.5.3.2 Modelos Ocultos de Markov

Un modelo oculto de Markov (HMM, Hidden Markov Model) se define como un proceso doblemente embebido siendo uno de los procesos estocásticos no observable. El proceso oculto sólo puede ser evaluado a través de otro conjunto de procesos que generan secuencias que sí pueden ser observadas (Rabiner & Juang, 1993). En una radio cognitiva, un HMM puede ser utilizado como un proceso de observación para reconocer o clasificar el entorno observado ya que son capaces de modelar procesos estadísticos complejos. Además, como el HMM puede reproducir las secuencias con las que ha sido entrenado, también puede ser utilizado para predecir en función de lo aprendido anteriormente (He et al., 2010).

Los HMMs han sido muy utilizados como modelos y detectores en aplicaciones de reconocimiento de voz (Rabiner & Juang, 1993). Recientemente también han sido aplicados a sistemas de radio cognitiva para la detección de actividad de usuarios primarios y para la predicción de su actividad, obteniendo resultados muy significativos. Un detector basado en varios HMMs, cada uno entrenado para una respuesta en frecuencia de señales diferentes, se presentó en (Z. Chen et al., 2009). Por otro lado, (Park et al., 2007) y (Z. Chen & Qiu, 2010) propusieron modelos de predicción de la actividad en un canal basados en HMMs. El modelo presentado en (Park et al., 2007) predecía la actividad cuando las secuencias de observación era deterministas y periódicas; no podía predecir secuencias no periódicas como son las medidas reales de cualquier banda de frecuencias. Otros modelos para predicción de actividad de usuarios primarios fueron propuestos en (Akbar & Tranter, 2007) y (Ahmadi et al., 2011), donde se asumía que el tráfico de los usuarios primarios seguía una distribución de Poisson con un porcentaje de ocupación superior al 50 %. Un escenario diferente al de los trabajos anteriores fue considerado en (Sharma et al., 2008). En este trabajo, se propuso que los usuarios secundarios accedían al espectro con una estrategia *underlay* basada en la medida de la temperatura de interferencia. Es por ello que se propuso un modelo basado en HMMs de la variación de la temperatura de interferencia para su posterior uso como sistema de predicción.

Finalmente, cabe destacar que pocos de los modelos basados en HMMs para la predicción de la actividad de los usuarios primarios han sido evaluados en escenarios reales. Éste es el caso de los trabajos propuestos en (Z. Chen & Qiu, 2010), (Z. Chen et al., 2011) y (Chatziantoniou et al., 2013). El modelo presentado en (Z. Chen & Qiu, 2010) y (Z. Chen et al., 2011) fue entrenado con señales WiFi, mientras que el modelo presentado en (Chatziantoniou et al., 2013) fue entrenado con señales WiFi y Bluetooth de la banda de 2.4 GHz. Además, la precisión de las predicciones realizadas con el modelo presentado en (Ahmadi et al., 2011) fue evaluada en (Ahmadi et al., 2013) y (Macaluso et al., 2015) con datos reales de la bandas ISM de 2.4 GHz y GSM 1800 adquiridas por la Universidad RWTH Aachen (Wellens & Mähönen, 2010).

A.5.4 Estrategias para la toma de decisiones en Radio Cognitiva

Uno de los modelos de acceso más utilizados en la literatura relacionada con radio cognitiva es el acceso oportunista al espectro. Múltiples soluciones han sido propuestas como estrategias de toma de decisiones (*decision-making*) de usuarios secundarios que quieren acceder de manera oportunista al espectro. Algunas de estas propuestas han sido diseñadas para escenarios con un único usuario secundario mientras que otras han sido diseñadas para escenarios con múltiples usuarios secundarios accediendo al espectro de manera oportunista tal y como se muestra en la Figura A.7.

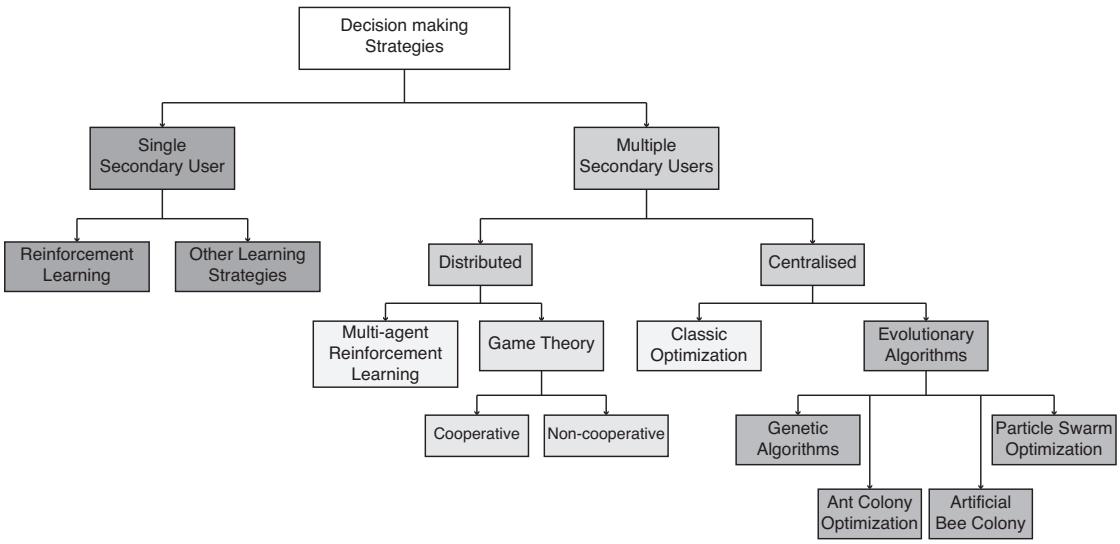

FIGURA A.7. Estrategias para la toma de decisiones.

A.5.4.1 *Reinforcement Learning* en escenarios con un único usuario secundario

Reinforcement Learning engloba los problemas de aprendizaje en los que el aprendizaje se adquiere al interactuar con el entorno, sin requerir modelos de la actividad del entorno (Sutton & Barto, 1998). *Reinforcement Learning* consiste en un agente que interactúa con el entorno siguiendo una política que describe su comportamiento en función de los cambios del entorno. A diferencia de otras técnicas de aprendizaje, en *reinforcement learning* el sistema que aprende debe descubrir qué acciones generan la mayor recompensa a partir de su experiencia (Sutton & Barto, 1998).

En el contexto de la toma de decisiones en radio cognitiva, un escenario OSA puede ser descrito como un problema de *reinforcement learning* donde el agente es un usuario secundario y el entorno es el espectro de los usuarios primarios al que pretende acceder. El conjunto de acciones se corresponde con el conjunto de posibles canales a los que el usuario secundario puede acceder si existen oportunidades de transmisión. Finalmente, la recompensa que recibe el usuario secundario le informará si ha seleccionado un canal que estaba disponible o no, o alguna métrica que le indique la calidad de la transmisión realizada en ese canal.

Los problemas *Multi-armed bandit* (MAB) (Robbins, 1952) y los procesos de decisión *Markov Decision Processes* (MDP) (Sutton & Barto, 1998) son dos marcos teóricos que describen el problema de *reinforcement learning*, siendo el MAB una versión simplificada del MDP donde se considera un único estado y no un conjunto de estados como en el MDP. MAB es una estrategia que se puede implementar directamente para la toma de decisiones en escenarios OSA donde el agente sólo puede estar en un determinado estado y el conjunto de acciones se corresponde con el conjunto de posibles canales de transmisión. Sin embargo, cuando un MDP es utilizado para modelar un escenario OSA, existen múltiples estados en los que puede permanecer el agente y cuyas transiciones represen-

tan la complejidad de cambiar de un canal a otro (Berthold et al., 2008). Los escenarios OSA han sido definidos como MAB en (Berthold et al., 2008; Jouini et al., 2009; Jiang, Grace, & Liu, 2011; Robert et al., 2014), como MDP en (Berthold et al., 2008; Hamdaoui et al., 2009), o como un MDP parcialmente observable (POMDP) en (Hoang et al., 2009; Unnikrishnan & Veeravalli, 2010), donde un POMDP es un MDP en el que los estados no son directamente observables (Sutton & Barto, 1998).

Para resolver estos escenarios se han propuesto diferentes algoritmos en la literatura. Dichos algoritmos tienen en común la búsqueda del compromiso entre exploración y explotación, es decir, el compromiso entre la selección de un canal que ha dado buena recompensa en el pasado y la búsqueda de nuevos canales que podrían dar una mayor recompensa. Los algoritmos *softmax action-selection* (Sutton & Barto, 1998), *Upper Confidence Bound* (UCB) (Agrawal, 1995; Auer et al., 2002), y *weight-driven* (Jiang, Grace, & Liu, 2011) han sido propuestos para problemas MAB, mientras que los métodos *time-difference learning* como *Q-learning* (Watkins & Dayan, 1992), *Sarsa* (Sutton & Barto, 1998) y *actor-critic methods* (Sutton & Barto, 1998) han sido propuestos para MDP.

En el caso de escenarios OSA modelados con MAB se han seleccionado: *softmax action-selection* en (Berthold et al., 2008), UCB en (Jouini et al., 2009, 2010), y *weight-driven* en (Jiang, Grace, & Liu, 2011; Jiang, Grace, & Mitchell, 2011). Además, se ha realizado una comparativa entre UCB y *weight-driven* en escenarios OSA en (Robert et al., 2014). En el caso de escenarios OSA modelados con MDP, se propuso *Q-learning* en (Hamdaoui et al., 2009; Yau et al., 2010; Macaluso et al., 2013) y *actor-critic methods* en (Berthold et al., 2008).

A.5.4.2 Estrategias en escenarios con múltiples usuarios secundarios

En el caso de la toma de decisiones con múltiples usuarios secundarios, existen dos tipos de escenarios: distribuidos o centralizados, tal y como se muestra en la Figura A.7. En los escenarios distribuidos, cada usuario secundario toma su decisión según sus observaciones y las de otros usuarios secundarios. Por otro lado, en un escenario centralizado, la toma de decisiones se lleva a cabo en una entidad central.

Algunos trabajos han propuesto soluciones basadas en *multi-agent reinforcement learning* y teoría de juegos para escenarios distribuidos con múltiples usuarios secundarios que acceden simultáneamente al espectro. Éste es el caso de *Q-learning*, que fue modificado en (Galindo-Serrano & Giupponi, 2010) para una versión no centralizada de diferentes usuarios secundarios siguiendo el estándar IEEE 802.22 (Cordeiro et al., 2005). Además, para garantizar que no se produjeran situaciones inestables, se introdujo el término *docition* en (Giupponi et al., 2010) para referirse al hecho de que los usuarios secundarios pueden enseñar a otros el comportamiento del entorno a través del intercambio de información sobre el mismo, lo que resultó en una mejora del proceso de aprendizaje.

La teoría de juegos es una herramienta matemática que intenta reflejar el comportamiento de entidades racionales en entornos de conflicto (Bkassiny et al., 2013). Dado que uno de los retos en OSA es la interacción entre los usuarios secundarios (Xu et al., 2013), se han propuesto diversas soluciones basadas en teoría de juegos para la toma de decisiones en escenarios con múltiples usuarios secundarios. Éstos pueden cooperar o no en la toma de decisiones (Tragos et al., 2013; B. Wang et al., 2010). Algunas de estas propuestas están incluidas en (Nie & Comaniciu, 2006) y (Ji & Liu, 2007).

En el caso de los escenarios centralizados, se han propuesto diferentes trabajos basados en técnicas de optimización clásicas y algoritmos evolutivos para distribuir el espectro disponible. El problema de distribución del espectro, potencia y tasa de datos de múltiples usuarios secundarios se resuelve en (Masmoudi et al., 2015) y (Ngo & Le-Ngoc, 2011) con un algoritmo del sub-gradiente. Del conjunto de algoritmos evolutivos, los algoritmos genéticos (Goldberg, 1989; Tragos et al., 2013) han sido propuestos para la toma de decisiones en escenarios centralizados en (Thilakawardana & Moessner, 2007; Kim et al., 2008; Z. Zhao et al., 2009). Por otro lado, el algoritmo basado en los enjambres de abejas (*Artificial Bee Colony, ABD*) (Karaboga & Basturk, 2007) es propuesto en (Cheng & Jiang, 2011) para optimizar los recursos espectrales de manera eficiente y justa.

A.5.5 Radios metacognitivas

Los algoritmos que dotan a una radio cognitiva con las capacidades de aprendizaje y toma de decisiones se denominan en la literatura como el motor o máquina cognitiva de una radio cognitiva (Gadhiok et al., 2011). Sucede que dichos algoritmos no pueden ser fiables ni realizables en todos las situaciones, es por ello que se adoptó el concepto de *metacognition* de psicología a la radio cognitiva en (Gadhiok et al., 2011) y (Asadi et al., 2015).

Una radio metacognitiva se define como una radio cognitiva formada por varias máquinas cognitivas y que tiene la capacidad de adaptarse a las condiciones del entorno, es decir, selecciona la máquina cognitiva más apropiada en función de lo previamente observado (Asadi et al., 2015). De esta manera, las prestaciones no están limitadas a las prestaciones de una única máquina cognitiva.

A.5.6 Radio Cognitiva y comunicaciones HF

Pocos trabajos en la literatura de radio cognitiva han sido enfocados a la aplicación de radio cognitiva en las comunicaciones HF. Aunque el protocolo ALE ha sido definido como una forma primitiva y limitada de radio cognitiva (Fette, 2009), se requiere un mecanismo más dinámico que el protocolo ALE para poder aplicar eficientemente los principios de radio cognitiva en HF.

Tomando el protocolo ALE como punto de partida, (Furman & Koski, 2009) y (Koski

& Furman, 2009) propusieron nuevas especificaciones para este protocolo basadas en radio cognitiva. Además, (Vanninen et al., 2014) también analizó las limitaciones actuales de las comunicaciones HF con el protocolo ALE para incluir nuevas mejoras basadas en los principios de radio cognitiva. Ninguno de estos trabajos presentó alguna estrategia evaluada en un entorno real o bajo simulación que estuviera basada en las propuestas de modificación del ALE. No obstante, (Shahid et al., 2010) analizó cómo los sistemas de detección de usuarios primarios descritos previamente podían conseguir mejores prestaciones que la técnica LBT en el protocolo ALE. Por otro lado, (Shukla et al., 2012) propuso mejoras de las comunicaciones HF basadas en radio cognitiva con el estándar IEEE 802.22 (Cordeiro et al., 2005), pero no demostró ninguna evidencia sobre su aplicación.

Aunque las técnicas de aprendizaje tienen un papel importante en radio cognitiva, hay pocos trabajos relacionados con aprendizaje para radio cognitiva en HF. Un modelo de actividad en términos de congestión sufrida por los usuarios de radiodifusión en HF se propuso en (Haralambous & Papadopoulos, 2009). Dicho modelo estaba basado en redes neuronales y fue entrenado con medidas reales de la banda. Además de este trabajo, diversas técnicas de aprendizaje sí han sido utilizadas para modelar las características de propagación de la banda de HF como en (Altinay et al., 1997) y (Chu & Conn, 1999).

A.6 Base de datos de medidas de la banda de HF

Durante el desarrollo de esta Tesis se han adquirido diferentes medidas de banda ancha de la banda de HF que han sido posteriormente utilizadas para evaluar las propuestas basadas en radio cognitiva para la banda de HF. El sistema de adquisición estaba situado en las instalaciones del IDeTIC en Las Palmas de Gran Canaria y está representado en la Figura A.8. Se ha utilizado el transceptor HF de banda ancha previamente desarrollado en el grupo de investigación (Pérez-Díaz et al., 2009) junto con un analizador vectorial de señales (VSA, Vector Signal Analyzer) (Agilent Technologies, 2010b) y el programa SystemVue (Agilent Technologies, 2010a), ambos de Agilent Technologies, para recoger la información temporal de la antena Yagi y trasladarla al dominio de la frecuencia haciendo uso de la transformada rápida de Fourier (FFT, Fast Fourier Transform). Para realizar una correcta adquisición de la información, deben ajustarse varios parámetros incluyendo el span, el ancho de banda de resolución y el número de bins de la FFT.

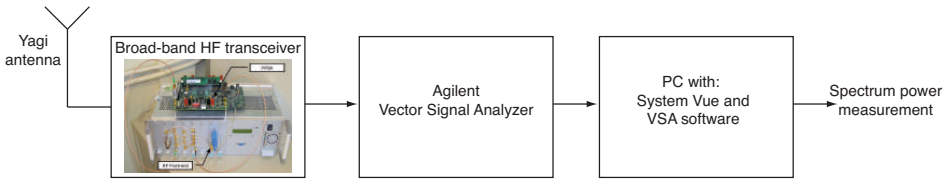

FIGURA A.8. Sistema de adquisición de medidas situado en las instalaciones del IDeTIC en Las Palmas de Gran Canaria, España.

A.6.1 Transceptor HF de banda ancha

Como la sensibilidad del VSA no era suficientemente alta para detectar la mayor parte de señales de la banda, se introdujo el transceptor HF de banda ancha diseñado en (Pérez-Díaz et al., 2009) en el sistema de adquisición de medidas. De esta manera, el transceptor recogía la señal de la antena y la transmitía al VSA, según se muestra en la Figura A.8. Este transceptor digital tiene un ancho de banda de 1 MHz y cubre la banda de HF (3-30 MHz). A pesar de su ancho de banda, fue diseñado para la transmisión simultánea por varios canales en lugar de un único canal de 1 MHz de ancho de banda (Pérez-Díaz et al., 2009).

La arquitectura de este transceptor está basada en la de un receptor superheterodino de doble conversión. Además, incluye una etapa digital de conversión implementada en una FPGA (Pérez-Díaz et al., 2009). Sin embargo, la señal que se transmite al VSA en el sistema de adquisición de medidas de la Figura A.8 es la señal a la salida de la segunda etapa de conversión, junto antes de ser digitalizada. Esta señal ya ha sido adaptada por el AGC para permanecer dentro del rango dinámico del conversor analógico-digital. Por tanto, sufre del efecto de las interferencias de banda estrecha tal y como se detallará en la Sección A.7 de este apéndice.

A.6.2 Campaña de medidas

Se han realizado medidas secuenciales de las bandas de radioaficionados en 14 MHz, 21 MHz y 28 MHz durante varios días y detalladas en las Tablas A.1 y A.2. Dichas medidas contienen la información espectral en términos de potencia y fueron adquiridas en bloques de 9 ó 10 minutos de duración, separados por intervalos de 10-15 minutos. Además, la resolución temporal es de aproximadamente 2 segundos ya que el VSA calcula la FFT de la señal de banda ancha cada 2 segundos.

La adquisición de medidas se ha restringido a estas bandas y, principalmente a la banda de 14 MHz, debido a las limitaciones de la antena receptora. No obstante, la alta actividad que hay en la banda de 14 MHz y la presencia de diferentes tipos de transmisiones, tanto de voz como de datos, hacen que estas medidas sean representativas de la banda de HF y un escenario adecuado donde validar las técnicas cognitivas propuestas en esta Tesis. Tal y como se muestra en las Tablas A.1 y A.2, se han grabado varios concursos de radioaficionados en los que se encuentra una gran cantidad de patrones de transmisión en un entorno saturado.

Se han creado dos bases de datos a partir de las medidas realizadas en la banda de 14 MHz: La base de datos HFSA_IDeTIC_F1_V01 (ver Tabla A.3) que ha sido utilizar para evaluar las propuestas de las Secciones A.8, A.9 y A.10 de este apéndice, mientras que la base de datos HFSA_IDeTIC_F1_V02 (ver Tabla A.4) ha sido utilizada para evaluar la propuesta de la Sección A.7.

TABLA A.1. Campaña de medidas en la banda de 14 MHz.

Fecha	Ancho de banda	Concurso de radioaficionados
3 Junio 2011	640 kHz	– (Grabada entre semana)
10 Junio 2011	640 kHz	– (Grabada entre semana)
24 Septiembre 2011	640 kHz	First Greek Telegraphy Club CW Cup
23-24 Junio 2012	640 kHz	ARRL Field Day 2012
14-15 Julio 2012	1.28 MHz	IARU HF World Championship 2012
25-26 Mayo 2013	640 kHz	CQ World Wide WPX CW Contest 2013
22-23 Junio 2013	640 kHz	ARRL Field Day 2013
13-14 Julio 2013	640 kHz	IARU HF World Championship 2013
23-24 Noviembre 2013	640 kHz	CQ World Wide DX CW Contest 2013
15 Febrero 2014	640 kHz	ARRL Int. DX CW Contest 2014
1-2 Marzo 2014	640 kHz	ARRL Int. DX Phone Contest 2014
28-29 Junio 2014	640 kHz	ARRL Field Day 2014
12-13 Julio 2014	640 kHz	IARU HF World Championship 2014
25-26 Octubre 2014	640 kHz	CQ World Wide DX SSB Contest 2014
21-22 Febrero 2015	640 kHz	ARRL Int. DX CW Contest 2015
27-28 Junio 2015	640 kHz	ARRL Int. DX Phone Contest 2015
11-12 Julio 2015	640 kHz	IARU HF World Championship 2015

TABLA A.2. Campaña de medidas de otras bandas de radioaficionados: 21 MHz y 28 MHz.

Fecha	Ancho de banda	Banda	Concurso de radioaficionados
16-17 Febrero 2013	640 kHz	21 MHz	ARRL Int. DX CW Contest 2013
14-15 Diciembre 2013	1.28 MHz	28 MHz	ARRL 10 m Contest 2013
13-14 Diciembre 2014	1.28 MHz	28 MHz	ARRL 10 m Contest 2014

La banda de radioaficionados en 14 MHz cubre las frecuencias desde 14000 kHz hasta 14350 kHz. Para poder cubrir toda la información espectral de esta banda se ha seleccionado 14175 kHz como frecuencia central de las medidas y un ancho de banda de 500 kHz

TABLA A.3. Selección de medidas de banda ancha de la banda de 14 MHz incluidas en la base de datos HFSA_IDeTIC_F1_V01.

Fecha	Ancho de banda	Número de Medidas	Concurso de radioaficionados
3 Junio 2011	640 kHz	20	– (Grabada entre semana)
10 Junio 2011	640 kHz	29	– (Grabada entre semana)
24 Septiembre 2011	640 kHz	14	First Greek Telegraphy Club CW Cup

TABLA A.4. Selección de medidas de banda ancha de la banda de 14 MHz incluidas en la base de datos HFSA_IDeTIC_F1_V02.

Fecha	Ancho de banda	Número de Medidas	Concurso de radioaficionados
3 Junio 2011	640 kHz	20	– (Grabada entre semana)
10 Junio 2011	640 kHz	29	– (Grabada entre semana)
24 Septiembre 2011	640 kHz	14	First Greek Telegraphy Club CW Cup
23-24 Junio 2012	640 kHz	72	ARRL Field Day 2012
14-15 Julio 2012	1.28 MHz	72	IARU HF World Championship 2012

ó 1 MHz. Debido a las características del VSA, éstas tienen un ancho de banda mayor, 640 kHz y 1.28 MHz, respectivamente. Con estas especificaciones se han adquirido medidas de la banda de radioaficionados y también de otros canales con diferente uso. En el caso de las medidas adquiridas en la banda de 21 MHz (21000-21450 kHz), la frecuencia central ha sido 21225 kHz y el ancho de banda 640 kHz, y en las medidas de la banda de 28 MHz (28000-29700 kHz), la frecuencia central ha sido 28500 kHz con un ancho de banda de 1.28 MHz.

A.6.3 *Spectrum Sensing* con detector de energía

La estrategia de observación del espectro seleccionada en esta Tesis está basada en la detección de usuarios primarios a través de un detector de energía. Durante la adquisición de medidas de la banda de HF se pudo comprobar que esta banda es un entorno heterogéneo donde se pueden observar múltiples tipos y patrones de transmisión diferentes. Un usuario secundario de la banda de HF no tiene información previa sobre el comportamiento de los usuarios primarios, por lo tanto, el detector de energía es la téc-

nica más apropiada para llevar a cabo *spectrum sensing* en la banda de HF.

El detector de energía calcula la potencia media de la señal adquirida en el dominio de la frecuencia y en un periodo de tiempo determinado. Después, la detección de las señales de los usuarios se realiza al comparar la potencia media de la señal con un umbral definido previamente en función del piso de ruido (Urkowitz, 1967).

Una vez el VSA ha capturado la información espectral con la FFT, se procesan las medidas en el dominio de la frecuencia para obtener muestras que representen la potencia media de un canal HF de 3 kHz en un intervalo temporal de 2 segundos. A continuación, la potencia media de cada canal es promediada en una ventana temporal de los 8 segundos previos para caracterizar mejor la evolución temporal de las transmisiones. Así mismo, se omiten aquellas muestras que representen los nulos del canal HF o el ruido impulsivo de la banda. Finalmente, se plantea la detección de señales de usuarios primarios a través de la transformación de las muestras de potencia en valores normalizados que representen la actividad de dichos usuarios. Para ello, se plantea el problema de detección de la Ecuación A.1.

El detector que maximiza la probabilidad de detección para una determinada probabilidad de falsa alarma se define a través del test del cociente de probabilidad especificado por el lema de Neyman-Pearson (Kay, 1998):

$$L(\mathbf{y}) = \frac{p\left(\mathbf{y}; H_1\right)}{p\left(\mathbf{y}; H_0\right)} > \lambda \tag{A.2}$$

donde $p\left(\mathbf{y}; H_1\right)$ es la función de distribución de probabilidad de las muestras de canales ocupados, $p\left(\mathbf{y}; H_0\right)$ la función de distribución de probabilidad de las muestras de canales con ruido y el umbral λ del detector se calcula a partir de la restricción en la probabilidad de falsa alarma

$$P_{FA} = \int_{\lambda}^{\infty} p\left(\mathbf{y}; H_0\right) d\mathbf{y} = \gamma. \tag{A.3}$$

La mejor forma de evaluar este detector es a través de las curvas de las características operativas del receptor (ROC, receiver operating characteristics) que representan la probabilidad de detección (P_D) frente a la probabilidad de falsa alarma (P_{FA}) para diferentes valores del umbral λ. Dada una determinada probabilidad de falsa alarma γ, el valor del umbral que maximiza la probabilidad de detección se obtiene a partir de la curva ROC estimada.

Para las medidas adquiridas, se estiman las funciones de distribución de probabilidad de ambas hipótesis calculando el histograma normalizado de las muestras de canales con ruido y de las muestras de canales ocupados. Estas estimaciones están representadas en la Figura A.9 y a partir de ellas se calcula el umbral de decisión λ. Además, para poder evaluar las curvas ROC, la distribución de probabilidad de los canales con ruido ha sido ajustada a una distribución normal $N(\mu_0, \sigma_0)$ con media $\mu_0 = -58{,}82$, desviación

estándar $\sigma_0 = 3{,}23$ y función de densidad de probabilidad

$$p\left(\mathbf{y};H_0\right) = \frac{1}{\sigma_0\sqrt{2\pi}} e^{-\frac{(y-\mu_0)^2}{2\sigma_0^2}}, \tag{A.4}$$

mientras que la distribución de probabilidad de canales ocupados ha sido ajustada a una distribución GEV (Generalised Extreme Value) con parámetros $\mu = -47{,}125$, $\sigma = 3{,}882$, $\xi = -0{,}015$ y función de densidad de probabilidad

$$p\left(\mathbf{y};H_1\right) = \frac{1}{\sigma}\left(1+\xi\frac{y-\mu}{\sigma}\right)^{-\frac{\xi+1}{\xi}} e^{-\left(1+\xi\frac{y-\mu}{\sigma}\right)^{-\frac{1}{\xi}}}. \tag{A.5}$$

Al contrario que una distribución normal, la distribución GEV puede utilizarse para ajustar datos con una distribución asimétrica como los correspondientes a los canales ocupados en la Figura A.9.

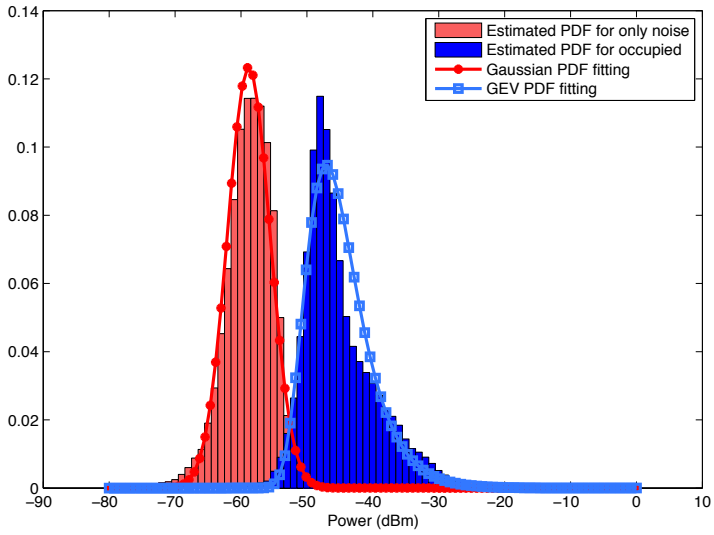

FIGURA A.9. Estimación y ajuste estadístico de la distribución de probabilidad de las muestras de canales de sólo ruido y de canales ocupados.

Después de ajustar ambas distribuciones, se calculan la probabilidad de falsa alarma (P_{FA}) y la probabilidad de detección (P_D) para representar la curva ROC analítica de la Figura A.10, donde

$$P_{FA} = \int_\lambda^\infty p\left(\mathbf{y};H_0\right)dy = \int_\lambda^\infty \frac{1}{\sigma_0\sqrt{2\pi}} e^{-\frac{(y-\mu_0)^2}{2\sigma_0^2}} dy = Q\left(\frac{\lambda-\mu_0}{\sigma_0}\right) \tag{A.6}$$

$$\begin{aligned} P_D &= \int_\lambda^\infty p\left(\mathbf{y};H_1\right)dy = \\ &= \int_\lambda^\infty \frac{1}{\sigma}\left(1+\xi\frac{y-\mu}{\sigma}\right)^{-\frac{\xi+1}{\xi}} e^{-\left(1+\xi\frac{y-\mu}{\sigma}\right)^{-\frac{1}{\xi}}} dy = 1 - e^{-\left(1+\xi\frac{\lambda-\mu}{\sigma}\right)^{-\frac{1}{\xi}}} \end{aligned} \tag{A.7}$$

y λ es el umbral de detección.

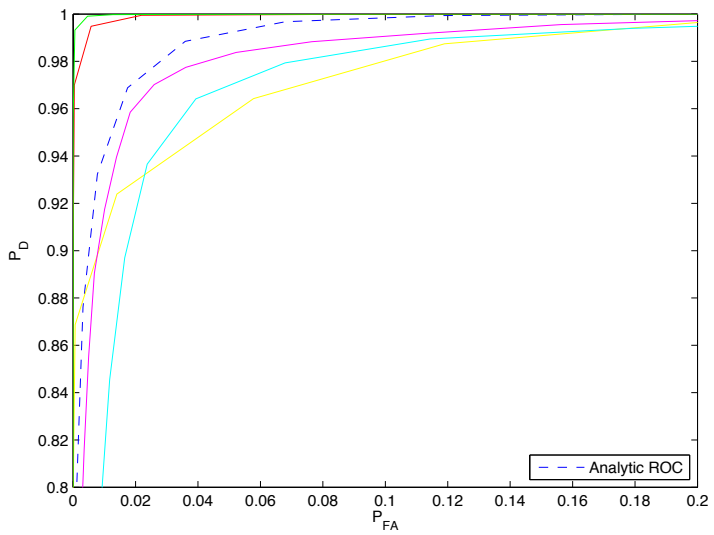

FIGURA A.10. Curvas de las características operativas del receptor (ROC)

A.7 Detección de interferencias de banda estrecha con *Compressive Sensing*

Aunque las comunicaciones HF se establecen generalmente con transceptores de banda estrecha de 3 kHz (Maslin, 1987), nuevos transceptores de banda ancha han sido recientemente especificados en el estándar MIL-STD-188-110C. Además de alcanzar mayores tasas de datos, nuevas estrategias basadas en comunicaciones multicanal pueden ser implementadas en ellos y así lograr un uso más eficiente de la banda. Entre estas estrategias destaca la aplicación de radio cognitiva (Haykin, 2005), tal y como se propone en esta Tesis, ya que las estaciones HF pueden ser dotadas con nuevas capacidades como adaptabilidad y conocimiento para explotar mejor el espectro de frecuencias.

Sin embargo, el uso de receptores de banda ancha conlleva nuevos retos como hacer frente al efecto de las interferencias de banda estrecha (NBI, narrowband interference). Además de la propagación a través de reflexiones en la ionosfera, la posibilidad de establecer un enlace sin saltos a través de la superficie terrestre provoca la aparición de señales de muy alta potencia que han sido transmitidas desde una estación cercana geográficamente al receptor. La presencia de NBI en la señal recibida fuerza la adaptación de la señal de banda ancha recibida al rango dinámico del conversor analógico-digital (ADC, analog-to-digital converter), es decir, el número efectivo de bits utilizados para digitalizar las señales de interés se reduce y el ruido de cuantificación supera al ruido térmico y a la señal de interés (Pérez-Díaz et al., 2012). Es por ello que se requiere algún método para detectar y mitigar el efecto de la NBI en el dominio analógico y, así, aumentar el número efectivo de bits utilizados para digitalizar las señales de interés en el ADC del receptor de banda ancha y la relación señal a ruido.

En esta Tesis se propone un detector de NBI de baja complejidad basado en *Compressive Sensing* (CS). Dicho detector, que tiene un ADC de baja velocidad, será utilizado

conjuntamente con un receptor de banda ancha ejecutando la tarea de *spectrum sensing*. Por lo tanto, el mayor objetivo a lograr es detectar NBI eficientemente a la vez que la radio cognitiva monitoriza múltiples canales simultáneamente. Además, se evalúan sus prestaciones con la base de datos HFSA_IDeTIC_F1_V02 de medidas reales de la banda de HF, donde tanto las transmisiones deseadas como las interferencias son señales de banda estrecha. Es por ello que las propuestas presentadas en (G. Chen et al., 2010; Kanterakis & Bruno, 1994; F. Wang & Tian, 2008) no pueden ser aplicadas aquí porque consideran señales deseadas de banda ancha. Tampoco son viables las soluciones basadas en CS para mitigación de NBI de (Davenport et al., 2009), (Davenport et al., 2010) y (Hwang et al., 2010) porque asumen que la localización de la NBI es previamente conocida, suposición que no se considera en esta Tesis.

El esquema de detección propuesto está descrito en la Figura A.11 como fase de detección, siendo un sistema que trabaja en paralelo al receptor de banda ancha antes de digitalizar de la señal recibida. De esta manera, se garantiza la detección y mitigación de NBI en el dominio analógico para posteriormente garantizar también un número suficiente de bits para digitalizar las transmisiones deseadas. Para ello, el detector de NBI se auto-configura en función del estado del control automático de ganancia (AGC, automatic gain control).

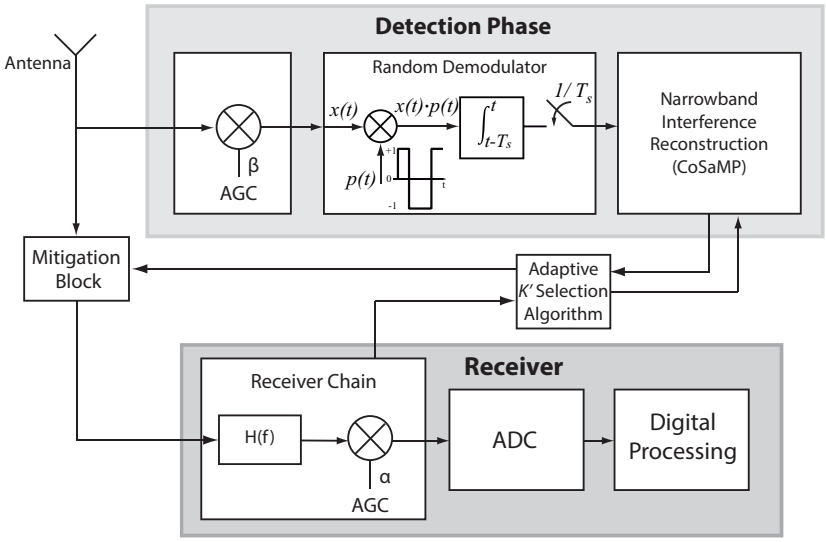

FIGURA A.11. Arquitectura de un receptor de banda ancha junto al detector de NBI propuesto.

La baja complejidad del sistema propuesto radica en la aplicación de CS. Actualmente, los ADCs son llevados al límite para cumplir con el teorema de Nyquist en la digitalización de señales de banda ancha (Tropp et al., 2010). Sin embargo, las técnicas CS son aplicadas a las señales que contienen poca información cuando son representadas en un determinado dominio (Candès, 2006)(Donoho, 2006), denominadas dispersas, aprovechan sus características para digitalizarlas con una tasa de muestreo inferior a la del teorema de Nyquist, haciendo uso de ADC de menor velocidad. Éste es el caso de la banda de HF donde el espectro, tras la transformada de Fourier de una señal de banda ancha en el tiempo, está formado por múltiples señales de banda estrecha con múltiples *spectrum*

holes entre ellas.

A.7.1 Efecto de NBI en receptores de banda ancha

El comportamiento del detector de NBI propuesto en esta Tesis está basado en la respuesta del AGC del receptor de banda ancha desarrollado en (Pérez-Díaz et al., 2009). El AGC es responsable de adaptar la potencia de entrada al rango dinámico del ADC del receptor de banda ancha. Cuando la potencia de la señal de entrada es baja, la ganancia del AGC es máxima. A medida que la potencia de entrada aumenta, la ganancia va disminuyendo hasta que se llega al punto en el que el AGC está saturado. Cuando esto ocurre, la salida del AGC no puede ser adaptada al rango dinámico del ADC y se produce un efecto de *clipping* en la conversión de la señal analógica en digital, degradando las prestaciones finales del transceptor. Este efecto suele ocurrir cuando hay NBI a la entrada del transceptor, de ahí la importancia de detectar NBI en el dominio analógico.

La Figura A.12 muestra un ejemplo real del efecto de NBI en el receptor HF de banda ancha. Esta medida, incluida en la base de datos HFSA_IDeTIC_F1_V02, muestra una señal interferente en cerca de 14.1 MHz cuya potencia es 40 dB superior al resto de transmisiones de banda estrecha. Cuando está presente provoca la adaptación de toda la señal al rango dinámico del ADC atenuando todas las señales deseadas por debajo del piso de ruido.

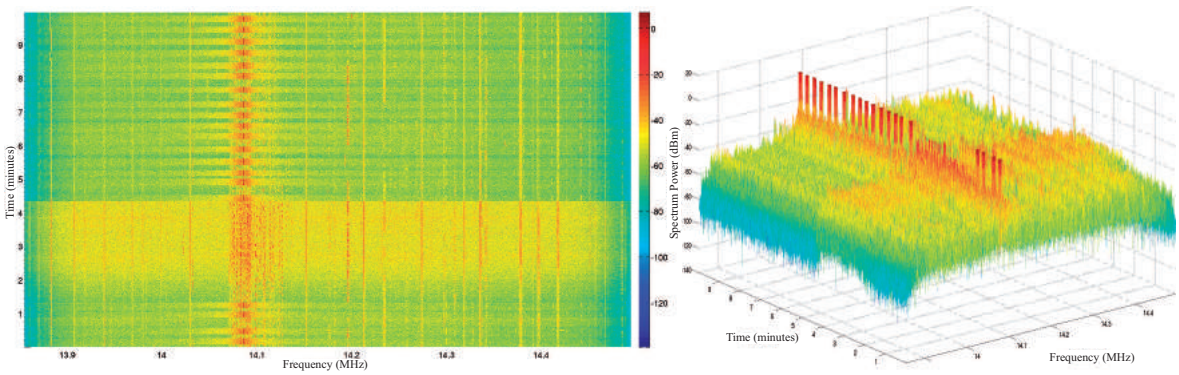

FIGURA A.12. Ejemplo de una medida de 600 kHz de ancho de banda en la banda de 14 MHz durante 10 minutos con una NBI intermitente en 14.09 MHz.

A.7.2 *Compressive Sensing*

Compressive sensing (CS) establece una estrategia nueva de adquisición de señales de banda ancha con ADCs de velocidad muy inferior a la de Nyquist (Candès, 2006)(Donoho, 2006). Las medidas $\mathbf{y} \in \mathbb{R}^M$ del procedimiento de adquisición CS se expresan como

$$\mathbf{y} = \mathbf{\Phi x} + \mathbf{e} = \mathbf{\Phi \Psi s} + \mathbf{e}, \tag{A.8}$$

donde $\mathbf{x} \in \mathbb{R}^N$ representa las muestras de la señal en el tiempo muestreadas a la tasa de Nyquist en una determinada ventana de tiempo, $\mathbf{\Phi}$ es una matriz $M \times N$ llamada matriz

de medidas, $\mathbf{e} \in \mathbb{R}^M$ es un término de error, $\mathbf{\Psi}$ es una base ortonormal, y $\mathbf{s}$ contiene los coeficientes de la señal en el dominio *compressive*. En concreto, CS está enfocado a escenarios en los que el número de medidas adquiridas es muy inferior al número de muestras especificadas por el teorema de Nyquist, i.e., $M \ll N$. La teoría de CS está enfocada a señales $\mathbf{s}$ donde sólo unos pocos coeficientes en la base $\mathbf{\Psi}$ contienen la energía de la señal, mientras que el resto son cercanos a cero. En este contexto, se define $\mathbf{s}$ como una señal K-dispersa si tiene K coeficientes diferente de cero (Candès, 2006)(Donoho, 2006). Éste es el caso del espectro tras la transformada de Fourier de una señal de banda ancha compuesta por múltiples señales de banda estrecha y *spectrum holes* entre ellas.

Además, la adquisición de medidas en un sistema CS debe asegurar que la información de la señal original no se daña por la reducción dimensional (Candès, 2006). Para ello, la propiedad *Restricted Isometry Property* (RIP) (Candès & Tao, 2005) determina si se garantiza la reconstrucción en un sistema caracterizado por la matriz de sistema $\mathbf{A} = \mathbf{\Phi\Psi}$. Se define la RIP de orden K para la matriz de sistema $\mathbf{A}$ y para cualquier señal K-dispersa $\mathbf{s}$ como (Candès & Tao, 2005)

$$(1-\delta_K)\|\mathbf{s}\|_{l_2}^2 \leq \|\mathbf{As}\|_{l_2}^2 \leq (1+\delta_K)\|\mathbf{s}\|_{l_2}^2, \tag{A.9}$$

donde $\|\cdot\|_{l_2}$ es la norma euclídea y la constante $\delta_K \in (0,1)$ determina cuánta energía de la señal original ha sido conservada en el proceso de medidas (Candès & Tao, 2005). Es habitual afirmar que el sistema de medidas satisface la RIP si la constante δ_K tiene un valor cercano a cero (Candès & Tao, 2005).

Una vez que las medidas, $\mathbf{y}$, han sido adquiridas cumpliendo (A.9), el siguiente paso es la reconstrucción de la señal original $\mathbf{s} \in \mathbb{R}^N$. Como expuso (Candès et al., 2006), una reconstrucción precisa se obtiene de

$$\begin{aligned} \underset{\mathbf{s}\in\Re^N}{\text{minimize}} \quad & \|\mathbf{s}\|_{l_1} \\ \text{subject to} \quad & \|\mathbf{As}-\mathbf{y}\|_{l_2} \leq \epsilon \end{aligned} \tag{A.10}$$

dado que $\delta_{2K} < \sqrt{2}-1$. Aquí, $\|\mathbf{s}\|_{l_1}$ es la norma l_1 y ϵ es la constante que limita el ruido en las medidas $\|e\|_{l_2} \leq \epsilon$.

A.7.3 Detector de NBI basado en *Compressive Sensing*

En el diseño propuesto en la Figura A.11, la señal de recibida en la antena, que contiene NBI, se envía al detector de NBI (*detection phase*) y al bloque de mitigación situado a la entrada del receptor de banda ancha. La estructura del detector de NBI tiene dos partes: la adquisición de la señal de banda ancha con una tasa de muestreo inferior a la de Nyquist pero cumpliendo la RIP (A.9) y su reconstrucción (A.10). En el detector propuesto, la señal es adquirida con un *random demodulator* (Tropp et al., 2010) que digitaliza la señal con un ADC de baja velocidad. Después, ésta es reconstruida con el algoritmo CoSaMP (Needell & Tropp, 2009). Este algoritmo extrae la localización en el

dominio de la frecuencia de las transmisiones de banda estrecha con más potencia en la banda. Dichas localizaciones son enviadas posteriormente al bloque de mitigación para que aplique técnicas de cancelación y garantizar así que el funcionamiento del transceptor no se ve afectado por NBI. Durante este proceso se asume que el transceptor conoce las frecuencias en las que establece la comunicación para no cancelar señales deseadas.

Cabe destacar que el sistema propuesto funciona acorde al estado del AGC del transceptor de banda ancha, es decir, dependiendo de si está saturado o no. Si la señal recibida no puede ser procesada, el bloque de mitigación actúa en las frecuencias indicadas por el algoritmo CoSaMP para atenuar la NBI. De esta manera, la entrada del receptor de banda ancha no contendrá NBI. Por otro lado, si la señal de entrada está en el rango de trabajo del AGC, el bloque de mitigación no entra en funcionamiento.

Una de las características del algoritmo CoSaMP es que requiere como parámetro de entrada el orden K' de la señal dispersa a reconstruir. En el caso de un escenario real como el que se propone implica que K' puede controlar el número de señales interferentes a detectar ya que coincide con el número de componentes en la frecuencia que el algoritmo va a reconstruir. Es por ello que, para poder detectar todas las interferencias presentes a la entrada del transceptor de banda ancha, el orden K' de reconstrucción se controla de acuerdo con el estado del AGC siguiendo el algoritmo diseñado en la Figura A.13.

A.7.4 Experimentos

Un detector de NBI basado en CS y con una tasa de muestreo ocho veces inferior a la de Nyquist ha sido diseñado para demostrar los beneficios del mismo. Se trata de una reducción de la tasa de muestreo de la señal compleja de 1 MHz a 125 kHz. Particularmente, bloques de $N = 4096$ muestras obtenidas con una tasa de Nyquist en una ventana de tiempo determinada son introducidos en el *random demodulator*. De estas muestras, el *random demodulator* produce $M = 512$ muestras en el dominio *compressive* que serán entregadas al algoritmo CoSaMP para obtener la localización de NBI en el dominio de la frecuencia.

Dada la variabilidad de la actividad en la banda de HF, las medidas de la base de datos HFSA_IDeTIC_F1_V02 han sido clasificadas en tres categorías: 41.67 % de ellas se corresponden a un escenario normal (días entre semana), 41.67 % en escenarios de alta actividad (fin de semana) y 16.66 % en medidas con NBI como la de la Figura A.12. Todas las medidas de los escenarios de actividad normal y alta no tienen NBI presente y fueron adquiridas con el AGC en su rango de trabajo.

Con el algoritmo presentado previamente en la Figura A.13 se varía el orden K'. Es por ello que, para demostrar la importancia de seleccionar un valor de K' adecuado, en los próximos párrafos se detalla el análisis del comportamiento del detector de NBI al variar K'. Se calcula la tasa de detección y de falsa alarma del detector de NBI comparando el conjunto de componentes reconstruidas por el algoritmo CoSaMP con las componentes

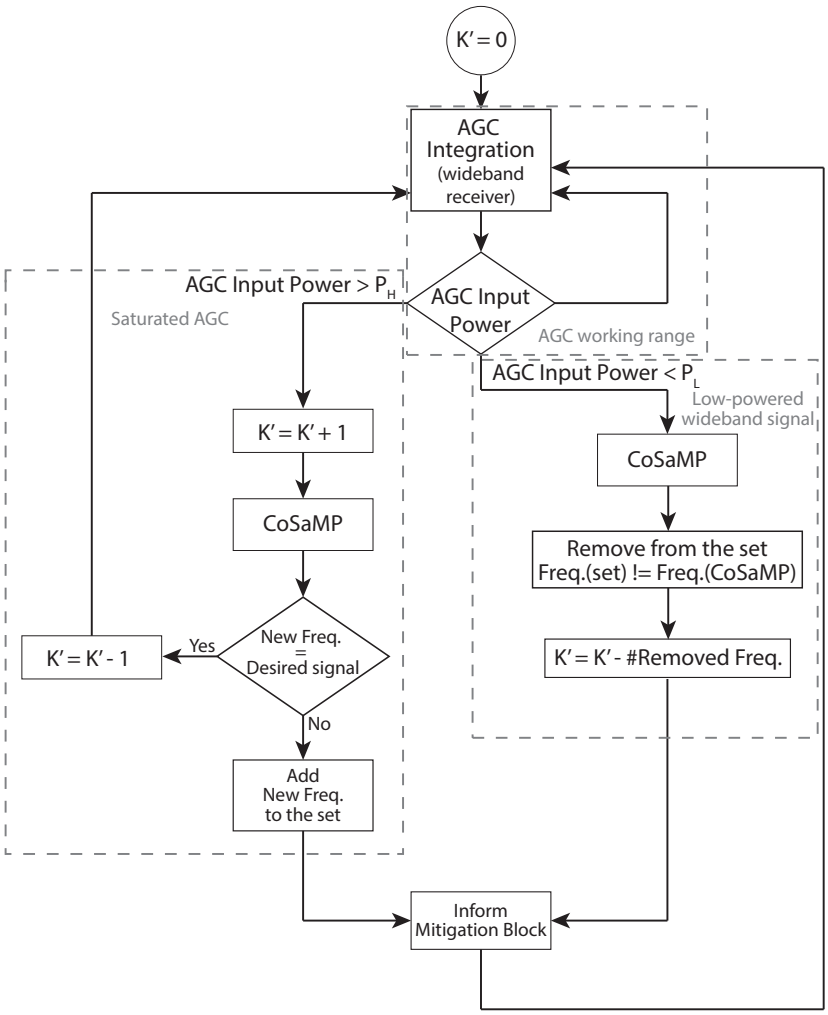

FIGURA A.13. Diagrama de flujoe del algoritmo de selección del orden K' de reconstrucción.

existentes en la señal original. Los resultados de ambas tasas están representados en las Figuras A.14 y A.15, donde se muestra que las prestaciones del detector de NBI dependen del orden K' y de la actividad en la banda.

Cuando sólo hay una NBI que se desea detectar, $K' = 1$, las prestaciones son mejores en los escenarios en los que hay una única NBI: la tasa de detección asciende al 92 % y la de falsa alarma es igual al 8 %. Sin embargo, existe una mejora cuando el orden K' asciende a $K' = 5$ debido a las características de las medidas, ya que cada componente frecuencial es de 600 Hz y el ancho de banda habitual en las comunicaciones de HF de 3 kHz. Dicho de otro modo, existen varias componentes frecuenciales que el algoritmo CoSaMP reconstruye que pertenecen a la misma transmisión.

En las Figuras A.14 y A.15 se muestra la importancia de seleccionar un valor de K' adecuado. En escenarios de alta actividad, donde hay múltiples señales de banda estrecha con niveles de potencia altos y similares, tanto la tasa de detección como la de falsa alarma mejoran con $K' = 15$ a $K' = 30$, alcanzando un 97.8 % de detección y un 4 % de falsa alarma. Sin embargo, en los escenarios en los que no hay múltiples señales representativas como el de actividad normal o el de sólo NBI, a medida que K' crece también

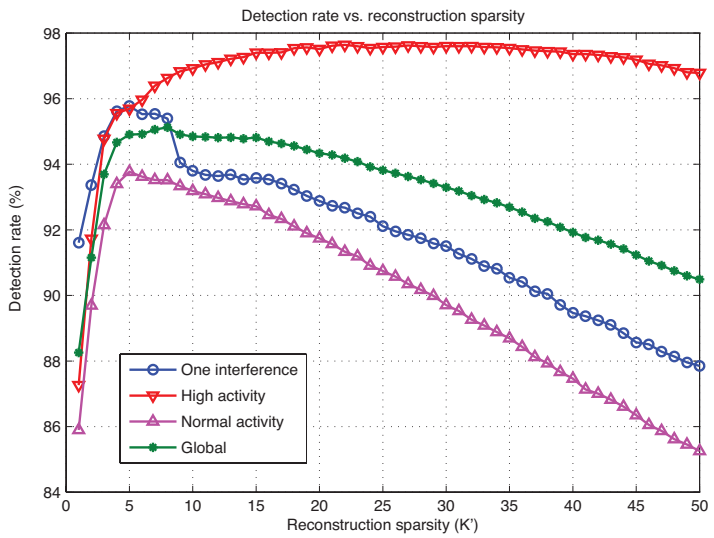

FIGURA A.14. Tasa de detección respecto al orden K'.

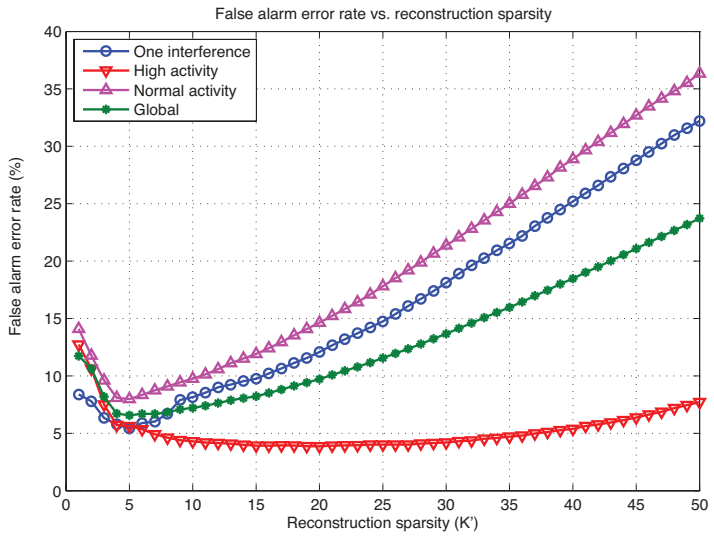

FIGURA A.15. Tasa de falsa alarma respecto al orden K'.

lo hace el error. Ello se debe a la diferencia en potencia entre las señales de mayor potencia y el resto, i.e., una vez que todas las componentes de las transmisiones de mayor potencia son reconstruidas, el resto de coeficientes aparecen en puntos donde no hay señales representativas.

A.7.5 Caracterización del RD en escenarios reales

Los resultados obtenidos en los experimentos descritos en la Sección A.7.4 permiten caracterizar el comportamiento del RD en un escenario real, a diferencia de su estudio teórico en (Tropp et al., 2010) en un escenario controlado. En (Tropp et al., 2010), se utilizó una regla empírica para relacionar la tasa de muestreo R necesaria para identificar una señal K-dispersa con un ancho de banda W utilizando el RD y el modelo de señal propuesto en (Tropp et al., 2010). Este mismo procedimiento es utilizado en esta Tesis con

las medidas reales de la banda de HF. En este caso, el ancho de banda es el del transceptor HF de banda ancha, 1 MHz, y debido al ruido y los diferentes tipos de transmisiones presentes en las medidas reales, se calcula la tasa de muestreo R mínima con la que se obtiene una tasa de falsa alarma del 10 %. Los resultados obtenidos están dibujados en la Figura A.16 para un orden K de 2 a 100 y una tasa de muestreo R resultante del coeficiente W/P con P siendo un valor entero $P = 3, 4, ..., 10$ (líneas horizontales azules de la Figura A.16).

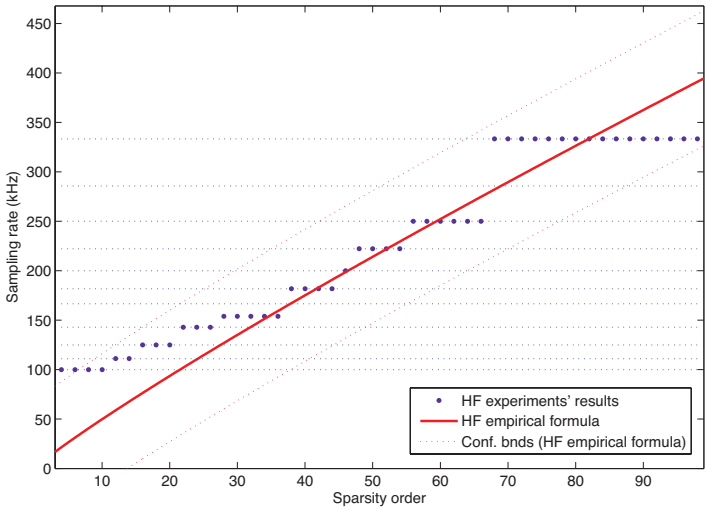

FIGURA A.16. Resultados del ajuste a la fórmula empírica (A.11).

Se realiza el ajuste de los resultados obtenidos a la fórmula empírica propuesta en (Tropp et al., 2010):

$$R \approx CK \log\left(\frac{W}{K} + 1\right), \tag{A.11}$$

donde log es logaritmo neperiano y C la constante de ajuste de los resultados. El test de bondad del ajuste demuestra que los resultados de los experimentos están dentro de los márgenes de confianza. Además, el valor de la métrica R-square, que es igual a 0.8594, demuestra que el ajuste realizado con los resultados de los experimentos es capaz de explicar el 85.94 % de las variaciones en los datos con respecto a la media. Asimismo, se muestra que las prestaciones en términos de detección con el *random demodulator* en escenarios reales es muy similar a las prestaciones teóricas mostradas en (Tropp et al., 2010).

A.8 Modelo de la actividad de los usuarios primarios en la banda HF

Un modelo de la actividad de los usuarios primarios puede ser de gran ayuda para predecir su actividad en un futuro a partir del conocimiento previamente adquirido. En esta Tesis se desarrolla un modelo para realizar predicciones a largo plazo basado en modelos ocultos de Markov (HMM, Hidden Markov Models). Este modelo es entrenado y validado con la base de datos de medidas de la banda HFSA_IDeTIC_F1_V01. Se propone

el uso de HMMs ya que son una herramienta muy robusta para modelar procesos estocásticos, obteniendo gran precisión con modelos de baja complejidad. Además, tienen un fundamento matemático fuerte y son abordables (Akbar & Tranter, 2007), propiedad que no siempre está garantizada con las redes neuronales (Blum & Rivest, 1992).

A.8.1 Modelos ocultos de Markov

Un modelo oculto de Markov se define como un proceso doblemente embebido con uno de los procesos estocásticos no observable. Este proceso oculto sólo puede ser evaluado a través de otro conjunto de procesos que generan la secuencia que sí puede ser observada (Rabiner & Juang, 1993). Un HMM para observaciones discretas se define con los siguientes elementos:

- **A**: Matriz de la distribución de probabilidad de las transiciones entre estados.
- **B**: Matriz de la distribución de probabilidad de los símbolos observados en cada estado.
- π: Vector con la distribución de probabilidad del estado inicial.
- **O**: Secuencia de observaciones.

Por lo tanto, una definición completa de un HMM incluye dos parámetros (N el número de estados del modelo y M el número de observaciones posibles), la especificación de los símbolos observables y la definición de **A**, **B** y π, lo que se resume en la notación compacta de un HMM:

$$\lambda = (\mathbf{A}, \mathbf{B}, \pi)\,. \tag{A.12}$$

Existen dos tipos de HMM según su estructura. Los HMM ergódicos o totalmente conectados permiten transiciones entre todos los estados del modelo, mientras que los HMM *left-right* o de Bakis tienen la propiedad de que a medida que aumenta el tiempo también lo hace el índice del estado o permanece en el mismo estado. Este tipo de HMM fue introducido para modelar señales que variaban a lo largo del tiempo. Además, otra característica de los HMM *left-right* es que la secuencia de estados empieza en el estado 1 y termina en el estado N.

Finalmente, existen tres tareas principales que deben ser llevadas a cabo en un HMM para que éste sea útil en la aplicación para la que ha sido diseñado (Rabiner & Juang, 1993):

1. *Evaluación*: Dada una secuencia de observaciones y un conjunto de modelos a comparar, se evalúa la probabilidad de que la secuencia de observación dada ha sido generada por cada uno de los modelos, $P\left(O|\lambda_k\right)$. Se calcula con la suma de las variables *forward* definidas en el algoritmo *forward-backward* (Rabiner & Juang, 1993).

2. *Decodificación*: Dada una secuencia de observaciones, se selecciona la secuencia de estados que es óptima en algún sentido. El criterio más utilizado es el de encontrar la secuencia de estados que maximiza la probabilidad $P(Q, O = |\lambda)$ utilizando el algoritmo de Viterbi (Forney, 1973).

3. *Aprendizaje*: Es la tarea en la que los parámetros de un determinado modelo se ajustan para maximizar su verosimilitud cuando se utiliza una secuencia de observaciones que le corresponde. Se suele referir como el entrenamiento del modelo en el que se buscan los parámetros que mejor describen la secuencia de observaciones utilizada. El método Baum-Welch (Rabiner & Juang, 1993) es el más utilizado para maximizar la verosimilitud del modelo definida por la probabilidad $P(O|\lambda)$.

En las Secciones A.8.4, A.8.5 y A.8.6 se describe como las tres tareas fueron ejecutadas para entrenar y validar el modelo, así como para su uso una vez entrenado como sistema de predicción a largo plazo.

A.8.2 HFSA_IDeTIC_F1_V01: clasificación y segmentación de medidas

Al realizar la tarea de *spectrum sensing*, las medidas de banda ancha adquiridas en la base de datos HFSA_IDeTIC_F1_V01 han sido transformadas en secuencias de observación binarias que representan un canal de HF con ancho de banda de 3 kHz y nueve o diez minutos de duración. En cada secuencia, '0' representa las muestras con sólo ruido mientras que '1' representa las muestras de canales ocupados. A continuación, para reducir la variabilidad en las estrategias de aprendizaje seleccionadas en esta Tesis, se han segmentado las secuencias correspondientes a cada canal en secuencias más pequeñas de un minuto y éstas han sido posteriormente clasificadas.

Debido a la diferencia de actividad observada en la banda de HF, los usuarios secundarios de la banda tienen diferentes opciones de transmisión. Por ello, las secuencias de un minuto han sido clasificadas en:

- *Canales disponibles* donde el usuario secundario puede transmitir.
- *Canales no disponibles* donde un usuario primario está transmitiendo y, por lo tanto, un usuario secundario no puede transmitir.
- *Canales parcialmente disponibles* en los que hay pequeños intervalos en los que un usuario secundario puede transmitir hasta que un usuario primario vuelva a aparecer.

Las secuencias de nueve y diez minutos de duración han sido segmentadas en secuencias de un minuto tal y como se muestra en la Figura A.17 y posteriormente clasificadas en canales *disponibles*, *no disponibles* o *parcialmente disponibles* y codificados como $\{1, 2, 3\}$, respectivamente, para reducir la complejidad del modelo de actividad propuesto en la Sección A.8.3.

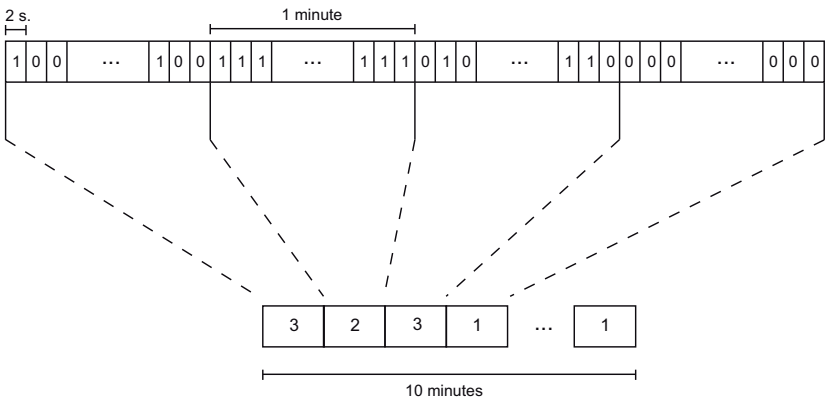

FIGURA A.17. Clasificación y segmentación de los datos.

A.8.3 Definición del modelo de actividad de usuarios primarios de HF

Dada la clasificación de las secuencias de observaciones realizada en la Sección A.8.2, el modelo diseñado tiene una estructura jerárquica y se define como un HMM ergódico con tres estados que conecta tres submodelos, uno para cada clase definida, i.e., disponible, no disponible y parcialmente disponible, tal y como se muestra en la Figura A.18.

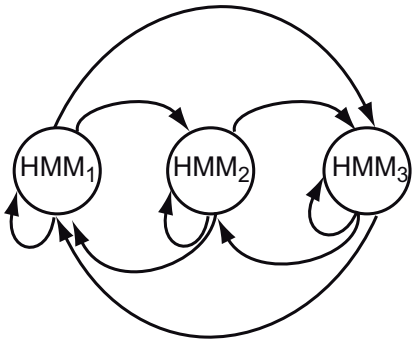

FIGURA A.18. HMM principal del modelo de actividad de usuarios primarios de HF.

Se entrena cada submodelo con un conjunto de secuencias de observaciones de un minuto de la clase correspondiente para generar un modelo adecuado a dicha clase. Por lo tanto, el primer modelo caracteriza las secuencias de canales disponibles, el segundo caracteriza las secuencias de canales no disponibles y el tercero, las secuencias de canales parcialmente disponibles. Los tres submodelos son implementados como HMM *left-right* ya que la estructura de su matriz de transiciones es adecuada para modelar la evolución temporal de las muestras de las secuencias de observaciones con un número reducido de parámetros, comparado con los modelos ergódicos. En resumen, el modelo de actividad de los usuarios primarios de HF está construido a partir de un modelo principal, un HMM ergódico con tres estados, siendo cada estado una de las clases definidas: disponible, no disponible y parcialmente disponible. Además, cada estado emite una secuencia de observaciones de un minuto de duración que es generada por el submodelo correspondiente.

Para simplificar el entrenamiento y la validación del modelo principal propuesto, se

entrenó como un HMM independiente en el que cada estado generaba un valor que representaba la secuencia de observaciones que generaría el submodelo que le corresponde: {1 (canales disponibles), 2 (canales no disponibles), 3 (canales parcialmente disponibles)}. Además, mientras los submodelos caracterizan las secuencias de observaciones de un minuto de canales disponibles, no disponibles o parcialmente disponibles, el modelo principal caracteriza la evolución temporal de un determinado canal de HF durante nueve o diez minutos, siendo cada estado el valor correspondiente a la clase de la secuencia de un minuto.

Una vez definido el modelo, se entrena y valida con las medidas de la base datos HFSA_IDeTIC_F1_V01. Un 70 % de las secuencias de observaciones se utiliza en la fase de entrenamiento de la Sección A.8.4, mientras que el 30 % restante se utiliza en el proceso de validación de la Sección A.8.5.

A.8.4 Entrenamiento del modelo

Para el entrenamiento se plantea la tarea de aprendizaje en la que se buscan los parámetros del HMM que maximicen $P(O|\lambda)$. Se utiliza el algoritmo Baum-Welch (Rabiner & Juang, 1993) para entrenar tanto los submodelos como el modelo principal. Dado que no había un conocimiento previo sobre la estructura de las secuencias de entrenamiento, se utilizaron matrices inicializadas de forma aleatoria en la primera iteración del algoritmo Baum-Welch.

Dos protocolos de entrenamiento son definidos porque la estructura del modelo principal difiere de la de los submodelos. Mientras el modelo principal tiene un número de estados pre-establecido (3), todavía queda por elegir el número de estados de los submodelos. Por un lado, la principal tarea en el entrenamiento del modelo principal es la inicialización de los parámetros de manera que la estructura sea independiente del punto de partida de ejecución. Es por ello que se utilizan diferentes semillas aleatorias para estimar los parámetros de la matriz de transiciones **A**. Por otro lado, los submodelos son entrenados con las matrices **A** y **B** inicializadas de manera aleatoria, diferentes números de estados entre 20 y 45, tal y como se muestra en la Figura A.19, y con las secuencias de observaciones de un minuto correspondientes.

Una vez entrenados con diferente número de estados, se compara la verosimilitud en escala logarítmica de cada uno de ellos, que se obtiene ejecutando la tarea de evaluación de la Sección A.8.1, y se selecciona el modelo con la máxima verosimilitud. De los resultados mostrados en la Figura A.19 se extrae que éstos tienen un máximo local en cuarenta estados para los submodelos de canales no disponibles y parcialmente disponibles. Por otro lado, los resultados del submodelo de canales disponibles son muy pequeños para cualquier número de estados, con lo que no existirían diferencias significativas en las prestaciones de este submodelo si el número de estados está entre 20 y 45. Desde un punto de vista práctico, el entrenamiento y el posterior uso de los submodelos para pre-

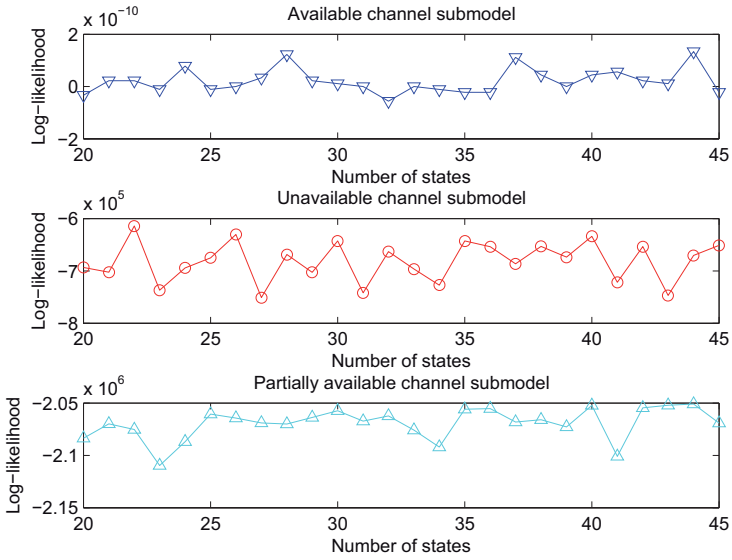

FIGURA A.19. Evolución de las verosimilitudes de los submodelos respecto al número de estados.

dicción se simplifican si los tres submodelos tienen el mismo número de estados. Por lo tanto, los submodelos son HMM *left-right* de cuarenta estados, como compromiso de los resultados anteriores, y con transiciones de hasta tres estados.

Cada submodelo con cuarenta estados es entrenado con un 70 % de las secuencias de observaciones de su clase para obtener los parámetros que maximizan $P(O|\lambda)$. El algoritmo Baum-Welch se ejecuta con matrices inicializadas de manera aleatoria y se seleccionan las matrices **A** y **B** tras diez iteraciones del algoritmo para obtener modelos estables y evitar *over-fitting*.

A.8.5 Validación del modelo

El 30 % restante de las secuencias de observaciones se utiliza para validar los modelos previamente entrenados. Dada la estructura definida, la validación se divide en dos pasos: primero, se evalúa la verosimilitud de los submodelos con las secuencias de un minuto, posteriormente, se calculan las probabilidades del modelo principal con las secuencias correspondientes a un canal de HF durante diez o nueve minutos.

Se ejecuta la tarea de evaluación en cada uno de los submodelos con cada secuencia de un minuto y se selecciona el submodelo con mayor probabilidad de haber generado dicha secuencia. Con estas decisiones se construye una matriz de valores $\{1, 2, 3\}$ siendo cada fila de la matriz una secuencia de observación de nueve o diez minutos. Posteriormente, dada la definición del modelo principal en el que las secuencias de observaciones son iguales a las transiciones entre estados del mismo, se compara la matriz generada con la original, resultando en un 5 % de errores en las decisiones realizadas a partir de los submodelos.

Finalmente, para validar el modelo principal se ejecuta la tarea de decodificación con el algoritmo de Viterbi (Forney, 1973). Este algoritmo fue diseñado para identificar la secuencia de transiciones entre estados que maximice $P(Q, O|\lambda)$. Dada la estructura del modelo principal, esta secuencia puede ser comparada con la matriz original de observaciones. El porcentaje de error logrado en este paso es el mismo que el obtenido al validar los submodelos, indicando que el modelo principal puede generar secuencias de observaciones como las utilizadas en esta fase de validación.

A.8.6 Predicción con el modelo de actividad de usuarios primarios de HF

En esta Tesis, se propone el uso del modelo de actividad de usuarios primarios de HF diseñado para la predicción de actividad a largo plazo, en este caso, en el próximo minuto. Se toma un minuto como periodo de predicción para permitir el establecimiento de transmisiones más largas. El sistema de predicción propuesto está representado en la Figura A.20. Mientras un usuario secundario está observando la actividad de los canales para seleccionar uno sin interferir con un usuario primario, debe procesar el espectro observado durante el último minuto de un determinado canal y utilizarlo como secuencia de observaciones O_T para evaluarla en cada uno de los submodelos. A través del algoritmo *forward-backward*, se calcula la probabilidad de que cada submodelo haya generado la secuencia O_T observada. En lugar de seleccionar el de mayor verosimilitud, se incluyen las probabilidades en la matriz de observaciones B del modelo principal. A continuación, se evalúa el algoritmo *forward-backward* en el modelo principal con la secuencia de estados correspondientes a los T minutos anteriores y las tres posibles opciones en el siguiente minuto: {1 (canales disponibles), 2 (canales no disponibles), 3 (canales parcialmente disponibles)}. De esta manera se calcula la probabilidad de que en el próximo minuto exista una de las clases de actividad de canal en función de lo observado anteriormente. Finalmente, se selecciona el estado con el que se obtiene la mayor probabilidad y este estado representa la actividad en el próximo minuto.

El error medio cometido por el modelo de predicción está representado en la Figura A.21. Debido a las restricciones del proceso de adquisición de medidas de la banda de HF, la mayoría de las secuencias tiene una duración de nueve minutos, lo que se traduce en un tiempo máximo de observación de ocho minutos para la predicción de la actividad en el siguiente minuto. Además de los resultados globales del modelo, se han diferenciado los resultados para dos escenarios de actividad comunes en la banda de HF: actividad normal (medidas adquiridas entre semana) y alta actividad (medidas adquiridas en fin de semana).

En términos globales, cuando el usuario secundario sólo conoce lo ocurrido en el minuto previo, el error medio asciende al 10.3 % pero éste disminuye a medida que el usuario secundario conoce la actividad durante más tiempo. Si esta actividad engloba lo ocurrido en los ocho minutos previos, el error medio se reduce a un 5.8 %.

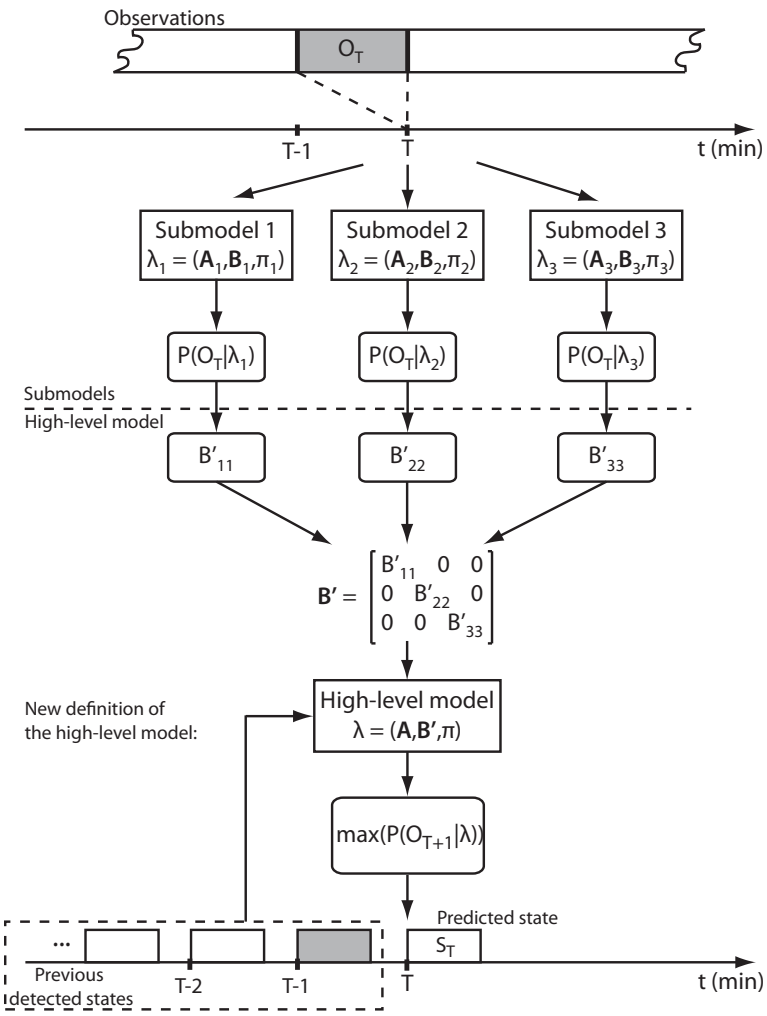

FIGURA A.20. Diagrama de bloques del sistema de predicción.

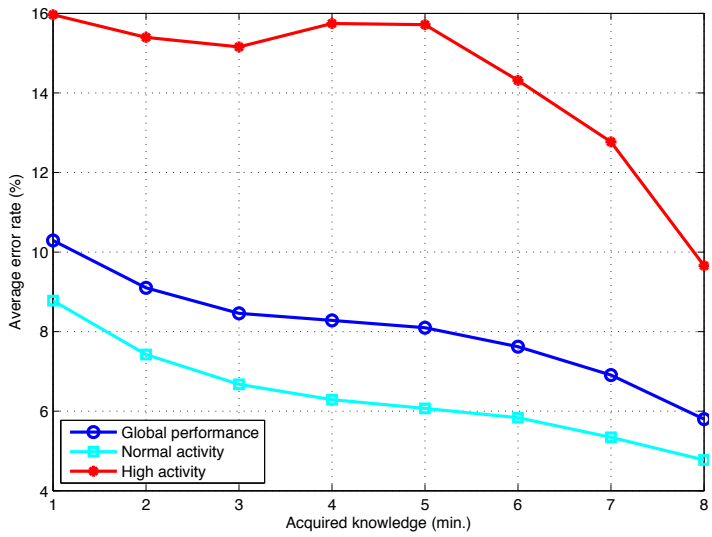

FIGURA A.21. Error medio cometido por el sistema de predicción.

A.9 Toma de decisiones con algoritmos *Upper Confidence Bound*

El modelo de predicción basado en HMM propuesto en la Sección A.8 permite aumentar la duración de las transmisiones de los usuarios de HF al realizar predicciones sobre la actividad de un canal de HF en el próximo minuto con baja complejidad. Sin embargo, su aplicación directa a un escenario de acceso oportunista al espectro (OSA) implica el uso de tantos modelos basados en HMM como el número de canales a observar y transmitir. Por lo tanto, se requiere una estrategia de toma de decisiones así como un esquema de predicción a corto plazo para complementar el modelo de predicción basado en HMM en una estación de HF cognitiva.

En esta Tesis se propone el uso de los algoritmos *Upper Confidence Bound* (UCB) para un acceso oportunista al espectro como se propuso en (Jouini et al., 2009). Este mecanismo ayuda a los usuarios de HF a decidir cuál es el mejor canal en términos de disponibilidad. Además, permite realizar predicciones a corto plazo durante su ejecución.

Como se describió en la Sección A.5.4.1, la toma de decisiones en OSA se puede modelar de forma directa con los MAB utilizados en *reinforcement learning*. Del conjunto de algoritmos detallados en la Sección A.5.4.1 para resolver MAB, el algoritmo UCB ha sido presentado como una solución eficiente de los mismos (Auer et al., 2002). Además, el intenso trabajo realizado en (Jouini et al., 2009, 2010; Robert et al., 2014) ha demostrado que los algoritmos UCB son viables en radio cognitiva para la toma de decisiones tanto en entornos simulados como reales. Es por ello que el algoritmo UCB puede ser también una solución viable para la aplicación de radio cognitiva en HF.

Se utiliza una selección de medidas de la base de datos HFSA_IDeTIC_F1_V01 para demostrar la viabilidad de este algoritmo en la banda de HF. Esta selección contiene exclusivamente canales de 3 kHz de la banda de radioaficionados de 14.07 MHz a 14.14 MHz cuando esta banda estaba altamente ocupada. Para una mejor comprensión, el intervalo de 2 segundos de la base de datos se denomina de aquí en adelante como T_{UCB} y la duración total de las medidas de 10 minutos como T_{TEST}.

A.9.1 Algoritmo *Upper Confidence Bound*

El algoritmo UCB, basado en *reinforcement learning* (RL), fue propuesto en (Agrawal, 1995) y (Auer et al., 2002) como una estrategia para resolver los problemas MAB (Robbins, 1952). El MAB es análogo a las máquinas tragaperras con más de una palanca. En (Jouini et al., 2009), este algoritmo fue propuesto para que usuarios secundarios en radio cognitiva pudieran acceder al espectro de manera oportunista siguiendo un problema MAB. En él, el espectro se divide en N canales, cada uno con el mismo ancho de banda y esquema de modulación, y cada uno representa una de las palancas del MAB. En cada instante de tiempo, el algoritmo puede jugar con una o varias palancas y obtiene una recompensa de cada una de ellas.

El algoritmo UCB permite la toma de decisiones en escenarios OSA para maximizar las oportunidades de transmisión de los usuarios secundarios. El modelo de escenario OSA utilizado es: en cada instante, sólo un canal (*single-channel* UCB) o M canales (*multi-channel* UCB) de un grupo de N canales ($M < N$) son observados pero todos los N canales son evaluados. Si los canales seleccionados están libres, podrán ser utilizados para transmitir y obtendrán una recompensa. Si están ocupados por otros usuarios, no se establecerá una transmisión ni se obtendrá recompensa alguna para evitar colisionar con otros usuarios primarios. Este algoritmo aprende de las recompensas previas, ya que está basado en RL, empezando desde cero sin conocimiento previo. El algoritmo UCB aprende continuamente (fase de exploración) y predice cuál es el siguiente estado disponible para transmitir (fase de explotación) durante toda su ejecución. Incluso es capaz de explotar oportunidades cuando el conocimiento no es lo suficientemente maduro (Robert et al., 2014). Durante su ejecución, existe un balance entre exploración y explotación para un mejor manejo del dilema de exploración versus explotación.

En cada instante de tiempo t, el algoritmo actualiza los índices UCB llamados $B_{t,k,T_k(t)}$, donde $T_k(t)$ es el número de veces que el canal k ha sido seleccionado anteriormente, y devuelve el canal k con mayor índice UCB (ver Algoritmo A.1). De los diferentes índices UCB propuestos en la literatura, se ha seleccionado el índice UCB_1 (Auer et al., 2002) para ser evaluado con un canal (UCB_1) o múltiples canales (UCB_1-M, UCB_1-*multiple plays*) y seleccionar así los canales disponibles. El índice UCB_1 se define como:

$$B_{t,k,T_k(t)} = \overline{X}_{k,T_k(t)} + A_{t,k,T_k(t)}, \tag{A.13}$$

donde $\overline{X}_{k,T_k(t)}$ y $A_{t,k,T_k(t)}$ son los términos que representan la explotación y la exploración, respectivamente. $\overline{X}_{k,T_k(t)}$ es la media empírica y se define como

$$\overline{X}_{k,T_k(t)} = \frac{\sum_{m=0}^{t-1} r_m \mathbf{1}_{\{a_m=k\}}}{T_k(t)}, \tag{A.14}$$

donde r_m y a_m son la recompensa recibida y el canal seleccionado, respectivamente, en el intervalo de tiempo m, y la señal

$$\mathbf{1}_{\{a_m=k\}} = \begin{cases} 1 & \text{if } a_m = k \\ 0 & \text{if } a_m \neq k \end{cases} \tag{A.15}$$

La media empírica es también proporcional al *throughput* acumulado por el algoritmo UCB_1 cuando el canal k ha sido seleccionado. $A_{t,k,T_k(t)}$ es el *bias* del UCB_1 (Auer et al., 2002) y se define como

$$A_{t,k,T_k(t)} = \sqrt{\frac{\alpha \ln(t)}{T_k(t)}}, \tag{A.16}$$

donde α es el factor de explotación-exploración del algoritmo. Si α crece, el *bias* del UCB_1 $A_{t,k,T_k(t)}$ domina y el algoritmo UCB_1 explora nuevos canales. Por lo contrario, si α disminuye, el *bias* del UCB_1 también lo hace y $\overline{X}_{k,T_k(t)}$ domina el índice UCB_1 forzando al algoritmo a explotar los canales previamente seleccionados (Jouini et al., 2009).

Algorithm A.1 Algoritmo UCB_1

Require: $N, \alpha, \{a_0, r_0, a_1, r_1, \ldots, a_{t-1,} r_{t-1}\}$

Init.: a_t

1: **loop**

2: **if** $t \leq N$ **then**

3: $a_t = t + 1$

4: **else**

5: $T_k(t) \leftarrow \sum_{m=0}^{t-1} \mathbf{1}_{\{a_m=k\}}, \forall k$

6: $\overline{X}_{k,T_k(t)} \leftarrow \frac{\sum_{m=0}^{t-1} r_m \mathbf{1}_{\{a_m=k\}}}{T_k(t)}, \forall k$

7: $A_{t,k,T_k(t)} \leftarrow \sqrt{\frac{\alpha \ln(t)}{T_k(t)}}, \forall k$

8: $B_{t,k,T_k(t)} \leftarrow \overline{X}_{k,T_k(t)} + A_{t,k,T_k(t)}, \forall k$

9: $a_t = \arg\max_k \left(B_{t,k,T_k(t)}\right)$

10: **end if**

11: **return** a_t

12: **end loop**

A.9.2 Estrategias analizadas en la evaluación

Los algoritmos UCB_1 y UCB_1-M están evaluados en esta Tesis desde un punto de vista de comunicaciones en un contexto de radio cognitiva en lugar de utilizar las métricas habituales en *machine learning*. En un contexto de radio cognitiva, el objetivo es lograr encontrar y utilizar cualquier canal disponible para transmitir, sin importar si es el que está disponible durante más tiempo. De esta manera, se aprovechan mejor las oportunidades que surjan en el espectro. Nuevas métricas para algoritmos de RL fueron presentadas en (Robert et al., 2014) bajo este contexto de radio cognitiva. Están basadas en el porcentaje de tiempo que el algoritmo selecciona un canal disponible, denominado como *porcentaje de pruebas satisfactorias*, que también puede ser visto como la tasa de transmisiones con éxito (*successful transmission rate*) alcanzada por el algoritmo.

En esta tesis se utiliza la tasa de transmisiones con éxito para evaluar las prestaciones de los algoritmos UCB_1 y UCB_1-M. Esta métrica se define como el porcentaje de oportunidades de transmisión que han sido correctamente detectadas y utilizadas por un usuario secundario durante todo el periodo de ejecución del algoritmo. Para demostrar las prestaciones de los algoritmos UCB_1 y UCB_1-M en estos términos y facilitar comparaciones, se definen las siguientes estrategias de selección:

- *Selección aleatoria uniforme*: la primera pregunta que se plantea es "¿merece la pena aplicar *reinforcement learning* para la toma de decisiones en el entorno HF?", si es así, "¿cuánto mejoran las prestaciones respecto a una estrategia no inteligente?" Por ello, se calcula la tasa de transmisiones con éxito de una selección aleatoria de canales siguiendo una distribución uniforme.

- *Mejor canal*: dentro de cada grupo de canales, se trata del canal que está disponible durante el mayor periodo de tiempo durante la ejecución del algoritmo (10 minutos), lo que se considera como la mejor estrategia desde la perspectiva de *machine learning*.

- *Peor canal*: es el canal de los pertenecientes a un determinado grupo que está disponible durante el menor periodo de tiempo durante la ejecución del algoritmo.

- *Mejor selección oportunista*: puesto que la evaluación de los algoritmos se realiza para un contexto de radio cognitiva, las prestaciones se comparan con una *genie-aided policy* en la que el usuario secundario tiene un conocimiento perfecto del entorno, sabe dónde se encuentran las oportunidades de transmisión y aprovechará cualquiera de ellas para transmitir.

A.9.3 El dilema exploración vs. explotación en UCB_1

Antes de la ejecución del algoritmo *single-channel* UCB_1 se deben especificar dos parámetros: N, el número de canales de cada grupo de evaluación y α, el factor de explotación-exploración. Mientras N está definido por las restricciones del sistema final como el número de canales asignados, α varía en función de las condiciones del entorno en términos de actividad. En esta sección se muestra cómo la selección de ambos parámetros influye en las prestaciones finales, lo que se denomina como el dilema exploración vs. explotación.

La estrategia de *mejor selección oportunista* se utiliza como referencia de las mejores prestaciones posibles ya que tiene conocimiento perfecto de la actividad del entorno. Para ello, se calcula el porcentaje medio de la tasa de transmisiones con éxito de cada estrategia de selección con respecto a la tasa de transmisiones con éxito de esta estrategia tras $\mathrm{T}_{\mathrm{TEST}}$, que se corresponde con la máxima tasa de transmisiones con éxito alcanzable. Los resultados obtenidos de la comparación entre esta estrategia y el algoritmo UCB_1 están representados en la Figura A.22 para $\alpha \in [0, 5]$ y grupos de $N = \{4, 8, 16\}$ canales. Para todos los valores de N se obtienen las mejores prestaciones cuando $\alpha = 0{,}4$. Si $N = 4$, el algoritmo UCB_1 logra un 81 % de la tasa de transmisiones con éxito que logra la *mejor selección oportunista* para $\alpha \in [0{,}4, 1{,}8]$, y se mantiene cerca de este máximo para $\alpha > 1{,}8$. No obstante, cuando el número de canales en un grupo aumenta a $N = 8$ y $N = 16$, el número de canales que el algoritmo tiene que explorar también aumenta. Por lo tanto, si el factor α es alto, el algoritmo está forzado a explorar más que explotar los canales previamente detectados como disponibles. Esto explica que, cuando $N = 8$,

las mejores prestaciones (77 %) se obtienen para $\alpha \in [0{,}3, 0{,}4]$, mientras que éstas son iguales al 79 % para $N = 16$ y $\alpha \in [0{,}2, 0{,}4]$.

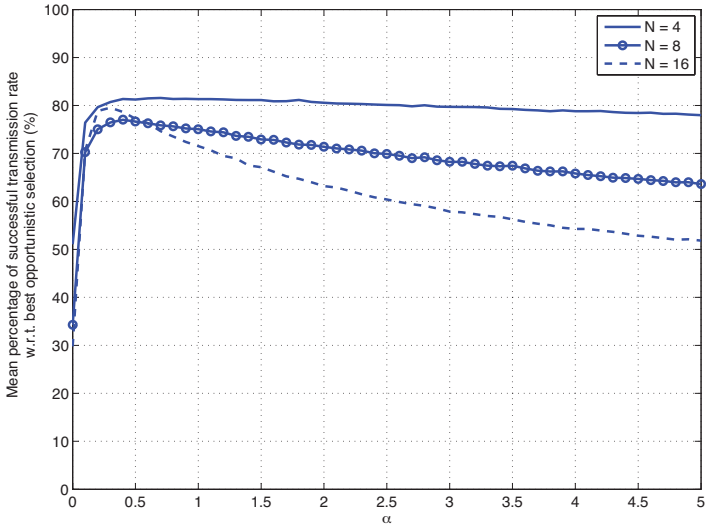

FIGURA A.22. UCB_1: Porcentaje medio de la tasa de transmisiones con éxito con respecto a la de la mejor selección oportunista vs. α con $N = \{4, 8, 16\}$.

También se comparan las prestaciones de las estrategias de selección del mejor canal, el peor canal y la selección aleatoria uniforme en términos de porcentaje medio de tasa de transmisiones con éxito con respecto a la mejor selección oportunista en la Tabla A.5.

TABLA A.5. Selección de un canal de transmisión: Porcentaje medio de tasa de transmisiones con éxito alcanzada por cada estrategia con respecto a la mejor selección oportunista.

	$N = 4$	$N = 8$	$N = 16$
UCB_1 ($\alpha = 0{,}4$)	81 %	77 %	79 %
Selección del mejor canal	83 %	81 %	88 %
Selección aleatoria uniforme	53 %	39 %	35 %
Selección del peor canal	27 %	9 %	3 %

Finalmente, se evalúa el porcentaje medio de mejora en la tasa de transmisiones con éxito si se compara el algoritmo UCB_1 con una estrategia de selección no inteligente, i.e., la selección aleatoria uniforme, ya que refleja los beneficios de aplicar técnicas de aprendizaje para la toma de decisiones en HF. Este porcentaje está representado en la Figura A.23 con $\alpha \in [0, 5]$, y grupos de $N = \{4, 8, 16\}$ canales. Si $N = 4$, este porcentaje es cercano al 178 % (casi el doble con respecto a la selección aleatoria) para cualquier valor de α en el intervalo $[0{,}4, 5]$. Sin embargo, para valores de N mayores, el mayor porcentaje de mejora se logra con $\alpha = 0{,}4$, siendo del 228 % para $N = 8$ y del 245 % para $N = 16$. Al igual que en la Figura A.22, a medida que el número de canales en un determinado grupo aumenta, el algoritmo tiende a explorar más que a explotar los canales previos si α también crece, resultando en un descenso del porcentaje de mejora con respecto a la selección aleatoria de canales. Por tanto, se puede concluir de los resultados mostrados

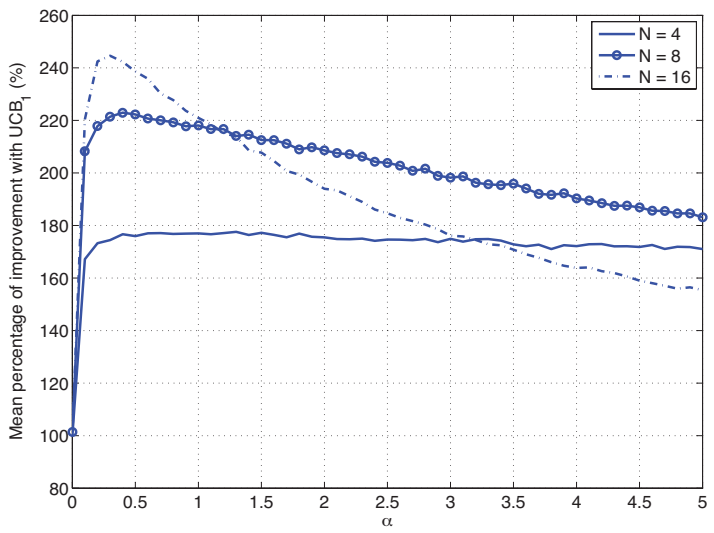

FIGURA A.23. Porcentaje de mejora con UCB_1 con respecto a una selección aleatoria uniforme de canales vs. α con $N = \{4, 8, 16\}$.

en las Figuras A.22 y A.23 que las mejores prestaciones del algoritmo UCB_1 se obtienen cuando α tiene un valor próximo a 0,4.

A.9.4 El dilema exploración vs. explotación en UCB_1-M

Para la evaluación del algoritmo *multi-channel* UCB_1 que permite seleccionar múltiples canales de transmisión en cada iteración, se sigue el mismo procedimiento que en la evaluación del algoritmo *single-channel* UCB_1. A diferencia del algoritmo UCB_1 que requiere dos parámetros N y α, el algoritmo UCB_1-M requiere un nuevo parámetro M, que es el número de canales de transmisión que puede seleccionar el algoritmo en cada iteración, siendo $M < N$.

Los resultados obtenidos en términos de porcentaje medio de tasa de transmisiones con éxito respecto a la tasa de transmisiones con éxito de la *mejor selección oportunista* se muestran en la Figura A.24. Están representados para valores de $\alpha \in [0, 5]$, y relaciones $M/N = \{1/8, 1/4, 1/2\}$ con $12 \leq N \leq 30$. Cuando la relación M/N es alta ($M/N = 1/2$), i.e., un porcentaje mayor de canales de N pueden ser seleccionados simultáneamente por el algoritmo, se obtiene el mayor porcentaje de tasa de transmisiones con éxito con el algoritmo UCB_1-M, que es igual al 88 % de la tasa de transmisiones con éxito alcanzada por la *mejor selección oportunista* de canales para cualquier valor de α en el intervalo estudiado. Por lo que se puede concluir que las prestaciones no dependen significativamente del valor de α cuando $M/N = 1/2$. No obstante, cuando M/N disminuye porque se reduce el número de canales de transmisión ($M/N = 1/4$ y $M/N = 1/8$), las mejores prestaciones se obtienen para $\alpha \in [0{,}2, 0{,}4]$ cuando $M/N = 1/8$, y $\alpha = 0{,}4$ si $M/N = 1/4$. Este comportamiento es idéntico al observado con el algoritmo *single-channel* UCB_1. En este caso, el algoritmo UCB_1-M tiene un grupo de canales mayor que explorar y, a medida que aumenta α, tiene que explorar más, y por tanto, pierde oportunidades de transmisión.

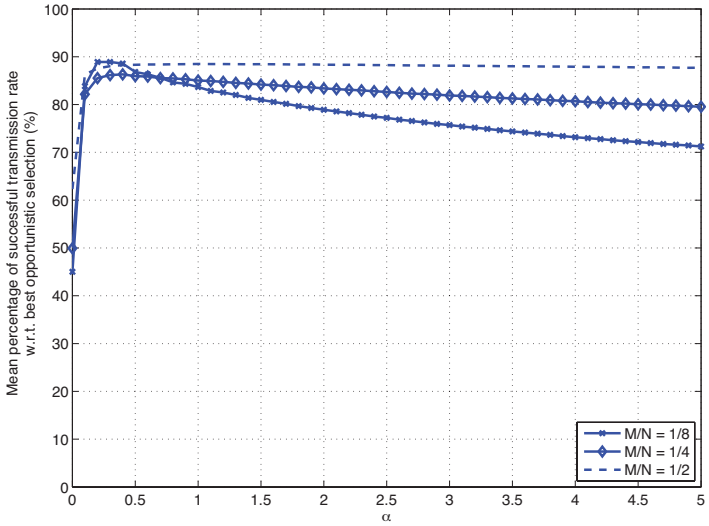

FIGURA A.24. UCB_1-M: Porcentaje medio de la tasa de transmisiones con éxito con respecto a la de la mejor selección oportunista vs. α con $M/N = \{1/8, 1/4, 1/2\}$.

La Tabla A.6 incluye los resultados de la comparación entre las diferentes estrategias de selección en términos de porcentaje medio de tasa de transmisiones con éxito con respecto a la mejor selección oportunista.

TABLA A.6. Selección de múltiples canales de transmisión: Porcentaje medio de tasa de transmisiones con éxito alcanzada por cada estrategia con respecto a la mejor selección oportunista.

	$M/N = 1/8$	$M/N = 1/4$	$M/N = 1/2$
UCB_1-M ($\alpha = 0{,}4$)	88 %	86 %	88 %
Selección del mejor canal	100 %	92 %	92 %
Selección aleatoria uniforme	48 %	52 %	64 %
Selección del peor canal	4 %	14 %	37 %

Por último se presenta el porcentaje medio de mejora con el algoritmo UCB_1-M con respecto a la selección aleatoria de canales para valores de $\alpha \in [0, 5]$ y $M/N = \{1/8, 1/4, 1/2\}$. Cuando el número de canales que el algoritmo UCB_1-M puede seleccionar es alto, i.e., $M/N = 1/2$, el porcentaje de mejora es del 140 % si $\alpha \in [0{,}4, 5]$. Si la relación M/N disminuye, el porcentaje de mejora aumenta. Cuando $M/N = 1/4$, éste es igual al 180 % para $\alpha \in [0{,}3, 0{,}7]$, mientras que para $M/N = 1/8$, el mayor porcentaje de mejora se obtiene con $\alpha \in [0{,}3, 0{,}4]$ y es igual al 190 %, siendo la tasa de transmisiones con éxito del algoritmo UCB_1-M casi tres veces superior a la de la selección aleatoria de canales.

De los resultados mostrados en las Figuras A.24 y A.25, se puede concluir que las mejores prestaciones del algoritmo UCB_1-M en el entorno de HF se obtienen cuando α tiene un valor cercano a 0,4 y $M/N = 1/8$.

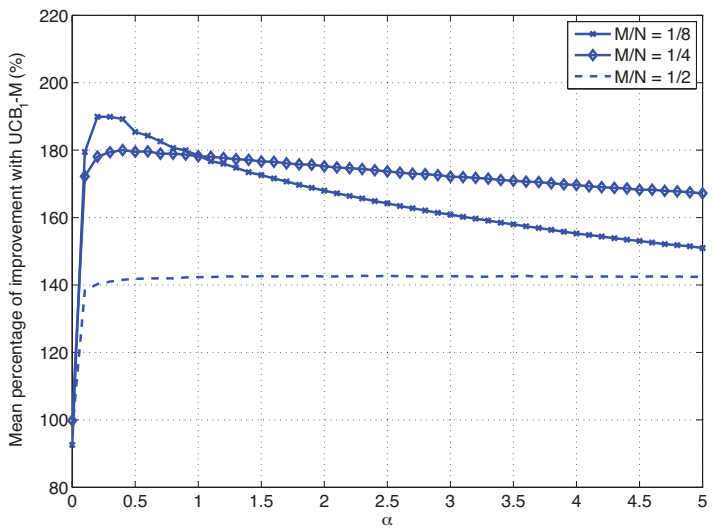

FIGURA A.25. Porcentaje de mejora con UCB_1-M con respecto a una selección aleatoria uniforme de canales vs. α con $M/N = \{1/8, 1/4, 1/2\}$.

A.10 Sistema híbrido UCB-HMM: una propuesta metacognitiva

Los sistemas metacognitivos han sido propuestos recientemente en la literatura como agentes de alto nivel que seleccionan de forma dinámica una determinada máquina cognitiva en función de los cambios observados en el entorno (Asadi et al., 2015).

En esta Tesis se han presentado dos métodos de aprendizaje que pueden ser considerados como máquinas cognitivas independientes: el modelo de actividad de usuarios primarios de HF basado en HMM y el algoritmo UCB_1-M. El modelo de predicción basado en HMM ha sido diseñado para realizar predicciones a largo plazo (un minuto de duración) de un determinado canal de HF con una baja complejidad. Sin embargo, se necesitan tantos modelos como canales a observar cuando se realiza un acceso oportunista al espectro. Por otro lado, el algoritmo UCB_1-M ha sido presentado como una solución para seleccionar los mejores canales para transmisión de datos. A diferencia del modelo de predicción basado en HMM, el algoritmo UCB_1-M permite realizar predicciones a corto plazo (2 segundos duración) y permite además la toma de decisiones entre varios canales.

Uno de los aspectos no considerados hasta ahora es que se requiere señalización para coordinar a transmisor y receptor. Ambos extremos del enlace pueden realizar una gestión del enlace con un canal en banda o fuera de banda. Los sistemas de radio cognitiva también necesitan gestionar el enlace, y un canal piloto (CPC, Cognitive Pilot Channel) fue propuesto en (Cordier *et al.*, 2006). La gestión del enlace se realizaba a través de un canal en banda o fuera de ella que informaba al usuario secundario sobre el estado del canal. En esta Sección se considera la señalización de canal para coordinar al transmisor y al receptor de un sistema de comunicaciones HF. Debido a las limitaciones en la tasa de datos y la variabilidad del enlace HF, sea cual sea la solución de señalización utilizada,

es vital manejar eficientemente la cantidad de datos de señalización que se intercambia entre transmisor y receptor. Es por ello que en esta Tesis se define la señalización de canal (*channel signalling*) como la cantidad de transmisiones que son necesarias para informar al receptor sobre los canales seleccionados para transmisión.

En esta Tesis se propone una solución híbrida que combina el modelo de predicción basado en HMM con el algoritmo UCB_1-M basado en *reinforcement learning* como una propuesta metacognitiva. Si las condiciones del entorno permiten transmisiones de datos a largo plazo, éstas se harán según las predicciones del modelo basado en HMM y, por tanto, se reduce notablemente la cantidad de señalización a enviar si se compara con un sistema de predicción a corto plazo como el algoritmo UCB_1-M. Por lo contrario, si las condiciones del entorno empeoran, se establecerán transmisiones de datos a corto plazo a pesar de que la cantidad de señalización aumenta. Por lo tanto, los tres objetivos principales a cumplir con el sistema híbrido UCB-HMM son: (1) reducir la cantidad de señalización de canal intercambiada entre transmisor y receptor, (2) reducir la complejidad de múltiples modelos HMM trabajando en paralelo, y (3) adaptar los periodos de transmisión de datos a las condiciones del entorno. Finalmente, cabe destacar que la aplicación de esta solución metacognitiva en el entorno HF genera nuevas especificaciones en los sistemas HF actuales que serán detalladas en la Sección A.11.

A.10.1 Descripción del sistema híbrido UCB-HMM

Los dos métodos de aprendizaje se ejecutan en paralelo en el sistema propuesto siguiendo dos intervalos de transmisiones; uno a corto plazo de 2 segundos con UCB_1-M (T_{UCB}), y uno a largo plazo de 1 minuto con el HMM (T_{HMM}). Además se considera la misma segmentación de medidas de la base de datos HFSA_IDeTIC_F1_V01 de la Sección A.8.2.

El sistema híbrido propuesto adapta automáticamente su configuración ante los cambios en la actividad del entorno, lo que significa que, si hay múltiples canales disponibles para transmisiones de un minuto, el sistema híbrido UCB-HMM realizará transmisiones a largo plazo siguiendo las predicciones del los M modelos de predicción basados en HMM trabajando en paralelo (M-HMMs), siendo $M < N$. Por lo contrario, si las condiciones cambian y la mayoría de los canales no están disponibles o están parcialmente no disponibles, transmitirá en el corto plazo siguiendo las predicciones del algoritmo UCB_1-M. Este comportamiento es el que sigue un sistema metacognitivo (Asadi et al., 2015).

Si sólo se realizan transmisiones cortas, la señalización de canal utilizada para la gestión del enlace entre transmisor y receptor crece. Esto ocurriría si sólo el algoritmo UCB_1-M se utiliza en el sistema híbrido, ya que predice la actividad cada 2 segundos, y requiere un mayor número de transmisiones para señalización. No obstante, la cantidad de señalización disminuye en el sistema híbrido cuando éste selecciona M-HMMs para transmitir durante un minuto, enviando una única vez en ese minuto la información de

señalización. De esta manera, se reduce en treinta veces ($T_{\text{HMM}}/T_{\text{UCB}}$) la señalización de canal, factor que se mantiene constante durante toda la ejecución del sistema híbrido ya que los M-HMMs son entrenados antes de su uso para predicción.

Además, el sistema híbrido permite reducir la complejidad de N modelos de predicción basados en HMM trabajando en paralelo, ya que la combinación con el algoritmo UCB_1-M sólo requiere M modelos basados en HMM con $M < N$ y el propio algoritmo UCB_1-M, que no tiene tanta complejidad (Melián-Gutiérrez, Modi, et al., 2015b). En las próximas secciones se detalla cómo se explota en el sistema híbrido UCB-HMM lo mejor de ambos métodos de aprendizaje.

El sistema híbrido está descrito en el Algoritmo A.2 y en la Figura A.26. Durante su ejecución, el algoritmo UCB_1-M selecciona los M mejores canales con predicciones cortas en intervalos T_{UCB}, y estos canales son los que posteriormente son introducidos en los M-HMMs para realizar predicciones a largo plazo, T_{HMM}. Por otro lado, se modifican dos conjuntos para evitar conflictos entre los dos métodos: ID_{UCB}, que contiene los índices de los M canales seleccionados por el algoritmo UCB_1-M y ID_{HMM} que incluye los índices de los canales identificados como disponibles en el siguiente T_{HMM} por los M-HMMs. Ambos conjuntos son actualizados cada T_{HMM} (ver líneas 9 y 12 del Algoritmo A.2).

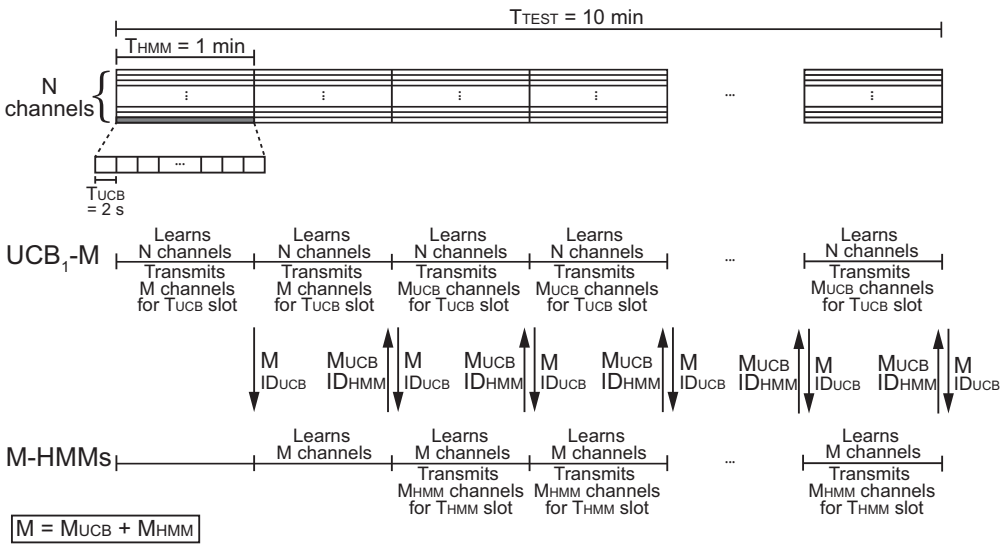

FIGURA A.26. Ejecución temporal del sistema híbrido UCB-HMM con M modelos de predicción basados en HMM y el algoritmo UCB_1-M.

En la fase de inicialización del sistema híbrido, sólo el algoritmo UCB_1-M se ejecuta durante T_{HMM} sobre los N canales y extrae los M mejores canales disponibles (línea 11 del Algoritmo A.2 y Figura A.26). Después del primer intervalo T_{HMM}, éste transmite los M mejores canales en el conjunto ID_{UCB} a los M-HMMs. En el segundo intervalo T_{HMM}, cada HMM aprenderá de uno de los M mejores canales para predecir cuáles estarán disponibles, parcialmente disponibles o no disponibles en el siguiente intervalo T_{HMM}. Mientras los M-HMMs aprenden, el algoritmo UCB_1-M continúa su ejecución y transmite en M canales como máximo cada T_{UCB}. Una vez que los M-HMMs han aprendido durante

Algorithm A.2 Algoritmo del sistema híbrido UCB-HMM

Require: N, M, α

Init.: $\mathrm{M_{UCB}} = M$, $\mathrm{M_{HMM}} = 0$, slot $= 0$, $\mathrm{T_{UCB}} = 2$ s, $\mathrm{T_{HMM}} = 1$ min, $\mathrm{ID_{UCB}} = \varnothing$, $\mathrm{ID_{HMM}} = \varnothing$

```
loop
    if t = slot + T_HMM then
        slot ← t
        if ID_UCB ≠ ∅ then
            Predict with M-HMMs
            ID_HMM ← indices (channels predicted as free)
            M_HMM ← size (ID_HMM)
            M_UCB ← M − M_HMM
            M-HMMs SEND UCB_1-M: M_UCB, ID_HMM
        end if
        ID_UCB ← indices (M highest B_{t,k,T_k(t)})
        UCB_1-M SENDS M-HMMs: M, ID_UCB
    end if
    t ← t + T_UCB
    Compute UCB_1-M
    TX in M_UCB channels ∈ N \ ID_HMM
    if ID_UCB ≠ ∅ then
        M-HMMs save sensing information of ID_UCB channels
        if ID_HMM ≠ ∅ then
            TX in M_HMM channels ∈ ID_HMM
        end if
    end if
end loop
```

un intervalo T_{HMM}, se incluye en el conjunto de canales ID_{HMM} los canales que estarán disponibles en el siguiente intervalo T_{HMM} y se enviará al algoritmo UCB_1-M junto con el máximo número de canales M_{UCB} donde el algoritmo UCB_1-M puede transmitir en el siguiente intervalo T_{HMM} (ver líneas 4-10 del Algoritmo A.2). En este momento (al comienzo del tercer intervalo T_{HMM}) ambos métodos de aprendizaje pueden transmitir en los canales que les corresponden, M-HMMs en M_{HMM} canales del conjunto ID_{HMM} y el algoritmo UCB_1-M en M_{UCB} canales del complemento relativo de ID_{HMM} en N ($N \setminus ID_{HMM}$), siendo $M = M_{UCB} + M_{HMM}$. Así, el sistema híbrido UCB-HMM siempre intenta transmitir en el máximo de canales permitido M. Cabe destacar que la ejecución de los M-HMMs está restringida a T_{TEST}-2·T_{HMM} debido a la inicialización del sistema híbrido propuesto.

A.10.2 Evaluación del sistema híbrido UCB-HMM

En las siguientes secciones se muestran los beneficios de la combinación de ambos métodos de aprendizaje en el sistema híbrido UCB-HMM. Se ha utilizado la misma selección de medidas de la base de datos HFSA_IDeTIC_F1_V01 utilizada en la Sección A.9, que contiene canales de 3 kHz de la banda de radioaficionados cuando ésta estaba altamente ocupada. De acuerdo con los resultados obtenidos en la Sección A.9.4, el factor de explotación-exploración seleccionado es $\alpha = 0{,}4$ y la relación entre los canales de transmisión (M) y el número total de canales (N) es igual a $M/N = \{1/8, 1/4, 1/2\}$ donde M cambia pero N es constante e igual a 24.

A.10.2.1 Tasa de transmisiones con éxito

En primer lugar se realiza la evaluación de la tasa de transmisiones con éxito al igual que con el algoritmo UCB_1-M en la Sección A.9.4 donde las mejores prestaciones se lograban con $\alpha = 0{,}4$ y $M/N = 1/8$. La Figura A.27 muestra la tasa de transmisiones con éxito del sistema híbrido UCB-HMM y del algoritmo UCB_1-M con $\alpha = 0{,}4$ y $M/N = \{1/8, 1/4, 1/2\}$. Se puede observar que tanto el aprendizaje del algoritmo UCB_1-M como el del sistema híbrido UCB-HMM crecen gradualmente al igual que la tasa de transmisiones con éxito desde el minuto 1 al minuto 1.7. En este punto, ambos están cerca de las máximas prestaciones para todos los valores de M/N. La mejor tasa de transmisiones con éxito se alcanza cuando $M/N = 1/8$ y es igual al 99 % de todas las oportunidades de transmisión a partir del tercer minuto de ejecución, que es cuando los M-HMMs han empezado a a transmitir. Esta tasa de transmisiones con éxito es un 4% superior a la obtenida con $M/N = 1/4$ y un 20 % superior a la obtenida con $M/N = 1/2$.

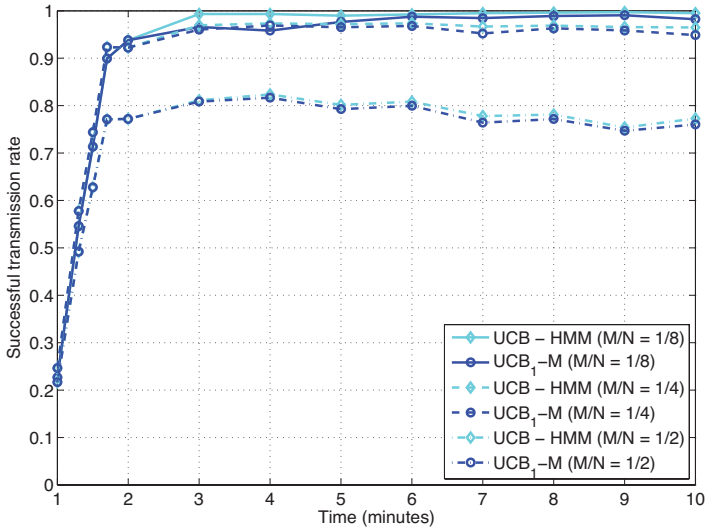

FIGURA A.27. Tasa de transmisiones con éxito del sistema híbrido UCB-HMM y del algoritmo UCB_1-M con $\alpha = 0{,}4$ y $M/N = \{1/8, 1/4, 1/2\}$.

A.10.2.2 Estrategia metacognitiva

La adaptabilidad que presentan los sistemas metacognitivos está reflejada en el sistema híbrido UCB-HMM propuesto cuando éste selecciona uno de los métodos de aprendizaje en función del estado del entorno. Si las condiciones del entorno son buenas, realiza transmisiones a largo plazo mientras que si las condiciones empeoran, realiza transmisiones en el corto plazo. La Figura A.28 muestra cómo el sistema híbrido adapta las transmisiones en función de las condiciones del entorno cuando $M/N = \{1/8, 1/4, 1/2\}$. Se representa el porcentaje medio de canales utilizados para transmisión por cada uno de los métodos respecto a las condiciones del entorno: un escenario bueno donde la mayoría de los N canales están disponibles, un escenario regular donde la mayoría de los N canales están parcialmente disponibles y un escenario malo donde la mayoría de los N canales no están disponibles.

La Figura A.28 muestra que a medida que mejoran las condiciones del entorno también crece el porcentaje de canales utilizados para transmisiones largas con los M-HMMs mientras que disminuyen las transmisiones cortas con el algoritmo UCB_1-M. El porcentaje de incremento de transmisiones a largo plazo es del 16 % para $M/N = 1/8$, 31 % para $M/N = 1/4$ y del 50 % para $M/N = 1/2$. El mayor incremento ocurre con $M/N = 1/2$ porque al crecer M, el número de canales de transmisión aumenta, y, en escenarios malos, es más complicado aprovechar todas las oportunidades de transmisión existentes dentro del grupo de N canales.

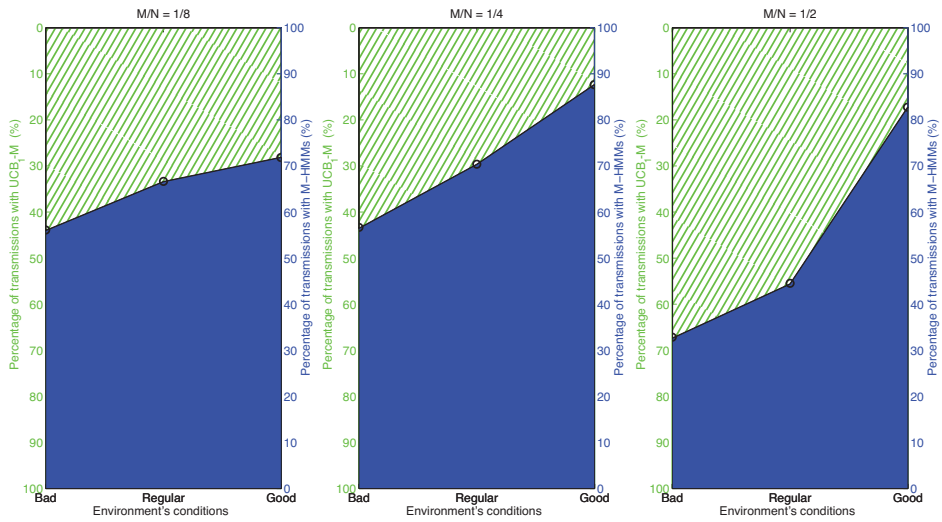

FIGURA A.28. Porcentaje medio de transmisiones a largo plazo (M-HMMs) y a corto plazo (UCB_1-M) en el sistema híbrido UCB-HMM con $M/N = \{1/8, 1/4, 1/2\}$ vs. condiciones del entorno.

A.10.2.3 Análisis de la duración de las transmisiones de datos

También debe tenerse en cuenta un análisis sobre la duración de las transmisiones de datos realizadas según las predicciones de cada uno de los métodos del sistema híbrido UCB-HMM. Las Figuras A.29 y A.30 muestran el histograma de la duración de las transmisiones de datos realizadas según las predicciones del algoritmo UCB_1-M y de los M-HMMs, respectivamente, para configuraciones del sistema híbrido con $M/N = \{1/8, 1/4, 1/2\}$.

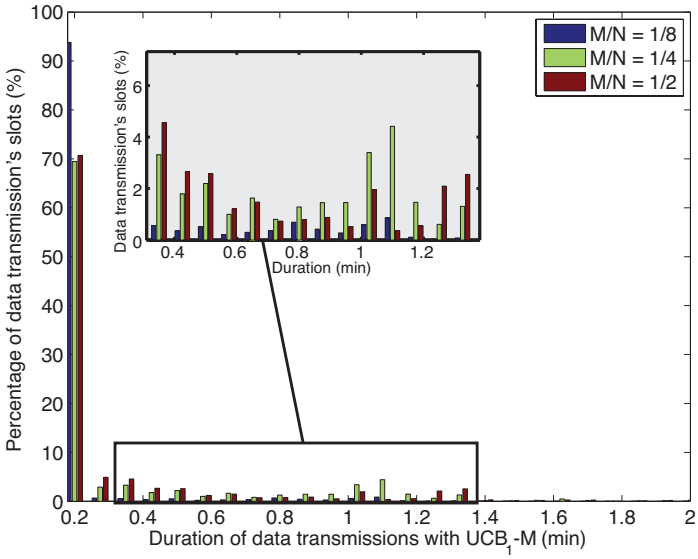

FIGURA A.29. Histograma de la duración de las transmisiones de datos realizadas según las predicciones del algoritmo UCB_1-M en el sistema híbrido UCB-HMM.

La Figura A.29 muestra que para $M/N = 1/8$, el 94% de las transmisiones realizadas tras las predicciones del algoritmo UCB_1-M tienen una duración inferior a 12 segundos. Cuando M/N crece, también lo hace el número de canales de transmisión, y las transmi-

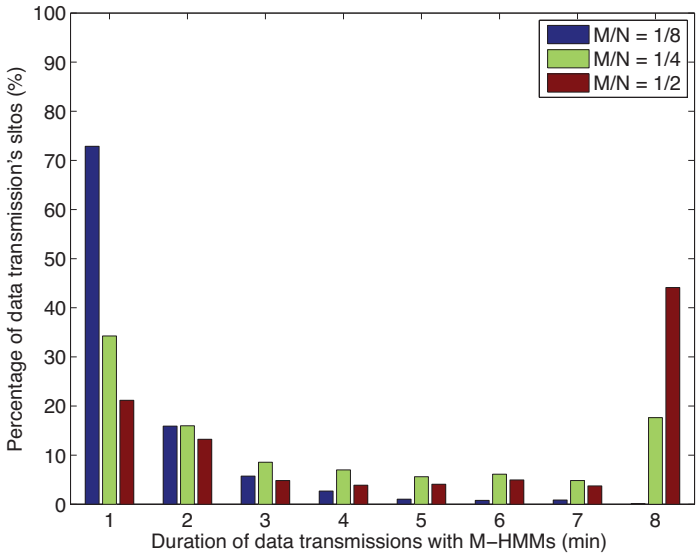

FIGURA A.30. Histograma de la duración de las transmisiones de datos realizadas según las predicciones de los M-HMMs en el sistema híbrido UCB-HMM.

siones tienen una duración de 2 minutos como máximo, reduciéndose al 70 % el número de transmisiones con una duración inferior a 12 segundos. Se debe a que al aumentar M, también aumenta la probabilidad de encontrar canales disponibles durante intervalos de tiempo más largos. El mismo efecto se observa en la Figura A.30, donde se representa el histograma de la duración de las transmisiones de datos realizadas con las predicciones de los M-HMMs. Cuando $M/N = 1/8$, un 73 % de las transmisiones tiene una duración de un minuto. No obstante, a medida que aumenta M/N, este porcentaje disminuye al 34 % con $M/N = 1/4$ y al 21 % con $M/N = 1/2$. También sucede que, al aumentar M/N, también aumenta el porcentaje de transmisiones de mayor duración (8 minutos) sin cambiar de canal según las predicciones de los M-HMMs (18 % con $M/N = 1/4$ y 44 % con $M/N = 1/2$). Por lo que M/N debe ser fijado a 1/4 ó 1/2 para aprovechar las transmisiones de datos más largas.

A.10.2.4 Mejora en la señalización de canal

Dos de los objetivos a lograr con el sistema híbrido UCB-HMM son la reducción en complejidad de N modelos de predicción basados en HMMs ejecutándose en paralelo y la simplificación de la señalización de canal en la gestión del enlace. Esta simplificación se puede ver como la reducción de la señalización al realizar transmisiones a largo plazo ($T_{\mathbf{HMM}} = 1$ min.) con las predicciones de los M-HMMs, en lugar de transmisiones cortas ($T_{\mathrm{UCB}} = 2$ s) con las predicciones del algoritmo UCB_1-M. Esta sección demuestra además que la carga de señalización requerida por el sistema híbrido UCB-HMM es abordable en el entorno de HF.

La Figura A.31 muestra la comparación en términos de cantidad de transmisiones de señalización realizadas por el sistema híbrido UCB-HMM, y los M modelos basados

en HMM en paralelo y el algoritmo UCB_1-M trabajando independientemente. La señalización que el sistema híbrido UCB-HMM requiere con $M/N = \{1/8, 1/4, 1/2\}$ después de T_{TEST} es superior a la de los M-HMMs pero inferior a la del algoritmo UCB_1-M. Cabe destacar que la señalización de las tres estrategias aumenta a medida que aumenta M/N puesto que es M, el número de canales de transmisión, el valor que aumenta. Sin embargo, aunque se considere el valor máximo de $N = 30$, la cantidad de señalización de canal es totalmente abordable en el entorno HF, incluso si se aplican codificación y redundancia para proteger la información de señalización.

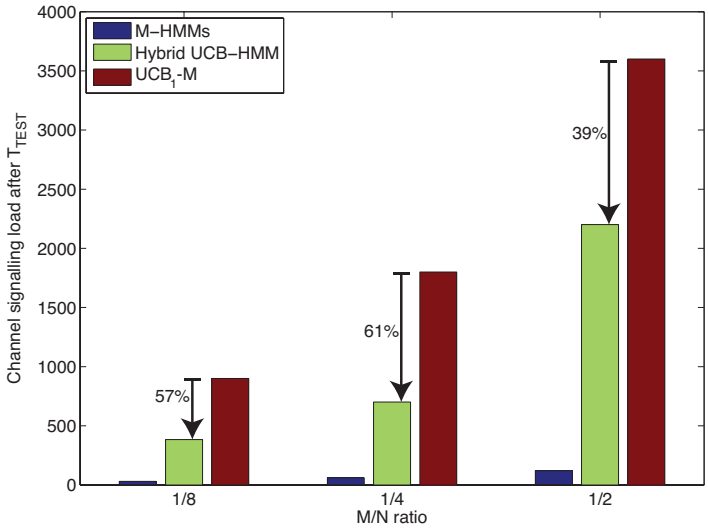

FIGURA A.31. Señalización requerida por los M-HMMs, el algoritmo UCB_1-M y el sistema híbrido UCB-HMM vs. M/N.

De la Figura A.31 también se puede extraer la reducción de señalización que requiere el sistema híbrido UCB-HMM con respecto a la del algoritmo UCB_1-M, que es el que más requiere. La señalización con el sistema híbrido UCB-HMM se reduce un 57 % cuando $M/N = 1/8$, un 61 % cuando $M/N = 1/4$ y un 39 % cuando $M/N = 1/2$, mostrando los beneficios de la combinación de M-HMMs y el algoritmo UCB_1-M en el sistema híbrido propuesto.

Finalmente, para poder explotar todas las capacidades del sistema híbrido UCB-HMM se debe lograr un compromiso entre la tasa de transmisiones con éxito, la duración de las transmisiones de datos y la reducción de la cantidad de señalización. Los resultados mostrados revelan que este compromiso se puede alcanzar cuando $M/N = 1/4$. Con esta configuración, el sistema híbrido UCB-HMM logra un 95 % de tasa de transmisiones con éxito y reduce hasta un 61 % la cantidad de señalización requerida si es comparada con la que requiere el algoritmo UCB_1-M.

A.11 Contribuciones y conclusiones

En esta Tesis se ha propuesto la aplicación de los principios de Radio Cognitiva como una posible solución del uso ineficiente de la banda de HF. Para ello, y tomando como punto de partida el ciclo de tareas cognitivas presentado por Mitola en (Mitola & Maguire, 1999; Mitola, 2000) que ha sido simplificado en tres tareas principales: OBERVAR, APRENDER y DECIDIR & ACTUAR, se ha propuesto una solución para cada una ellas en el entorno de HF.

OBSERVAR

Una radio cognitiva debe escuchar el entorno que la rodea para ser consciente de los cambios que se producen en el mismo. A su vez, debe ejecutar la tarea de *spectrum sensing* en la que transforma la información adquirida del entorno en datos que indiquen la existencia de oportunidades de transmisión.

En primer lugar, se ha creado una base de datos de medidas reales de la banda de HF para demostrar la viabilidad de la aplicación de radio cognitiva en esta banda. Esta base de datos contiene medidas de banda ancha de la potencia de 200-300 canales de HF con 3 kHz de ancho de banda y grabados simultáneamente durante 10 minutos. La banda grabada ha sido principalmente la banda de radioaficionados de 14 MHz debido a la variedad de transmisiones existentes.

Un detector de energía ha sido propuesto para ejecutar la tarea de *spectrum sensing*. Este detector de energía transforma las muestras de potencia en valores normalizados que representan la actividad de los usuarios primarios. En este caso se ha seleccionado el detector de energía dada la heterogeneidad de la banda de HF.

Uno de los problemas observados durante la adquisición de medidas de banda ancha es el efecto de las interferencias de banda estrecha (NBI) en receptores de banda ancha. La presencia de NBI en la señal de banda ancha recibida provoca una reducción del número efectivo de bits utilizados para la digitalización de las señales de interés, por lo tanto, el ruido de cuantificación puede sobrepasar al ruido término y a la señal deseada en sí (Pérez-Díaz et al., 2012).

El primer paso a realizar cuando esto sucede es la detección de NBI. En esta Tesis se ha propuesto un detector de NBI basado en *compressive sensing* que tiene una baja complejidad al utilizar un conversor analógico-digital de baja velocidad. La adquisición de la señal se realiza con el *random demodulator* (Tropp et al., 2010) y la identificación de las componentes frecuenciales más potentes de la señal a partir de las muestras *compressive* se realiza con el algoritmo CoSaMP (Needell & Tropp, 2009).

El detector de NBI propuesto se ejecuta en paralelo con un receptor de banda ancha. Su comportamiento se ajusta al estado del control automático de ganancia (AGC) del receptor de banda ancha. Es por ello que sus prestaciones han sido caracterizadas en

función del número de señales interferentes a detectar. Cuando sólo existe una señal interferente, alcanza un 92 % de tasa de detección y un 8 % de falsa alarma si se indica que sólo una señal debe ser detectada. No obstante, en los escenarios donde hay más de una señal representativa, el detector de NBI propuesto alcanza una tasa de detección de 97.8 % y un 4 % de falsa alarma si se desea detectar más de 15 componentes.

Por último, el comportamiento del *random demodulator* ha sido caracterizado en escenarios reales para ser comparado con el estudio teórico realizado en (Tropp et al., 2010). Los resultados obtenidos muestran que las prestaciones en escenarios reales siguen la misma tendencia que las prestaciones en el marco teórico.

APRENDER

Quizás la característica más representativa de una radio cognitiva sea su capacidad de aprendizaje. Al aprender del entorno, una radio cognitiva puede predecir la actividad de los usuarios primarios para hacer un uso más eficiente del espectro.

Se han propuesto dos métodos de aprendizaje en esta Tesis basados en dos intervalos de predicción. Un modelo de predicción basado en modelos ocultos de Markov (HMM) (Rabiner & Juang, 1993) que realiza predicciones a largo plazo, y los algoritmos *Upper Confidence Bound* (UCB) (Agrawal, 1995; Auer et al., 2002) basados en *reinforcement learning* para predicciones a corto plazo.

El modelo de predicción basado en HMM modela la actividad de los usuarios primarios de la banda de HF. A su vez, permite predecir la actividad en un determinado canal durante el próximo minuto con una estructura de poca complejidad. Su estructura está basada en HMM dado que se trata de una herramienta robusta de modelado de procesos estocásticos. El modelo propuesto está formado por tres submodelos que están conectados entre sí en un modelo principal. Cada submodelo describe un tipo de canal en función de la actividad: canales disponibles, canales no disponibles y canales parcialmente disponibles.

Los resultados obtenidos con las medidas reales de la banda de HF indican que el modelo puede predecir la actividad de un determinado canal en el próximo minuto con un error medio del 10.3 % si sólo ha observado durante el último minuto. Si su conocimiento se amplía hasta los ocho minutos previos, el error medio se reduce al 5.8 %.

Un segundo método de aprendizaje basado en *reinforcement learning* ha sido propuesto para la predicción de la actividad de los usuarios primarios de la banda de HF en el corto plazo y para la toma de decisiones en el escenario de acceso oportunista al espectro.

DECIDIR & ACTUAR

El siguiente paso a realizar es la toma de decisiones teniendo en cuenta lo previamente observado y aprendido. En este momento, la radio cognitiva debe seleccionar cuáles son los mejores canales para transmitir y cuál es la configuración más adecuada para las condiciones del entorno observadas. En muchas de las propuestas, así como en esta

Tesis, el aprendizaje y la toma de decisiones se pueden ejecutar simultáneamente. Esto sucede cuando los algoritmos UCB_1 y UCB_1-M propuestos en esta Tesis son utilizados, ya que aprenden de lo observado y también seleccionan cuáles son los mejores canales de transmisión en el siguiente intervalo de tiempo.

Ambos algoritmos han sido propuestos para acceder de manera oportunista al espectro de HF. Mientras UCB_1 selecciona el mejor canal en términos de disponibilidad de un conjunto de N canales observados, UCB_1-M selecciona M canales del conjunto de N, siendo $M < N$. A diferencia del modelo de predicción basado en HMM, ambos algoritmos se ejecutan en intervalos de tiempo cortos de 2 segundos para predecir la actividad y decidir en el corto plazo. Ambos algoritmos han sido evaluados con las medidas de la banda de HF y se ha demostrado su viabilidad en la misma con el análisis del dilema de exploración vs. explotación.

Para la evaluación de los algoritmos UCB_1 y UCB_1-M se ha propuesto la métrica de tasa de transmisiones con éxito que se define como el porcentaje de oportunidades de transmisión detectadas correctamente y utilizadas para transmitir por el usuario secundario durante el tiempo de ejecución de los algoritmos. Esta métrica ha sido utilizada para comparar las prestaciones de los algoritmos UCB_1 y UCB_1-M con las de la selección del mejor canal en términos de disponibilidad, la selección del peor canal en los mismos términos, la selección aleatoria de canales siguiendo una distribución uniforme, y por último, con la mejor selección oportunista de canales que tiene un conocimiento perfecto de las oportunidades de transmisión existentes y las aprovecha en todo momento.

Los resultados obtenidos muestran que los algoritmos UCB_1 y UCB_1-M tienen el mejor compromiso entre exploración de nuevos canales y explotación de canales disponibles seleccionados previamente cuando $\alpha = 0{,}4$. También reflejan los beneficios de aplicar *reinforcement learning* para la toma de decisiones en el entorno HF, ya que el porcentaje medio de mejora sobre una selección aleatoria de canales puede ser de hasta un 245 % para el algoritmo UCB_1 y de un 190 % para UCB_1-M.

Finalmente, se ha propuesto un sistema híbrido UCB-HMM como un sistema metacognitivo que combina dos métodos de aprendizaje: el modelo de predicción basado en HMM y el algoritmo UCB_1-M. En función de las condiciones del entorno observadas en términos de disponibilidad se selecciona uno u otro. Ambos métodos se ejecutan en paralelo en el sistema híbrido propuesto con dos intervalos de predicción: uno a largo plazo con el modelo de predicción basado en HMM y otro a corto plazo con el algoritmo UCB_1-M, y el sistema híbrido permite la toma de decisiones en ambos intervalos de tiempo de acuerdo con las predicciones de cada uno de los métodos.

El sistema híbrido UCB-HMM surge como una solución de menor complejidad que el uso de N modelos de predicción basados en HMM ejecutándose en paralelo en un sistema multi-canal. Además, al establecer transmisiones a largo plazo, se reduce la cantidad de señalización de canal necesaria entre transmisor y receptor comparado con la necesaria por el algoritmo UCB_1-M. Por lo tanto, este sistema híbrido UCB-HMM ha sido diseñado

con los siguientes objetivos: disminuir la cantidad de señalización de canal requerida para la gestión del enlace, reducir la complejidad de N modelos de predicción basados en HMM ejecutándose en paralelo y adaptar las transmisiones de datos a las condiciones de disponibilidad en el entorno.

El sistema híbrido propuesto ha sido evaluado con las medidas reales de la banda de HF y se ha demostrado que es capaz de adaptar su configuración a los cambios del entorno. Las mejores prestaciones se han obtenido cuando el factor de explotación-exploración $\alpha = 0{,}4$ y la relación entre el número de canales de transmisión y el número de canales de exploración $M/N = 1/4$. Con esta configuración, el sistema híbrido UCB-HMM consigue una tasa de transmisiones con éxito del 95 % mientras se adapta a los cambios del entorno. Un 88 % de las transmisiones de datos son establecidas a largo plazo según las predicciones de los M-HMMs cuando la actividad en la banda disminuye, mientras que un 44 % de las transmisiones de datos son establecidas en el corto plazo siguiendo las predicciones del algoritmo UCB_1-M cuando la actividad de la banda aumenta. Además, la señalización requerida para la gestión del enlace se reduce en un 61 % comparada con la requerida por el algoritmo UCB_1-M.

A.11.1 Líneas futuras

Una vez demostrada en esta Tesis la viabilidad de los principios de radio cognitiva en sistemas de comunicaciones HF, una posible línea futura sería su implementación en hardware, haciendo uso de ASIC o FPGA. Sin embargo, existen algunas consideraciones a tomar en cuenta antes de llevarla a cabo.

Los sistemas clásicos de HF, como STANAG 4285 o STANAG 4539, son sistemas basados en modulaciones monoportadora que, para que sean robustos, requieren entrelazados largos de varios segundos, ecualizadores y altas densidades de pilotos. Esta sobrecarga puede superar notablemente el intervalo de tiempo de corto plazo de 2 segundos considerado en esta Tesis. Además, los estándares actuales de gestión del enlace en HF como STANAG 5066, requieren más sobrecarga y no soportan un acceso dinámico al espectro como la radio cognitiva. Por lo tanto, nuevas estrategias han de ser consideradas en las comunicaciones HF para implementar la propuesta cognitiva de esta Tesis.

Actualmente, uno de los módems multiportadora para la banda de HF, denominado *HF Data+Voice Link* (HFDVL), ha sido diseñado y evaluado en la banda de HF por el grupo de investigación donde se ha desarrollado esta Tesis (Pérez-Álvarez et al., 2003; Santana-Sosa, Zazo-Bello, et al., 2006; Pérez-Álvarez et al., 2009). Este sistema está basado en *Orthogonal Frequency Division Multiplexing - Code Division Multiplexing* (OFDM-CDM), que no requiere entrelazados y tiene un retado punto a punto de 125 ms con una tasa de datos neta de 2460 bps. Por lo tanto, es una plataforma válida como capa física para la implementación de la propuesta cognitiva de esta Tesis.

Sin embargo, la propuesta de un protocolo de gestión del enlace con menor sobrecarga

que STANAG 5066 sí sería una línea futura de esta Tesis. El nuevo protocolo debe ser diseñado de manera que pueda mantener el intercambio de señalización de canal del sistema híbrido UCB-HMM propuesto. A nivel de carga de datos se ha demostrado que es viable incluso si se utiliza codificación y redundancia para proteger la información de señalización. Las tareas pendientes serían el diseño e implementación de un mecanismo más simple que tenga poca sobrecarga para la gestión del enlace.

Finalmente, otro tema propuesto como línea futura de esta Tesis es el diseño de un esquema de mitigación de interferencias de banda estrecha (NBI). Se ha recalcado la importancia de detectar y mitigar NBI en el dominio analógico, antes de la digitalización de la señal. Aunque implica una mayor complejidad en el sistema de mitigación, no hay alternativa para ser implementado en el dominio digital porque no se puede revertir el efecto de la interferencia de banda estrecha.

References

3GPP TS 36.201. (2015). *LTE; Evolved Universal Terrestrial Radio Access (E-UTRA); LTE physical layer; General description Release 12.* European Telecommunications Standards Institute.

AGILENT TECHNOLOGIES. (2010a). *SystemVue Documentation* (Tech. Rep.). Retrieved from `http://edocs.soco.agilent.com/display/sv201007/Home`

AGILENT TECHNOLOGIES. (2010b). *VSA 89600. technical Overview* (Tech. Rep.). Retrieved from `http://cp.literature.agilent.com/litweb/pdf/5989-1679EN.pdf`

AGRAWAL, R. (1995, December). Sample Mean Based Index Policies with O(log n) Regret for the Multi-Armed Bandit Problem. *Advances in Applied Probability*, *27*(4), 1054 - 1078.

AHMADI, H., CHEW, Y. H., TANG, P. K., & NIJSURE, Y. (2011, September). Predictive opportunistic spectrum access using learning based hidden Markov models. In *22nd IEEE International Symposium on Personal Indoor and Mobile Radio Communications (PIMRC 2011)* (p. 401-405). Toronto, Canada.

AHMADI, H., MACALUSO, I., & DASILVA, L. (2013, June). The effect of the spectrum opportunities diversity on opportunistic access. In *IEEE International Conference on Communications (ICC 2013)* (p. 2829-2834). Budapest, Hungary.

AKBAR, I., & TRANTER, W. (2007, March). Dynamic spectrum allocation in cognitive radio using hidden Markov models: Poisson distributed case. In *Proceedings of the IEEE SoutheastCon 2007* (p. 196-201). Richmond, USA.

AKYILDIZ, I. F., LEE, W.-Y., VURAN, M. C., & MOHANTY, S. (2006). Next generation/dynamic spectrum access/cognitive radio wireless networks: A survey. *Computer Networks*, *50*(13), 2127 - 2159.

AKYILDIZ, I. F., LO, B. F., & BALAKRISHNAN, R. (2011). Cooperative spectrum sensing in cognitive radio networks: A survey. *Physical Communication*, *4*(1), 40 - 62.

ALTINAY, O., TULUNAY, E., & TULUNAY, Y. (1997). Forecasting of ionospheric critical frequency using neural networks. *Geophysical Research Letters*, *24*(12), 1467–1470.

APPLETON, E. (1932). Wireless studies of the ionosphere. *Journal of the Institution of Electrical*

Engineers, *71*(430), 642-650.

ARSLAN, H. (Ed.). (2007). *Cognitive Radio, Software Defined Radio, and Adpative Wireless Systems*. Springer.

ASADI, H., VOLOS, H., MAREFAT, M., & BOSE, T. (2015, April). Metacognitive Radio Engine Design and Standardization. *IEEE Journal on Selected Areas in Communications*, *33*(4), 711-724.

AUER, P., CESA-BIANCHI, N., & FISCHER, P. (2002, May). Finite-time Analysis of the Multiarmed Bandit Problem. *Machine Learning*, *47*(2-3), 235 - 256.

BALDO, N., TAMMA, B., MANOJ, B., RAO, R., & ZORZI, M. (2009, June). A Neural Network Based Cognitive Controller for Dynamic Channel Selection. In *IEEE International Conference on Communications (ICC 2009)* (p. 1-5). Dresden, Germany.

BERTHOLD, U., FU, F., VAN DER SCHAAR, M., & JONDRAL, F. (2008, October). Detection of Spectral Resources in Cognitive Radios Using Reinforcement Learning. In *3rd IEEE Symposium on New Frontiers in Dynamic Spectrum Access Networks (DySPAN 2008)* (p. 1-5). Chicago, USA.

BKASSINY, M., LI, Y., & JAYAWEERA, S. (2013, Third Quarter). A Survey on Machine-Learning Techniques in Cognitive Radios. *IEEE Communications Surveys Tutorials*, *15*(3), 1136-1159.

BLUM, A. L., & RIVEST, R. L. (1992). Training a 3-Node Neural Network is NP-Complete. *Neural Networks*, *5*, 117-127.

BOURDENA, A., KORMENTZAS, G., PALLIS, E., & MASTORAKIS, G. (2012, June). A centralised broker-based CR network architecture for TVWS exploitation under the RTSSM policy. In *IEEE International Conference on Communications (ICC 2012)* (p. 5685-5689). Ottawa, Canada.

BRENT, R. P., & ZIMMERMANN, P. (2010). *Modern Computer Arithmetic*. Cambridge University Press.

BROWN, T. (2005, November). An analysis of unlicensed device operation in licensed broadcast service bands. In *First IEEE International Symposium on New Frontiers in Dynamic Spectrum Access Networks (DySPAN 2005)* (p. 11-29). Baltimore, USA.

BUDDHIKOT, M. (2007, April). Understanding Dynamic Spectrum Access: Models,Taxonomy and Challenges. In *2nd IEEE International Symposium on New Frontiers in Dynamic Spectrum Access Networks (DySPAN 2007)* (p. 649-663). Dublin, Ireland.

CABRIC, D., MISHRA, S., & BRODERSEN, R. (2004, November). Implementation issues in spectrum sensing for cognitive radios. In *38th Asilomar Conference on Signals, Systems and Computers* (Vol. 1, p. 772-776). Pacific Grove, USA.

CABRIC, D., TKACHENKO, A., & BRODERSEN, R. (2006, October). Spectrum Sensing Measurements of Pilot, Energy, and Collaborative Detection. In *IEEE Military Communications Conference (MILCOM 2006)* (p. 1-7). Washington DC, USA.

CANDÈS, E. (2006, August). Compressive Sampling. In *Proceedings of the International Congress of Mathematicians* (pp. 1433–1452). Madrid, Spain.

CANDÈS, E., ROMBERG, J., & TAO, T. (2006). Stable signal recovery from incomplete and inaccurate measurements. *Communications on pure and applied mathematics*, *59*(8), 1207–1223.

CANDÈS, E., & TAO, T. (2005). Decoding by linear programming. *IEEE Transactions on Information Theory*, *51*(12), 4203–4215.

CHALLAPALI, K., MANGOLD, S., & ZHONG, Z. (2004, March). Spectrum Agile Radio: Detection Spectrum Opportunities. In *International Symposium on Advanced Radio Technologies*. Boulder, USA.

CHATZIANTONIOU, E., ALLEN, B., & VELISAVLJEVIC, V. (2013, September). An HMM-based spectrum occupancy predictor for energy efficient cognitive radio. In *24th IEEE International Symposium on Personal Indoor and Mobile Radio Communications (PIMRC 2013)* (p. 601-605). London, UK.

CHEN, G., ZHAO, Z., ZHU, G., HUANG, Y., & LI, T. (2010, July). HF Radio-Frequency Interference Mitigation. *IEEE Geoscience and Remote Sensing Letters*, *7*(3), 479-482.

CHEN, Z., GUO, N., HU, Z., & QIU, R. (2011, May). Experimental Validation of Channel State Prediction Considering Delays in Practical Cognitive Radio. *IEEE Transactions on Vehicular Technology*, *60*(4), 1314-1325.

CHEN, Z., HU, Z., & QIU, R. (2009, October). Quickest Spectrum Detection Using Hidden Markov Model for Cognitive Radio. In *Proceedings of the IEEE Military Communications Conference (MILCOM 2009)*. Boston, USA.

CHEN, Z., & QIU, R. (2010, March). Prediction of Channel State for Cognitive Radio Using Higher-Order Hidden Markov Model. In *Proceedings of the IEEE SoutheastCon 2010* (p. 276-282). Concord, USA.

CHENG, X., & JIANG, M. (2011, September). Cognitive radio spectrum assignment based on artificial bee colony algorithm. In *13th IEEE International Conference on Communication Technology (ICCT 2011)* (p. 161-164). Jinan, China.

CHIANG, R., ROWE, G., & SOWERBY, K. (2007, April). A Quantitative Analysis of Spectral Occupancy Measurements for Cognitive Radio. In *65th IEEE Vehicular Technology Conference (VTC Spring 2007)* (p. 3016-3020). Dublin, Ireland.

CHU, A., & CONN, D. (1999, September). Neural network prediction of HF ionospheric propagation loss. *Electronics Letters*, *35*(20), 1774-1776.

CLANCY, T. (2009, August). Dynamic spectrum access using the interference temperature model. *Annals of Telecommunications - Annales des télécommunications*, *64*(7), 573-592.

CLANCY, T. C. (2007). Formalizing the interference temperature model. *Wireless Communications*

and Mobile Computing, *7*(9), 1077–1086.

CORDEIRO, C., CHALLAPALI, K., BIRRU, D., & SAI SHANKAR, N. (2005, November). IEEE 802.22: the first worldwide wireless standard based on cognitive radios. In *First IEEE International Symposium on New Frontiers in Dynamic Spectrum Access Networks (DySPAN 2005)* (p. 328-337). Baltimore, USA.

CORDIER *et al.*, P. (2006). E^2R Cognitive Pilot Channel concept. In *IST Mobile Summit*. Mykonos, Greece.

DAVENPORT, M. A., BOUFOUNOS, P. T., & BARANIUK, R. G. (2009, April). Compressive Domain Interference Cancellation. In *Workshop on Signal Processing with Adaptive Sparse Structured Representations (SPARS 2009)*. Saint-Malo, France.

DAVENPORT, M. A., SCHNELLE, S. R., SLAVINSKY, J., BARANIUK, R. G., WAKIN, M. B., & BOUFOUNOS, P. T. (2010). A wideband compressive radio receiver. In *IEEE Military Communications Conference (MILCOM 2010)* (pp. 1193–1198). San Jose, USA.

DERAKHSHANI, M., LE-NGOC, T., & NASIRI-KENARI, M. (2011, November). Efficient Cooperative Cyclostationary Spectrum Sensing in Cognitive Radios at Low SNR Regimes. *IEEE Transactions on Wireless Communications*, *10*(11), 3754-3764.

DONOHO, D. (2006). Compressed Sensing. *IEEE Transactions on Information Theory*, *52*(4), 1289–1306.

DORIGO, M., & BLUM, C. (2005). Ant colony optimization theory: A survey. *Theoretical Computer Science*, *344*(2–3), 243-278.

DOYLE, L. (2009). *Essentials of Cognitive Radio*. Cambridge University Press.

ELECTRONIC COMMUNICATIONS COMMITTEE. (2014, February). *ECC Report 205. Licensed Shared Access (LSA)*.

ETSI EN 301 701. (2008). *Digital Video Broadcasting (DVB); OFDM modulation for microwave digital terrestrial television V1.1.1*. European Telecommunications Standards Institute.

FARHANG-BOROUJENY, B. (2008, May). Filter Bank Spectrum Sensing for Cognitive Radios. *IEEE Transactions on Signal Processing*, *56*(5), 1801-1811.

FED-STD-1045A. (1993, October). *Telecommunications: HF Radio Automatic Link Establishment.* General Services Administration, National Communications System Office of Technology & Standards.

FEDERAL COMMUNICATIONS COMMISION. (2002, November). *Spectrum Policy Task Force Report* (ET Docket No. 02-135).

FEDERAL COMMUNICATIONS COMMISION. (2003, November). *Notice of inquiry and notice of proposed rule making: Establishment of an interference and to expand available unlicensed oper-*

ation in certain fixed, mobile and satellite frequency bands (ET Docket No. 03-237).

FEDERAL COMMUNICATIONS COMMISSION. (2000a, November). *Notice of proposed rulemaking in the matter of promoting efficient use of spectrum through elimination of barriers to the development of secondary markets* (FCC No. 00-402).

FEDERAL COMMUNICATIONS COMMISSION. (2000b, December). *Policy statement in the matter of principles for promoting the efficient use of spectrum by encouraging the development of secondary markets* (FCC No. 00-401).

FEDERAL COMMUNICATIONS COMMISSION. (2004, May). *Notice of proposed rule making: Unlicensed operation in TV broadcast bands* (ET Docket No. 04-186).

FEDERAL COMMUNICATIONS COMMISSION. (2005, February). *Notice of proposed rule making and order: Facilitating opportunities for flexible, efficient, and reliable spectrum use employing cognitive radio technologies* (ET Docket No. 03-108).

FETTE, B. A. (2009). *Cognitive Radio Technology*. Academic Press.

FITZEK, F. H. P., & KATZ, M. D. (Eds.). (2007). *Cognitive Wireless Networks. Concepts, Methodologies and Visions Inspiring the Age of Enlightenment of Wireless Communications*. Springer.

FORNEY, G. (1973, March). The Viterbi Algorithm. *Proceedings of the IEEE*, *61*(3), 268-278.

FUJII, T., & SUZUKI, Y. (2005, November). Ad-hoc cognitive radio - development to frequency sharing system by using multi-hop network. In *First IEEE International Symposium on New Frontiers in Dynamic Spectrum Access Networks (DySPAN 2005)* (p. 589-592). Baltimore, USA.

FURMAN, W., & KOSKI, E. (2009, April). Next Generation ALE Concepts. In *11th International Conference on Ionospheric Radio Systems and Techniques (IRST09)*. Edinburgh, UK.

GADHIOK, M., AMANNA, A., PRICE, M., & REED, J. (2011, February). Metacognition: Enhancing the performance of a cognitive radio. In *IEEE First International Multi-Disciplinary Conference on Cognitive Methods in Situation Awareness and Decision Support (CogSIMA 2011)* (p. 198-203). Miami Beach, USA.

GALINDO-SERRANO, A., & GIUPPONI, L. (2010, May). Distributed Q-Learning for Aggregated Interference Control in Cognitive Radio Networks. *IEEE Transactions on Vehicular Technology*, *59*(4), 1823-1834.

GANESAN, G., & LI, Y. (2005, November). Cooperative spectrum sensing in cognitive radio networks. In *First IEEE International Symposium on New Frontiers in Dynamic Spectrum Access Networks (DySPAN 2005)* (p. 137-143). Baltimore, USA.

GARCÍA-FRÍAS, J., & CRESPO, P. M. (1997). Hidden Markov Models for Burst Error Characterization in Indoor Radio Channels. *IEEE Transactions on Vehicular Technology*, *46*(4), 1006-1020.

GARDNER, W. A. (1987). *Statistical Spectral Analysis. A Nonprobabilistic Theory*. Prentice Hall.

GHASEMI, A., & SOUSA, E. (2005, November). Collaborative spectrum sensing for opportunistic access in fading environments. In *First IEEE International Symposium on New Frontiers in Dynamic Spectrum Access Networks (DySPAN 2005)* (p. 131-136). Baltimore, USA.

GIUPPONI, L., GALINDO-SERRANO, A., BLASCO, P., & DOHLER, M. (2010, August). Docitive networks: an emerging paradigm for dynamic spectrum management. *IEEE Wireless Communications*, *17*(4), 47-54.

GOH, L. P., LEI, Z., & CHIN, F. (2007, August). Feature Detector for DVB-T Signal in Multipath Fading Channel. In *2nd International Conference on Cognitive Radio Oriented Wireless Networks and Communications (CrownCom 2007)* (p. 234-240). Orlando, USA.

GOLDBERG, D. E. (1989). *Genetic Algorithms in Search, Optimization, and Machine Learning*. Addison-Wesley Publishing Company.

GURNEY, D., BUCHWALD, G., ECKLUND, L., KUFFNER, S., & GROSSPIETSCH, J. (2008, October). Geo-Location Database Techniques for Incumbent Protection in the TV White Space. In *3rd IEEE Symposium on New Frontiers in Dynamic Spectrum Access Networks (DySPAN 2008)* (p. 1-9). Chicago, USA.

HAMDAOUI, B., VENKATRAMAN, P., & GUIZANI, M. (2009, November). Opportunistic Exploitation of Bandwidth Resources through Reinforcement Learning. In *IEEE Global Telecommunications Conference (GLOBECOM 2009)* (p. 1-6). Honolulu, USA.

HARALAMBOUS, H., & PAPADOPOULOS, H. (2009, March). 24-Hour Neural Network Congestion Models for High-Frequency Broadcast Users. *IEEE Transactions on Broadcasting*, *55*(1), 145-154.

HAYKIN, S. (1998). *Neural Networks: A Comprehensive Foundation* (2nd ed.). Prenticel Hall.

HAYKIN, S. (2005, February). Cognitive Radio: Brain-Empowered Wireless Communications. *IEEE Journal on Selected Areas in Communications*, *23*(2), 201-220.

HE, A., BAE, K. K., NEWMAN, T., GAEDDERT, J., KIM, K., MENON, R., ... TRANTER, W. (2010, May). A Survey of Artificial Intelligence for Cognitive Radios. *IEEE Transactions on Vehicular Technology*, *59*(4), 1578-1592.

HERTZ, H. R. (1893). *Electric Waves: Being Researches on the Propagation of Electric Action with Finite Velocity through Space*. Macmillan and Co.

HOANG, A. T., LIANG, Y.-C., WONG, D., ZENG, Y., & ZHANG, R. (2009, March). Opportunistic spectrum access for energy-constrained cognitive radios. *IEEE Transactions on Wireless Communications*, *8*(3), 1206-1211.

HOSSAIN, E., & BHARGAVA, V. K. (Eds.). (2007). *Cognitive Wireless Communication Networks*. Springer.

HOSSAIN, E., NIYATO, D., & HAN, Z. (2009). *Dynamic Spectrum Access and Management in Cognitive Radio Networks*. Cambridge University Press.

HULBERT, A. (2005, September). Spectrum sharing through beacons. In *IEEE 16th International Symposium on Personal, Indoor and Mobile Radio Communications (PIMRC 2005)* (Vol. 2, p. 989-993). Berlin, Germany.

HWANG, S., JANG, S., KIM, D., & SEO, J. (2010, February). An MMSE-based compressive domain interference cancellator for wideband systems. In *2nd International Conference on Computer and Automation Engineering (ICCAE)*. Singapore.

IEEE COMMUNICATIONS SOCIETY. (2008, September). *IEEE Std. 1900.1. IEEE Standard Definitions and Concepts for Dynamic Spectrum Access: Terminology Relating to Emerging Wireless Networks, System Functionality, and Spectrum Management.*

ISLAM, M., KOH, C., OH, S. W., QING, X., LAI, Y., WANG, C., ... TOH, W. (2008, May). Spectrum Survey in Singapore: Occupancy Measurements and Analyses. In *3rd International Conference on Cognitive Radio Oriented Wireless Networks and Communications (CrownCom 2008)* (p. 1-7). Singapore.

ITU-R. (2009, September). *Report ITU-R SM.2152. Definitions of Software Defined Radio (SDR) and Cognitive Radio System (CRS)*.

JALLON, P. (2008, January). An Algorithm for Detection of DVB-T Signals Based on Their Second-order Statistics. *EURASIP Journal on Wireless Communications and Networking*, *2008*, 1-9.

JAMES, G., WITTEN, D., HASTIE, T., & TIBSHIRANI, R. (2013). *An Introduction to Statistical Learning with Applications in R*. Springer.

JI, Z., & LIU, K. (2007, May). COGNITIVE RADIOS FOR DYNAMIC SPECTRUM ACCESS - Dynamic Spectrum Sharing: A Game Theoretical Overview. *IEEE Communications Magazine*, *45*(5), 88-94.

JIANG, T., GRACE, D., & LIU, Y. (2011, March). Two-stage reinforcement-learning-based cognitive radio with exploration control. *IET Communications*, *5*(5), 644-651.

JIANG, T., GRACE, D., & MITCHELL, P. (2011, July). Efficient exploration in reinforcement learning-based cognitive radio spectrum sharing. *IET Communications*, *5*(10), 1309-1317.

JONDRAL, F. K. (2005, August). Software-defined Radio: Basics and Evolution to Cognitive Radio. *EURASIP Journal on Wireless Communications and Networking*, *2005*(3), 275–283.

JOUINI, W., ERNST, D., MOY, C., & PALICOT, J. (2009, November). Multi-armed bandit based policies for cognitive radio's decision making issues. In *3rd International Conference on Signals, Circuits and Systems (SCS)*. Medenine, Tunisia.

JOUINI, W., ERNST, D., MOY, C., & PALICOT, J. (2010, May). Upper Confidence Bound Based Decision Making Strategies and Dynamic Spectrum Access. In *IEEE International Conference*

on Communications (ICC). Cape Town, South Africa.

KANTERAKIS, E., & BRUNO, F. (1994, May). Wideband frequency selective limiter. In *Proceedings of the Tactical Communications Conference* (Vol. 1, p. 421-430). Fort Wayne, USA.

KARABOGA, D., & BASTURK, B. (2007). A powerful and efficient algorithm for numerical function optimization: artificial bee colony (ABC) algorithm. *Journal of Global Optimization*, *39*(3), 459-471.

KAY, S. M. (1998). *Fundamentals of statistical signal processing: Detection theory* (Vol. II). Prentice-Hall.

KENNEDY, J., & EBERHART, R. (1995, November). Particle swarm optimization. In *IEEE International Conference on Neural Networks* (Vol. 4, p. 1942-1948). Perth, Australia.

KENNELLY, A. (1902, March). On the Elevation of the Electrically-Conducting Strata of the Earth's Atmosphere. *Electrical World and Engineer*, *39*(11), 473.

KIM, J. M., SOHN, S. H., HAN, N., ZHENG, G., KIM, Y. M., & LEE, J. K. (2008, May). Cognitive Radio Software Testbed using Dual Optimization in Genetic Algorithm. In *3rd International Conference on Cognitive Radio Oriented Wireless Networks and Communications (CrownCom 2008)* (p. 1-6). Singapore.

KOSKI, E., & FURMAN, W. (2009, April). Applying Cognitive Radio Concepts to HF Communications. In *11th International Conference on Ionospheric Radio Systems and Techniques (IRST09)*. Edinburgh, UK.

LA, C., & DO, M. (2006, October). Tree-Based Orthogonal Matching Pursuit Algorithm for Signal Reconstruction. In *IEEE International Conference on Image Processing* (p. 1277-1280). Atlanta, USA.

LÓPEZ-BENÍTEZ, M., & CASADEVALL, F. (2012, May). Improved energy detection spectrum sensing for cognitive radio. *IET Communications*, *6*(8), 785-796.

LÓPEZ-BENÍTEZ, M., CASADEVALL, F., UMBERT, A., PÉREZ-ROMERO, J., HACHEMANI, R., PALICOT, J., & MOY, C. (2009, June). Spectral occupation measurements and blind standard recognition sensor for cognitive radio networks. In *4th International Conference on Cognitive Radio Oriented Wireless Networks and Communications (CrownCom 2009)* (p. 1-9). Hannover, Germany.

LÓPEZ-BENÍTEZ, M., UMBERT, A., & CASADEVALL, F. (2009, April). Evaluation of Spectrum Occupancy in Spain for Cognitive Radio Applications. In *69th IEEE Vehicular Technology Conference (VTC Spring 2009)* (p. 1-5). Barcelona, Spain.

LUNDÉN, J., KOIVUNEN, V., HUTTUNEN, A., & POOR, H. (2009, November). Collaborative Cyclostationary Spectrum Sensing for Cognitive Radio Systems. *IEEE Transactions on Signal Processing*, *57*(11), 4182-4195.

MA, J., LI, G., & JUANG, B. H. (2009, May). Signal Processing in Cognitive Radio. *Proceedings of the IEEE*, *97*(5), 805-823.

MA, J., ZHAO, G., & LI, Y. (2008, November). Soft Combination and Detection for Cooperative Spectrum Sensing in Cognitive Radio Networks. *IEEE Transactions on Wireless Communications*, *7*(11), 4502-4507.

MACALUSO, I., AHMADI, H., & DASILVA, L. (2015, April). Fungible Orthogonal Channel Sets for Multi-User Exploitation of Spectrum. *IEEE Transactions on Wireless Communications*, *14*(4), 2281-2293.

MACALUSO, I., FINN, D., OZGUL, B., & DASILVA, L. (2013, November). Complexity of Spectrum Activity and Benefits of Reinforcement Learning for Dynamic Channel Selection. *IEEE Journal on Selected Areas in Communications*, *31*(11), 2237-2248.

MALANCHINI, I., CESANA, M., & GATTI, N. (2009, November). On Spectrum Selection Games in Cognitive Radio Networks. In *IEEE Global Telecommunications Conference (GLOBECOM 2009)* (p. 1-7). Honolulu, USA.

MANGOLD, S., JAROSCH, A., & MONNEY, C. (2006). Operator Assisted Cognitive Radio and Dynamic Spectrum Assignment with Dual Beacons - Detailed Evaluation. In *First International Conference on Communication System Software and Middleware (Comsware 2006)* (p. 1-6). Delhi, India.

MANGOLD, S., ZHONG, Z., CHALLAPALI, K., & CHOU, C.-T. (2004, November). Spectrum agile radio: radio resource measurements for opportunistic spectrum usage. In *IEEE Global Telecommunications Conference (GLOBECOM '04)* (Vol. 6, p. 3467-3471). Dallas, USA.

MASLIN, N. M. (1987). *HF Communications: A Systems Approach*. Pitman Publishing.

MASMOUDI, R., BELMEGA, E., FIJALKOW, I., & SELLAMI, N. (2015, June). Joint scheduling and power allocation in Cognitive Radio systems. In *IEEE International Conference on Communications Workshops (ICC Workshops 2015)* (p. 399-404). London, UK.

MATINMIKKO, M., MUSTONEN, M., ROBERSON, D., PAAVOLA, J., HÖYHTYA, M., YRJOLA, S., & RONING, J. (2014, April). Overview and comparison of recent spectrum sharing approaches in regulation and research: From opportunistic unlicensed access towards licensed shared access. In *IEEE International Symposium on Dynamic Spectrum Access Networks (DySPAN 2014)* (p. 92-102). McLean, USA.

MAXWELL, J. C. (1873). *A Treatise on Electricity and Magnetism*. Oxford Clarendon Press.

MELIÁN-GUTIÉRREZ, L., GARCIA-RODRIGUEZ, A., PÉREZ-ÁLVAREZ, I., & ZAZO, S. (2015). Compressive Narrowband Interference Detection for Wideband Cognitive HF Front-Ends. *Springer Wireless Personal Communications (Submitted)*.

MELIÁN-GUTIÉRREZ, L., MODI, N., MOY, C., BADER, F., PÉREZ-ÁLVAREZ, I., & ZAZO, S. (2016). Hy-

brid UCB-HMM: A Machine Learning Strategy for Cognitive Radio in HF Band. *IEEE Transactions on Cognitive Communications and Networking*. doi: 10.1109/TCCN.2016.2527021

MELIÁN-GUTIÉRREZ, L., MODI, N., MOY, C., PÉREZ-ÁLVAREZ, I., BADER, F., & ZAZO, S. (2015a, May). DSA with Reinforcement Learning in HF Band. In *1st URSI Atlantic Radio Science Conference (AT-RASC)*. Gran Canaria, Spain.

MELIÁN-GUTIÉRREZ, L., MODI, N., MOY, C., PÉREZ-ÁLVAREZ, I., BADER, F., & ZAZO, S. (2015b, June). Upper Confidence Bound Learning Approach for Real HF Measurements. In *IEEE International Conference on Communications Workshops (ICC Workshops)* (p. 281-286). London, UK.

MELIÁN-GUTIÉRREZ, L., ZAZO, S., BLANCO-MURILLO, J., PÉREZ-ÁLVAREZ, I., GARCÍA-RODRÍGUEZ, A., & PÉREZ-DÍAZ, B. (2012, May). Efficiency improvement of HF communications using cognitive radio principles. In *12th International Conference on Ionospheric Radio Systems and Techniques (IRST12)* (p. 1-5). York, UK.

MELIÁN-GUTIÉRREZ, L., ZAZO, S., BLANCO-MURILLO, J., PÉREZ-ÁLVAREZ, I., GARCÍA-RODRÍGUEZ, A., & PÉREZ-DÍAZ, B. (2013). HF spectrum activity prediction model based on HMM for cognitive radio applications. *Elsevier Physical Communication*, *9*, 199 - 211.

MIL-STD-188-110C. (2011, September). *Interoperability and Performance Standards for Data Modems.* U.S. Dept. of Defense.

MIL-STD-188-141A. (1988, September). *Interoperability and Performance Standards for Medium and High Frequency Radio Equipment.* U.S. Dept. of Defense.

MIL-STD-188-141B. (1999, March). *Interoperability and Performance Standards for Medium and High Frequency Radio Equipment.* U.S. Dept. of Defense.

MITOLA, J. (1999, November). Cognitive radio for flexible mobile multimedia communications. In *IEEE International Workshop on Mobile Multimedia Communications.* San Diego, USA.

MITOLA, J. (2000). *Cognitive radio: An integrated agent architecture for software defined radio* (Doctoral Dissertation). Royal Institute of Technology (KTH), Stockholm, Sweden.

MITOLA, J., & MAGUIRE, G. Q. (1999, August). Cognitive Radio: Making software radios more personal. *IEEE Personal Communications*, *6*(4), 13-18.

MOY, C. (2014, March). Reinforcement Learning Real Experiments for Opportunistic Spectrum Access. In *Karlsruhe Workshop on Software Radios.* Karlsruhe, Germany.

MUECK, M., DI RENZO, M., DEBBAH, M., & RENK, T. (2010, August). Combination of centralized & decentralized database and terminal-based spectrum sensing for secondary spectrum access. In *IEEE International Conference on Wireless Information Technology and Systems (ICWITS 2010)* (p. 1-4). Honolulu, USA.

MURTY, R., CHANDRA, R., MOSCIBRODA, T., & BAHL, P. (2012, February). SenseLess: A Database-

Driven White Spaces Network. *IEEE Transactions on Mobile Computing*, *11*(2), 189-203.

NASTASE, C.-V., MARTIAN, A., VLADEANU, C., & MARGHESCU, I. (2014, November). An accurate average energy detection algorithm for spectrum sensing in cognitive radio systems. In *11th International Symposium on Electronics and Telecommunications (ISETC)* (p. 1-4). Timisoara, Romania.

NEEDELL, D., & TROPP, J. (2009). CoSaMP: Iterative signal recovery from incomplete and inaccurate samples. *Applied and Computational Harmonic Analysis*, *26*(3), 301–321.

NEEDELL, D., TROPP, J., & VERSHYNIN, R. (2008, October). Greedy signal recovery review. In *42nd Asilomar Conference on Signals, Systems and Computers* (p. 1048-1050). Pacific Grove, USA.

NEEDELL, D., & VERSHYNIN, R. (2009, April). Uniform Uncertainty Principle and Signal Recovery via Regularized Orthogonal Matching Pursuit. *Foundations of Computational Mathematics*, *9*(3), 317–334.

NGO, D. T., & LE-NGOC, T. (2011, September). Distributed Resource Allocation for Cognitive Radio Networks With Spectrum-Sharing Constraints. *IEEE Transactions on Vehicular Technology*, *60*(7), 3436-3449.

NIE, N., & COMANICIU, C. (2006). Adaptive Channel Allocation Spectrum Etiquette for Cognitive Radio Networks. *Mobile Networks and Applications*, *11*(6), 779-797.

NTIA/ITS. (1998). *High Frequency Radio ALE Application Handbook*. NTIA/ITS.

PARK, C.-H., KIM, S.-W., LIM, S.-M., & SONG, M.-S. (2007, December). HMM Based Channel Status Predictor for Cognitive Radio. In *Proceedings of Asia-Pacific Microwave Conference* (p. 1-4). Bangkok, Thailand.

PEHA, J. M., & PANICHPAPIBOON, S. (2004). Real-time secondary markets for spectrum. *Telecommunications Policy*, *28*(7–8), 603 - 618.

PÉREZ-ÁLVAREZ, I., LÓPEZ-PÉREZ, J., ZAZO-BELLO, S., RAOS, I., PÉREZ-DÍAZ, B., & JIMÉNEZ-YGUACEL, E. (2009, April). Real link of a high data rate OFDM modem: description and performance. In *11th International Conference on Ionospheric Radio Systems and Techniques (IRST09)*. Edinburgh, UK.

PÉREZ-ÁLVAREZ, I., RAOS, I., ZAZO, S., MENDIETA-OTERO, E., SANTANA-SOSA, H., & PÁEZ-BORRALLO, J. (2003, June). Interactive Digital Voice over HF. In *9th International Conference on Ionospheric Radio Systems and Techniques (IRST03)* (p. 31-36). Bath, UK.

PÉREZ-DÍAZ, B., JIMÉNEZ-YGUACEL, E., LÓPEZ-PÉREZ, J., PÉREZ-ÁLVAREZ, I., ZAZO-BELLO, S., & MENDIETA-OTERO, E. (2009, April). Design and construction of a broadband (1 MHz) digital HF transceiver for multicarrier and multichannel modulations. In *11th International Conference on Ionospheric Radio Systems and Techniques (IRST09)*. Edinburgh, UK.

PÉREZ-DÍAZ, B., ZAZO, S., PÉREZ-ÁLVAREZ, I., LÓPEZ-PÉREZ, J., MELIÁN-GUTIÉRREZ, L., & JIMÉNEZ-YGUACEL, E. (2012, May). Theory and practice for modelling the broadband acquisition in HF transmissions. In *12th International Conference on Ionospheric Radio Systems and Techniques (IRST12)*. York, UK.

PRESIDENT'S COUNCIL OF ADVISORS ON SCIENCE AND TECHNOLOGY. (2012, July). *Report to the President: Realizing the Full Potential of Government-held Spectrum to Spur Economic Growth.*

PROAKIS, J. G. (2000). *Digital communications* (4th ed.). McGraw Hill.

PUVANESWARI, M., & SIDEK, O. (2004, September). Wideband analog front-end for multistandard software defined radio receiver. In *15th ieee international symposium on personal, indoor and mobile radio communications (pimrc 2004)* (Vol. 3, p. 1937-1941). Barcelona, Spain.

RABINER, L., & JUANG, B.-H. (1993). *Fundamentals of Speech Recognition*. Prentice-Hall.

RADIO SPECTRUM POLICY GROUP. (2011, November). *RSPG11-392. Report on Collective Use of Spectrum (CUS) and other spectrum sharing approaches.*

RADIO SPECTRUM POLICY GROUP. (2013, November). *RSPG13-538. Opinion on Licensed Shared Access.*

RAMAN, C., YATES, R., & MANDAYAM, N. B. (2005, November). Scheduling variable rate links via a spectrum server. In *First IEEE International Symposium on New Frontiers in Dynamic Spectrum Access Networks (DySPAN 2005)* (p. 110-118). Baltimore, USA.

RATCLIFFE, J. (1974, September). Scientists' reactions to Marconi's transatlantic radio experiment. *Proceedings of the Institution of Electrical Engineers*, *121*(9), 1033-1039.

RIBEIRO, J., RIBEIRO, J., RODRIGUEZ, J., DIONISIO, R., ESTEVES, H., DUARTE, P., & MARQUES, P. (2012, August). Testbed for combination of local sensing with geolocation database in real environments. *IEEE Wireless Communications*, *19*(4), 59-66.

ROBBINS, H. (1952, September). Some aspects of the sequential design of experiments. *Bulletin of the American Mathematical Society*, *58*(5), 527 - 535.

ROBERT, C., MOY, C., & WANG, C.-X. (2014, June). Reinforcement learning approaches and evaluation criteria for opportunistic spectrum access. In *IEEE International Conference on Communications (ICC)*. Sidney, Australia.

SAHAI, A., HOVEN, N., & TANDRA, R. (2004, October). Some Fundamental Limits on Cognitive Radio. In *42nd Allerton Conference on Communication, Control, and Computing.*

SANTANA-SOSA, H., PÉREZ-ÁLVAREZ, I., ZAZO-BELLO, S., MENDIETA-OTERO, E., RAOS, I., & LÓPEZ-PÉREZ, J. (2006, July). Performance over a real link of a HF software radio modem for interactive digital voice communication. In *10th International Conference on Ionospheric Radio Systems and Techniques (IRST06)* (p. 207-211). London, UK.

SANTANA-SOSA, H., ZAZO-BELLO, S., PÉREZ-ÁLVAREZ, I., RAOS, I., MENDIETA-OTERO, E., & LÓPEZ-PÉREZ, J. (2006). Validation of a HF spread spectrum multi-carrier technology through real-link measurements. *European Transactions on Telecommunications*, *17*(6), 651-657.

SHAHID, A., AHMAD, S., AKRAM, A., & KHAN, S. (2010, March). Cognitive ALE for HF Radios. In *Second international conference on computer engineering and applications (iccea 2010)* (Vol. 2, p. 28-33). Bali, Indonesia.

SHARMA, M., SAHOO, A., & NAYAK, K. (2008, October). Channel modeling based on interference temperature in underlay cognitive wireless networks. In *IEEE International Symposium on Wireless Communication Systems (ISWCS '08)* (p. 224-228). Reykjavik, Iceland.

SHUKLA, A., JACKSON-BOOTH, N., & ARTHUR, P. (2012, May). "Cognitive radios" and their relevance to HF radio systems. In *12th IET International Conference on Ionospheric Radio Systems and Techniques (IRST 2012)* (p. 1-6). York, UK.

SIMONS, R. (1996). Guglielmo Marconi and Early Systems of Wireless Communication. *GEC Review*, *11*(1), 37-55.

STANAG 4285. (1989, February). *Characteristics of 1200/2400/3600 bits per second single tone modulators/demodulators for HF radio links.* North Atlantic Treaty Organization (NATO).

STANAG 4538. (2000). *Technical Standards for an Automatic Radio Control System (ARCS) for HF Communication Links.* North Atlantic Treaty Organization (NATO).

STANAG 4539. (2005). *Technical Standards for Non-hopping HF Communications Waveforms.* North Atlantic Treaty Organization (NATO).

STANAG 5066. (2008, December). *Profile for HF Radio Communications Ed. 2.* North Atlantic Treaty Organization (NATO).

SURIS, J., DASILVA, L., HAN, Z., & MACKENZIE, A. (2007, June). Cooperative Game Theory for Distributed Spectrum Sharing. In *IEEE International Conference on Communications (ICC 2007)* (p. 5282-5287). Glasgow, UK.

SUTTON, R. S., & BARTO, A. G. (1998). *Reinforcement Learning: An Introduction*. MIT Press.

TANG, H. (2005, November). Some physical layer issues of wide-band cognitive radio systems. In *First IEEE International Symposium on New Frontiers in Dynamic Spectrum Access Networks (DySPAN 2005)* (p. 151-159). Baltimore, USA.

THE SDR FORUM. (2008, September). *Cognitive Radio Definitions and Nomenclature.*

THILAKAWARDANA, D., & MOESSNER, K. (2007, August). A Genetic Approach to Cell-by-Cell Dynamic Spectrum Allocation for Optimising Spectral Efficiency in Wireless Mobile Systems. In *2nd International Conference on Cognitive Radio Oriented Wireless Networks and Communications (CrownCom 2007)* (p. 367-372). Orlando, USA.

TIAN, Z., & GIANNAKIS, G. (2006, June). A Wavelet Approach to Wideband Spectrum Sensing for Cognitive Radios. In *1st International Conference on Cognitive Radio Oriented Wireless Networks and Communications (CrownCom 2006)* (p. 1-5). Mykonos, Greece.

TIAN, Z., & GIANNAKIS, G. B. (2007). Compressed sensing for wideband cognitive radios. In *IEEE International Conference on Acoustics, Speech and Signal Processing (ICASSP)* (Vol. 4, p. 1357-1360). Honolulu, USA.

TRAGOS, E., ZEADALLY, S., FRAGKIADAKIS, A., & SIRIS, V. (2013, Third Quarter). Spectrum Assignment in Cognitive Radio Networks: A Comprehensive Survey. *IEEE Communications Surveys Tutorials*, *15*(3), 1108-1135.

TROPP, J., & GILBERT, A. (2007, December). Signal recovery from random measurements via orthogonal matching pursuit. *IEEE Transactions on Information Theory*, *53*(12), 4655-4666.

TROPP, J., LASKA, J., DUARTE, M., ROMBERG, J., & BARANIUK, R. (2010). Beyond Nyquist: Efficient sampling of sparse bandlimited signals. *IEEE Transactions on Information Theory*, *56*(1), 520–544.

TUMULURU, V., WANG, P., & NIYATO, D. (2010, May). A Neural Network Based Spectrum Prediction Scheme for Cognitive Radio. In *IEEE International Conference on Communications (ICC 2010)* (p. 1-5). Cape Town, South Africa.

UNNIKRISHNAN, J., & VEERAVALLI, V. (2010, February). Algorithms for Dynamic Spectrum Access With Learning for Cognitive Radio. *IEEE Transactions on Signal Processing*, *58*(2), 750-760.

UNNIKRISHNAN, J., & VEERAVALLI, V. V. (2008, February). Cooperative Sensing for Primary Detection in Cognitive Radio. *IEEE Journal of Selected Topics in Signal Processing*, *2*(1), 18-27.

URKOWITZ, H. (1967, April). Energy detection of unknown deterministic signals. *Proceedings of the IEEE*, *55*(4), 523-531.

VANNINEN, T., LINDEN, T., RAUSTIA, M., & SAARNISAARI, H. (2014, June). Cognitive HF - New perspectives to use the high frequency band. In *9th International Conference on Cognitive Radio Oriented Wireless Networks and Communications (CrownCom 2014)*. Oulu, Finland.

WANG, B., & LIU, K. (2011, February). Advances in cognitive radio networks: A survey. *IEEE Journal of Selected Topics in Signal Processing*, *5*(1), 5-23.

WANG, B., WU, Y., & LIU, K. R. (2010, October). Game theory for cognitive radio networks: An overview. *Computer Networks*, *54*(14), 2537 - 2561.

WANG, F., & TIAN, Z. (2008, July). Wideband receiver design in the presence of strong narrowband interference. *IEEE Communications Letters*, *12*(7), 484-486.

WATKINS, C., & DAYAN, P. (1992). Q-learning. *Machine Learning*, *8*(3-4), 279-292.

WELLENS, M., & MÄHÖNEN, P. (2010, June). Lessons Learned from an Extensive Spectrum Oc-

cupancy Measurement Campaign and a Stochastic Duty Cycle Model. *Mobile Networks and Applications*, *15*(3), 461-474.

WELLENS, M., WU, J., & MÄHÖNEN, P. (2007, August). Evaluation of Spectrum Occupancy in Indoor and Outdoor Scenario in the Context of Cognitive Radio. In *2nd International Conference on Cognitive Radio Oriented Wireless Networks and Communications (CrownCom 2007)* (p. 420-427). Orlando, USA.

WIRELESS INNOVATION FORUM. (2012, December). *Top 10 most wanted innovations version 2.0.*

WU, Y., WANG, B., LIU, K., & CLANCY, T. (2009, April). Repeated open spectrum sharing game with cheat-proof strategies. *IEEE Transactions on Wireless Communications*, *8*(4), 1922-1933.

XU, Y., ANPALAGAN, A., WU, Q., SHEN, L., GAO, Z., & WANG, J. (2013, Fourth Quarter). Decision-Theoretic Distributed Channel Selection for Opportunistic Spectrum Access: Strategies, Challenges and Solutions. *IEEE Communications Surveys Tutorials*, *15*(4), 1689-1713.

YATES, R., RAMAN, C., & MANDAYAM, N. B. (2006, June). Fair and Efficient Scheduling of Variable Rate Links via a Spectrum Server. In *IEEE International Conference on Communications (ICC 2006)* (Vol. 11, p. 5246-5251). Istanbul, Turkey.

YAU, K.-L., KOMISARCZUK, P., & TEAL, P. (2010, May). Applications of Reinforcement Learning to Cognitive Radio Networks. In *IEEE International Conference on Communications Workshops (ICC 2010)* (p. 1-6). Cape Town, South Africa.

YU, L., LIU, C., & HU, W. (2010, June). Spectrum allocation algorithm in cognitive ad-hoc networks with high energy efficiency. In *International Conference on Green Circuits and Systems (ICGCS 2010)* (p. 349-354). Shangai, China.

YUCEK, T., & ARSLAN, H. (2009). A survey of spectrum sensing algorithms for cognitive radio applications. *IEEE Communications Surveys Tutorials*, *11*(1), 116-130.

ZENG, Y., & LIANG, Y.-C. (2009, May). Spectrum-Sensing Algorithms for Cognitive Radio Based on Statistical Covariances. *IEEE Transactions on Vehicular Technology*, *58*(4), 1804-1815.

ZHAO, J., ZHENG, H., & YANG, G.-H. (2005, November). Distributed coordination in dynamic spectrum allocation networks. In *First IEEE International Symposium on New Frontiers in Dynamic Spectrum Access Networks (DySPAN 2005)* (p. 259-268). Baltimore, USA.

ZHAO, Q., & SADLER, B. (2007, May). A Survey of Dynamic Spectrum Access. *IEEE Signal Processing Magazine*, *24*(3), 79-89.

ZHAO, Z., PENG, Z., ZHENG, S., & SHANG, J. (2009, September). Cognitive radio spectrum allocation using evolutionary algorithms. *IEEE Transactions on Wireless Communications*, *8*(9), 4421-4425.